

**CORRECTION FACTOR TECHNIQUES
FOR IMPROVING
AERODYNAMIC PREDICTION METHODS**

By

J. P. Giesing
T. P. Kalman
W. P. Rodden

MAY 1976

Prepared under Contract No. NAS1-13835 By
MCDONNELL DOUGLAS CORPORATION
DOUGLAS AIRCRAFT COMPANY
LONG BEACH, CALIFORNIA

For

National Aeronautics And Space Administration

CONTENTS

	Page
SUMMARY	1
INTRODUCTION	3
LIST OF SYMBOLS	6
THEORETICAL DEVELOPMENT	10
Basic Method	10
Premultiplying Correction Factor Matrix	10
Multiple Modes	14
Postmultiplying Correction Factor Matrix	15
Modifications of the Basic Method	18
Estimates	18
Correction Factor Modes	21
Limits	22
A New Postmultiplying Correction Factor Matrix	24
Transonic Effects Using Local Mach Number	27
Direct Application of Local Mach Number	27
A New Transonic Effects Method	28
CORRELATION STUDIES	35
Local Mach Number Studies	35
Subsonic Cases	40
Oscillating Wing with Control Surface	40
Wing With and Without Leading Edge Droop	45
Transonic Cases	48
Supersonic Cases	54
RECOMMENDATIONS FOR DATA ACQUISITION	56
CONCLUDING REMARKS	58
Conclusions	58
Recommendations for Further Studies	63
CORRECTION FACTOR COMPUTER PROGRAM	64
Introduction	64
Program Input	67
Overview of Data	67

	Page
Input Sheets	69
Description of Input Data	72
Tape Description	85
Test Cases	91
Subroutine Description	142
Listing	203
REFERENCES	238

CORRECTION FACTOR TECHNIQUES FOR
IMPROVING AERODYNAMIC PREDICTION METHODS*

By Joseph P. Giesing, Terez P. Kalman
and William P. Rodden **
Douglas Aircraft Company

SUMMARY

This report describes a method for correcting lifting surface theory so that it reflects known experimental data. Specifically the theoretical pressure distribution is modified such that imposed constraints are satisfied (e.g., lift, moment, etc.) while minimizing the change to the theoretical pressure distribution. It is assumed that a finite element or discretized lifting surface method is used, such as either the Doublet or Vortex Lattice Methods.

There are several ways in which the theoretical pressures are modified. One is a direct application of a set of correction factors to the pressures. This is accomplished by premultiplying the pressures with a diagonal matrix of correction factors. A second approach to correcting the theory is to modify the downwash. This modification can be accomplished by either multiplying the downwash by a diagonal matrix of correction factors or by adding an incremental downwash (which is proportioned to the pressure) to the theoretical downwash. In any case the correction factors are adjusted so that the imposed experimental constraints are satisfied by the corrected pressure distribution while the changes in the pressure distribution are minimized.

There are several features that have been built into the basic method and these include: (1) the ability to consider together experimental data

* The authors wish to acknowledge Dr. Edward Albano for interesting discussions of alternate formats (non-diagonal) of correction matrices and their potential derivations.

** Consulting Engineer

from more than one mode (e.g., control surface rotation, pitch, camber, etc.), (2) the ability to limit the excursions of the correction factors (i.e., establish minimum and maximum values for them) and (3) the ability to use correction factor mode shapes (i.e., construct correction factors from known distributions or functions).

The methods developed have been implemented on the computer and many correlations and calculations made. Specifically cases involving all three Mach Number ranges are considered. For instance in the subsonic speed range a swept wing with an oscillating partial span flap and a swept wing with a leading edge droop are discussed. In the transonic speed range a two-dimensional symmetric airfoil with an oscillating flap is treated in detail. An arrow wing with and without camber is used in the supersonic analysis.

The computer program used to generate the correction factors for these cases is also fully described in this report and test cases are provided.

Finally, a new, simple method for accounting for transonic effects in the lifting surface theory is described and correlated for the two-dimensional case. Basically, a transformed distance between the sending element and receiving point is employed. The transformation depends on the time delay encountered by a signal traveling from the sending point to the receiving point.

INTRODUCTION

Wind tunnel data have provided the basis for semi-empirical methods of aeroelastic analysis for many years, whether in the estimation of stability and control characteristics, the calculation of structural loads, or in flutter analysis by modified strip methods. These semi-empirical methods have been tailored to aerodynamic lifting-line theory or to strip theory and not to the more general (and more accurate) lifting-surface methods. The use of a diagonal correction matrix to be applied as a premultiplying factor to matrices of aerodynamic influence coefficients obtained from lifting surface theory has been considered by a number of authors. A premultiplier may be regarded as a correction to the pressure distribution; as an alternative, a postmultiplier would be regarded as a correction to the downwash to account for thickness effects and for camber induced by boundary-layer displacement effects. Rodden and Revell (refs. 1 - 4) considered a real correction matrix derived from static wind tunnel measurements and theoretical load predictions. Bergh and Zwaan (refs. 5 and 6) investigated a complex correction matrix derived from oscillatory wind-tunnel pressure measurements and theoretical predictions. These authors assumed measurements were available only for a single mode, a steady angle of attack or an oscillatory pitching (or yawing) mode.

Current interest in using actively controlled aerodynamic surfaces to minimize aeroelastic response requires an improvement in accuracy in predicting unsteady aerodynamic characteristics of lifting surfaces equipped with control surfaces. The correction matrix provides one means of improving the accuracy but it requires experimental data on control surface characteristics in addition to the angle of attack characteristics of the surface. Hence, an extension of references 1 - 4 is necessary to obtain the correction matrix for more than one aerodynamic mode. Furthermore, the discrepancies between theory and experiment in predicting trailing-edge control surface loads are most likely caused by boundary-layer displacement effects on the effective downwash. Hence, another extension is necessary to obtain a postmultiplying correction matrix. These two extensions are considered in the present

development. The diagonal format has been retained* and complex pre- and postmultiplying correction matrices have been derived which satisfy the constraints of matching experimental data from multiple aerodynamic downwash modes.

The use of correction matrices is in the time-honored engineering tradition of empirical correction factors. It retains the generality of the theory while approaching the limiting values of the test results. Such a posteriori adjustment obviously cannot be regarded as addressing any of the fundamental causes of the discrepancies. Other possibilities exist whereby empirical corrections can be introduced directly into the theoretical solution. Ashley (ref. 7) has discussed two such "irrational correction methods". The first of these is of interest here and concerns the calculation of the downwash boundary condition and the pressure distribution by "local linearization" in terms of the local velocity V_L rather than the free stream velocity U_∞ . The dimensionless downwash then becomes

$$\frac{w}{U_\infty}(x,y,0,t) = \frac{1}{U_\infty} \left[\frac{\partial h}{\partial t} + V_L(x,y) \frac{\partial h}{\partial x} \right]$$

where $h(x,y,t)$ is the deflection of the mean surface. Applications of this "local linearization" to the downwash boundary condition (but not to the kernel function nor pressure coefficient) have been made for control surfaces by Ashley and Rowe (ref. 8) and by Rowe, Winther, and Redman (ref. 9), and improved correlations have been obtained. Tijdeman and Zwaan (ref. 10) have also employed the local linearization of the downwash boundary condition but have suggested another modification for use in the Doublet-Lattice Method for high subsonic flows, viz., that the free stream Mach number be replaced by a mean Mach number M_{j1} for each panel (lifting element or box). The downwash induced at box i by the lifting pressure on box j then becomes

* The format of a full matrix was briefly investigated but it was found to destroy the distributional character of the theoretical aerodynamic influence coefficients, and was not considered further.

$$\frac{w_i}{U_\infty} = D_{ij} (M_{j1}, k_r) \Delta C_{pj}$$

where $D_{ij} (M_{j1}, k_r)$ is the downwash influence coefficient between the j th lifting element and the i th downwash collocation point and its functional dependence on M_{j1} and the reduced frequency k_r is indicated. Tijdeman and Zwaan denote the freestream Mach number by M_∞ and the local Mach number at the surface of box i by M_{i2} , so that the locally linearized downwash for harmonic motion becomes

$$\frac{w_i}{U_\infty} = \frac{M_{i2}}{M_\infty} \frac{\partial h_i}{\partial x} + i \frac{\omega}{U_\infty} h_i$$

The values of M_1 and M_2 for a certain box are not equal, in general, because M_1 has to reflect the influence of the Mach number distribution normal to the surface ranging from M_2 at the surface to the freestream Mach number far away from the wing. Preliminary results from NLR calculations have shown that M_1 can be chosen simply to be the average value of M_2 and M_∞ .

LIST OF SYMBOLS

A	Matrix that gives pressures in terms of downwash. Inverse of D
a_∞	Speed of sound in the free stream
\tilde{a}	Constraining power of a constraint. If $\tilde{a} = 1$ constraint is 100% effective. If $\tilde{a} = 0$ constraint has no effect at all
B	Wing bending moment (about x-axis)
b/2	Semi span of wing
C	Aerodynamic coefficient (e.g. lift or moment coefficient). C_e is used as an experimental constraint
C_L	Lift coefficient
C_M	Moment coefficient
C_B	Wing root bending moment coefficient
\bar{c}	Reference chord length
c_l	Section lift coefficient
c_m	Section moment coefficient
c_h	Section hinge moment coefficient
D	Matrix that gives downwash (normalwash) in terms of pressures
h	Deflection normal to lifting surface
i_a	Unit vector in direction of axis
k_r	Reduced frequency $\frac{\omega \bar{c}}{2U_\infty}$
M_1	An average Mach Number between M_2 and M_∞

M_2	Local Mach Number at wing surface
M_∞	Free stream Mach Number
\bar{M}_∞	Average Mach Number between sending and receiving point
R	Compressible radius (see Eqn. 73)
S	Matrix that integrates pressures into aerodynamic parameters (e.g., C_L , C_M , c_ℓ , etc.)
S_p	[S] $[\Delta C_{p_t}]$ see Equation (9)
S_w	[S] [A][w] see Equation (30)
\bar{S}	See Equation (45)
\bar{S}	[S] $\begin{bmatrix} \phi' & 0 \\ 0 & I \end{bmatrix}$ See Equation (54)
S_p^*	See Equation (67)
T	Weights given to the correction factors $\bar{\epsilon}$ for the minimization process, $\sum T \bar{\epsilon}^2 = \min$
t	Time
U_∞	Free stream velocity
V_L	Local surface speed
W	Correction factor = $1 + \epsilon$ (Called CF in computer program)
w	Downwash (or normalwash) (Called W in computer program)
wT	Weights in the minimization process for estimates
x,y,z	Cartesian coordinates right handed system x aft, y lateral (starboard), z vertical
α	Angle-of-attack, also direction cosine for force or moment axis
B	$\sqrt{1 - M_\infty^2}$
γ	Direction cosine for force or moment axis

$\bar{\gamma}$	Dihedral of lifting surface
ΔC_p	Lower surface minus upper surface pressure coefficient
ΔA	Box area
ϵ	Incremental correction factors = $W - 1$
$\bar{\epsilon}$	Generalized incremental correction factors $\epsilon = \phi \bar{\epsilon}$
$\tilde{\epsilon}$	$\epsilon \sqrt{T}$
ϕ	Correction factor mode shapes
ϕ_d	Doublet potential function
ω	Circular Frequency

Subscripts and Superscripts

a	Stands for either p or w
d	Designated or known correction factors
e	Experimental
q	Identifies estimates as opposed to constraints
H	Hermetian transpose
mod.	Modified values
p	Identifies pressure modifying terms in the correction factor procedure
t	Theoretical values
u	Undesignated or unknown correction factors
w	Identifies downwash modifying terms
1	Deflection mode 1
2	Deflection mode 2
3/4	Three quarter chord point
1/4	One quarter chord point

Matrix Notation

{ }	Column Matrix
[]	Rectangular
[]	Diagonal

THEORETICAL DEVELOPMENT

Basic Method

Premultiplying Correction Factor Matrix. - A derivation of a real premultiplying correction matrix constrained to match aerodynamic data from a single downwash mode is presented in references 1 - 4. The use of Lagrange multipliers considerably simplifies the derivation so we present this alternative derivation here. As an introduction we will rederive the same case first, i.e., the premultiplier for a single mode; then we will consider multiple modes and the postmultiplier. Whether the correction matrix is real or complex depends only on the experimental data: static data lead to a real matrix and oscillatory data lead to a complex matrix.

Assume that we have a matrix $[A]$ of theoretical aerodynamic influence coefficients (AIC's) that relates the theoretical pressures $\{C_{p_t}\}$ on a set of aerodynamic finite elements to the dimensionless downwashes $\{w\}$ at the same aerodynamic elements by

$$\{\Delta C_{p_t}\} = [A] \{w\} \quad (1)$$

The AIC's correspond to the reduced frequency of the experimental data and, hence, are real for static data and complex for oscillatory data. The premultiplying correction matrix $[W_p]$ is used to obtain an estimate of the experimental pressure distribution $\{\Delta C_{p_e}\}$ from the theoretical distribution from

$$\{\Delta C_{p_e}\} = [W_p] \{\Delta C_{p_t}\} \quad (2)$$

The subscript p refers to modification of the pressure distribution. The experimental force distribution is usually not known from the test data but only the integrated force and moment coefficients $\{C_e\}$ are measured. An integration matrix $[S]$ relates the experimental force distribution to the measured force coefficients through;

$$\{C_e\} = [S] \{\Delta C_{p_e}\} \quad (3)$$

Combining equations (1) - (3) yields

$$\{C_e\} = [S] [W_p] [A] \{w\} \quad (4)$$

which is the equation to be solved for the correction matrix $[W_p]$ given all the remaining terms in the equation. The remaining terms are all known: $\{C_e\}$ and $\{w\}$ are obtained from the test data, and $[S]$ and $[A]$ are known from the mathematical model and the theoretical aerodynamic analysis of the configuration. In general, equation (4) is underdetermined, i.e., there are many more unknowns than equations. The method of least squares provides a solution. We require that changes in the theoretical load distribution shall be as uniform as possible or, in least-squares terminology, the weighted sum of the squares of the deviations shall be a minimum, where the deviation $\{\epsilon_p\}$ is defined as the difference between the correction factors and unity.

$$\{\epsilon_p\} = \{W_p - I\} \quad (5)$$

We denote the weighting function by T_p ; it will be discussed below. The weighted least-squares condition then becomes

$$\begin{aligned} \sum T_p \epsilon_p^2 &= \{\epsilon_p\}^H [T_p] \{\epsilon_p\} \\ &= \text{a minimum} \end{aligned} \quad (6)$$

where H denotes a Hermitian (complex conjugate) transpose. The Lagrange multipliers may be introduced by defining the error functional

$$f_p = (1/2) \{\epsilon_p\}^H [T_p] \{\epsilon_p\} \quad (7)$$

and rewriting the measured generalized force coefficients (the constraints) as

$$\begin{aligned}\{C_e\} &= [S] [1 + \epsilon_p] \{\Delta C_{p_t}\} \\ &= [S] \{\Delta C_{p_t}\} + [S] [\Delta C_{p_t}] \{\epsilon_p\}\end{aligned}$$

The term $[S] \{\Delta C_{p_t}\}$ is just the theoretical integrated pressures which are the theoretical coefficients, $\{C_t\}$. Thus

$$\{C_t\} = [S] \{\Delta C_{p_t}\} \quad (8)$$

Introducing also the following

$$[S_p] = [S] [\Delta C_{p_t}] \quad (9)$$

$$\{\Delta C_e\} = \{C_e\} - \{C_t\}$$

gives finally

$$\{\Delta C_e\} = [S_p] \{\epsilon_p\} \quad (10)$$

The variation of the error functional f_p is

$$\delta f_p = \{\epsilon_p\}^H [T_p] \{\delta \epsilon_p\} \quad (11)$$

and the variations of the incremental constraints, ΔC_e , given by equation (10) are

$$\{\delta \Delta C_e\} = [S_p] \{\delta \epsilon_p\} \quad (12)$$

$$= 0$$

The condition for the minimum subject to the constraints is then a linear combination of equations (11) and (12) set to zero in which the linear factors

are the Lagrange multipliers λ_p ,

$$\delta f_p + \{\lambda_p\}^H \{\delta \Delta C_e\} = 0 \quad (13)$$

Substituting equations (11) and (12) into equation (13) yields

$$(\{\epsilon_p\}^H [T_p] + \{\lambda_p\}^H [S_p]) \{\delta \epsilon_p\} = 0$$

Since the variation $\{\delta \epsilon_p\}$ is arbitrary,

$$\{\epsilon_p\}^H [T_p] + \{\lambda_p\}^H [S_p] = 0$$

or, after Hermitian transposition.

$$[T_p] \{\epsilon_p\} + [S_p]^H \{\lambda_p\} = 0 \quad (14)$$

The simultaneous solution of equations (5), (10) and (14) yields the desired solution. The simultaneous solution leads first to the Lagrange multipliers and then to ϵ_p as follows:

$$\{\lambda_p\} = -([S_p] [T_p]^{-1} [S_p]^H)^{-1} \{\Delta C_e\} \quad (15)$$

$$\{\epsilon_p\} = -[T_p]^{-1} [S_p]^H \{\lambda_p\} \quad (16)$$

and the correction factors are then

$$\{W_p\} = \{I\} + \{\epsilon_p\} \quad (17)$$

The premultiplying correction factors are written in a diagonal format for use in subsequent aeroelastic analyses as in equation (2).

The above results can be restated in summary form as follows:

$$\text{Solution of } \rightarrow \{\Delta C_e\} = [S_p] \{\epsilon_p\} \quad (18)$$

$$\text{subject to } \rightarrow \sum \epsilon_p^2 T_p = \min. \quad (19)$$

$$\text{is } \rightarrow \{\hat{\epsilon}\} = [\tilde{S}_p]^H ([\tilde{S}_p][\tilde{S}_p]^H)^{-1} \{\Delta C_e\} \quad (20)$$

$$\text{where } [\tilde{S}_p] = [S_p] [\sqrt{T_p}]^{-1} \quad (21)$$

$$\text{and } \{\epsilon_p\} = \{\hat{\epsilon}\} / \sqrt{T_p} \quad (22)$$

The weighting function T_p is arbitrary; the only requirement on it is that it should be positive. However, engineering judgment provides some guidance: if only a single constraint, e.g., the lift curve slope, is available, one would prefer all the correction factors to be simply the ratio of its experimental value to its theoretical estimate. Accordingly, the recommended choice for the weighting function for the premultiplier is

$$\{T_p\} = |[A] \{I\}| \quad (23)$$

However, other choices may be deserving of further investigation:

Multiple Modes. - We next consider multiple experimental downwash modes. The derivation will be presented using two modes $\{w_1\}$ and $\{w_2\}$. For these two modes, the theoretical pressure distributions are

$$\{\Delta C_{p_{t1}}\} = [A] \{w_1\}$$

$$\{\Delta C_{p_{t2}}\} = [A] \{w_2\}$$

so the incremental experimental force coefficients ΔC_{e_1} and ΔC_{e_2} become

$$\begin{aligned} \{\Delta C_{e_1}\} &= \{C_e\} - [S] [\Delta C_{p_{t1}}] \{W_p\} \\ &\equiv \{C_e\} - [S_{p1}] \{W_p\} \end{aligned} \quad (24)$$

$$\begin{aligned} \{\Delta C_{e2}\} &= \{C_e\} - [S] \begin{bmatrix} \Delta C_{p1} \\ \Delta C_{p2} \end{bmatrix} \{W_p\} \\ &\equiv \{C_e\} - [S_{p2}] \{W_p\} \end{aligned} \quad \text{(Continued)(24)}$$

These two equations may be combined into one set as follows:

$$\{\Delta C_e\} = [S_p] \{\epsilon_p\} \quad (25)$$

where

$$\{\Delta C_e\} = \begin{Bmatrix} \Delta C_{e1} \\ \Delta C_{e2} \end{Bmatrix}$$

and

$$[S_p] = \begin{bmatrix} S_{p1} & \\ & S_{p2} \end{bmatrix} \quad (26)$$

If again we impose the minimization condition

$$\sum \epsilon_p^2 T_p = \min \quad (27)$$

then the solution is identical to equation (20) since equations (25) and (27) are identical to (18) and (19).

Postmultiplying Correction Factor Matrix. - Now we consider the postmultiplying correction matrix. It is only necessary to consider a single downwash mode; the multiple mode case can be generalized by reference to equations (25) and (26). Since the postmultiplier modifies the downwash mode it defines an effective experimental downwash given by

$$\{w_e\} = [W_w] \{w\}$$

in which the subscript w refers to modification of the downwash. Our new estimate of the experimental pressure distribution becomes:

$$\begin{aligned}
\{\Delta C_{p_e}\} &= [A] \{w_e\} \\
&= [A] [W_w] \{w\}
\end{aligned}
\tag{28}$$

The experimental generalized forces or force coefficients are again given by equation (3) which with equation (28) becomes

$$\begin{aligned}
\{C_e\} &= [S] [A] [1+\epsilon_w] \{w\} \\
&= [S] \{\Delta C_{p_t}\} + [S] [A] [w] \{\epsilon_w\}
\end{aligned}
\tag{29}$$

And again noting that $[S] \{\Delta C_{p_t}\} = \{C_t\}$ and introducing

$$[S_w] = [S] [A] [w] \tag{30}$$

gives

$$\{C_e\} - \{C_t\} = [S_w] \{\epsilon_w\}$$

or since

$$\{C_e\} - \{C_t\} = \{\Delta C_e\}$$

$$\{\Delta C_e\} = [S_w] \{\epsilon_w\} \tag{31}$$

Again the minimization condition is imposed,

$$\sum \epsilon_w^2 T_w = \min. \tag{32}$$

The solution for ϵ_w is then identical to equation (20) since equations (31) and (32) are identical to equations (18) and (19). Again the correction factors are calculated from ϵ_w as follows:

$$\{W_w\} = \{I\} + \{\epsilon_w\} \tag{33}$$

The weighting function T_w is also arbitrary. However, the considerations that led to the recommendation of equation (23), in the premultiplying case, also lead to

$$\{T_w\} = | \{I\}^T [A] | \quad (34)$$

which is to say that the weighting function is the lift coefficient induced by a unit downwash at each lifting element. Equation (34) is the recommended choice for the weighting function in the postmultiplying case, although other choices may still warrant further investigation.

For multiple modes, say two, equations (31) and (32) provide the following:

$$\{\Delta C_{e_1}\} = [S_{w_1}] \{\epsilon_w\} \quad (35)$$

$$\{\Delta C_{e_2}\} = [S_{w_2}] \{\epsilon_w\} \quad (36)$$

$$\sum \epsilon_w^2 T_w = \min \quad (37)$$

Again equations (35) and (36) can be combined into one as follows:

$$\{\Delta C_e\} = [S_w] \{\epsilon_w\} \quad (38)$$

where

$$\{\Delta C_e\} = \begin{Bmatrix} \Delta C_{e_1} \\ - \\ \Delta C_{e_2} \end{Bmatrix}$$

and where

$$[S_w] = \begin{bmatrix} S_{w_1} & \\ & S_{w_2} \end{bmatrix} \quad (39)$$

Equations (38) and (37) are now identical to equations (18) and (19) respectively and thus the solution is the same as before, i.e., equation (20).

Modifications to the Basic Method

In some instances correction factors become unrealistic. In order to correct this situation when it occurs or to minimize the probability of its occurrence initially, various modifications can be introduced. Three such modifications are discussed here, i.e., estimates, correction factor modes and limits. Estimates are like constraints except that the "constraining power" can be varied. Correction factor modes constrain the distribution of correction factors such that the final distribution is a superposition of a limited set of well behaved, user input mode shapes. The "limit" feature constrains the correction factors (or any subset of them) to be above a given minimum and below a given maximum.

Estimates. - In some instances data will be available in the form of estimates. These estimates can be based on past data, data from related configurations, two-dimensional data, empirical methods, or just past experience. In any case they do not have equal weight with the experimental data considered so far. Consider the case where some experimental data are available, leading to $\{\Delta C_e\}$, then the usual equation applies to these data:

$$\{\Delta C_e\} = [S_a] \{\epsilon_a\}$$

where the subscript "a" stands for either p or w. If estimates exist, leading to $\{\Delta C_g\}$, then it is desirable to minimize the difference between these estimates and the modified theoretical values. Let this difference be termed $\{\epsilon_g\}$, then:

$$\{\Delta C_g\} = [S_g] \{\epsilon_a\} + \{\epsilon_g\}$$

where $\{\Delta C_g\} = \{C_g - C_t\}$ and S_g is analogous to S_a with the exception that it refers to the estimates C_g and not the constraints C_e . Thus we wish to minimize both $\{\epsilon_a\}$ and $\{\epsilon_g\}$ together and this is done as follows:

$$\begin{Bmatrix} \Delta C_e \\ \Delta C_g \end{Bmatrix} = \begin{bmatrix} S_a & | & 0 \\ \hline S_g & | & I \end{bmatrix} \begin{Bmatrix} \epsilon_a \\ \epsilon_g \end{Bmatrix}$$

This equation can then be solved in the usual manner producing the following result:

$$\sum T\epsilon_a^2 + \sum \epsilon_g^2 = \min$$

If it is desired to give the ϵ_g values more or less weight in the minimization scheme, then the ϵ_g values must be weighted.

$$\sum T\epsilon_a^2 + \sum (wT \epsilon_g)^2 = \min. \quad (40)$$

The equations for the constraints then become

$$\begin{Bmatrix} \Delta C_e \\ \Delta C_g \end{Bmatrix} = \begin{bmatrix} S_a & | & 0 \\ \hline S_g & | & \frac{1}{wT} \end{bmatrix} \begin{Bmatrix} \epsilon_a \\ \epsilon_{wT} \end{Bmatrix} \quad (41)$$

where

$$\{\epsilon_{wT}\} = [wT] \{\epsilon_g\} \quad (42)$$

and where the values wT are the weights assigned to the errors ϵ_g . If the estimates are of high quality then the weights will be large. In the limit as $wT \rightarrow \infty$, ΔC_g becomes a constraint instead of an estimate and equation (41) reduces to the form of equation (18). Equation (41) can also be cast into the same form as equation (18) for the general case, i.e., wT finite, as follows:

$$\{\Delta C_e\} = [\bar{S}] \{\epsilon\} \quad (43)$$

with

$$\{\Delta C_e\} = \begin{Bmatrix} \Delta C_e \\ - \\ \Delta C_g \end{Bmatrix} \quad (44)$$

$$[\bar{S}] = \begin{bmatrix} S_a & | & 0 \\ -a & | & - \\ S_g & | & \frac{1}{wT} \end{bmatrix} \quad (45)$$

$$\{\epsilon\} = \begin{Bmatrix} \epsilon_a \\ - \\ \epsilon_{wT} \end{Bmatrix} \quad (46)$$

Equation (40) can be written in terms of ϵ as:

$$\sum T^* \epsilon^2 = \min \quad (47)$$

where

$$T^* = \begin{cases} T & \text{for constraints} \\ \frac{1}{(wT)^2} & \text{for estimates} \end{cases}$$

Thus equation (43) and (47) are formally identical to equation (18) and (19) and thus have the same solution, i.e., equation (20).

Currently the term $\frac{1}{wT}$ is obtained from a term \tilde{a} where

$$\frac{1}{wT} = \frac{1-\tilde{a}}{\tilde{a}} \quad (48)$$

$$10^{-4} \leq \tilde{a} \leq 1.0$$

where \tilde{a} is called the constraining power of the estimate C_g .

Correction Factor Modes. - The correction factors can be expressed in terms of a set of modes ϕ as follows:

$$\{\epsilon\} = [\phi] \{\bar{\epsilon}\} \quad (49)$$

Placing equation (49) into (43) gives

$$\begin{aligned} \{\Delta C_e\} &= [\bar{S}] [\phi] \{\bar{\epsilon}\} \\ &= [\bar{S}] \{\bar{\epsilon}\} \end{aligned} \quad (50)$$

where

$$[\bar{S}] = [\bar{S}] [\phi] \quad (51)$$

If the minimization process is applied to $\bar{\epsilon}$ as usual

$$\sum \bar{\epsilon}^2 = \min \quad (52)$$

Here the weight T is missing since it is usually not used with modes. Equations (50) and (52) are then identical to equations (18) and (19) and thus have the same solution, i.e., equation (20). A similar expression exists for the postmultiplying correction factors. This approach allows a bias based on experience and past tests and physical reasoning, to be built into the correction factors. When estimates are considered equation (50) must be altered since the ϵ_{wT} are not fitted with correction factor modes. Thus

$$\{\epsilon\} = \begin{Bmatrix} \epsilon_a \\ \epsilon_{wT} \end{Bmatrix} = \begin{bmatrix} \phi & | & 0 \\ 0 & | & I \end{bmatrix} \begin{Bmatrix} \bar{\epsilon}_a \\ \epsilon_{wT} \end{Bmatrix} \quad (53)$$

and thus

$$[\bar{S}] = [\bar{S}] \begin{bmatrix} \phi & | & 0 \\ 0 & | & I \end{bmatrix} \quad (54)$$

and then the solution proceeds as before.

Limits. - If certain basic properties of the weight factors are known, they could be limited to fall within a given set of bounds. If for instance the sign of an incremental weight factor is known to be positive, then it could be constrained to be positive. Also, for practical reasons, the maximum value of the weight factors should be limited and thus the incremental weight factors are constrained to lie below this maximum. In general, the weight factors can be constrained to lie between a maximum and a minimum.

$$\bar{\epsilon}_{\min} \leq \bar{\epsilon} \leq \bar{\epsilon}_{\max} \quad (55)$$

Notice that the generalized incremental correction factors, $\bar{\epsilon}$, are the ones limited in the solution and not the actual ones, ϵ . The values of $\bar{\epsilon}$ are the coefficients of the correction factor modes, ϕ , and not the incremental correction factors themselves.

The basic procedure would be to set any generalized incremental weight factor to its maximum or minimum value if it exceeded these limits. This would require a multistep operation: (1) solving for the factors, (2) checking and setting those that exceeded the limits to the limit values, and (3) resolving. Before this can be done a capability must exist for assigning weight factors special values. This is easily accomplished as follows:

$$\{\Delta C_e\} = [\bar{S}_u | \bar{S}_d] \begin{Bmatrix} \bar{\epsilon}_u \\ \bar{\epsilon}_d \end{Bmatrix} \quad (56)$$

where $[\bar{S}]$ is defined in equation (51). The subscript u indicates those factors that are undesignated and d indicates those that are designated. This equation can be solved for $\{\epsilon_u\}$ in terms of the known quantities:

$$\{\Delta C_e\} - [\bar{S}_d] \{\bar{\epsilon}_d\} = [\bar{S}_u] \{\bar{\epsilon}_u\} \quad (57)$$

Equation (57) effectively eliminates the designated factors from the minimi-

zation process. This equation can then be solved in the usual manner for $\{\bar{\epsilon}_u\}$ since $\{\bar{\epsilon}_d\}$ is given. Specifically

$$\{\Delta C_{e_{\text{mod}}}\} = [\bar{S}_u] \{\bar{\epsilon}_u\} \quad (58)$$

where

$$\{\Delta C_{e_{\text{mod}}}\} = \{\Delta C_e\} - [\bar{S}_d] \{\bar{\epsilon}_d\} \quad (59)$$

The minimization scheme is then

$$\sum T^* \bar{\epsilon}_u^2 = \min \quad (60)$$

Equations (58) and (60) are now formally identical to equations (18) and (19) and thus the solution is identical to equation (20). In the computer program the final $\bar{\epsilon}$ array that are modified or have reached their limits, is called $\bar{\bar{\epsilon}}$.

A New Postmultiplying Correction Factor Matrix

The postmultiplying correction factor matrix developed in a previous section has been applied successfully to wings operating in pitch. Problems arise however when control surface modes are used. The discussion to be presented in the "Correlation Studies" section describes some of these problems. As a result of these, a new postmultiplying correction factor matrix was developed and it is derived here.

Viscous effects on airfoils can be thought of in terms of a displacement thickness added to the airfoil. The difference between the upper and lower surface displacement thicknesses produces a "decambering" of the airfoil or a change in the downwash w .

$$w_e = w + \delta w \quad (61)$$

The changes in downwash, δw , exist over the entire airfoil or wing and not just in the region where w is non zero. These changes are a function of the pressure distribution on the airfoil. Usually the displacement thickness at a point is an integral function of the pressure distribution upstream of that point. If the general case of correction factor mode shapes is assumed then the downwash correction δw can be expressed as:

$$\{\delta w\} = [\phi] \{\delta \bar{e}\} \quad (62)$$

where $\{\delta \bar{e}\}$ is proportional to the integrated pressures, $[\ell]$.

$$\{\delta \bar{e}\} = [\ell] \{\bar{\epsilon}\} \quad (63)$$

where $[\ell]$ is given in terms of an integration matrix $[N]$ and the pressures $\{\Delta C_p\}$.

$$\{\ell\} = [N] \{\Delta C_p\} \quad (64)$$

Combining equations (63) with (62) and using the result to obtain the corrected pressures leads to

$$\begin{aligned} \{\Delta C_{p_e}\} &= [A] \{w_e\} \\ &= [A] \{w + [\phi] [\ell] \{\bar{\epsilon}\}\} \end{aligned} \quad (65)$$

The constraints $\{C_e\}$ are obtained by integrating $\{\Delta C_{p_e}\}$ as follows:

$$\begin{aligned} \{C_e\} &= [S] \{\Delta C_{p_e}\} \\ &= [S] \{\Delta C_{p_t}\} + [S_p^*] \{\epsilon_w\} \end{aligned} \quad (66)$$

where

$$[S_p^*] = [S] [A] [\phi] [\ell] \quad (67)$$

Noting that $\{\Delta C_e\} = \{C_e\} - \{C_t\}$ equation (65) can be written as:

$$\{\Delta C_e\} = [S_p^*] \{\epsilon_w\} \quad (68)$$

Equation (68) has a form identical to that of equation (18) except $[S_p]$ is replaced by $[S_p^*]$ and thus has the same solution, i.e., equation (20). Once found, $\{\epsilon_w\}$ can be placed into the expression for $\{\Delta C_{p_e}\}$, in equation (65), and the desired modified pressure found.

Currently in the computer program the matrix $[N]$ is simply either the identity matrix or the matrix $[\phi]^T$. The identity matrix implies that the correction to the downwash is proportional to the local lifting pressure. In addition the above derivation is good for only one mode and thus the multiple mode option can not be used with the new postmultiplier. The new postmultiplier can be extended to multiple modes by simply replacing

$$\{\Delta C_e\} \text{ with } \begin{Bmatrix} \Delta C_{e_1} \\ -1 \\ \Delta C_{e_2} \end{Bmatrix} \quad (69)$$

and

$$[S_p^*] \text{ with } \begin{bmatrix} S_{p_1}^* \\ S_{p_2}^* \end{bmatrix} \quad (70)$$

but this has not yet been tried.

Transonic Effects Using Local Mach Number

Empirical modification of theory is most meaningful if the theory qualitatively matches experimental data. If the theory misses an important feature of the data the modified theory will also usually miss it. Transonic effects fall in this category. The classic lifting surface theory makes no provision for transonic effects and it is the purpose of this section to investigate some simple modifications to help remedy this situation.

Direct Application of Local Mach Number. - Several methods based on the steady local Mach Number distribution have been tried and the results are discussed in later sections.

One of these methods, discussed in the Introduction, consists of making a simple substitution of a local Mach Number distribution in place of its free stream value both in the kernel function and in the boundary conditions and pressure equation (see refs. 7 and 10). The local Mach Number distribution is taken from steady flow results. For the kernel function, application of a Mach Number distribution that lies somewhere in between the surface values and the free stream value was used. Tijdeman and Zwaan (ref. 10) suggest a local Mach Number distribution that lies half way in between the actual local and the free stream values. The reason for this is that acoustic signals propagate to the surface along various paths out in the fluid and thus propagate at some average between the surface value and free stream value. For the kernel, the local receiving point value of Mach Number and the free stream values were averaged and used in place of the free stream value.

For the normalwash boundary condition and pressure evaluation the local Mach Number on the surface was used. Specifically, if $M_2(x)$ is the local surface steady Mach Number distribution then the normalwash boundary condition w is (see ref. 10):

$$\frac{w}{U_\infty} = \frac{M_2(x)}{M_\infty} \frac{\partial h}{\partial x} + i \frac{\omega}{U_\infty} h \quad (71)$$

The second order Bernoulli Equation for steady flow is (see ref. 7):

$$\Delta C_{p_{so}} = \Delta C_p \left[1 + \beta^2 \left(\frac{M_2(x)}{M_\infty} - 1 \right) \right] \quad (72)$$

where ΔC_p and $\Delta C_{p_{so}}$ are the first and second order pressures respectively. This method did not prove to be all that was hoped for and thus a second method was investigated.

A New Transonic Effects Method. - In this section a derivation of the newly developed Douglas transonic effects method is presented. The basic method was conceived under the McDonnell-Douglas IRAD program however its implementation in two-dimensions and its application to the airfoil-control surface problem was done under the current contract.

The lifting surface method is based on the following expression for the potential of a doublet, ϕ_d :

$$\phi_d = \frac{\partial}{\partial n} \left\{ \frac{e^{i\omega t} e^{i\lambda[M_\infty(x-\xi)-R]}}{R} \right\} \quad (73)$$

where

$$\lambda = \frac{\omega M_\infty}{\beta^2 U_\infty}, \quad R = \sqrt{(x-\xi)^2 + \beta^2 r^2}$$

and n is the direction normal to the lifting surface. This expression can be rewritten as:

$$\phi_d = \frac{\partial}{\partial n} \left\{ \frac{e^{i\omega(t-\tau)}}{R} \right\} \quad (74)$$

where

$$\tau = \frac{M_\infty}{\beta^2 U_\infty} [R - M_\infty(x-\xi)] \quad (75)$$

It can be shown that τ has a physical significance. The term τ is the acoustic time delay between the sending and receiving points. That is, τ is the time it takes an acoustic signal, originating at the point ξ, η, ζ to reach the point x, y, z as the acoustic pulse washes downstream.

This statement can be illustrated by the example of figure 1.

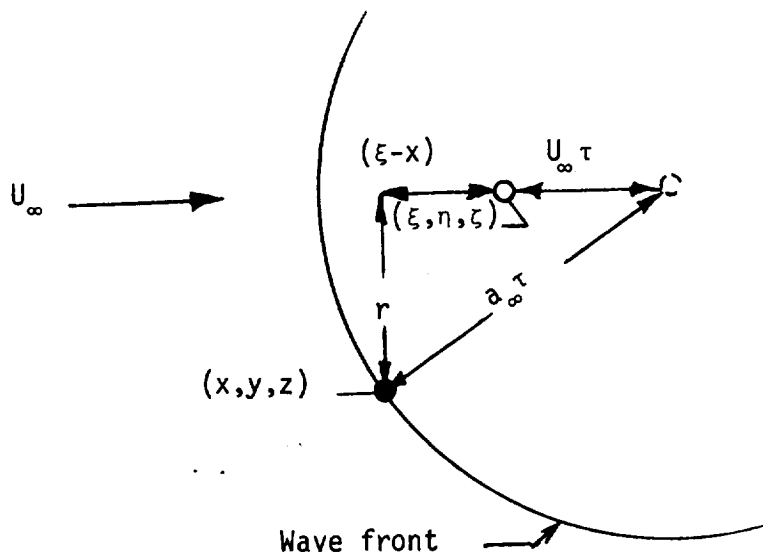


Figure 1

A signal is emitted at (ξ, η, ζ) at time $\tau = 0$. At time τ the wave front, traveling at the speed of sound, a_∞ , has reached the receiving point at (x, y, z) . During this time the wave center has travelled a distance $U_\infty \tau$. Using the right triangle relations gives:

$$r^2 + (\xi - x + U_\infty \tau)^2 = a_\infty^2 \tau^2 \quad (76)$$

Solving for τ using the solution for a quadratic equation gives:

$$\tau = \frac{M_\infty}{U_\infty \beta^2} (M_\infty (\xi - x) + R)$$

which is exactly what is given in equation 75.

Thus τ in the expression for ϕ_d has physical significance and it is the acoustic time delay between the sending and receiving points in a fluid moving with uniform velocity. This physical insight can form the basis of a correction factor for the theory. For instance if the wave is in a flow field whose velocity varies in the longitudinal direction then the distance d travelled by the wave center is not $U_\infty \tau$ but is:

$$d = \int_0^\tau U(t) dt \quad (77)$$

If we consider $U(t)$ to be made up of $U_\infty + \delta U(t)$ then d also can be so split.

$$d = U_\infty \tau + \delta d \quad (78)$$

$$\delta d = \int_0^\tau \delta U(t) dt \quad (79)$$

The wave center velocity U is being discussed, however this is not the velocity of the fluid particle located at the wave center as is the case for a uniform flow. The velocity U actually reflects the wave front speed and location and is the speed of an imagined wave center for the wave that strikes the receiving point. The wave front speed varies around the circumference of the wave, but the most important part of the wave is that part that strikes the receiving point. Thus the velocity $U(t)$ is the time history of the wave center corresponding to that part of the wave that strikes the receiving point (x, y, z) . As an approximation to the location of this part of the wave, it is assumed that it lies along a line connecting the receiving and sending points (shown dotted in figure 2). Thus δU is the difference between the local velocity and the free stream velocity along the dotted line. If a

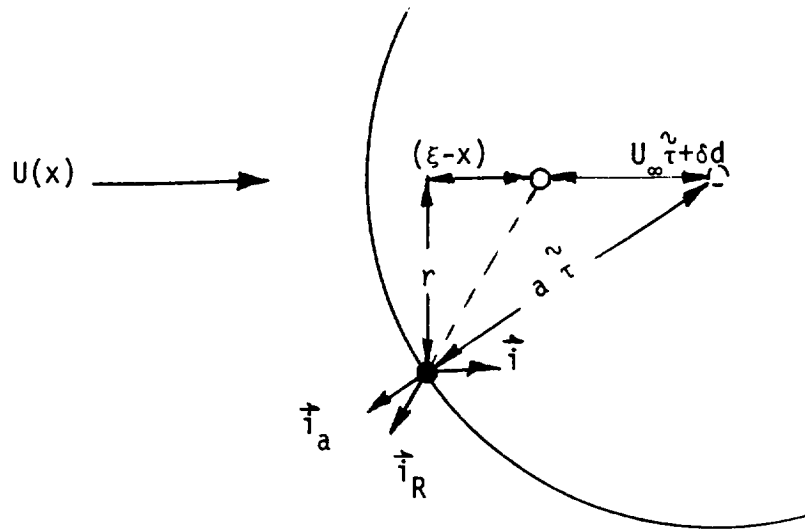


Figure 2

coordinate \bar{R} is defined lying along this line then the integral in time of equation (79) can be converted into a space integral in \bar{R} as follows:

$$\delta d = \int_0^R \delta U(\bar{R}) \frac{dt}{d\bar{R}} d\bar{R}$$

where \bar{R} is defined below equation (73) and where $\frac{d\bar{R}}{dt}$ is the speed with which the wave front moves along the radial coordinate.

$$\frac{d\bar{R}}{dt} = (a_{\infty} \vec{i}_a + U(\bar{R}) \vec{i}) \cdot \vec{i}_R$$

The unit vectors \vec{i}_a , \vec{i} and \vec{i}_R are defined in figure 2.

For example, in the two-dimensional analysis for coplanar surfaces:

$$\delta d = \int_x^\xi \Delta U \frac{dt}{d\bar{x}} d\bar{x}$$

$$\frac{d\bar{x}}{dt} = a - U(\bar{x}) \quad (80)$$

Thus

$$\delta d = \int_\xi^x \frac{M(\bar{x}) - U_\infty/a}{1 - M(\bar{x})} d\bar{x} \quad (81)$$

where $M(\bar{x})$ is the local Mach Number distribution. As an approximation set $U_\infty/a = U_\infty/a_\infty = M_\infty$.

The time $\tilde{\tau}$ can now be calculated using the right-triangle relations and the quadratic formula solution.

$$[U_\infty \tilde{\tau} + \delta d + \xi - x]^2 + r^2 = a_\infty^2 \tilde{\tau}^2$$

Solving for $\tilde{\tau}$ gives:

$$\tilde{\tau} = \frac{M_\infty}{U_\infty \beta^2} \{M_\infty(\xi - \tilde{x}) + \tilde{R}\} \quad (82)$$

where

$$\tilde{R}^2 = (\xi - \tilde{x})^2 + \beta^2 r^2 \quad (83)$$

$$\tilde{x} = x - \delta d \quad (84)$$

It is immediately evident that $\tilde{\tau}$ has exactly the same form as τ (see equation (75)) except that x is replaced, in the expression for τ , by $x - \delta d$ in the expression for $\tilde{\tau}$. In essence then the receiving and sending points

have increased their separation (in the x-direction) as far as the acoustic time delay τ is concerned. Is there any reason to carry this increase in distance to other parts of the potential function, specifically, to the radius term in the denominator? It seems so. First, this radial distance is already modified in the expression for $\tilde{\tau}$, see equation (82). Second it is known that transonic effects exist in steady flow ($\omega = 0$) where τ has no effect; i.e., $\phi_d = \frac{\partial}{\partial n} (1/R)$. Thus it seems appropriate to add $-\delta d$ to all $x - \xi$ terms. Thus

$$\tilde{\phi}_d(x - \xi, y - \eta, z - \zeta, \omega, M_\infty) = \phi_d(x - \xi - \delta d, y - \eta, z - \zeta, \omega, M_\infty) \quad (85)$$

where $\tilde{\phi}_d$ is the potential modified for transonic effects.

This method has been implemented for the two-dimensional case and the results are discussed subsequently.

One variation of this method that is possible is to use an average Mach Number between sending and receiving points and define δU as the difference between the local value of velocity and this average. Thus the term M_∞ is replaced with \bar{M}_∞ where

$$\bar{M}_\infty = \frac{1}{(x-\xi)} \int_{\xi}^x M(\bar{x}) dx \quad (86)$$

This method has also been tried and results using this variation are also discussed subsequently.

A final consideration is the determination of the local Mach Number distribution, $M(\bar{x})$. Tijdeman and Zwaan (ref. 10) note that the local surface Mach Number distribution should not be used but that some average between it and the free stream Mach Number should be used. This is because the signal arriving at a point has traveled both in the vicinity of the airfoil and out in the flow field. The recommendation of Tijdeman and Zwaan has been adopted in the present method.

Other work by Tijdeman and Bergh (ref. 11) can also be brought to bear on this work. Specifically a fully two-dimensional acoustic solution of a source pulse located at the control surface hinge was calculated for the case of a nonuniform flow field. This solution produced the exact time lag $\tilde{\tau}$ from the hinge line to all other points on the airfoil. The equivalent distance \tilde{x} , and also \tilde{R} , from the hinge line to the receiving point can then be calculated using this information and the equation relating $\tilde{\tau}$ to \tilde{x} . Thus

$$\xi - \tilde{x} = \sqrt{\tilde{\tau}^2 U_\infty^2 \beta^2 - r^2}$$

If acoustic solutions were obtained for all other sending points then all the necessary \tilde{x} for this theory would be available. This method would be accurate, however it would require many expensive acoustic solutions. It appears that each of these solutions requires a computing effort comparable to a direct solution, by finite difference, of the original problem. This conclusion however, remains to be seen and further study is required.

CORRELATION STUDIES

Local Mach Number Studies

Several methods of accounting for local steady Mach Number variations in the oscillatory lifting surface theory have been studied for the two-dimensional case. A mathematical description of these methods has been presented in the Theoretical Development section. The cases considered here are for a two-dimensional symmetric airfoil (NACA 65A006) with an oscillating 25% chord flap. The local Mach Number variations over the airfoil at zero angle of attack are given in reference 11.

The first and simplest of the methods studied involves simply making a direct substitution of the steady local Mach Number in place of its free stream value. In general, this approach does not produce substantial changes in the pressures from their classical values.

In figure 3 the symbols marked by triangles indicate the pressures calculated using the local Mach Number in the downwash boundary condition. The pressures are reduced from their classical values (indicated by dots and a dashed line) as expected, but not by very much.

The circles indicate the pressures calculated using the local Mach Number in the downwash as well as in the kernel function. In the kernel function the average between the local receiving point Mach Number and the free stream value is used. The pressures again are generally reduced but not by any substantial amount.

The use of local Mach Number in the second order Bernoulli equation (Ashley, ref. 7) also produces very little change. In figure 5 this change is observed as the difference between the circles and triangles. This change is about the same order of magnitude as the other changes except it is generally in the opposite direction.

The second method studied is new and is described in the Theoretical

Development section. The basic idea of this method is to transform the longitudinal distance between sending and receiving points depending on the time it takes an acoustic signal to travel that distance. A variation of this method is simply to replace the free stream Mach Number, M_∞ , by \bar{M}_∞ , an integrated average of the Mach Number distribution between sending element and receiving point defined in equation (86).

On the face of it the new method gives the best correlation when M_∞ and not \bar{M}_∞ is used. Figure 4 presents a comparison between the two methods at a Mach Number of 0.875. Near the leading edge the basic method designated "Present Method (M_∞)" and indicated by triangles produces the best agreement between experiment and calculation. Near the position of the steady shock wave however the peak pressure is better predicted by the variation of the basic method designated "Present Method (\bar{M}_∞)" and indicated by circles. The location of the calculated peak is slightly forward of the experimentally observed peak. Either method, however, is better than the classic theory (indicated by dots) for predicting pressures as comparisons with experimental data shown.

Two features of the experimental pressure distribution illustrate transonic effects. One of these is the reduced leading edge pressure levels, and a second is the bump or peak in pressure near the location of the steady shock wave location. The new method qualitatively reproduces these features. However there is reason to suspect that the basic version of the new method (triangle) under-predicts the leading edge pressure. The reason for this lies in the fact that, even though the calculated and experimental pressures agree near the leading edge, viscous effects have not yet been accounted for and these effects reduce the calculated loads even further. A drop in the leading edge loading caused by application of viscous effects to the (\bar{M}_∞) variation of the basic method (circles), renders this method more acceptable than before. However these effects are not large enough to bring the calculated pressures in line with the experimental values (see fig. 38). Further study is required in this area to decide which method is best or to discover other more accurate variations of the basic method.

The application of the new transonic method to a lower Mach Number, (0.85), is shown in figure 5. The agreement is good near the leading edge but only a slight indication of the shock bump is given by the theory. Also shown in this figure is the effect of local Mach Number on the Bernoulli equation (see equation (72)). The difference between the circles and triangles indicates this effect.

All applications thus far have been for the steady case. Figure 6 presents a comparison of the Present Method (new transonic theory) for the case of the control surface oscillating at a reduced frequency $k_r = \frac{\omega C}{2U_\infty} = 0.059$. Also shown in this figure is a calculation done using the Traci et al method (ref. 12) and a calculation done using the classic theory. The finite element theory of Traci et al predicts the bump at the shock wave fairly accurately however is not as good as the Present Method elsewhere. One part of the pressure distribution that does not seem to be predicted by any of the theories is the depth of the dip in pressure behind the shock.

Figure 7 presents a comparison similar to that in Figure 6 but at a lower Mach Number (0.85). Also instead of in phase (Real) and out of phase (Imaginary) parts given, amplitude $\Delta C_p = \sqrt{(\text{Re}\Delta C_p)^2 + (\text{Im}\Delta C_p)^2}$ and phase angle $= \tan^{-1} (\text{Im}\Delta C_p / \text{Re}\Delta C_p)$ are presented. Again, as in the steady case the bump at the shock is barely noticeable in the Present Method and of course absent altogether in the classic theory.

Figure 8 presents a comparison of the Present Method, classic theory and experimental data for a case similar to that presented in figure 7 except that the Mach Number is 0.875 and the reduced frequency, $k_r = 0.176$. Again pressure amplitude and phase angle are shown. The two variations of the Present Method are in better agreement with the experimentally obtained pressure amplitudes than is the classic theory. However the same can not be said of the phase angles. The Present Method follows the experimental phase angle curve from about the 40% chord on to the trailing edge. However none of the theories follows the curve forward of that point. Tijdeman and Bergh (ref. 11) present a modified phase angle curve based on a full two-dimensional

acoustic solution of a pulse located at the control surface leading edge (see section on New Transonic Effects Method). This approach gives very good agreement with the experimental phase angle data (see figure 31 of reference 11). The correction was applied only to the phase angles and not the pressure amplitudes. The calculated phase angle was simply corrected using the additional time lag over and above that experienced in uniform flow. This additional phase lag was not used internal to the theory but applied after the theoretical calculation was completed. The section of this report entitled "A New Transonic Effects Method" describes how this acoustic type of information can be used internally with the theory so that the pressure amplitudes are also effected. This approach has not yet been tried.

A possible explanation of the phase angle differences between theory and experiment might be due to the fact that signal fronts, which emanated from the control surface, do not exactly travel normal to the flow as assumed in the Present Method. Tijdeman and Bergh have shown that the wave fronts are actually inclined to the flow to a considerable degree, within the supersonic zone. This being the case the wave fronts impinge on the forward part of the airfoil (forward of the shock wave) with very little longitudinal time delay. This would explain the flattening of the phase angle curve in front of the shock.

Thus far detailed pressure distributions have been discussed. Attention is now focused on the forces and moments these pressures produce. Figures 9 through 12 present comparisons of the present method with the classic theory and experimental data. In figure 9 the Traci, Farr, Albano theory is also plotted. This figure shows that the Present Method (M_∞) is in better agreement with the data than is the classic method. As expected the Present Method and classic theory tend to coalesce at low Mach Numbers, out of the transonic region. The transonic peak lift, predicted by the Present Method, occurs earlier, as Mach Number is increased, than does the experimental data. Also the dip occurring after this peak is not nearly as deep as shown by the experimental data.

Both theories show values of lift coefficient that are higher than the

experimental values. This is due to reduced flap effectivity caused by the viscous boundary layers.

Figure 10 presents a comparison similar to the previous figure except that pitching and hinge moment coefficients are considered. Of particular note is the over prediction of hinge moment by both theories. Again this is due to viscous effects on the flap.

The last two figures have dealt with force and moment coefficients in steady flow for an airfoil with a deflected flap. Figures 11 and 12 present the same data for the oscillatory case. (The reduced frequency varies from 0.098 at $M_\infty = 0.5$ to 0.057 at $M_\infty = 0.901$ in these figures.) Generally speaking the same trends and conclusions hold for these figures as for the previous two figures.

Subsonic Cases

Oscillating Wing with Control Surface. - Extensive low speed wind tunnel measurements of static and oscillatory pressure data have been made by Hertrich (refs. 14 and 15) on straight and swept wings with a full span control surface. The wings had no taper and the control surface had a 30% chord; two aspect ratios, 2.5 and 3.1, were tested by changing the exposed span in the tunnel. The swept wings had a sweep angle of 25° . A later oscillatory test of the swept wing was made by Förshing, Triebstein, and Wagener (ref. 16) in which the full span control surface was split approximately in half (the inboard flap had 46.59% of the span) and the aspect ratio was set at 2.94.

The pressure data from the first tests (refs. 14 and 15) were integrated by Hertrich to obtain lift and moment coefficients and the static values for the swept wing with aspect ratio 3.1 have been used here as constraints to determine correction factors. The static values corrected for wind-tunnel wall interference are: lift curve slope $C_{L_{\alpha}} = L/q\bar{c} = 3.13$ per radian, pitching moment curve slope $C_{m_{\alpha}} = M/qS\bar{c}\alpha = 0.148$ per radian, flap lift effectiveness $C_{L_{\delta}} = L/qS\delta = 1.95$ per radian, flap pitching moment effectiveness $C_{m_{\delta}} = M/qS\bar{c}\delta = -0.432$ per radian, and the flap hinge moment coefficient $C_{h_{\delta}} = H/qS\bar{c}\delta = -0.0350 \cos 25^{\circ} = -0.03172$ per radian where the sweep correction is added to give the moment about the hinge axis; the reference area is $S = 0.564 \text{ m}^2$, the reference chord is $\bar{c} = 0.6 \text{ m}$, and the pitch axis is located at 61.5% of the root chord.

Rolling moment coefficients were not derived from the pressure data and neither was the hinge moment due to angle of attack $C_{h_{\alpha}}$. The available data permitted a maximum of five constraints, and two sets of constraints were investigated; the first set used two constraints from the angle of attack data, $C_{L_{\alpha}}$ and $C_{m_{\alpha}}$, and the second set used all five constraints. The use of the flap rotation data alone without the angle of attack data was not considered.

The theoretical basis for the correction factors is the Doublet-Lattice Method (DLM) of reference 17. The idealization of the lifting surface consists of 110 boxes resulting from 11 strips and 10 equal chordwise divisions. The chordwise division on each strip result in 7 boxes on the primary surface and 3 boxes on the control surface. The strip widths Δy_i are chosen so that the strip centerlines fall along the lines of pressure taps. The span of 0.940 m is divided into the following strip widths from root to tip: $\Delta y_1 = 0.110$ m, $\Delta y_2 = 0.080$ m, $\Delta y_3 = 0.075$ m, $\Delta y_4 = \Delta y_5 = \Delta y_6 = \Delta y_7 = \Delta y_8 = \Delta y_9 = \Delta y_{10} = 0.090$ m, and $\Delta y_{11} = 0.045$ m. The pressure stations correspond to the strips as follows: pressure station VII is on Strip 1, VI on Strip 4, V on 6, IV on 8, III on 9, and finally station II is on Strip 10. Pressure station I is too close to the tip to permit a meaningful calculation.

The theoretical pressure distributions are compared to the experimental measurements in figures 13 through 24. The theoretical estimates of the five constraint parameters are: $C_{L_\alpha} = 3.207462$, $C_{m_\alpha} = 0.179494$, $C_{L_\delta} = 2.131577$, $C_{m_\delta} = -0.463554$, and $C_{h_\delta} = -0.057784$. Three additional parameters are also of interest. These are the locations of the spanwise aerodynamic centers for angle of attack, \bar{y}_α/s , and for flap deflection, \bar{y}_δ/s , and the hinge moment coefficient for angle of attack, C_{h_α} . Their theoretical estimates are $\bar{y}_\alpha/s = 0.452071$, $\bar{y}_\delta/s = 0.464614$ and $C_{h_\alpha} = -0.021034$.

A typical set of correction factors is shown in table I; it is for a premultiplying matrix and is based on five constraints. The factors are listed in order from leading edge to trailing edge on each strip beginning at the root; factors 1 to 10 are on Strip 1, and factors 101 to 110 are on Strip 11. The first seven factors on each strip apply to the primary surface and the last three apply to the control surface. The general trends seen in table I are a spanwise increase in factors from root to tip and a chordwise increase toward the hinge line. The minimum correction factor in table I is a 0.255873 for Box No. 10 and the maximum factor is 2.00893 for Box No. 108.

TABLE I

CORRECTION FACTORS			**	PREMULTIPLIER	CASE			
1	0.848278E+00	0.0	2	0.863580E+00	0.0	3	0.877532E+00	0.0
4	0.885935E+00	0.0	5	0.884442E+00	0.0	6	0.863395E+00	0.0
7	0.795167E+00	0.0	8	0.351261E+00	0.0	9	0.377085E+00	0.0
10	0.255873E+00	0.0	11	0.817065E+00	0.0	12	0.894144E+00	0.0
13	0.907865E+00	0.0	14	0.516395E+00	0.0	15	0.916132E+00	0.0
16	0.899734E+00	0.0	17	0.845436E+00	0.0	18	0.431832E+00	0.0
19	0.430533E+00	0.0	20	0.295866E+00	0.0	21	0.901404E+00	0.0
22	0.920260E+00	0.0	23	0.935662E+00	0.0	24	0.946287E+00	0.0
25	0.949498E+00	0.0	26	0.935449E+00	0.0	27	0.897291E+00	0.0
28	0.510927E+00	0.0	29	0.475718E+00	0.0	30	0.330467E+00	0.0
31	0.928828E+00	0.0	32	0.950033E+00	0.0	33	0.967959E+00	0.0
34	0.981803E+00	0.0	35	0.989602E+00	0.0	36	0.986787E+00	0.0
37	0.958193E+00	0.0	38	0.607972E+00	0.0	39	0.530440E+00	0.0
40	0.366155E+00	0.0	41	0.960566E+00	0.0	42	0.984268E+00	0.0
43	0.100520E+01	0.0	44	0.102273E+01	0.0	45	0.103556E+01	0.0
46	0.104067E+01	0.0	47	0.102777E+01	0.0	48	0.721815E+00	0.0
49	0.591196E+00	0.0	50	0.400920E+00	0.0	51	0.993722E+00	0.0
52	0.101983E+01	0.0	53	0.104356E+01	0.0	54	0.106452E+01	0.0
55	0.108209E+01	0.0	56	0.109509E+01	0.0	57	0.109904E+01	0.0
58	0.840227E+00	0.0	59	0.646701E+00	0.0	60	0.424058E+00	0.0
61	0.102803E+01	0.0	62	0.105634E+01	0.0	63	0.108254E+01	0.0
64	0.110650E+01	0.0	65	0.112847E+01	0.0	66	0.114958E+01	0.0
67	0.117262E+01	0.0	68	0.965580E+00	0.0	69	0.692697E+00	0.0
70	0.428853E+00	0.0	71	0.106328E+01	0.0	72	0.109351E+01	0.0
73	0.112173E+01	0.0	74	0.114814E+01	0.0	75	0.117424E+01	0.0
76	0.120438E+01	0.0	77	0.125149E+01	0.0	78	0.110761E+01	0.0
79	0.726251E+00	0.0	80	0.410725E+00	0.0	81	0.109930E+01	0.0
82	0.113103E+01	0.0	83	0.116048E+01	0.0	84	0.118864E+01	0.0
85	0.121911E+01	0.0	86	0.126123E+01	0.0	87	0.134366E+01	0.0
88	0.129296E+01	0.0	89	0.749826E+00	0.0	90	0.379618E+00	0.0
91	0.113593E+01	0.0	92	0.116805E+01	0.0	93	0.119719E+01	0.0
94	0.122676E+01	0.0	95	0.126399E+01	0.0	96	0.132572E+01	0.0
97	0.146760E+01	0.0	98	0.159211E+01	0.0	99	0.791950E+00	0.0
100	0.407107E+00	0.0	101	0.116343E+01	0.0	102	0.119185E+01	0.0
103	0.121559E+01	0.0	104	0.125326E+01	0.0	105	0.130061E+01	0.0
106	0.138609E+01	0.0	107	0.159604E+01	0.0	108	0.200893E+01	0.0
109	0.949436E+00	0.0	110	0.615306E+00	0.0			

TABLE II

Type of Correction Matrix	Number of Constraints	\bar{y}_α/s	\bar{y}_δ/s	C_{h_α}	C_{h_δ}
None	0	0.452071	0.464614	-0.021034	-0.057784
Pre-	2	0.456751	0.469814	-0.021746	-0.059959
Pre-	5	0.484939	0.522318	-0.010117	-0.031721
Post-	2	0.453096	0.465632	-0.022409	-0.057711
Post-	5	0.469176	0.491720	+0.013014	-0.031721

The modified static pressure distributions for angle of attack are shown in figures 13 and 14, and for flap deflection are in figures 15 and 16. Perusal of these figures indicates the following results. For the angle of attack loading, both the premultiplying and postmultiplying corrections move the theoretical results slightly away from the experimental data, the postmultiplier causing a little greater change. The effect of five constraints is greater than that of two. For the flap loading, both the pre- and postmultipliers based on two constraints have small effect. The corrections based on five constraints improve the correlations on the control surface but increase the discrepancies on the wing. The postmultiplier causes a much larger change and, although the data show a pressure reversal near the trailing edge, the postmultiplier exaggerates this reversal to the extent that the sign of the hinge moment is reversed. Table II shows the effects of the four correction matrices on the aerodynamic centers and hinge moments. All of the correction matrices resulted in an outboard shift of the aerodynamic centers, the largest shift coming from the 5-constraint premultiplier.

Two constraints did not improve the hinge moment prediction; and the 5-constraint postmultiplier lead to an unreasonable prediction of $C_{n\alpha}$. The effect of additional constraints based on estimates is a topic deserving further investigation.

We can anticipate similar discrepancies when the correction factors derived from static data are applied to the oscillatory cases, and, indeed, they are shown in figures 17 through 20 for the angle of attack oscillating at $k_r = 0.622$, and in figures 21 through 24 for the flap oscillating at $k_r = 0.752$. The theoretical loading for the oscillating angle of attack is not changed significantly by either the premultiplier or the postmultiplier based on two constraints and both the real and imaginary parts are affected about the same. In some regions the theory is shifted toward the data and in others the theory is moved away from the data. The effects of five constraints are more extreme. The 5-constraint premultiplier improves the correlation for the real part but only improves the agreement for the imaginary part on the control surface while diverging on the wing. The 5-constraint postmultiplier

is substantially worse in correcting the real part but is no worse than the premultiplier in modifying the imaginary part. Again, the theoretical load distribution from the oscillating control surface is not changed significantly by either the 2-constraint pre- or postmultipliers. However, some improvement is noted with the 5-constraint corrections although it is only slight. As in the static case, an outboard shift in loading occurs with all correction matrices and for both modes of motion.

The above applications of correction matrices have achieved very limited, if any, success. The lack of improvement in the most elementary case, however, is rather puzzling. This was the case of the static loading at angle of attack for which the correction factors were derived using the two constraints of lift and pitching moment. The pitching moment constraint was expected to shift the theoretical chordwise center of pressure in such a manner that the predicted pressure distribution would be closer to the experimental data. Two explanations for the lack of improvement appear possible. The first is that the theoretical loading in the leading edge region differs so much from the data that it dominates the correction factor calculation and results in a distorted loading. The second possibility is that the limited number of pressure taps near the leading edge prevented an accurate evaluation of the leading edge contribution to the pitching moment. A strain gage measurement of pitching moment would have shed some light on this possible difference.

A number of options were not pursued with these data which may have shown better correlation. First, only one configuration was studied here, the swept wing with aspect ratio 3.1; as noted above, straight wings with two aspect ratios and a swept wing with another aspect ratio were also tested. Next, only the reported integrated loads were used as constraints: the two angle of attack coefficients and the three additional control surface coefficients. The three control surface coefficients were not used as constraints by themselves, nor were additional constraints used based on estimates of rolling or bending moments. The new postmultiplying matrix was also not investigated. Finally, it would have been interesting to apply complex correction factors derived from the oscillatory angle of attack data at

$k_r = 0.622$ to the oscillatory control surface data at $k_r = 0.752$; however, this would have required integration of the published oscillatory pressure data to obtain the complex constraint coefficients.

Wing With and Without Leading Edge Droop. - Trailing edge control surfaces are studied in several other sections of this report. In this section, an attempt is made to study leading edge control surfaces. Usable data for such devices is very scarce. Several references have been investigated; however, only reference 18 proved in any way useful. The leading edge device described in this reference is a wing droop of 6° . The droop was applied to the first 19% of the wing chord along its entire span (see fig. 25). The idealization shown in this figure is for the Doublet Lattice Method (DLM). The fuselage was simplified as simply a wing extension to the centerline.

A steady case at $M = 0.80$ is considered and the uncorrected calculated results using the DLM for $\alpha = 4^\circ$, (no droop) agree very well with the experimental data (see fig. 25). Only a lateral shift in the center of pressure seems evident. Correction factors were developed for this case to correct this slight deviation in the theory. The constraints used are lift, pitching moment and bending moment coefficients. These coefficients were summed on strips outboard of the station $y/(b/2) = 0.11$ and are defined as:

$$C_L = \frac{L}{qA}, \quad \frac{A}{c_{\text{root}}^2} = 1.28$$

$$C_M = \frac{M}{qAc}, \quad c/c_{\text{root}} = .815 \text{ (moment taken about } x/c_{\text{root}} = 1.0)$$

$$C_B = \frac{B}{qA \cdot b/2}, \quad b/2/c_{\text{root}} = 1.6 \text{ (moment taken about } x\text{-axis)}$$

For the various modes the coefficients are:

	Pitch $\alpha = 4^{\circ}$	$\alpha = 10^{\circ}$	6° Droop
C_L	.2282	.5356	-.0215
C_M	-.0233	-.065	-.008
C_B	.0563	0.128	-.00536

A premultiplier and a postmultiplier (new type) were tried with equally good results on the span loading. Figure 26 illustrates the effect of the correction factors on the spanwise distribution of aerodynamic center. The correction factors increased the accuracy of the aerodynamic center inboard, but decreased it outboard.

The single mode application of both pre- and postmultipliers, also produces good results for leading edge droop span loadings (fig. 27). Notice that the unmodified results are approximately half of the experimental values. The experimental data were difficult to read on the plots (open squares). Thus, the pressure distributions were integrated to produce the darkened squares. The pressure distributions themselves were difficult to integrate accurately since there were down loads at the nose and uploads near the bend in the chord, such that the total loads were small. If the correction factors possessed only a slight variation in the chordwise direction, the balance of integrated load could shift drastically as a percent of the total.

The flow field near the wing changes at approximately $\alpha = 8^{\circ}$. Here the flow is to a large extent separated from the upper outboard surface. A comparison of uncorrected theory and experimental data, for the case of $\alpha = 10^{\circ}$, no wing droop, in figure 28, shows a loss of lift outboard of the 40% semi-span. Application of both pre- and postmultipliers (New), using C_L , C_M and C_B (bending moment at the centerline), show a much improved prediction of span loading. Also, shown in this figure is the application of the premultiplier correction factors, obtained at $\alpha = 4^{\circ}$ to the $\alpha = 10^{\circ}$ case (diamond symbols). The span loads are improved which shows that data obtained at one angle of attack can be profitably applied to other angles of attack. The corrections generated at $\alpha = 4^{\circ}$ are not as large as those generated at

$\alpha = 10^\circ$ because flow separation exist in the latter case. However, both corrections are in the same direction. Therefore, application of correction factors for $\alpha = 4^\circ$ improves the results for the 10° case. In general, the reverse may not hold; i.e., the correction factors obtained at $\alpha = 10^\circ$ (or larger angles) may be too large and an excessive correction may result leaving the corrected data further from the experimental data than there were originally. It does seem safe, however, to apply correction factors obtained at one angle of attack to other nearby angles if the flow is qualitatively similar (e.g., no great changes in flow pattern).

Transonic Cases

In this section applications of the correction factor technique are made to the same cases considered in the "Local Mach Number Studies" section. Specifically a two-dimensional symmetric airfoil (NACA 65A006) with an oscillating 25% chord flap is used.

Figure 29 illustrates the difference in results obtained when the classic theory (subsonic compressible) and the new transonic theory (Present Method (M_∞)) are corrected. A premultiplying set of correction factors were obtained using three constraints; lift, moment (1/4 chord) and control surface hinge-moment (3/4 chord). Each theory was corrected to the proper experimental constraints, i.e.,

$$\begin{array}{ll} c_{\ell} & = 4.93 & M_\infty & = .875 \\ c_{m_{1/4}} & = -1.57 & k_r & = 0.0 \\ c_{h_{3/4}} & = -0.053 & & \end{array}$$

where the characteristic length is the chord and the downwash over the control surface is unity. The classic theory does not have the bulge in pressure, near the compression (or shock) region for the steady flow as does the experimental data and applying correction factors will not make it appear. Thus correction factors can not make a qualitative feature appear where none existed before. The corrected classic theory does not compare well with the experimental data and the correction factors themselves, $(1 + \epsilon)$, show fairly large deviations from unity especially near the leading and trailing edges.

The Present Method (M_∞) however possesses a qualitative similarity with the experimental data and thus it is a better candidate for correction. Figure 29 shows such a correction. The bulge in pressure as calculated by the present method is amplified as it should be. The loading on the flap however is reduced, again as it should be, however the shape of the flap load is distorted. The correction factors themselves are better behaved for the

Present Method, (M_∞), showing large deviations from unity only on the flap surface.

Figure 30 presents the results of applying the premultiplying correction factors, obtained for the steady case, to an unsteady case. That is, the correction factors shown at the bottom of figure 29 are applied to the oscillatory results of the Present Method (M_∞) and the classic theory ($k_r = \omega \bar{c} / 2U_\infty = 0.059$). Since the correction factors are real they do not effect the phase angles of the pressures but only the amplitudes, $|\Delta C_p|$. Also shown in the figure is a pressure distribution corrected using factors based on the complex lift moment (1/4 chord) and hinge moment obtained for the unsteady case. Specifically

$$\begin{aligned} c_\ell &= 3.5 - i 1.18 & M_\infty &= 0.875 \\ c_{m_{1/4}} &= -1.66 + i 0.07 & k_r &= 0.059 \\ c_{h_{3/4}} &= -0.057 - i 0.016 \end{aligned}$$

The correction factors obtained in this manner produce pressures that are close to those obtained using the steady correction factors (except near the flap) even though the constraints in lift are considerably different in the two cases. There is one slight anomaly in the phase angle for the complex constraint case ($k_r = 0.059$) and it exists on the last two pressure points on the flap. The phase angle there is quite large however these angles do not have a large effect since the amplitude of pressures is very small there.

The question arises; to what extent can static correction factors be applied with accuracy to the oscillatory case? Figures 31 and 32 illustrate the effect of static correction factors on lift, moment and hinge moment coefficient versus reduced frequency for a Mach Number of 0.85. Considering first the lift coefficient it is noticed that the accuracy of the imaginary part is increased up to $k_r = 0.2$. Beyond this point application of correction factors decreases the accuracy of the theory. For the real part of the lift the corrected theory is more accurate only below a reduced frequency of 0.06. For the pitching moment and hinge moment the cross over point is roughly

$k_r = 0.1$. On the average then the static correction factors are useful up to about a reduced frequency of 0.1. Beyond this point it is better to use the original theory.

It is probably true that the accuracy of extrapolating correction factors versus reduced frequency depends on Mach Number. Figure 33 gives an indication that as Mach Number is reduced the accuracy increases. Specifically, static correction factors have been applied to the oscillatory case ($k_r = 0.098$) with very good results. Both amplitude and phase angle are improved.

The theory used in figures 31, 32 and 33 is a variation of the new transonic method presented previously. Specifically the variation utilizes an average local Mach Number (\bar{M}_∞) in place of the free stream Mach Number, M_∞ . Figures 31 and 32 show the application of two separate types of correction factors; a premultiplier type, the type used in figures 29 and 30, and a postmultiplier type. The postmultiplier is actually an additive viscous type of correction. It can be seen that this correction does not extrapolate to higher frequencies as well as the premultiplier type (as far as the lift coefficient is concerned). As the frequency is increased the experimental data approach the unmodified theory. One interpretation of this fact is that as the frequency is increased viscous effects are reduced.

The postmultiplying correction factor (designated as "New Post") used in figures 31 and 32 is the new postmultiplying correction factor discussed in the Theoretical Development section. The reason a new type of postmultiplier was needed is because the original one seemed to fail when control surfaces are considered. Postmultipliers correct the downwash matrix. When all downwash values are non zero, e.g., wing pitch, the method seems to work. However, when this is not the case, e.g., control surface deflections, the method fails entirely. The corrected downwash values are either large and erratic themselves or they cause large and erratic pressures due to the modified downwash.

It was hoped that the introduction of correction factor mode shapes would smooth out the corrected downwash and produce accurate results. This did not

happen. Even though smooth, well behaved functions were used the results were unrealistic. Although not tried, it seems that limiting the maximum and minimum values of the correction factors probably would not help very much either.

This failure of the postmultiplying correction factors led to an interesting investigation and subsequent development of the "New Postmultiplier". The investigation consisted in finding out what downwash in the theory would produce the experimental pressure distribution. Specifically the theoretical influence coefficient matrix was multiplied by the vector of experimental pressures to produce a vector of downwash values.

Figure 34 shows the results of this type of analysis (designated as Experimental) for a steady subsonic case ($M_\infty = 0.5$). Also shown is the theoretical downwash, i.e., unity over the flap. One thing is noticed immediately, there is a change in downwash ahead of the flap even though it is theoretically zero there. This downwash change is like a negative pitch of the entire airfoil. Figure 35 shows the camber (designated $M_\infty = 0.5$) associated with the downwash given in figure 34 and indeed it is like a negative or nose down pitch. This fact suggests that an additive type of correction factor, whereby all downwash values are changed, is necessary. This resulted in the development of the "New Postmultiplier" as described in the Theoretical Development section. This name is somewhat of a misnomer since the correction factor is additive and not multiplicative although the correction factors are proportional to the theoretical pressures.

The results of applying the new postmultiplying correction factors are also shown in figure 34. Again lift, moment ($c/4$) and hinge moment ($c3/4$) coefficient were used as the constraints

$$\begin{aligned} c_l &= 3.2 \\ c_{m_{1/4}} &= -.70 \\ c_{h_{3/4}} &= -.0528 \end{aligned}$$

The corrected values of downwash (circular symbols) agree well with the experimentally deduced downwash. The disagreements at the leading edge of the air-

foil and ahead of the flap are due to the fact that downwash is a sensitive function of pressure and slight variations cause large variations in downwash. With this in mind the agreement is very good especially over the flap itself.

Applying this corrected downwash to the theory produces the results given in figure 36 for the pressure distribution. The results of the New Postmultiplier agree very well with the experimental pressures. For reference, corrections by a premultiplier are also shown and these are also very good. The uncorrected theory is also presented for reference.

At the low Mach Numbers used in the last few figures ($M_\infty = 0.5$) transonic effects are not present and any differences between theory and experiment are, in all probability, due to viscous effects. Figure 35 has shown that viscous effects modify not only the downwash over the flap but also over the forward part of the airfoil as well. This comes about due to the fact that the deflected flap causes an induced upwash over the forward portion of the airfoil which in turn generates a difference in boundary layer displacement thickness on the upper and lower surfaces. This difference in displacement thicknesses causes an effective nose down pitch.

It stands to reason that the correction factors generated at $M_\infty = 0.5$ could be used to increase the accuracy of the theory at all Mach Numbers since viscous effects are present at all Mach Numbers. Figure 35 shows the effective cambers at $M_\infty = 0.5$ and $M_\infty = 0.875$ using the (\bar{M}_∞) variation of the new transonic theory. Notice that the transonic camber can be thought of as composed of two pieces; one viscous piece very similar to that found at $M_\infty = 0.5$ and one transonic piece with the shape of a bump. This indicates that the accuracy of the corrected camber (or downwash) at transonic Mach Numbers can be increased if the subsonic ($M_\infty = 0.5$) results are known and used since it represents one part of the correction.

Figures 37, 38, 39 and 40 give examples of applying correction factors obtained at $M_\infty = 0.5$ to other Mach Numbers for both pressures and aerodynamic coefficients. Specifically figures 37 and 38 present the results for Mach Numbers of 0.85 and 0.875 respectively. Up to three separate corrected

pressure distributions are shown in each figure. One is the result of applying a premultiplying correction factor matrix to the (M_∞) variation of the new transonic method. A second is the result of applying a new postmultiplier to the same theory; and third is the result of applying a new postmultiplier to the (\bar{M}_∞) variation of the new transonic method. The last pressure distribution is seen to be the most accurate and a definite improvement over the unmodified (\bar{M}_∞) theory (see fig. 4).

Figures 39 and 40 give a clear picture of the effect of applying corrections obtained at $M_\infty = 0.5$ to other Mach Numbers. Figure 39 presents the lift coefficients associated with corrected and uncorrected pressure distributions. Two types of corrections are used; both pre- and postmultiplier (New). The theory used is the (\bar{M}_∞) variation of the new transonic method. Figure 40 presents similar results for the pitching moment and hinge moment coefficients. The corrections developed at $M_\infty = 0.5$ greatly improve the theory as far as the lift coefficient is concerned. The pitching moment is not changed much because it was very close to the data to begin with. The hinge moment also is not changed much.

Figures 39 and 40 show that corrections obtained at low Mach Numbers can be applied to the theories to improve accuracy at higher Mach Numbers.

Figure 41 presents the results of correcting the theory with both a postmultiplier (New) and a premultiplier. First the theory is corrected using a new postmultiplier obtained at $M_\infty = 0.5$. This represents a viscous type of correction. A premultiplier is then applied to the previously corrected results to account for transonic effects. This process produces a pressure distribution that approaches the data more closely than any of the others when it is combined with the (\bar{M}_∞) variation of the new transonic method.

Figure 42 presents typical correction factors for the steady two-dimensional cases considered in this section. The theory used is the Present Method (M_∞). There is a greater change in premultiplying correction factors between $M_\infty = 0.85$ and 0.875 than there is between $M_\infty = 0.5$ and 0.85 .

Supersonic Case

The arrow wing, shown in figure 43, has been chosen to illustrate the application of the correction factor technique to the supersonic case. The Douglas Supersonic Doublet Method (SDM) (ref. 20) has been used to determine the theoretical loads. The box idealization used is also shown in the figure. Notice that the tip of the wing has been clipped to reduce the number of boxes. Two modes are considered; (1) pitch ($\alpha = 4^\circ$) and (2) camber. The wing is operating at a Mach Number of 2.05 and a reduced frequency of zero.

Figure 43 presents a comparison of uncorrected theory (dotted line), corrected theory and experimental data. The experimental values lie below the theoretical (uncorrected) values over the entire span.

Four different methods of correcting the theory were tried. A pre- and postmultiplier (New) were applied using the pitch mode only and the results are very encouraging. The only real difference between the theory, corrected in this manner, and the experimental data appears at the wing tip. A multiple mode case was tried using the pitch and camber modes and the results are good but not as good as the previous two corrections. The fourth method is the application, to the pitch case, of a premultiplier correction factor matrix that was derived for the camber case. Thus a correction factor derived for one mode (camber) is applied to another mode (pitch). The results are not very accurate on the inboard part of the wing but agree as well as the other methods on the outboard part. The constraints used are summarized as follows:

	Pitch $\alpha = 4^\circ$	Camber
C_L	0.1213	0.1297
C_M	-0.035	-0.022
C_B	0.025	0.02196
$C_L =$	$\frac{L}{qA}$	$\frac{A}{c_{root}^2} = 0.28$
$C_m =$	$\frac{M}{qA\bar{c}}$	$\bar{c}/c_{root} = 0.665$
		Moment about $x/c_{root} = 0.68$

$$C_B = \frac{B}{qAb/2}$$

$$(b/2)/c_{\text{root}} = 0.564$$

B ≡ Moment about x-axis

A similar set of corrections were applied to the camber case and the results are shown in figure 44. Specifically pre- and postmultiplying correction factors were obtained using the camber mode. In addition a multiple mode (pitch, camber) premultiplying correction factor matrix was derived using six constraints; i.e., C_L , C_M , C_B for both modes. All three of these corrections give approximately the same good results except right at the wing tip.

Two other types of correction factors are applied to the theory and these refer to applying the correction factors derived for pitch to the camber mode. On the inboard portion of the wing these correction factors over-correct the theory, but are accurate on the outboard portion of the wing. On the inboard portions of the wing the correction factors move the corrected theory further from the data than it was originally in its uncorrected state.

Figure 45 illustrates how correction factors modify the pressure distribution over the wing (in pitch) using a premultiplier. It seems that the reduction in lift due to the correction factors is taken out at the trailing edge rather than the leading edge as the experimental pressures would indicate. This fact might be explained if the experimental pitching moment were inaccurate.

The postmultiplier does not directly modify the pressures but modifies the downwash. Modified downwash can be expressed in terms of modified camber. It is of interest to know how the postmultiplier (New) modifies the wing camber and figure 46 presents such a modification. The camber is reduced, by the correction factors, over most of the wing just as expected, since the boundary layer and separation regions act to reduce the effective wing camber. The postmultiplier, then, acts in a way that is consistent with physical processes.

RECOMMENDATIONS FOR DATA ACQUISITION

Most of the data utilized in this study were pressure data, and the correction factors were derived using constraints that were obtained in some instances from integrations of the pressures. Certain errors are associated with integrations of pressures to obtain generalized forces, arising primarily from the limited number of pressure pickup points on a practical model. The forces and moments should be measured directly in addition to the pressures. Control surface hinge moments should be measured and so should rolling moments, i.e., root bending moments, because of the importance of the spanwise aerodynamic center location. For swept surfaces it would be desirable to measure not only pitching and rolling moments in the streamwise coordinate system but also root bending moment and torque about some swept coordinate system, e.g., the 25% or 50% chord lines.

Two significant deficiencies were observed in available experimental data besides the absence of combined pressure and force data. One was a lack of any systematic variation in reduced frequency in covering the range from steady flow to high frequency, i.e., k_r of order unity. The correction factors are frequency dependent, and it is not reliable to use factors derived from low frequency data to predict pressure distributions at high frequencies. The second deficient area is the effect of Reynolds number. An important source of discrepancy between theory and test is the neglect of viscosity in the theory. When extensions of oscillatory lifting surface theory are made to account for viscous effects, data will be needed to verify the accuracy of the improved theory. However, these data are also needed to determine the accuracy with which correction factors derived from data at one Reynolds number can be used to predict pressures at another Reynolds number. This is particularly important for trailing edge control surfaces.

A number of suggestions can be made for future wind tunnel tests in addition to those indicated above. Leading edge control surfaces should be tested; spoilers might also be considered. Very little data are available for these configurations. Models should be designed so that components can be

tested in their principal modes of motion. Complete models usually have moveable control surfaces but a moveable fin, horizontal tail, and engine pylon should also be considered to distinguish between component loads and interference loads. More oscillatory transonic data are needed. In two-dimensions, pitch data should be measured in addition to control surface data; in three-dimensions, data on both straight and swept wings are required.

CONCLUDING REMARKS

CONCLUSIONS

The basic conclusions arrived at as a result of the calculations and correlations presented are outlined as follows:

(1) One Set of Correction Factors Is Not Good For All Modes

Application of correction factors, determined from one mode, to other modes has not met with much success. Specifically, correction factors obtained using a pitch mode can not be applied to pressures due to control surface deflections. The converse is also true. In addition, application of correction factors, obtained using a pitch mode, to pressures due to a camber mode (and vice versa) have not proved to be very accurate either. Bergh and Zwaan, reference 6, on the other hand have concluded that correction factors calculated using a pitch mode can be applied to a roll mode. These two modes, however, are similar. One of them has a constant angle-of-attack along the span while the other has a linearly varying angle-of-attack along the span.

Further study is required to find out what types of correction factors are required for the various modes encountered in flutter and other dynamic aeroelastic analyses. The practical method of implementing such a correction procedure also requires further study.

The fact that one set of correction factors can not be applied to all modes has certain implications for testing procedures. It may be that more rigid body types of modes will be required (e.g., pylon yaw, wing alone pitch, tail alone pitch, outer wing pitch, inner wing pitch, fuselage alone pitch, etc.) than are now considered.

A second approach to the problem of obtaining one set of correction factors for both a pitch and a control surface mode was attempted using the "multiple mode" capability of the program. This capability allows the theory to be constrained to produce the correct lift and moment coefficient, etc., for each of several modes. The resulting span loading and/or pressures were not improved for either the pitch or control surface modes.

Even within a single mode problems can occur for different amplitudes. For instance high angle-of-attack flow fields can be basically different (separated) from those at low angles-of-attack. However correction factors obtained at low angles-of-attack can result in improved predictions for all angles-of-attack. The basic reason being that the viscous corrections, although smaller for the unseparated case, are still in the same direction as that for the separated case.

(2) A Bending Moment Constraint Is Needed For Swept Wings

Lift and pitching moment constraints are not enough for the swept wing case. A bending moment constraint is also required so that the loading is not shifted outboard to accommodate an aft shift in aerodynamic center of pressure. Without the constraint on the bending moment the correction factors will cause the wing loading to be moved toward the wing tip instead of moving the load aft along the chordline.

(3) Correction Factors Can Be Extrapolated More Accurately To Other Mach Numbers Than To Other Frequencies

When correction factors are determined at low Mach Numbers they are caused primarily by viscous effects. Since viscous effects exist at all Mach Numbers an increase in accuracy will result if the low Mach Number correction factors are applied to the high Mach Number cases.

Extrapolation in frequency has not been as successful as extrapolation in Mach Number. For the two dimensional case studied it seems that extrapolation further than $\Delta k_r = 0.1$ (based on the half chord and a Mach Number of 0.85) will lead to a decrease in accuracy as k_r is increased. It is believed that extrapolation in reduced frequency is more accurate at lower Mach Numbers.

It appears that as the frequency is increased the viscous effects are reduced. This is an important fact and if steady wind tunnel results are to be used for correcting data then a good estimate of the reduction in the viscous effect must be known. One way to accomplish this without testing every configuration is to test a representative sample of configurations over

a range of frequencies and construct general trends to be used in conjunction with steady data to estimate the frequency effect on correction factors.

(4) Qualitative Features Missing From The Theory Can Not Be Generated By Correction Factors

Correction factors tend to produce quantitative changes to the theory and not qualitative ones. For instance, in transonic flow, the bulge in pressure at the shock location cannot be induced with correction factors if one did not exist in the basic theory.

(5) Downwash Correction Factors Must Be Additive, Not Multiplicative

It was found that postmultiplying correction factors did not work for control surface modes (they did work for pitch modes however). That is, scaling the downwash to reproduce the imposed experimental constraints (C_L , C_M , etc.) led to unusable results. Smoothing of the results was obtained by introducing correction factor modes; however, the levels of correction were still unrealistic. An analysis was performed to see what downwash was required to produce the experimental pressures and it became evident that the downwash had to be corrected everywhere and not just on the control surface. This suggested an additive downwash correction. A new method was developed and executed successfully.

Downwash correction factors essentially reflect the physical fact that viscous effects tend to change the effective airfoil camber (and thus the downwash). The camber is changed over the entire airfoil.

(6) Premultiplying And (New) Postmultiplying Correction Factors Are Equally Accurate

In the cases studied the accuracy of the corrected theory is improved equally well (approximately) by either type of correction factor matrix. The downwash correcting factors (New Postmultipliers) are physically more meaningful if interpreted as viscous corrections while premultipliers are more meaningfully interpreted as compressibility corrections.

Since transonic experimental data reflect both viscous and compressibility effects a very accurate way to obtain correction factors, if data permit, is to combine pre- and postmultipliers together. First a postmultiplier (New) is developed at low Mach Number where viscous effects dominate. This correction is then applied to the transonic case. The modified theory is then corrected further for transonic effects using a premultiplier. Correction factors produced in this way are more accurate than most.

(7) New Transonic Method Useful But Requires Further Investigation

Various methods of applying local Mach Number were tried. Simple procedures based on the substitution of the local steady Mach Number (or some average between surface and free stream) for the freestream value in the boundary conditions, kernel, and pressure equations have been tried. The results have only shown minor changes and have not even given qualitatively good results.

A new method was developed at Douglas (under the McDonnell Douglas IRAD program) and is based on a transformation of the distance between sending and receiving points based on acoustic travel time between the two points. This method was implemented for the two-dimensional case and correlated in the present study. The results are encouraging since the predicted pressures are qualitatively similar to the experimental data. That is, the new method predicts a bump in the pressure which is centered at the shock wave location and predicts a lowering of the pressure forward of the shock wave. This bump, however, is forward of the experimentally observed bump, and is usually smaller in amplitude.

The theoretically determined phase angles of the pressures are not in good agreement with the experimental data forward of the 40 percent point (for the case of a control surface rotation). One possible reason for this is the fact that the wave fronts emanating from points on the flap tend to move up and over the shock wave and arrive at the forward portions of the airfoil in nearly a horizontal configuration. On the other hand, in the theory, the paths of the wave fronts are assumed to be normal to the free stream flow with the wave fronts vertical, and this difference causes the phase angles to be greater for the theory than for the data. Further investigation of this

discrepancy and its solution is required. It may be possible to use a more exact phase lag time computation in the theory, such as the one used by Tijdeman and Bergh in reference 11.

When trying to decide which theory is best it is important to account for viscous effects. Without such a correction the new transonic method, designated as (M_∞) , seems best. However, when viscous effects are accounted for, the variation designated (M_∞) is best.

With the current method of computation the new transonic method is probably not reliable past $M_\infty = 0.90$. This may not be too restrictive since most wings are swept which reduces the normal Mach Numbers to values lower than 0.90.

(8) Overview of Conclusions

The concept of correcting theoretical pressure or load distributions so that they reflect associated experimental data works well with the correction factor technique, especially if the proper experimental data are available (e.g. bending moments.) It was hoped however that a set of correction factors, once developed, would be applicable to a wide variety of other cases. The range of applicability however has not been as wide as hoped for. Success in extrapolating correction factors was obtained for Mach Number and to a limited extent for frequency. Attempts to apply correction factors to dissimilar mode shapes however has not met with much success. Therefore more than one set of correction factors is required. The use of several sets of correction factors to correct oscillatory aerodynamic generalized forces for use in dynamic aeroelastic analyses requires further investigation.

Also concluded from the present analysis is that correction factors can not change the character of the load distribution. If a fundamental feature is missing from the theoretical loading then the correction factors will not make it appear. Thus theoretical methods must possess at least qualitative accuracy.

Recommendations for Further Studies

Further studies may be profitably pursued in several areas. The successes and failures of the correction factor technique, presented here, furnish a guide to such studies.

First, it seems advisable to exercise more of the various options in the present method and include more types of force data (integrated from pressure data) for some of the cases treated in this report. For instance such a case would be the Hertrich wing (refs. 14, 15). It would also be desirable to obtain new data similar to that obtained by Hertrich, in which both force and pressure data are available. It would be interesting to compare force data with integrated pressure data.

Second, it is now clear that one set of correction factors is not sufficient for all deflection modes. Thus a method for including multiple sets of correction factors into the determination of generalized oscillatory aerodynamic forces for various modes is required. This method may require special testing procedures whereby each major component or subcomponent is systematically given a rigid body rotation.

Third, the studies on viscous effects initiated in this report should be continued. Specifically the technique of determining theoretical camber lines that reproduce experimental pressure distributions seems valuable and could lead to a semiempirical method for viscous effects when combined with boundary layer theory.

Fourth, the new transonic method illustrated in this report should be refined and extended. Initially the two-dimensional capability should be refined in the areas of; 1) pressure phase angle and, 2) unsteady shock wave motion. Subsequent to this a three-dimensional method should be developed.

In addition, an investigation should be undertaken to explore the possibility of developing a semiempirical transonic method. The local steady Mach Number can be used as an adjustable parameter so as to produce the pressure distribution changes necessary to satisfy experimental constraints (lift moment etc.).

CORRECTION FACTOR COMPUTER PROGRAM

Introduction

As described in the Theoretical Development Section this method generates a set of correction factors that can be applied to a set of data (e.g., theoretical pressure) such that the data satisfies certain imposed (e.g., experimental) constraints.

For convenience this data will be referred to as pressure data since this is the most common application. However the correction factor procedure is not restricted to pressures and can be applied to other data sets (e.g., span loads, etc.).

For this procedure it is assumed that one or more theoretical pressure distributions, ΔC_{p_j} , ($j = 1$, number of pressure modes) are input. Associated with these pressures are: an area distribution, ΔA , a set of coordinates, (x, y, z) , and a dihedral angle distribution $\bar{\gamma}$ which are input via cards, tape or both. As an option the aerodynamic influence coefficient matrix, $[A] = [D]^{-1}$, along with one or more normalwash distributions, w_j , can be input in place of ΔC_{p_j} ; and as a matter of fact these must be input for postmultiplier correction matrices (i.e., correction factor matrices for the normalwash).

Constraint data (experimental data) are input as force or moment coefficients. If a force coefficient, C_e , is considered it is defined as

$$C_e = \frac{1}{\tilde{c}} \sum_a^b \Delta A \Delta C_p \vec{n} \cdot \vec{i}_a \quad (\text{force coef.}) \quad (87)$$

where \tilde{c} is a constant used to convert the dimensional sum into a coefficient form. For example if $C_e = C_L$ then \tilde{c} is equal to the reference area. The limits of the sum are also input to the program. The unit vector \vec{i}_a is in the direction of an input axis. A set of axes are input for use in the constraining and monitoring features of the program. Each axis can be input in one of two

ways; (1) a point and a direction or (2) by two points. The unit vector \vec{i}_a is calculated as follows:

$$\vec{i}_a = \vec{i} \cos\alpha + \vec{j} \cos\beta + \vec{k} \cos\gamma \quad (88)$$

The unit vector \vec{n} is in the direction of the lifting pressure which is given in terms of the dihedral angle of the lifting surface.

$$\vec{n} = \vec{j}(-\sin\bar{\gamma}) + \vec{k}(\cos\bar{\gamma}) \quad (89)$$

where \vec{j} and \vec{k} are unit vectors in the y and z directions respectively and where a right handed system is employed where z is up, y is out the starboard wing and x is aft.

If a moment coefficient, C_e , is considered then it is defined as follows:

$$C_e = \frac{1}{\hat{c}} \sum_a^b \Delta A C_p (\vec{r} \times \vec{n}) \cdot \vec{i}_a \quad (\text{moment coef.}) \quad (90)$$

where

$$\vec{r} = (x - \xi^{(1)})\vec{i} + (y - \eta^{(1)})\vec{j} + (z - \zeta^{(1)})\vec{k} \quad (91)$$

and where $\xi^{(1)}$, $\eta^{(1)}$, $\zeta^{(1)}$ are the coordinates of the first end point of the axis considered and where \vec{i}_a is its direction. The constant \hat{c} for the case of C_M has the dimensions of volume.

The program has various other capabilities and one of these is its ability to monitor the corrected or uncorrected pressures. The integrations performed in equations (87) and (90) can be performed using data without reference to constraints. Thus if span loads are desired for data that has been corrected (or uncorrected) then the proper summations are activated in the program in a manner similar to that for constraining the data.

The program also has the capability to use correction factor modes. That

is, the actual correction factors $\{\epsilon\}$ are related to a set of modal coordinates $\{\bar{\epsilon}\}$ as follows:

$$\{\epsilon\} = [\phi] \{\bar{\epsilon}\} \quad (92)$$

The modal matrix, ϕ , is either input directly by cards or certain built in modes can be activated.

The program has the capability to limit the excursion of any or all correction factors. The upper and lower bounds are simply input for the correction factors that are to be limited. If correction factor modes are used then the limits are placed on the modal coordinates, $\bar{\epsilon}$, and not on the correction factors themselves.

In addition to limits, a factor $\tilde{\alpha}$ is input for each constraint to indicate its "constraining power". The term $\tilde{\alpha}$ ranges from 0 to 1.0. If $\tilde{\alpha}$ is 1.0 the constraint has full power and is 100 percent effective as a constraint. If $\tilde{\alpha}$ is 0 then the constraining power is zero and the "constraint" has no effect. For values of $\tilde{\alpha}$ anywhere in between the constraint is said to be an estimate.

Finally, the program can be used to apply previously obtained correction factors to input pressure distributions. The program can also be used simply to monitor existing data without any constraints.

One nomenclature problem which might cause confusion is the fact that the normalwash w is called W in the program, while the correction factors W are called CF.

Program Input

The following table provides an overview of the card input data grouped according to their functions in the program. The layout of the input sheets and a detailed description of each input item are also given following the table.

Overview of Input Data

ITEMS	CARD NO.	WHEN NEEDED	COMMENTS
CONTROL DATA	1, 2, 3, 4	Always	Header card, control dimensions and control flags.
GEOMETRY AND PRESSURES	5, 6	If FLAGP=3	Geometry data is input on one card per i , $i=1$, NP (NP=number of pressures). Pressures are input either 6 real numbers per card (when FLAGI=1), or 3 complex numbers per card (when FLAGI=0). Repeat pressure input per pressure mode, symmetric modes first, antisymmetric modes (if any) last.
AXIS DATA	7, 8	Always	Axis data, 2 cards per i , $i=1$, NAXIS (NAXIS=number of input axes)
CONSTRAINT DATA	9, 10 11, 12	If NC \neq 0	Constraint data is input in a minimum of four cards per i , $i=1$, NC (NC=number of constraints)
MONITOR DATA	13, 14 15, 16	If NMØN \neq 0	Monitor data is input in a minimum of four cards per i , $i=1$, NMØN (NMØN= the number of monitored aerodynamic parameters)
LIMITS DATA	17	If NELIMS \neq 0	Minimum and maximum limit values on ϵ ; repeat per i , $i=1$, NELIMS (NELIMS=number of min. and max. limiting value pairs)

ITEMS	CARD NO.	WHEN NEEDED	COMMENTS
CORRECTION FACTOR MODES	18, 19 20, 21	If NEM \neq 0	Correction factor modes may be input according to two options depending on the flag TYPE (see detail description of data) either in cards 18, 19 and 21, or in cards 18, 20 and 21. Repeat per i, i = 1, NEM (NEM=number of correction factor modes)
DOWNWASH DATA	22, 23	If FLAGW=1	Downwash data is input in a minimum of two cards per mode (see detail description of data). Input symmetric modes first, antisymmetric modes (if any) last.

Computer program requires less than 200K OCTAL storage.

Input Sheets

ENGINEER _____

PHONE _____

DATE _____

73 74 75 76

E J I G C

PROGRAM NO.

53 64 65 66 67 68

CASE

PUNCH IN ALL CARDS

SEQ. NO.	CONTROL DATA										GEOMETRY AND PRESSURES		AXIS DATA		CONSTRAINT DATA	
77 78 79 80	1	2	3	4	5	6	7	8	9	10						
	HEADER															
	NP	NC	NEM	NELIMS	NMON	NAXIS										
	FLAGB	FLAGP	ELAGL	FLAGW	ELAGL	IPRINT										
	NMSYM	NMASYM														
	X _i	y _i	Z _i	γ _i	ΔA _i	i=L, NP										
			ΔC _{p_i}	j=L, NP												
	IAX	IFA														
	XII	EIAI	ZETAL	XI2/cosα	EIA2/cosβ	ZETA2/cosγ										
	JAX	IEF														
	NDI	MI	AIL	CIT	Re CIE	Im CIE										

DO NOT PUNCH BLANK COLUMNS NO UNDERPUNCHES IN SIGN FIELDS.

DIRECTIONS FOR KEYPUNCH

ENGINEER

PHONE

DATE

70

73 74 75 76

53 64 65 66 67 68

E J G C

PUNCH IN ALL CARDS

CASE

PROGRAM NO.

±		±		±		±		±		±		±		±		±		±		SEQ. NO.
1	2	3	4	5	6	7	8	9	10	11	12	13	14	15	16	17	18	19	20	77 78 79 80
LIMIT1		LIMIT2		LIMIT1		LIMIT2		LIMIT1		LIMIT2		LIMIT1		LIMIT2		LIMIT1		LIMIT2		11
MAX		IFN		ANT		CNT		LABEL												12
NDN		MN																		13
LIMIT1		LIMIT2																		14
																				15
																				16
LIMIT1		LIMIT2		LIMIT1		LIMIT2		LIMIT1		LIMIT2		LIMIT1		LIMIT2		LIMIT1		LIMIT2		17
MODENO		ITYPE		NL		AL		BL		Re ϵ_{min}		Im ϵ_{min}		Re ϵ_{max}		Im ϵ_{max}				18
J		Re ϕ_j		Im ϕ_j		J+1		Re ϕ_{j+1}		Im ϕ_{j+1}										19
LIMIT1		LIMIT2																		20

DIRECTIONS FOR KEYPUNCH DO NOT PUNCH BLANK COLUMNS NO UNDERPUNCHES IN SIGN FIELDS.

Description of Input Data

Control Data

These data items are required for all cases. They consist of a header, control numbers, flags, and tape (or scratch unit) numbers.

CARD	ITEM	MNEMONIC	DESCRIPTION
1	Header	HEADER	Alpha-numeric description of case in card columns 1 through 60
2	NP	NP	Number of ΔC_p elements, where ΔC_p may represent any type of quantity ($NP \leq 350$)
2	NC	NC	Number of constraints to be applied to the ΔC_p values ($NC \leq 35$)
2	NEMØDES	NEM	Number of correction factor modes if any ($NEM \leq 100$)
2	NELIMS	NELIMS	Number of input cards giving the minimum and maximum values of ϵ ($NELIMS \leq 100$)
2	NMONITOR	NMØN	Number of sets of monitoring data used to integrate ΔC_p into aerodynamic parameters ($NMON \leq 35$)
2	NAXIS	NAXIS	Number of axes input for use in integrating the ΔC_p data into forces and moments for constraint and monitoring purposes ($NAXIS \leq 25$)
3	FLAGB	FLAGB, IFB	FLAGB=0, correction matrix calculation FLAGB=1, monitor data only FLAGB=2, apply input correction factor matrices to input pressure distribution
3	FLAGP	FLAGP, IFP	FLAGP=0, geometry data and ΔC_p are input from tapes; calculate <u>pre</u> multiplying correction factors. (See Tape Description section for format) FLAGP=1, geometry data and D^{-1} (inverse aero matrix) are input from tapes, W (normalwash) input either from tape or on cards (see FLAGW below), calculate <u>post</u> -multiplying correction factors

CARD	ITEM	MNEMONIC	DESCRIPTION
			<p>FLAGP=2, input as for FLAGP=1; but calculate <u>pre</u>-multiplying correction factors</p> <p>FLAGP=3, geometry data and ΔC_p input on cards; calculate <u>pre</u>-multiplying correction factors</p> <p>FLAGP=4, geometry data and D^{-1} input from tapes, W input either from tape or on cards; calculate <u>modified post</u>-multiplying correction factors</p>
3	FLAGT	FLAGT	<p>FLAGT=0, weights for minimization process are absolute values of forces for unit deflections</p> <p>FLAGT=1, weights are unity</p>
3	FLAGW	FLAGW	<p>FLAGW=0, normalwash matrix, W^*, is input from tape, if needed</p> <p>FLAGW=1, normalwash matrix, W, is input on cards</p>
3	FLAGI	FLAGI	<p>FLAGI=0, ΔC_p values are input as complex numbers (either from tape or on cards)</p> <p>FLAGI=1, ΔC_p values are input as real numbers (i.e. not complex)</p>
3	IPRINT	IPRINT	<p>Detail print flag;</p> <p>IPRINT = 1, print rows of the SAI matrix, and rows of the SAN matrix (if any)</p> <p>IPRINT = 0, bypass printing of same</p>

* Cap. W is normalwash in the computer program where correction factors are called CF.

CARD	ITEM	MNEMONICS	DESCRIPTION
4	TS	NMSYM	Number of symmetric pressure modes (NMSYM, NMASYM \leq 10)
4	TA	NMASYM	Number of antisymmetric pressure modes
			Note that all data items in cards 2 through 4 are input as integers, right-justified* in their respective fields of ten card columns each (format I10) as shown on the input sheets.

* Right justified means input ending in the last (or right-most) card column of the field.

Geometry and Pressure Data

Data items defining the geometry of a case are usually available on tape; similarly, pressure data (if needed; see item FLAGP under Control Data) are usually input from tape. However, if this is not the case, these data items may be input from cards by specifying FLAGP=3, as shown below.

CARD	ITEM	MNEMONICS	DESCRIPTION
			The following two cards are input only if FLAGP=3.
5	x_i	X	x, y, z coordinates of pressure point i
5	y_i	Y	
5	z_i	Z	
5	$\bar{\gamma}_i$	GMA	Dihedral angle of pressure point i
5	ΔA_i	DELA	Area of box over which the pressure acts. Repeat card 5 for all points, $i=1, NP$
6	ΔC_p	DCP	Array of the ΔC_p values (lifting pressures) either 3 complex numbers per card (when FLAGI=0), or 6 real numbers per card (when FLAGI=1; see Control Data)
			The format used for cards 5 and 6 is 6F10.0.

Axis Data

The following data items are required for all cases. These input data are used to describe an axis in space. Axes can be described by either two endpoints or by one endpoint and a set of direction cosines. These axes are used in the integration of the pressures into force or moment coefficients. Forces are resolved in the direction of the axis, while moments are taken about the axis.

CARD	ITEM	MNEMONIC	DESCRIPTION
7	Axis number	IAX	Axis number
7	Axis type	IFA	IFA=0, axis endpoints are input IFA=1, a point and direction cosines are input
8	ξ_1 η_1 ζ_1	XI1 ETA1 ZETA1	Axis endpoint coordinates
8	$\xi_2/\cos\alpha$ $\eta_2/\cos\beta$ $\zeta_2/\cos\gamma$	XI2 ETA2 ZETA2	Second axis endpoint coordinates if IFA=0; direction cosines if IFA=1
			Card 7 format is 6I10; card 8 format is 6F10.0

Constraint Data

The correction factors modify the theoretical values of ΔC_p by a minimum amount so that specified forces and moments are reproduced. For example, if the total lift is known experimentally, then several data items must be input specifying the actual value of the lift coefficient and describing the way the ΔC_p values are to be integrated to obtain this coefficient. The lift coefficient is then called a constraint on the theoretical data.

CARD	ITEM	MNEMONIC	DESCRIPTION
9	Axis number	JAX	Number of the axis to be used for calculating the constraint force or moment
	F-M Flag	IFF	IFF=0, the constraint, C_e , is a force in the direction of the axis; IFF=1, the constraint, C_e , is a moment about the axis (right-hand-rule). Card format is 6I10
10	δ	NDI	$\delta=1$, symmetric pressure mode to be used; $\delta=-1$, antisymmetric pressure mode to be used
10	Press. mode	MI	Pressure mode number to be used with constraint C_e
10	\tilde{a}	AIT	Constraining effectiveness of C_e ; $0 \leq \tilde{a} \leq 1$. If $\tilde{a} = 1$, C_e is a constraint; if $\tilde{a} < 1$, C_e is only an estimate, and the resulting weighted (corrected) theory will only approximately reproduce C_e . If $\tilde{a}=0$, then C_e will not affect data.
10	\tilde{c}	CIT	Constant used to nondimensionalize integrated data. If C_e is a force, $\tilde{c} = \text{Area}$; if C_e is a moment, $\tilde{c} = \text{Area} \times \text{length}$.

CARD	ITEM	MNEMONIC	DESCRIPTION
10	C_e	CIE	Experimental (or any other) constraint on the data. Card format is 2I10, 4F10.0.
11	LIMI1, LIMI2	LIMI(1) LIMI(2)	Identification of a range of ΔC_p values (or boxes) from LIMI1 to LIMI2 defining the limits of integration for the pressures. There may be as many sets of ranges input as needed. Card format is 6I10.
12	-1	-1	The number -1; end indicator for the sets of data LIMI1, LIMI2
			Cards 9 through 12 are repeated for all constraints, i.e. NC times.

Monitor Data

The following data are input only if the control data item `NMONITOR` has a value different from zero. These data are used for the integration of the ΔC_p values into some meaningful parameters as a check on the effect of the correction factors on theory, whenever `FLAGB = 0`. Since often it is desirable to monitor the unmodified data as well, the setting `FLAGB = 1` is designed to integrate the ΔC_p values into parameters without calculating the correction factors. Another monitoring option can be activated by the setting `FLAGB = 2`; in this case the correction factors are input from tape (FT16) saved in a previous run and the weighted ΔC_p values are integrated into parameters as specified by the monitor data.

CARD	ITEM	MNEMONIC	DESCRIPTION
13	Axis number	NAX	Axis number used in the integration of the ΔC_p values into forces and moments
13	F-M flag	IFN	IFN=0, parameter to be determined is a force IFN=1, parameter to be determined is a moment. Card format is 6I10.
14	δ	NDN	$\delta=1$, symmetric pressure mode used $\delta=-1$, antisymmetric pressure mode used
14	Press. mode	MN	Pressure mode number
14	\tilde{a}	ANT	Not used
14	\tilde{c}	CNT	Constant used to nondimensionalize integrated data
14	LABEL	LABEL	Alphameric identifier of the integrated parameter (ten characters long) Card format is 2I10, 2F10.0, 10A1

CARD	ITEM	MNEMONIC	DESCRIPTION
15	LIMN1, LIMN2	LIMN(1) LIMN(2)	Identification of a range of ΔC_p values defining the limits of integration for the pressures. There may be as many sets of ranges input as needed. Card format is 6I10.
16	-1	-1	The number -1; end indicator for the sets of data LIMN1, LIMN2
			Cards 13 through 16 are repeated for all parameters, i.e., NMØNITØR times

Limits Data

It is sometimes desirable to place a restriction on the range of values of ϵ by specifying a minimum and a maximum bound on ϵ . In this case the control data item NELIMS is input as the number of ϵ limit pairs to be supplied, which are input as shown below. Note that this input (card 17) is omitted when NELIMS = 0.

CARD	ITEM	MNEMONIC	DESCRIPTION
17	LIM ϵ 1 LIM ϵ 2	LIMK(1) LIMK(2)	} A range of boxes, or ΔC_p elements, over which a limit is placed on ϵ
17	$\bar{\epsilon}_{\min}$ $\bar{\epsilon}_{\max}$	EBMIN EBMAX	
			Card 17 is repeated for all sets of ranges, i.e., NELIMS times.

Correction Factor Modes Data

In many instances it is desirable to restrict the incremental correction factors $\{\epsilon\}$ to a linear combination of a set of modes, $\{\epsilon\} = [\phi] \{\epsilon_g\}$. The mode shapes $[\phi]$ can be input directly per box, and per mode, or the mode shapes may be selected from a set of functions. This set of data is input only if the control data item NEM is different from zero.

CARD	ITEM	MNEMONIC	DESCRIPTION
18	ϵ MODE NUMBER	MØDENØ	Weight factor mode number
18	TYPE	ITYPE	TYPE=1, use $(x-a)^n$ TYPE=2, use $(y-a)^n$ TYPE=3, use $(z-a)^n$ TYPE=4, use $\exp[b(x-a)^n]$ TYPE=5, use $\exp [b(y-a)^n]$ TYPE=6, use $\exp [b(z-a)^n]$
			} as mode equation
18	n	NL	} Constants used in the mode equation Card format is 2I10, 4F10.0
18	a	AL	
18	b	BL	
19	J	J	Card 19 is input only if TYPE = 0. Box (or element) number for which the $\phi(J)$ applies
19	$\phi(J)$	PHI(J)	The modal value of the J-th value of ϵ
19	J + 1	J + 1	} Another set of ϕ -data Card format is 2(I10, 2F10.0). Repeat as needed, 2 sets of data per card. Note that only the non-zero elements need be input.
19	$\phi(J+1)$	PHI(J+1)	

CARD	ITEM	MNEMONIC	DESCRIPTION
20	LIML1 LIML2	LIML(1) LIML(2)	Omit card 20 if TYPE = 0. Range of boxes or ϵ 's over which the current ϵ -mode applies. There may be as many sets of ranges input as needed. Card format is 6I10.
21	-1	-1	The number -1; end indicator of data set for the current ϵ -mode (MØDENØ)
			Repeat cards 18 through 21 for all ϵ modes, i.e., NEM times.

Normalwash Data

If the normalwash matrix [W] is needed (see control data FLAGP), and it is not available on tape, the control flag FLAGW must be input as 1, and then the normalwash values are card input as shown below.

CARD	ITEM	MNEMONIC	DESCRIPTION
22	MØDE	MØDE(J)	Mode number for the current set of W values
22	δ	IDELW	Symmetry flag to aid in identifying the mode; note that δ=1 type values are expected to precede the δ=-1 type values
22	LIMW1	LIMW(1)	A range of boxes over which the W value applies
	LIMW2	LIMW(2)	
22	W	WIN	Normalwash, W, for the above range of boxes. Card format is 4I10, 2F10.0. Repeat card 22 as needed. Note that only the non zero W values need be input.
23	-1	-1	The number -1; end indicator for the normalwash input data

Tape Description

Program EIGC uses a minimum of four, and a maximum of twelve tapes and/or utility (scratch) units depending on the type of the case considered. In addition NPIT = 5 and NPOT = 6 are used throughout the program as the system input/output units respectively. These, as well as all tapes and utility units are defined in subroutine WEYT by means of a DATA statement specification under their respective names. The following table gives a summary of tape names and their use; the formats of those tapes that may be specified as input/output units are described in subsequent tables.

Summary of Tape Units

NAME	UNIT	WHEN NEEDED	USER SUBROUTINES	DESCRIPTION OF CONTENTS
NUTL1	1	Always	WEYT, WSWA, SDBL, EPSJ	Miscellaneous intermediate solutions
NUTL2	2	Always	WEYT, SDBL, DCPT, CEMN	
NTSAIJ	3	If $NC \neq 0$	WEYT, SAIJ, DELC, SDBL	SAI matrix rows
NTSANJ	4	If $NM \neq 0$	WEYT, SAIJ, CEMN	SAN matrix rows
NTPHIJ	8	If $NEM \neq 0$	WEYT, PHIJ, SDBL, EPSJ	ϕ matrix columns
MASTSB	9	Always	WEYT, SDBL, GINV	S matrix rows
NEWTSB	10	If $NELIMS \neq 0$	WEYT, MØDF, GINV	The modified S matrix rows
NTGEØM	11	If $FLAGP \neq 3$	WEYT	Geometry arrays; input tape
NTDCP	12	Always	WEYT, DCPB	ΔC_p matrix columns; either input tape or scratch unit depending on FLAGP
NTAPW	13	If $FLAGP \neq 0, 3$	WEYT, WSWA	W (normalwash) columns; input tape if $NTAPW = 0$, scratch unit otherwise
NTAPDI	14		WEYT, DCPB, SDBL, DCPT	Inverse downwash factor matrix $[D]^{-1}$
NEWDCP	15	If $FLAGI=1$ and $FLAGP = 0$	WEYT, DCPB	Complex ΔC_p columns, when ΔC_p is input as a real matrix
NTAPCF	16	If $FLAGB \neq 1$	WEYT, DCPT	CF, the correction factor matrix; NTAPCF is output tape (or scratch unit) for $FLAGB = 0$ cases; NTAPCF is an input tape for $FLAGB = 2$ cases

Input Tape NTGEØM

RECORD	WORD	ITEM	DESCRIPTION
1	1	LENGTH	Length of arrays in records 2 through 6 (LENGTH = NP)
2	1 - NP	X	x-coordinate array
3	1 - NP	Y	y-coordinate array
4	1 - NP	Z	z-coordinate array
5	1 - NP	GMA	Dihedral angle ($\bar{\gamma}$) array
6	1 - NP	DELA	Array of box areas

Input Tape (or Scratch Unit) NTDCP

RECORD	WORD	ITEM	DESCRIPTION
1	1	NP	Row dimension of the ΔC_p matrix (column length)
	2	NSYM	Number of ΔC_p columns for symmetric modes
	3	NASYM	Number of ΔC_p columns for antisymmetric modes
2	1 - NP	DCP	ΔC_p column for first symmetric mode
⋮	⋮	⋮	⋮
1+NSYM +NASYM	1 - NP	DCP	ΔC_p column for last antisymmetric mode*

* Note that if NASYM = 0, the last ΔC_p column refers to last symmetric mode

Input Tape (or Scratch Unit) NTAPW

RECORD	WORD	ITEM	DESCRIPTION
1	1	NP	Row dimension of the W (normalwash) matrix
	2	NSYM	Numbers of W columns for symmetric modes
	3	NASYM	Number of W columns for antisymmetric modes
2	1 - NP	W	W column for first symmetric mode
⋮	⋮	⋮	⋮
1 + NSYM +NASYM	1 - NP	W	W column for last anti-symmetric mode (if any)

Input Tape NTAPDI

RECORD	WORD	ITEM	DESCRIPTION
1	1	NP	Row dimension of matrix DI
	2	NP	Column dimension of matrix DI
	3	NCØL2	NCØL2 = NP if both symmetric and antisymmetric DI matrices are on tape; NCØL2 = 0 otherwise
2	1 - NP	DI	First row of DI, the inverse downwash factor matrix, $[D^{-1}]$ for symmetry
⋮	⋮	⋮	⋮
1 + NP	1 - NP	DI	Last DI-row for symmetry
			The following records may be omitted when antisymmetric modes are not desired.
2 + NP	1 - NP	DI	First DI-row for antisymmetry
⋮	⋮	⋮	⋮
1 + 2NP	1 - NP	DI	Last DI-row for antisymmetry

Input/Output Tape NTAPCF

RECORD	WORD	ITEM	DESCRIPTION
1	1	CØDE	Alphameric identifier of tape, 4 characters in length, left justified; CØDE = PRE, for pre-multiplier cases, CØDE = PØST for post-multiplier cases
2	1	LENGTH	Length of array CF. LENGTH should be equal to NP.
	2	NMSYM	Number of symmetric modes for case
	3	NMASYM	Number of antisymmetric modes for case Note that the last two items are not used when tape NTAPCF is an input tape
3	1 - NP	CF	Array of the complex correction factors

Test Cases. - The use of the program will be illustrated by two test cases. The first will be a premultiplier and will exercise most features of the program so that their use can be illustrated. The second test case will illustrate the use of the new postmultiplier, tape input, and downwash input on cards.

The theoretical pressures are taken from a two-dimensional analysis of an airfoil with a 25% chord flap. The new transonic procedure discussed previously will be used for the airfoil operating at a Mach Number of 0.875 and a reduced frequency of 0.0. Figure 47 illustrates the geometry, pressures and axes data for the airfoil for control surface rotation (Mode 1) and pitch (Mode 2). Also shown on the figure are the theoretical and experimental values of c_{ℓ} , $c_{m1/4}$ and $c_{h1/4}$ for mode 1 and c_{ℓ} for mode 2. The experimental values are used as the constraints. An experimental value for c_{ℓ} for mode 2 is not available thus an estimate is given in its place in the figure.

Test Case 1. - Table III presents the input cards for the first test case. The number of pressures, NP, is 19; the number of constraints, NC, is 4. For this case 19 correction factor modes, ϕ , will be used, thus NEM = 19. In addition limits will be placed on the values of $\bar{\epsilon}$. These limits will be described by one card thus NELIMS = 1. The number of axes, NAXIS, is 3. The program is able to monitor the corrected data, and in this test case the number of coefficients to be monitored, NMON, is 4 and they are c_{ℓ} , $c_{m1/4}$ and $c_{h3/4}$ for mode 1 and c_{ℓ} for mode 2. Thus the monitored coefficients should reproduce the input constraints. This, in fact, is the case as the output shows in Table IV.

Since correction factors are to be calculated rather than data monitored only, FLAGB = 0. Also since the geometrical data and pressure data are to be card input and a premultiplier is to be calculated FLAGP = 3. The usual weight factor T, (the absolute value of the force on an element) is not used, thus FLAGT = 1. Normalwash values are not input thus FLAGW = 0. Only real values of pressure are used thus FLAGI = 1; the detail print flag is input as IPRINT = 1. In this example there are two modes (call them symmetric) thus

NMSYM = 2 and NMASYM = 0. This marks the end of the control data.

The geometry data are taken from figure 47 and are given on cards designated as type 5. The 1/4-chord point of each box is input along with its area, $\Delta A = \Delta X$. The pressures at each 1/4-chord point of each box and for each mode are taken from figure 47 and are given on cards designated as type 6.

The axis data are encountered next. IAX identifies the axis number and IFA identifies how it is input (whether by two points or a point and a direction). In this case a point $(\xi^{(1)}, \eta^{(1)}, \zeta^{(1)})$ and direction $(\cos\alpha, \cos\beta, \cos\gamma)$ are input thus IFA = 1. These points and directions are taken from figure 47 and are input on card designated as type 8.

The constraint data is next. Input are four constraints c_ℓ , $c_{m1/4}$ and $c_{h3/4}$ for mode 1 and c_ℓ for mode 2 taken from the experimental values of these parameters given on figure 47. Each constraint has a 9 and 10 type card. JAX identifies the axis to be used with the constraint (axis 1 for c_ℓ , axis 2 for $c_{m1/4}$ and axis 3 for $c_{h3/4}$). The flag IFA identifies the coefficient type to be calculated whether the force type (IFA = 0) or moment type (IFA = 1). The terms MI and NDI denote the mode to be used. In this case modes 1 and 2 are symmetric. The constraining power AIT is taken as 1.0 for the constraints of mode 1 to ensure a full constraint. However AIT for c_ℓ of mode 2 is taken as .95 since this is an estimate. The nondimensionalizing constant CIT is the chord for the c_ℓ constraint and the chord squared for $c_{m1/4}$ and $c_{h3/4}$. The limits of integration LIM11, LIM12 span the entire surface for c_ℓ and $c_{m1/4}$ (from box 1 to box 19) but only range over the control surface (box 13 to box 19) for $c_{h3/4}$.

The monitor data found on card types 13, 14, 15, 16 are almost identical to that of the constraint data because in this case c_ℓ , $c_{m1/4}$ and $c_{h3/4}$ are the parameters to be monitored. Of course they could be any quantity or for that matter no quantities if monitoring is not desired. The only real difference between monitor data and constraint data is that an alpha-numeric identifier is input in place of the constraints for the monitor data.

As an example of the use of limiting values on $\bar{\epsilon}$, card type 17 is input for this test case. Specifically it is required that

$$-0.7 \leq \epsilon \leq 1.5$$

hold for all values of $\bar{\epsilon}$, 1 through 19 (LIMK1 = 1, LIMK2 = 19).

As a simple example of the use of correction factor mode shapes, ϕ , an identity matrix will be used;

$$[\phi] = [I] \quad (\text{ITYPE} = 0)$$

Card types 19 and 21 are used to input these modes.

The program output for this case is given in Table IV. The printed output, which fits on 8 1/2 x 11 sheets, contains most of the input. Integration matrices are then printed along with other intermediate steps in the process of solution. At the end of the printout a summary of the geometry data, incremental correction factors, ϵ , and modified pressures are printed. Next are the correction factors $\epsilon + 1$ and finally the aerodynamic parameters, calculated using the modified pressures, that have been monitored by the program.

Test Case 2. - Table V presents the input sheets for the second test case. This test case is the same as the test case 1 with the following exceptions: (1) the geometry and $[D]^{-1}$ are input from tape; (2) a new postmultiplier is developed; (3) one mode is used with three constraints; (4) correction factor modes are not used and (5) limits on incremental correction factors, ϵ , are not imposed.

For this case changes from test case 1 occur in the control data (cards 1 through 4). First, no correction factor modes (NEM = 0) are to be used. Second, the card giving limits on ϵ is omitted, thus NELIMS = 0. Third, $[D]^{-1}$ and the geometry are to be read in on tapes and the new postmultiplying

correction factor is desired, thus FLAGP = 4. In this case normalwash values are to be card read and so FLAGW = 1. Also only one mode is to be used (control surface rotation), thus NMSYM = 1. The geometry data remains the same as in test case 1.

Finally the normalwash is input on card type 22. The mode is a control surface rotation, thus $W^* = 1.0$ over boxes 13 through 19, i.e., LIMW1 = 13, LIMW2 = 19. The program output is given in Table VI.

* Remember W is downwash in this computer program

TABLE III
INPUT DATA - TEST CASE I

TEST CASE NO.	1	PRE-MULT.	CARD INPUT	M=.875, K=0	CONTROL DATA	GEOMETRY DATA	PRESSURE DATA	PRESSURE DATA	AXIS DATA	CONSTRAINT DATA
	19	4	19	4	3		6	6	7	9
	0	3	1	1	1				8	10
	2	0	0	0	1					11
										12
-93358	0.0	0.0	0.0	0.0256						
-0.94291	0.0	0.0	0.0	0.075						
-0.34502	0.0	0.0	0.0	0.119						
-0.70657	0.0	0.0	0.0	0.155						
-0.537	0.0	0.0	0.0	0.181						
-0.3479	0.0	0.0	0.0	0.194						
-0.1521	0.0	0.0	0.0	0.181						
0.03701	0.0	0.0	0.0	0.155						
0.20657	0.0	0.0	0.0	0.119						
0.34501	0.0	0.0	0.0	0.075						
0.44291	0.0	0.0	0.0	0.0256						
0.49358	0.0	0.0	0.0	0.0248						
0.50627	0.0	0.0	0.0	0.0694						
0.5545	0.0	0.0	0.0	0.1						
0.64153	0.0	0.0	0.0	0.111						
0.75	0.0	0.0	0.0	0.1						
0.8585	0.0	0.0	0.0	0.094						
0.9455	0.0	0.0	0.0	0.0248						
0.99373	0.0	0.0	0.0	0.14			1.267			
7.0114	2.45	1.61	1.28	12.65			17.0			
2.4884	9.69	8.94	10.24	3.41			1.79			
17.88	12.5	8.42	5.6							
5614	24.5187	15.4279	11.2879	8.77386			7.56652			
71.7527	14.2879	10.5817	8.97737	7.92188			6.79906			
8.20533	6.31302	5.50708	4.08903	2.72631			1.52178			
7.03546										
.437745										
0.0	1	0.0	0.0	0.0						
-0.5	2	0.0	0.0	1.0						
0.5	3	0.0	0.0	0.0						
-1	1	1	1.0	4.93						
-1	1	1	1.0	-1.57						
-1	1	1	1.0	-0.053						
-1	1	1	1.0	8.8						
-1	1	1	1.0	2.0						
-1	1	1	1.0	0.0						

						MONITOR DATA	
-1	1	0	1.0	2.0	CL		13
-1	1	1	1.0				14
-1	1	19					15
-1	2	1	1.0	4.0	CM-1/4		16
-1	1	1	1.0				
-1	1	19					
-1	3	1	1.0	4.0	CH-3/4		
-1	13	1	1.0				
-1	1	0	1.0	2.0	CL-ALPHA		
-1	1	2	1.0				
-1	1	19					
-1	1	19-0.7		0.0	1.5		17
-1	1	0	0.0	0.0	0.0	0.0	18
-1	1	1.0					19
-1	2	0	0.0	0.0	0.0		21
-1	2	1.0					
-1	3	0	0.0	0.0	0.0		
-1	3	1.0					
-1	4	0	0.0	0.0	0.0		
-1	4	1.0					
-1	5	0	0.0	0.0	0.0		
-1	5	1.0					
-1	6	0	0.0	0.0	0.0		
-1	6	1.0					
-1	7	0	0.0	0.0	0.0		
-1	7	1.0					
-1	8	0	0.0	0.0	0.0		
-1	8	1.0					
-1	9	0	0.0	0.0	0.0		
-1	9	1.0					
-1	10	0	0.0	0.0	0.0		
-1	10	1.0					
-1	11	0	0.0	0.0	0.0		
-1	11	1.0					
-1	12	0	0.0	0.0	0.0		
-1	12	1.0					

-1	13	1.0	0	0.0	0.0	0.0
-1	14	1.0	0	0.0	0.0	0.0
-1	15	1.0	0	0.0	0.0	0.0
-1	16	1.0	0	0.0	0.0	0.0
-1	17	1.0	0	0.0	0.0	0.0
-1	18	1.0	0	0.0	0.0	0.0
-1	19	1.0	0	0.0	0.0	0.0

TABLE IV

OUTPUT LISTING - TEST CASE 1

TEST CASE NO. 1 PRE-MULT., CARD INPUT, M=.875, K=0

98

CONTROL FLAGS ---
 FLAGB = 0 CORRECTION FACTORS CALCULATED
 FLAGP = 3 PREMULTIPLIER -- PRESSURE AND GEOMETRY TAKEN FROM CARDS
 FLAGT = 1 WEIGHTS = 1.0
 FLAGW = 0 NORMALWASH TAKEN FROM TAPE (IF NEEDED)
 IPRINT = 1 (DETAIL PRINT FLAG)

CONTROL DIMENSIONS ---
 NP = 19
 NC = 4
 NEM = 19
 NELIMS = 1
 NMON = 4
 NAXIS = 3

LIST OF INPUT/OUTPUT TAPES ---
 GEOMETRY TAPE = 11
 DELTA-CP TAPE = 12
 W TAPE = 13
 D-INVERSE TAPE = 14
 CORR. FACTORS = 16

CARD-READ OPTION IS SPECIFIED

I	X	Y	Z	GAMMA	DELTA-A
1	0.993580	0.0	0.0	0.0	0.025500
2	-0.942910	0.0	0.0	0.0	0.075000
3	-0.845020	0.0	0.0	0.0	0.119000
4	-0.706570	0.0	0.0	0.0	0.155000
5	-0.537000	0.0	0.0	0.0	0.181000
6	-0.347900	0.0	0.0	0.0	0.194000
7	0.152100	0.0	0.0	0.0	0.181000
8	0.206570	0.0	0.0	0.0	0.155000
9	0.342910	0.0	0.0	0.0	0.119000
10	0.493580	0.0	0.0	0.0	0.075000
11	0.506270	0.0	0.0	0.0	0.025500
12	0.493580	0.0	0.0	0.0	0.069400
13	0.554530	0.0	0.0	0.0	0.100000
14	0.641530	0.0	0.0	0.0	0.111000
15	0.750000	0.0	0.0	0.0	0.100000
16	0.858500	0.0	0.0	0.0	0.069400
17	0.945500	0.0	0.0	0.0	0.025500
18	0.993730	0.0	0.0	0.0	0.024800
19	0.0	0.0	0.0	0.0	0.0

SYMMETRIC DELTA-CP MATRIX

100

COLUMN 1

7.010000
1.140000
8.940000
17.880005
3.410000

0.0
0.0
0.0
0.0
0.0

2.450000
1.267000
10.240000
12.500000
1.730000

0.0
0.0
0.0
0.0
0.0

1.610000
2.484000
12.650000
8.420000
0.561400

0.0
0.0
0.0
0.0
0.0

1.280000
9.690000
17.000000
5.600000

0.0
0.0
0.0

COLUMN 2

71.752701
8.773860
10.581700
7.035460
2.726310

0.0
0.0
0.0
0.0
0.0

24.518707
7.566520
8.677370
6.813020
1.521780

0.0
0.0
0.0
0.0
0.0

15.427900
8.205330
7.921880
5.507080
0.499745

0.0
0.0
0.0
0.0
0.0

11.237900
14.287900
6.799060
4.089030

0.0
0.0
0.0

THE 3 SETS OF INPUT DATA FOR ALL AXES

AXISNO(R)	FLAGA(P)	XI1(R)	ETA1(R)	ZETA1(R)	XI2(R) (COSA(R))	ETA2(R) (COSB(R))	ZETA2(R) (COSG(R))
1	1	0.0	0.0	0.0	0.0	0.0	1.000000
2	1	-0.500000	0.0	0.0	0.0	1.000000	0.0
3	1	-0.500000	0.0	0.0	0.0	1.000000	0.0

THE 4 SETS OF INPUT DATA FOR ALL CONSTRAINTS

AXISNO(I)	FLAG(I)	DELTA	M	LIM1	LIM2	A-WIG(I)	C-WIG(I)	REAL C-E(I)	IMAG.
1	0	1	1			1.000000	0.200000E+01	4.930000	0.0
2	1	1	1	1	19	1.000000	0.400000E+01	-1.570000	0.0
3	1	1	1	13	19	1.000000	0.400000E+01	-0.053000	0.0
1	0	1	2	1	19	0.950000	0.200000E+01	8.800000	0.0

THE 4 SETS OF INPUT DATA FOR MONITORING

AXISNO(N)	FLAGF(N)	DELTA	M	LIM1	LIM2	A-WIG(N)	C-WIG(N)	LABEL
1	0	1	1	1	19	1.000000	0.200000E+01	CL
2	1	1	1	1	19	1.000000	0.400000E+01	CM-1/4
3	1	1	1	13	19	1.000000	0.400000E+01	CH-3/4
1	0	1	2	1	19	1.000000	0.200000E+01	CL-ALPHA

SAI MATRIX ROWS

0.012800	0.00	0.059500	0.00	0.077500	0.00
0.090500	0.00	0.097000	0.00	0.090500	0.00
0.077500	0.00	0.037500	0.00	0.012800	0.00
0.012400	0.00	0.050000	0.00	0.055500	0.00
0.050000	0.00	0.012400	0.00	0.008005	0.00
0.003159	0.00	0.010264	0.00	-0.024300	0.00
0.01674	0.00	-0.016873	0.00	-0.006359	0.00
-0.027380	0.00	-0.017680	0.00	-0.034688	0.00
-0.006239	0.00	-0.028538	0.00	0.00	0.00
-0.033962	0.00	-0.009261	0.00	0.00	0.00
0.00	0.00	0.00	0.00	0.00	0.00
0.00	0.00	0.00	0.00	-0.006938	0.00
0.000039	0.00	0.003538	0.00	0.077500	0.00
-0.008963	0.00	-0.003061	0.00	0.090500	0.00
0.012800	0.00	0.059500	0.00	0.012800	0.00
0.090500	0.00	0.097000	0.00	0.055500	0.00
0.077500	0.00	0.037500	0.00	0.00	0.00
0.012400	0.00	0.050000	0.00	0.00	0.00
0.050000	0.00	0.012400	0.00	0.00	0.00
0.003159	0.00	0.010264	0.00	0.00	0.00
0.01674	0.00	-0.016873	0.00	0.00	0.00
-0.027380	0.00	-0.017680	0.00	0.00	0.00
-0.006239	0.00	-0.028538	0.00	0.00	0.00
-0.033962	0.00	-0.009261	0.00	0.00	0.00
0.00	0.00	0.00	0.00	0.00	0.00
0.00	0.00	0.00	0.00	0.00	0.00
0.000039	0.00	0.003538	0.00	0.00	0.00
-0.008963	0.00	-0.003061	0.00	0.00	0.00
0.012800	0.00	0.059500	0.00	0.00	0.00
0.090500	0.00	0.097000	0.00	0.00	0.00
0.077500	0.00	0.037500	0.00	0.00	0.00
0.012400	0.00	0.050000	0.00	0.00	0.00
0.050000	0.00	0.012400	0.00	0.00	0.00

SAN MATRIX PDWS

0.012800	0.0	0.077500	0.0	0.059500	0.0	0.037500	0.0	0.012800	0.0	0.0	0.0
0.090500	0.0	0.090500	0.0	0.097000	0.0	0.097000	0.0	0.090500	0.0	0.0	0.0
0.012400	0.0	0.034700	0.0	0.034700	0.0	0.034700	0.0	0.012400	0.0	0.0	0.0
0.050000	0.0	0.034700	0.0	0.034700	0.0	0.034700	0.0	0.050000	0.0	0.0	0.0
0.003159	0.0	0.008305	0.0	0.008305	0.0	0.008305	0.0	0.003159	0.0	0.0	0.0
0.001674	0.0	0.007377	0.0	0.007377	0.0	0.007377	0.0	0.001674	0.0	0.0	0.0
-0.027380	-0.0	-0.025139	-0.0	-0.025139	-0.0	-0.025139	-0.0	-0.027380	-0.0	-0.0	-0.0
-0.006239	-0.0	-0.018296	-0.0	-0.018296	-0.0	-0.018296	-0.0	-0.006239	-0.0	-0.0	-0.0
-0.033962	-0.0	-0.025079	-0.0	-0.025079	-0.0	-0.025079	-0.0	-0.033962	-0.0	-0.0	-0.0
0.0	0.0	0.0	0.0	0.0	0.0	0.0	0.0	0.0	0.0	0.0	0.0
0.0	0.0	0.0	0.0	0.0	0.0	0.0	0.0	0.0	0.0	0.0	0.0
0.000039	0.0	0.000946	0.0	0.000946	0.0	0.000946	0.0	0.000039	0.0	0.0	0.0
-0.008963	-0.0	-0.007729	-0.0	-0.007729	-0.0	-0.007729	-0.0	-0.008963	-0.0	-0.0	-0.0
0.012800	0.0	0.037500	0.0	0.037500	0.0	0.037500	0.0	0.012800	0.0	0.0	0.0
0.090500	0.0	0.097000	0.0	0.097000	0.0	0.097000	0.0	0.090500	0.0	0.0	0.0
0.077500	0.0	0.059500	0.0	0.059500	0.0	0.059500	0.0	0.077500	0.0	0.0	0.0
0.012400	0.0	0.034700	0.0	0.034700	0.0	0.034700	0.0	0.012400	0.0	0.0	0.0
0.050000	0.0	0.034700	0.0	0.034700	0.0	0.034700	0.0	0.050000	0.0	0.0	0.0

```

EPSILON LIMITS  --
K   LIM-1(K)   LIM-2(K)   EPSILON-RAP-MIN   EPSILON-PAP-MAX
    REAL      REAL      REAL      REAL      REAL
1   1          19        -0.700000        1.500000        0.0

```

-PHI- MATRIX

COLUMN 1

```

1.000000
0.0
0.0
0.0
0.0

```

COLUMN 2

```

0.0
0.0
0.0
0.0
1.000000
0.0
0.0
0.0

```

COLUMN 3

```

0.0
0.0
0.0
0.0
0.0
0.0
0.0
1.000000

```

COLUMN 4

```

0.0
0.0
0.0
0.0
0.0
0.0
0.0
0.0
1.000000

```

COLUMN 5

```

0.0
0.0
0.0
0.0
1.000000
0.0
0.0
0.0

```

COLUMN 6

```

0.0
0.0
0.0
0.0
0.0
0.0
0.0
1.000000

```

COLUMN 7

```

0.0
0.0
0.0
0.0
0.0
0.0
1.000000
0.0

```

COLUMN 8

```

0.000000 0.000000 0.000000 0.000000 0.000000 0.000000 0.000000
0.000000 0.000000 0.000000 1.000000 0.000000 0.000000 0.000000
0.000000 0.000000 0.000000 0.000000 0.000000 0.000000 0.000000
0.000000 0.000000 1.000000 0.000000 0.000000 0.000000 0.000000
0.000000 0.000000 0.000000 0.000000 0.000000 0.000000 0.000000
0.000000 0.000000 0.000000 0.000000 0.000000 0.000000 0.000000
0.000000 0.000000 0.000000 0.000000 0.000000 0.000000 0.000000

```


0.0
0.0
0.0

0.0000	0.0000	0.0000
0.0000	0.0000	0.0000
0.0000	0.0000	0.0000

0.0
0.0
0.0
0.0
0.0

0.0000	0.0000	0.0000
0.0000	0.0000	0.0000
0.0000	0.0000	0.0000

0.0
0.0

0.0000	0.0000	0.0000
0.0000	0.0000	0.0000

0.0

0.0000	0.0000	0.0000
0.0000	0.0000	0.0000
0.0000	0.0000	0.0000

0.000000

0.0
0.0

0.0000	0.0000	0.0000
0.0000	0.0000	0.0000

0.0

0.0000	0.0000	0.0000
0.0000	0.0000	0.0000
0.0000	0.0000	0.0000

0.000000

0.0
0.0

0.0000	0.0000	0.0000
0.0000	0.0000	0.0000

0.0
0.0
0.0
0.0
0.0

COLUMN 1

0.000000

COLUMN 18

0.0000	0.0000	0.0000
0.0000	0.0000	0.0000
0.0000	0.0000	0.0000
0.0000	0.0000	0.0000

COLUMN 19

0.0000	0.0000	0.0000
0.0000	0.0000	0.0000
0.0000	0.0000	0.0000
0.0000	0.0000	0.0000

THE 2 COLUMNS OF THE DELTA-CP-RAR MATRIX

110	COLUMN 1			
	1	0.701000E+01	0.0	0.0
	4	0.128000E+01	0.0	0.0
	7	0.248400E+01	0.0	0.0
	10	0.102400E+02	0.0	0.0
	13	0.178800E+02	0.0	0.0
	16	0.560000E+01	0.0	0.0
	19	0.561400E+00	0.0	0.0
		2	0.245000E+01	0.0
		5	0.114000E+01	0.0
		8	0.969000E+01	0.0
		11	0.126500E+02	0.0
		14	0.125000E+02	0.0
		17	0.341000E+01	0.0
		3	0.161000E+01	0.0
		6	0.126700E+01	0.0
		9	0.894000E+01	0.0
		12	0.170000E+02	0.0
		15	0.842000E+01	0.0
		18	0.179000E+01	0.0

COLUMN 2

1	0.717527E+02	0.0					
4	0.112879E+02	0.0					
7	0.820533E+01	0.0					
10	0.897737E+01	0.0					
13	0.703546E+01	0.0					
16	0.408903E+01	0.0					
19	0.489745E+00	0.0					
2	0.245187E+02	0.0					
5	0.877386E+01	0.0					
8	0.142879E+02	0.0					
11	0.792188E+01	0.0					
14	0.681302E+01	0.0					
17	0.272631E+01	0.0					
3	0.154279E+02	0.0					
6	0.756652E+01	0.0					
9	0.105817E+02	0.0					
12	0.679906E+01	0.0					
15	0.550708E+01	0.0					
18	0.152178E+01	0.0					

DELTA-C

-0.411495 0.0 0.420184 0.0 0.074273 0.0 -1.207082 0.0

THEORETICAL C-VALUES

5.341496 0.0 -1.990184 0.0 -0.127273 0.0 10.007082 0.0

ONE S-BAR ROW

0.089728 0.0 0.091875 0.0 0.095795 0.0 0.099200 0.0
 0.103170 0.0 0.122899 0.0 0.240948 0.0 0.876945 0.0
 0.692850 0.0 0.609280 0.0 0.474375 0.0 0.217600 0.0
 0.221712 0.0 0.433750 0.0 0.421000 0.0 0.310800 0.0
 0.170500 0.0 0.062113 0.0 0.006961 0.0 0.0 0.0
 0.0 0.0 0.0 0.0 0.0 0.0 0.0 0.0

ONE S-BAR ROW

0.022144 0.0 0.020346 0.0 0.016526 0.0 0.010246 0.0
 0.001909 0.0 -0.009346 0.0 -0.041913 0.0 -0.235464 0.0
 -0.244773 0.0 -0.257424 0.0 -0.223646 0.0 -0.108101 0.0
 -0.11551 0.0 -0.228695 0.0 -0.240292 0.0 -0.194250 0.0
 -0.115812 0.0 -0.044892 0.0 -0.005199 0.0 0.0 0.0
 0.0 0.0 0.0 0.0 0.0 0.0 0.0 0.0

ONE S-BAR ROW

0.0 0.0 0.0 0.0 0.0 0.0 0.0 0.0
 0.0 0.0 0.0 0.0 0.0 0.0 0.0 0.0
 -0.000695 0.0 -0.011820 0.0 -0.029792 0.0 -0.038850 0.0
 -0.030562 0.0 -0.013836 0.0 -0.001719 0.0 0.0 0.0
 0.0 0.0 0.0 0.0 0.0 0.0 0.0 0.0

ONE S-BAR ROW

0.918435 0.0 0.919451 0.0 0.917960 0.0 0.874812 0.0
 0.794034 0.0 0.733952 0.0 0.795917 0.0 1.293055 0.0
 0.820082 0.0 0.534154 0.0 0.297070 0.0 0.087028 0.0
 0.087240 0.0 0.236412 0.0 0.275354 0.0 0.226941 0.0
 0.136315 0.0 0.052806 0.0 0.006073 0.0 0.0 0.0
 0.0 0.0 0.0 0.0 0.0 0.0 0.0 0.0

-S- MATRIX

0.255609E+01	0.0	0.0	0.0	0.0	0.0	0.0	0.0	0.0	0.0
0.322784E+01	0.0	0.0	0.0	0.0	0.0	0.0	0.0	0.0	0.0
0.216555E-01	0.0	0.0	0.0	0.0	0.0	0.0	0.0	0.0	0.0
0.216555E-01	0.0	0.0	0.0	0.0	0.0	0.0	0.0	0.0	0.0
0.322784E+01	0.0	0.0	0.0	0.0	0.0	0.0	0.0	0.0	0.0
0.804018E+01	0.0	0.0	0.0	0.0	0.0	0.0	0.0	0.0	0.0

-0.359801E-01	0.0
0.422131E+00	0.0
-0.359801E-01	0.0
-0.247821E-01	0.0
-0.247821E-01	0.0

-DC- COLUMN

-0.411495E+00	0.0	0.0	0.0	0.0	0.0	0.0	0.0	0.0	0.0
-0.120708E+01	0.0	0.0	0.0	0.0	0.0	0.0	0.0	0.0	0.0

0.742729E-01	0.0
--------------	-----

SOLUTION OF MATRIX EQ.

0.109207E+02	0.0	0.0	0.0	0.0	0.0	0.0	0.0	0.0	0.0
-0.206261E+01	0.0	0.0	0.0	0.0	0.0	0.0	0.0	0.0	0.0

-0.227097E+02	0.0
---------------	-----

OUTPUT OF GEN. INVERSE (EPS-TILDA)

-0.403892	0.0	0.0	0.0	0.0	0.0	0.0	0.0	0.0	0.0
-0.467087	0.0	0.0	0.0	0.0	0.0	0.0	0.0	0.0	0.0
0.230980	0.0	0.0	0.0	0.0	0.0	0.0	0.0	0.0	0.0
-0.315017	0.0	0.0	0.0	0.0	0.0	0.0	0.0	0.0	0.0
-0.395491	0.0	0.0	0.0	0.0	0.0	0.0	0.0	0.0	0.0

-0.466205	0.0
-0.023238	0.0
-0.589009	0.0
-0.834346	0.0
-0.017357	0.0
-0.108558	0.0

-0.484818	0.0
-1.480520	0.0
-0.295733	0.0
-0.670626	0.0

J	EPSILON-BAR	EPSILON-LIMIT	EPSILON-LAST
1	0.403892	0.0	0.0
2	0.423996	0.0	0.0
3	0.466205	0.0	0.0
4	0.464818	0.0	0.0
5	0.467087	0.0	0.0
6	0.387223	0.0	0.0
7	0.023238	0.0	0.0
8	1.480520	0.0	0.0
9	0.230980	0.0	0.0
10	0.383590	0.0	0.0
11	0.589009	0.0	0.0
12	0.295733	0.0	0.0
13	0.315017	0.0	0.0
14	0.75526	0.70000	0.0
15	0.834346	0.70000	0.0
16	0.670626	0.0	0.0
17	0.395491	0.0	0.0
18	0.151506	0.0	0.0
19	0.017357	0.0	0.0
20	0.0	0.0	0.0
21	0.0	0.0	0.0
22	0.0	0.0	0.0
23	0.108558	0.0	0.108558

THE 4 BY 23 S-DOUBLE-BAR MATRIX

116

ROW 1

1	0.897280E-01	0.0	0.0	0.918750E-01	0.0	0.0	0.957950E-01	0.0	0.0
4	0.992000E-01	0.0	0.0	0.103170E+00	0.0	0.0	0.122899E+00	0.0	0.0
7	0.240948E+00	0.0	0.0	0.876945E+00	0.0	0.0	0.692850E+00	0.0	0.0
10	0.609280E+00	0.0	0.0	0.474375E+00	0.0	0.0	0.217600E+00	0.0	0.0
13	0.221712E+00	0.0	0.0	0.0	0.0	0.0	0.0	0.0	0.0
16	0.310800E+00	0.0	0.0	0.170500E+00	0.0	0.0	0.621130E-01	0.0	0.0
19	0.696136E-02	0.0	0.0	0.0	0.0	0.0	0.0	0.0	0.0
22	0.0	0.0	0.0	0.0	0.0	0.0	0.0	0.0	0.0

ROW 2

1	0.221440E-01	0.0	0.0	0.203462E-01	0.0	0.0	0.165256E-01	0.0	0.0
4	0.102459E-01	0.0	0.0	0.190865E-02	0.0	0.0	0.934647E-02	0.0	0.0
7	-0.419129E-01	0.0	0.0	-0.235464E+00	0.0	0.0	-0.244773E+00	0.0	0.0
10	-0.257424E+00	0.0	0.0	-0.223646E+00	0.0	0.0	-0.108101E+00	0.0	0.0
13	-0.111551E+00	0.0	0.0	0.0	0.0	0.0	0.0	0.0	0.0
16	-0.194250E+00	0.0	0.0	-0.115812E+00	0.0	0.0	-0.448922E-01	0.0	0.0
19	-0.519919E-02	0.0	0.0	0.0	0.0	0.0	0.0	0.0	0.0
22	0.0	0.0	0.0	0.0	0.0	0.0	0.0	0.0	0.0

ROW 3

1	0.0	0.0	0.0	0.0	0.0	0.0	0.0	0.0	0.0
4	0.0	0.0	0.0	0.0	0.0	0.0	0.0	0.0	0.0
7	0.0	0.0	0.0	0.0	0.0	0.0	0.0	0.0	0.0
10	0.0	0.0	0.0	0.0	0.0	0.0	0.0	0.0	0.0
13	-0.695066E-03	0.0	0.0	0.0	0.0	0.0	0.0	0.0	0.0
16	-0.388500E-01	0.0	0.0	-0.305621E-01	0.0	0.0	-0.138357E-01	0.0	0.0
19	-0.171852E-02	0.0	0.0	0.0	0.0	0.0	0.0	0.0	0.0
22	0.0	0.0	0.0	0.0	0.0	0.0	0.0	0.0	0.0

ROW 4

1	0.918435E+00	0.0	0.0	0.919451E+00	0.0	0.0	0.917960E+00	0.0	0.0
4	0.874812E+00	0.0	0.0	0.794034E+00	0.0	0.0	0.733952E+00	0.0	0.0
7	0.795917E+00	0.0	0.0	0.129305E+01	0.0	0.0	0.820082E+00	0.0	0.0
10	0.534154E+00	0.0	0.0	0.297070E+00	0.0	0.0	0.870280E-01	0.0	0.0
13	0.872397E-01	0.0	0.0	0.0	0.0	0.0	0.0	0.0	0.0
16	0.226941E+00	0.0	0.0	0.136315E+00	0.0	0.0	0.528058E-01	0.0	0.0
19	0.607283E-02	0.0	0.0	0.0	0.0	0.0	0.0	0.0	0.0
22	0.0	0.0	0.0	0.526316E-01	0.0	0.0	0.0	0.0	0.0

DELTA-C-MOD

0.186830	0.0	0.091894	0.0	0.045145	0.0	-0.848846	0.0	0.0
----------	-----	----------	-----	----------	-----	-----------	-----	-----

-S- MATRIX

0.219071E+01	0.0	0.0	0.0	0.0	0.0	0.0	0.0	0.0	0.0
0.300937E+01	0.0	0.0	0.0	0.0	0.0	0.0	0.0	0.0	0.0
0.117937E-01	0.0	0.0	0.0	0.0	0.0	0.0	0.0	0.0	0.0
0.117937E-01	0.0	0.0	0.0	0.0	0.0	0.0	0.0	0.0	0.0
0.300937E+01	0.0	0.0	0.0	0.0	0.0	0.0	0.0	0.0	0.0
0.790847E+01	0.0	0.0	0.0	0.0	0.0	0.0	0.0	0.0	0.0

-DC- COLUMN

0.186830E+00	0.0	0.0	0.0	0.0	0.0	0.0	0.0	0.0	0.0
-0.848846E+00	0.0	0.0	0.0	0.0	0.0	0.0	0.0	0.0	0.0

SOLUTION OF MATRIX EQ.

0.112057E+02	0.0	0.0	0.0	0.0	0.0	0.0	0.0	0.0	0.0
-0.210554E+01	0.0	0.0	0.0	0.0	0.0	0.0	0.0	0.0	0.0

OUTPUT OF GEN. INVERSE (EPS-TILDA)

-0.401396	0.0	0.0	0.0	0.0	0.0	0.0	0.0	0.0	0.0
-0.470355	0.0	0.0	0.0	0.0	0.0	0.0	0.0	0.0	0.0
0.212602	0.0	0.0	0.0	0.0	0.0	0.0	0.0	0.0	0.0
-0.338055	0.0	0.0	0.0	0.0	0.0	0.0	0.0	0.0	0.0
-0.444962	0.0	0.0	0.0	0.0	0.0	0.0	0.0	0.0	0.0
0.0	0.0	0.0	0.0	0.0	0.0	0.0	0.0	0.0	0.0
0.422258	0.0	0.0	0.0	0.0	0.0	0.0	0.0	0.0	0.0
-0.390596	0.0	0.0	0.0	0.0	0.0	0.0	0.0	0.0	0.0
-0.422853	0.0	0.0	0.0	0.0	0.0	0.0	0.0	0.0	0.0
0.0	0.0	0.0	0.0	0.0	0.0	0.0	0.0	0.0	0.0
-0.172254	0.0	0.0	0.0	0.0	0.0	0.0	0.0	0.0	0.0
0.0	0.0	0.0	0.0	0.0	0.0	0.0	0.0	0.0	0.0
0.466105	0.0	0.0	0.0	0.0	0.0	0.0	0.0	0.0	0.0
-0.026817	0.0	0.0	0.0	0.0	0.0	0.0	0.0	0.0	0.0
-0.631618	0.0	0.0	0.0	0.0	0.0	0.0	0.0	0.0	0.0
0.0	0.0	0.0	0.0	0.0	0.0	0.0	0.0	0.0	0.0
-0.019850	0.0	0.0	0.0	0.0	0.0	0.0	0.0	0.0	0.0
-0.110818	0.0	0.0	0.0	0.0	0.0	0.0	0.0	0.0	0.0
0.486531	0.0	0.0	0.0	0.0	0.0	0.0	0.0	0.0	0.0
-1.501185	0.0	0.0	0.0	0.0	0.0	0.0	0.0	0.0	0.0
-0.317233	0.0	0.0	0.0	0.0	0.0	0.0	0.0	0.0	0.0
-0.743718	0.0	0.0	0.0	0.0	0.0	0.0	0.0	0.0	0.0

EPSILON-LAST

-0.401396
 -0.422258
 -0.466105
 -0.486531
 -0.470355
 -0.390596
 -0.026817
 1.500000
 0.212602
 -0.422853
 -0.631618
 -0.317233
 -0.338055
 -0.700000
 -0.700000
 -0.444962
 -0.172254
 -0.019850
 0.0
 0.0
 -0.110818

0.0
 0.0
 0.0
 0.0
 0.0
 0.0
 0.0
 0.0
 0.0
 0.0
 0.0
 0.0
 0.0
 0.0
 0.0
 0.0
 0.0
 0.0
 0.0

EPSILON-LIMIT

0.0
 0.0
 0.0
 0.0
 0.0
 0.0
 1.500000
 0.0
 0.0
 0.0
 0.0
 0.0
 0.700000
 0.700000
 0.0
 0.0
 0.0
 0.0
 0.0

0.0
 0.0
 0.0
 0.0
 0.0
 0.0
 0.0
 0.0
 0.0
 0.0
 0.0
 0.0
 0.0
 0.0
 0.0
 0.0
 0.0
 0.0

EPSILON-BAR

-0.401396
 -0.422258
 -0.466105
 -0.486531
 -0.470355
 -0.390596
 1.501185
 0.212602
 -0.422853
 -0.631618
 -0.317233
 -0.338055
 0.0
 0.743718
 -0.444962
 -0.172254
 -0.019850
 0.0
 0.0
 -0.110818

J 1
 1 2 3 4 5 6 7 8 9
 10
 11
 12
 13
 14
 15
 16
 17
 18
 19
 20
 21
 22
 23

THE 4 BY 23 S-DOUBLE-BAR MATRIX

ROW	1	2	3	4	5	6	7	8	9	10	11	12	13	14	15	16	17	18	19	20	21	22	23
1	0.897280E-01	0.918750E-01	0.203462E-01	0.919451E+00	0.0	0.0	0.0	0.0	0.0	0.0	0.0	0.0	0.0	0.0	0.0	0.0	0.0	0.0	0.0	0.0	0.0	0.0	0.0
4	0.992000E-01	0.103170E+00	0.190865E-02	0.794034E+00	0.0	0.0	0.0	0.0	0.0	0.0	0.0	0.0	0.0	0.0	0.0	0.0	0.0	0.0	0.0	0.0	0.0	0.0	0.0
7	0.240948E+00	0.0	0.0	0.0	0.0	0.0	0.0	0.0	0.0	0.0	0.0	0.0	0.0	0.0	0.0	0.0	0.0	0.0	0.0	0.0	0.0	0.0	0.0
10	0.609280E+00	0.474375E+00	-0.223646E+00	0.297070E+00	0.0	0.0	0.0	0.0	0.0	0.0	0.0	0.0	0.0	0.0	0.0	0.0	0.0	0.0	0.0	0.0	0.0	0.0	0.0
13	0.221712E+00	0.0	0.0	0.0	0.0	0.0	0.0	0.0	0.0	0.0	0.0	0.0	0.0	0.0	0.0	0.0	0.0	0.0	0.0	0.0	0.0	0.0	0.0
16	0.0	0.170500E+00	-0.0	0.136315E+00	0.0	0.0	0.0	0.0	0.0	0.0	0.0	0.0	0.0	0.0	0.0	0.0	0.0	0.0	0.0	0.0	0.0	0.0	0.0
19	0.696136E-02	0.0	0.0	0.0	0.0	0.0	0.0	0.0	0.0	0.0	0.0	0.0	0.0	0.0	0.0	0.0	0.0	0.0	0.0	0.0	0.0	0.0	0.0
22	0.0	0.0	0.0	0.526316E-01	0.0	0.0	0.0	0.0	0.0	0.0	0.0	0.0	0.0	0.0	0.0	0.0	0.0	0.0	0.0	0.0	0.0	0.0	0.0

ROW	2	3	4	5	6	7	8	9	10	11	12	13	14	15	16	17	18	19	20	21	22	23	
1	0.221440E-01	0.165256E-01	0.0	0.917960E+00	0.0	0.0	0.0	0.0	0.0	0.0	0.0	0.0	0.0	0.0	0.0	0.0	0.0	0.0	0.0	0.0	0.0	0.0	0.0
4	0.102459E-01	-0.934647E-02	0.0	0.733952E+00	0.0	0.0	0.0	0.0	0.0	0.0	0.0	0.0	0.0	0.0	0.0	0.0	0.0	0.0	0.0	0.0	0.0	0.0	0.0
7	-0.419129E-01	-0.244773E+00	0.0	0.820082E+00	0.0	0.0	0.0	0.0	0.0	0.0	0.0	0.0	0.0	0.0	0.0	0.0	0.0	0.0	0.0	0.0	0.0	0.0	0.0
10	-0.257424E+00	-0.108101E+00	0.0	0.870280E-01	0.0	0.0	0.0	0.0	0.0	0.0	0.0	0.0	0.0	0.0	0.0	0.0	0.0	0.0	0.0	0.0	0.0	0.0	0.0
13	-0.111551E+00	0.0	0.0	0.0	0.0	0.0	0.0	0.0	0.0	0.0	0.0	0.0	0.0	0.0	0.0	0.0	0.0	0.0	0.0	0.0	0.0	0.0	0.0
16	0.0	0.0	0.0	0.0	0.0	0.0	0.0	0.0	0.0	0.0	0.0	0.0	0.0	0.0	0.0	0.0	0.0	0.0	0.0	0.0	0.0	0.0	0.0
19	-0.519919E-02	-0.448922E-01	0.0	0.528058E-01	0.0	0.0	0.0	0.0	0.0	0.0	0.0	0.0	0.0	0.0	0.0	0.0	0.0	0.0	0.0	0.0	0.0	0.0	0.0
22	0.0	0.0	0.0	0.0	0.0	0.0	0.0	0.0	0.0	0.0	0.0	0.0	0.0	0.0	0.0	0.0	0.0	0.0	0.0	0.0	0.0	0.0	0.0

ROW	3	4	5	6	7	8	9	10	11	12	13	14	15	16	17	18	19	20	21	22	23		
1	0.0	0.0	0.0	0.918435E+00	0.0	0.0	0.0	0.0	0.0	0.0	0.0	0.0	0.0	0.0	0.0	0.0	0.0	0.0	0.0	0.0	0.0	0.0	0.0
4	0.0	0.0	0.0	0.874812E+00	0.0	0.0	0.0	0.0	0.0	0.0	0.0	0.0	0.0	0.0	0.0	0.0	0.0	0.0	0.0	0.0	0.0	0.0	0.0
7	0.0	0.0	0.0	0.795917E+00	0.0	0.0	0.0	0.0	0.0	0.0	0.0	0.0	0.0	0.0	0.0	0.0	0.0	0.0	0.0	0.0	0.0	0.0	0.0
10	0.0	0.0	0.0	0.534154E+00	0.0	0.0	0.0	0.0	0.0	0.0	0.0	0.0	0.0	0.0	0.0	0.0	0.0	0.0	0.0	0.0	0.0	0.0	0.0
13	-0.695066E-03	0.6095066E-03	0.0	0.872397E-01	0.0	0.0	0.0	0.0	0.0	0.0	0.0	0.0	0.0	0.0	0.0	0.0	0.0	0.0	0.0	0.0	0.0	0.0	0.0
16	0.0	0.0	0.0	0.0	0.0	0.0	0.0	0.0	0.0	0.0	0.0	0.0	0.0	0.0	0.0	0.0	0.0	0.0	0.0	0.0	0.0	0.0	0.0
19	-0.171852E-02	-0.171852E-02	0.0	0.0	0.0	0.0	0.0	0.0	0.0	0.0	0.0	0.0	0.0	0.0	0.0	0.0	0.0	0.0	0.0	0.0	0.0	0.0	0.0
22	0.0	0.0	0.0	0.0	0.0	0.0	0.0	0.0	0.0	0.0	0.0	0.0	0.0	0.0	0.0	0.0	0.0	0.0	0.0	0.0	0.0	0.0	0.0

DELTA-C-MOD

-0.911027 0.0 0.309115 0.0 0.017950 0.0 -2.629568 0.0

-S- MATRIX

0.132509E+01	0.0	0.507947E+00	0.0	-0.623628E-02	0.0
0.180490E+01	0.0	-0.507947E+00	0.0	0.218913E+00	0.0
0.424704E-02	0.0	-0.417531E+00	0.0	-0.623628E-02	0.0
0.424704E-02	0.0	0.112890E-02	0.0	-0.496776E-02	0.0
0.180490E+01	0.0	-0.417531E+00	0.0	-0.496776E-02	0.0
0.618498E+01	0.0				

-DC- COLUMN

-0.911027E+00	0.0	0.309115E+00	0.0	0.179497E-01	0.0
-0.262957E+01	0.0				

SOLUTION OF MATRIX EQ.

0.113088E+02	0.0	0.240208E+02	0.0	-0.213291E+02	0.0
-0.212086E+01	0.0				

OUTPUT OF GEN. INVERSE (EPS-TILDA)

-0.401236	0.0	-0.422297	0.0	-0.466577	0.0	-0.487404	0.0
-0.471456	0.0	-0.391275	0.0	-0.030033	0.0	0.0	0.0
0.216393	0.0	-0.426141	0.0	-0.637582	0.0	-0.320454	0.0
-0.342438	0.0	0.0	0.0	0.0	0.0	0.0	0.0
-0.490984	0.0	-0.192810	0.0	-0.022389	0.0	0.0	0.0
0.0	0.0	0.0	0.0	-0.111624	0.0	0.0	0.0

SYMMETRIC DELTA-CP-TILDA , MODE 1

J	X(J)	Y(J)	Z(J)	GAMMA(J)	DELTA-A(J)	EPS(J) REAL	EPS(J) IMAG.	DCP-TILDA(J) REAL	DCP-TILDA(J) IMAG.
1	-0.9936	0.0	0.0	0.0	0.0256	-0.401236	0.0	4.197338	0.0
2	-0.9429	0.0	0.0	0.0	0.0750	-0.422297	0.0	1.415373	0.0
3	-0.8450	0.0	0.0	0.0	0.1190	-0.466577	0.0	0.858811	0.0
4	-0.7066	0.0	0.0	0.0	0.1550	-0.487404	0.0	0.656123	0.0
5	-0.5370	0.0	0.0	0.0	0.1810	-0.471456	0.0	0.602541	0.0
6	-0.3479	0.0	0.0	0.0	0.1940	-0.391275	0.0	0.771254	0.0
7	-0.1521	0.0	0.0	0.0	0.1940	0.030033	0.0	2.558602	0.0
8	0.0370	0.0	0.0	0.0	0.1810	1.500000	0.0	24.224991	0.0
9	0.2066	0.0	0.0	0.0	0.1550	0.216393	0.0	10.874557	0.0
10	0.3429	0.0	0.0	0.0	0.1190	-0.426141	0.0	5.876318	0.0
11	0.4429	0.0	0.0	0.0	0.0750	-0.637582	0.0	4.584589	0.0
12	0.4936	0.0	0.0	0.0	0.0256	-0.320454	0.0	11.552276	0.0
13	0.5063	0.0	0.0	0.0	0.0248	-0.342438	0.0	11.757212	0.0
14	0.5415	0.0	0.0	0.0	0.0694	-0.700000	0.0	13.750000	0.0
15	0.6415	0.0	0.0	0.0	0.1000	-0.700000	0.0	2.526000	0.0
16	0.7500	0.0	0.0	0.0	0.1110	-0.700000	0.0	1.679999	0.0
17	0.8585	0.0	0.0	0.0	0.1000	-0.490984	0.0	1.735744	0.0
18	0.9455	0.0	0.0	0.0	0.0694	-0.192810	0.0	1.444869	0.0
19	0.9937	0.0	0.0	0.0	0.0248	-0.022389	0.0	0.548831	0.0

SYMMETRIC DELTA-CP-TILDA , MCDE 2									
J	X(J)	Y(J)	Z(J)	GAMMA(J)	DELTA-A(J)	REAL	IMAG.	REAL	IMAG.
1	-0.9936	0.0	0.0	0.0	0.0256	-0.401236	0.0	42.962952	0.0
2	-0.9429	0.0	0.0	0.0	0.0750	-0.422297	0.0	14.164542	0.0
3	-0.8450	0.0	0.0	0.0	0.1190	-0.466577	0.0	18.229603	0.0
4	-0.7066	0.0	0.0	0.0	0.1550	-0.487404	0.0	5.786134	0.0
5	-0.5379	0.0	0.0	0.0	0.1810	-0.471456	0.0	4.637374	0.0
6	-0.3479	0.0	0.0	0.0	0.1940	-0.391275	0.0	4.605927	0.0
7	-0.1521	0.0	0.0	0.0	0.1940	0.030033	0.0	8.451761	0.0
8	0.0370	0.0	0.0	0.0	0.1810	1.500000	0.0	35.719742	0.0
9	0.2066	0.0	0.0	0.0	0.1550	0.216393	0.0	12.871511	0.0
10	0.3450	0.0	0.0	0.0	0.1190	0.426141	0.0	15.151746	0.0
11	0.4429	0.0	0.0	0.0	0.0750	-0.637582	0.0	2.871033	0.0
12	0.4936	0.0	0.0	0.0	0.0256	-0.320454	0.0	4.626251	0.0
13	0.5063	0.0	0.0	0.0	0.0248	-0.342438	0.0	2.043905	0.0
14	0.5545	0.0	0.0	0.0	0.0694	-0.700000	0.0	1.652123	0.0
15	0.6415	0.0	0.0	0.0	0.1000	-0.700000	0.0	1.226708	0.0
16	0.7500	0.0	0.0	0.0	0.1110	-0.700000	0.0	1.387734	0.0
17	0.8585	0.0	0.0	0.0	0.1000	-0.490984	0.0	1.226708	0.0
18	0.9455	0.0	0.0	0.0	0.0694	-0.192810	0.0	1.226708	0.0
19	0.9937	0.0	0.0	0.0	0.0248	-0.022389	0.0	0.478780	0.0

CORRECTION FACTORS ** PREMUL TIPLIER CASE

1	0.598764E+00	0.0	0.577703E+00	0.0	0.533423E+00	0.0
4	0.512596E+00	0.0	0.528544E+00	0.0	0.608725E+00	0.0
7	0.103003E+01	0.0	0.250000E+01	0.0	0.121639E+01	0.0
10	0.573859E+00	0.0	0.362418E+00	0.0	0.679546E+00	0.0
13	0.657562E+00	0.0	0.300000E+00	0.0	0.300000E+00	0.0
16	0.300000E+00	0.0	0.509016E+00	0.0	0.807190E+00	0.0
19	0.977611E+00	0.0				
			2			
			5			
			8			
			11			
			14			
			17			
			3			
			6			
			9			
			12			
			15			
			18			

N	SYMMETRIC	CE-N	MODE	CF(N)	REAL	IMAG.
124			1			
1					0.493003E+01	0.0
2					-0.157000E+01	0.0
3					-0.530002E-01	0.0
4					0.493003E+01	0.0

CL-1/4
 CM-3/4
 CL-ALPHA

N	SYMMETRIC	CF-N	MODE	2	CE(N)	REAL	IMAG.
1						0.880589E+01	0.0
2						-0.145306E+01	0.0
3						-0.398661E-01	0.0
4						0.880589E+01	0.0

TABLE V
INPUT DATA - TEST CASE 2

TEST CASE	NO.	2	NEW POST-MULT.	TAPE	INPUT, M=.875, K=0	CONTROL DATA	13	14	15	16	22	23
1	0	3	0	0	0	3	1					
1	1	4	1	1	0	1						
1	1	0	0	0	0.0	0.0	0.0	1.0				
2	2	1	1	0.0	0.0	1.0	0.0	0.0				
3	3	1	1	0.0	0.0	1.0	0.0	0.0				
1	1	0	0	0	0.0	1.0	4.93	0.0				
1	1	19	1	1.0	2.0	4.93	0.0	0.0				
2	2	1	1	1.0	4.0	-1.57	0.0	0.0				
1	1	19	1	1.0	4.0	-1.57	0.0	0.0				
3	3	1	1	1.0	4.0	-0.053	0.0	0.0				
1	1	19	1	1.0	4.0	-0.053	0.0	0.0				
1	1	0	0	0	2.0	CL						
1	1	19	1	1.0	2.0	CL						
2	2	1	1	1.0	4.0	CM-1/4						
1	1	19	1	1.0	4.0	CM-1/4						
3	3	1	1	1.0	4.0	CH-3/4						
1	1	19	1	1.0	4.0	CH-3/4						
1	1	1	1	1.0	13	19-1.0						
1	1	1	1	1.0	13	19-1.0						

TABLE VI

OUTPUT LISTING - TEST CASE 2

TEST CASE NO. 2 NEW POST-MULT. TAPE INPUT, M=.875, K=0

CONTROL FLAGS --
 FLAG = 0 CORRECTION FACTORS CALCULATED
 FLAGP = 4 NEW POSTMULTIPLIER - DT INVERSE AND GEOMETRY TAKEN FROM TAPE
 FLAGT = 1 WEIGHTS = 1.0
 FLAGW = 1 NORMAL WASH TAKEN FROM CARDS (IF NEEDED)
 IPRINT = 1 (DETAIL PRINT FLAG)

CONTROL DIMENSIONS --
 NP = 19
 NC = 3
 NEM = 0
 NELIMS = 0
 NMON = 3
 NAXIS = 3

LIST OF INPUT/OUTPUT TAPES --
 GEOMETRY TAPE = 11
 DELTA-CP TAPE = 12
 W INVERSE TAPE = 13
 D-INVERSE TAPE = 14
 CORR. FACTORS = 16

THE 3 SETS OF INPUT DATA FOR ALL AXES

AXISNO(R)	FLAGA(R)	X11(R)	ETA1(R)	ZETA1(R)	XI2(R) (COSΔ(R))	ETA2(R) (COSβ(R))	ZETA2(R) (COSγ(R))
1	1	0.0	0.0	0.0	0.0	0.0	1.000000
2	1	-0.500000	0.0	0.0	0.0	1.000000	0.0
3	1	0.500000	0.0	0.0	0.0	1.000000	0.0

THE 3 SETS OF INPUT DATA FOR ALL CONSTRAINTS

AXISNO(I)	FLAGF(I)	DELTA	M	LIM1	LIM2	A-WIG(I)	C-WIG(I)	REAL C-F(I)	IMAG.
1	0	1	1	1	19	1.000000	0.200000E+01	4.930000	0.0
2	1	1	1	1	19	1.000000	0.400000E+01	-1.570000	0.0
3	1	1	1	13	19	1.000000	0.400000E+01	-0.053000	0.0

130 THE 3 SETS OF INPUT DATA FOR MONITORING

AXISNO(N)	FLAG(N)	DELTA	M	LIM1	LIM2	A-WIG(N)	C-WIG(N)	LABEL
1	0	1	1	1	19	1.000000	0.200000E+01	CL
2	1	1	1	1	19	1.000000	0.400000E+01	CM-1/4
3	1	1	1	13	19	1.000000	0.400000E+01	CH-3/4

SAI MATRIX ROWS

0.012800	0.0	0.059500	0.0	0.077500	0.0
0.009500	0.0	0.097000	0.0	0.090500	0.0
0.0077500	0.0	0.037500	0.0	0.012800	0.0
0.012400	0.0	0.050000	0.0	0.055500	0.0
0.050000	0.0	0.012400	0.0	0.08005	0.0
0.003159	0.0	0.010264	0.0	-0.024300	0.0
0.001674	0.0	-0.016873	0.0	-0.036359	0.0
-0.027380	0.0	-0.017680	0.0	-0.034687	0.0
-0.006239	0.0	-0.028538	0.0	0.0	0.0
-0.033962	0.0	-0.009261	0.0	0.0	0.0
0.0	0.0	0.0	0.0	0.0	0.0
0.0	0.0	0.0	0.0	0.0	0.0
-0.000039	0.0	0.0	0.0	-0.006937	0.0
-0.008962	0.0	-0.003538	0.0		
		-0.003061	0.0		

SAN MATRIX POWS

0.012800	0.0	0.059500	0.0	0.037500	0.0	0.012800	0.0	0.037500	0.0	0.077500	0.0	0.077500	0.0	0.0	0.0
0.090500	0.0	0.097000	0.0	0.097000	0.0	0.090500	0.0	0.097000	0.0	0.059500	0.0	0.059500	0.0	0.0	0.0
0.077500	0.0	0.037500	0.0	0.059500	0.0	0.077500	0.0	0.059500	0.0	0.097000	0.0	0.097000	0.0	0.0	0.0
0.012400	0.0	0.012400	0.0	0.034700	0.0	0.012400	0.0	0.034700	0.0	0.012400	0.0	0.012400	0.0	0.0	0.0
0.050000	0.0	0.010264	0.0	0.008305	0.0	0.050000	0.0	0.010264	0.0	0.008305	0.0	0.008305	0.0	0.0	0.0
0.003159	0.0	-0.016873	0.0	0.007377	0.0	0.003159	0.0	-0.016873	0.0	0.007377	0.0	0.007377	0.0	0.0	0.0
0.001674	0.0	-0.017680	0.0	-0.0025139	0.0	0.001674	0.0	-0.017680	0.0	-0.0025139	0.0	-0.0025139	0.0	0.0	0.0
0.027380	0.0	-0.028538	0.0	-0.018296	0.0	0.027380	0.0	-0.028538	0.0	-0.018296	0.0	-0.018296	0.0	0.0	0.0
-0.006239	0.0	-0.009261	0.0	-0.0025079	0.0	-0.006239	0.0	-0.009261	0.0	-0.0025079	0.0	-0.0025079	0.0	0.0	0.0
-0.033962	0.0	0.0	0.0	0.0	0.0	-0.033962	0.0	0.0	0.0	0.0	0.0	0.0	0.0	0.0	0.0
0.0	0.0	0.0	0.0	0.0	0.0	0.0	0.0	0.0	0.0	0.0	0.0	0.0	0.0	0.0	0.0
0.0	0.0	0.0	0.0	0.0	0.0	0.0	0.0	0.0	0.0	0.0	0.0	0.0	0.0	0.0	0.0
0.000039	0.0	0.003538	0.0	0.000946	0.0	0.000039	0.0	0.003538	0.0	0.000946	0.0	0.000946	0.0	0.0	0.0
-0.008962	0.0	-0.003061	0.0	-0.007729	0.0	-0.008962	0.0	-0.003061	0.0	-0.007729	0.0	-0.007729	0.0	0.0	0.0
0.0	0.0	0.0	0.0	0.0	0.0	0.0	0.0	0.0	0.0	0.0	0.0	0.0	0.0	0.0	0.0
0.0	0.0	0.0	0.0	0.0	0.0	0.0	0.0	0.0	0.0	0.0	0.0	0.0	0.0	0.0	0.0
0.0	0.0	0.0	0.0	0.0	0.0	0.0	0.0	0.0	0.0	0.0	0.0	0.0	0.0	0.0	0.0
0.0	0.0	0.0	0.0	0.0	0.0	0.0	0.0	0.0	0.0	0.0	0.0	0.0	0.0	0.0	0.0
0.0	0.0	0.0	0.0	0.0	0.0	0.0	0.0	0.0	0.0	0.0	0.0	0.0	0.0	0.0	0.0
0.0	0.0	0.0	0.0	0.0	0.0	0.0	0.0	0.0	0.0	0.0	0.0	0.0	0.0	0.0	0.0
0.0	0.0	0.0	0.0	0.0	0.0	0.0	0.0	0.0	0.0	0.0	0.0	0.0	0.0	0.0	0.0


```
--W-- IS CARO INPUT
MODE DELTA LIMITS          PEAL - W - IMAG.
  1   1   13   19      -1.000000  0.0
```

SYMMETRIC W MATRIX

THE 1 COLUMNS OF THE
 COLUMN 1
 1 0:0
 4 0:0
 7 0:0
 10 0:0
 13 -0:100000F+01
 16 -0:100000F+01
 19 -0:100000F+01

2 0:0
 5 0:0
 8 0:0
 11 0:0
 14 -0:100000F+01
 17 -0:100000F+01

3 0:0
 6 0:0
 9 0:0
 12 0:0
 15 -0:100000F+01
 18 -0:100000F+01

0:0
 0:0
 0:0
 0:0
 0:0
 0:0

THE 1 COLUMNS OF THE DELTA-CP-RAP MATRIX

COLUMN	1	2	5	8	11	14	17	3	6	9	12	15	18
1	0.716455E+01	-0.731030E+00	0.250015E+01	-0.250801E+00	0.117077E+01	-0.949423E-01	0.165207E+01	-0.159399E+00	0.1329571E+01	-0.868268E-01	0.922275E+01	-0.156961E+00	0.208988E+01
4	0.131495E+01	-0.118636E+00	0.117077E+01	-0.949423E-01	0.100245E+02	-0.220436E+00	0.922275E+01	-0.156961E+00	0.257012E+01	-0.109281E+00	0.154990E+02	-0.924698E-01	0.154990E+02
7	0.257012E+01	-0.109281E+00	0.100245E+02	-0.220436E+00	0.127522E+02	-0.110500E+00	0.127522E+02	-0.110500E+00	0.104787E+02	-0.129675E+00	0.908173E+01	-0.676048E-01	0.908173E+01
10	0.104787E+02	-0.129675E+00	0.127522E+02	-0.110500E+00	0.131619E+02	-0.883011E-01	0.131619E+02	-0.883011E-01	0.196969E+02	-0.944285E-01	0.208988E+01	-0.676048E-01	0.208988E+01
13	0.196969E+02	-0.944285E-01	0.131619E+02	-0.883011E-01	0.387184E+01	-0.297328E-01	0.387184E+01	-0.297328E-01	0.614658E+01	-0.472457E-01	0.908173E+01	-0.676048E-01	0.908173E+01
16	0.614658E+01	-0.472457E-01	0.387184E+01	-0.297328E-01	0.250015E+01	-0.250801E+00	0.250015E+01	-0.250801E+00	0.661877E+00	-0.499649E-02	0.908173E+01	-0.676048E-01	0.908173E+01
19	0.661877E+00	-0.499649E-02	0.250015E+01	-0.250801E+00	0.117077E+01	-0.949423E-01	0.165207E+01	-0.159399E+00	0.1329571E+01	-0.868268E-01	0.922275E+01	-0.156961E+00	0.208988E+01

DELTA-C

-0.630051 0.122550 0.519804 -0.018031 0.087867 -0.001059

THEORETICAL C-VALUES

5.560051 -0.122550 -2.080804 0.018031 -0.140867 0.001059

ONE S-BAR ROW

-0.035068 0.000612 -0.142536 0.002546 -0.302465 0.005638 0.009541
 -0.673939 0.013722 -0.746680 0.015803 -0.612309 0.012899 0.008227
 -0.437368 0.008864 -0.357380 0.007347 -0.204170 0.004221 0.000653
 -0.195771 0.004057 0.404510 0.008493 -0.636052 0.013583 0.019254
 -1.143060 0.025356 -1.426368 0.032111 -0.871221 0.019694 0.0
 0.0 0.0 0.0 0.0 0.0 0.0 0.0

ONE S-BAR ROW

-0.022906 -0.000047 -0.088104 0.000163 -0.170660 0.000274 0.000325
 -0.266833 -0.000338 -0.212600 -0.000411 -0.085731 -0.000688 -0.000793
 0.039684 -0.000944 0.054618 -0.000838 0.039468 0.000504 -0.000080
 0.043300 -0.000501 0.102894 0.001087 0.191509 0.001820 0.0002737
 0.453494 -0.003788 0.607809 0.004997 0.379680 0.003102 0.0
 0.0 0.0 0.0 0.0 0.0 0.0 0.0

ONE S-BAR ROW

-0.000135 -0.000005 -0.000559 0.000020 -0.001298 0.000043 0.000069
 -0.003637 -0.000094 -0.004861 -0.000103 -0.005300 -0.000088 -0.000065
 -0.007625 -0.000069 -0.008914 -0.000031 -0.007270 -0.000031 -0.000005
 -0.010606 -0.000030 -0.020665 -0.000059 -0.018662 0.000093 0.000005
 0.042317 -0.000217 0.085811 0.000315 0.059176 0.000202 0.000144
 0.0 0.0 0.0 0.0 0.0 0.0 0.0

```

-S-   MATRIX
0.776227E+01  0.0  -0.163754E+01  -0.168500E-01  -0.181983E+00  -0.273930E-02
-0.163754E+01  0.168500E-01  0.108984E+01  0.0  0.909225E-01  0.326475E-03
-0.181983E+00  0.273930E-02  0.909225E-01  -0.326475E-03  0.138484E-01  0.0

-DC-  COLUMN
-0.630051E+00  0.122550E+00  0.519804E+00  -0.180307E-01  0.878674E-01  -0.105876E-02

SOLUTION OF MATRIX EQ.
0.951395E-01  0.167979E-01  -0.304458E-01  -0.258064E-02  0.779167E+01  0.180770E+00

OUTPUT OF GEN. INVERSE (EPS-TILDA)
-0.003680  -0.000575  -0.015273  -0.033606  -0.002359  -0.0033606  -0.005084  -0.057116  -0.008387
-0.084121  -0.011875  -0.102196  -0.096750  -0.013584  -0.096750  -0.011589  -0.080137  -0.008222
-0.102091  -0.009162  -0.105001  -0.077203  -0.008042  -0.077203  -0.005017  -0.014564  -0.000841
-0.102517  -0.005489  -0.202497  -0.211533  -0.011175  -0.211533  -0.015178  -0.065944  -0.015800
-0.207560  -0.013562  0.514896  0.366935  -0.010769  0.366935  -0.005312  0.0  0.0
0.0  0.0  0.0  0.0  0.0  0.0  0.0  0.0  0.0

```

SYMMETRIC DELTA-CP-TILDA , MODE 1

J	X(J)	Y(J)	Z(J)	GAMMA(J)	DELTA-A(J)	REAL	IMAG.	REAL	IMAG.
1	-0.9936	0.0	0.0	0.0	0.0256	-0.003680	-0.000575	8.731648	-0.201151
2	-0.9429	0.0	0.0	0.0	0.0750	-0.015273	-0.002359	3.205733	-0.042868
3	-0.8450	0.0	0.0	0.0	0.1190	-0.033606	-0.005084	2.304436	0.0003822
4	-0.7066	0.0	0.0	0.0	0.1550	-0.057116	-0.008387	1.993573	0.031236
5	-0.5370	0.0	0.0	0.0	0.1810	-0.084121	-0.011875	1.857959	0.045195
6	-0.3479	0.0	0.0	0.0	0.1940	-0.102196	-0.013584	1.897981	0.036609
7	-0.1521	0.0	0.0	0.0	0.1810	-0.096750	-0.011589	2.755267	-0.010252
8	0.0370	0.0	0.0	0.0	0.1550	-0.080137	-0.008222	9.003983	-0.069108
9	0.2066	0.0	0.0	0.0	0.1190	-0.102091	-0.009162	8.396429	-0.024435
10	0.3450	0.0	0.0	0.0	0.0750	-0.105001	-0.008042	9.362289	-0.019947
11	0.4429	0.0	0.0	0.0	0.0256	-0.077203	-0.005017	11.350240	-0.014470
12	0.4936	0.0	0.0	0.0	0.0256	-0.014564	-0.000841	14.212420	0.003620
13	0.5063	0.0	0.0	0.0	0.0248	-0.102517	-0.005489	18.871185	0.040578
14	0.5545	0.0	0.0	0.0	0.0694	-0.202497	-0.011175	12.228393	0.065479
15	0.6415	0.0	0.0	0.0	0.1000	-0.211533	-0.015178	17.173484	0.053617
16	0.7500	0.0	0.0	0.0	0.1110	-0.065944	-0.015800	2.928123	0.019568
17	0.8585	0.0	0.0	0.0	0.1000	0.207560	-0.013562	0.046162	-0.011998
18	0.9455	0.0	0.0	0.0	0.0694	0.514896	-0.010769	-0.950595	-0.024853
19	0.9937	0.0	0.0	0.0	0.0248	0.366935	-0.005312	-0.634418	-0.029181

CORRECTION FACTORS ** POSTMIJITIPIER CASE

1	0.996320E+00	-0.574841E-03	2	0.984727E+00	-0.235866E-02	3	0.966394E+00	-0.508433E-02
4	0.942884E+00	-0.838712E-02	5	0.915879E+00	-0.118752E-01	6	0.897804E+00	-0.135835E-01
7	0.903250E+00	-0.115889E-01	8	0.919863E+00	-0.822229E-02	9	0.897909E+00	-0.916240E-02
10	0.894999E+00	-0.804217E-02	11	0.922797E+00	-0.501745E-02	12	0.985436E+00	-0.841083E-03
13	0.897483E+00	-0.548857E-02	14	0.797503E+00	-0.111750E-01	15	0.788467E+00	-0.151780E-01
16	0.934056E+00	-0.158000E-01	17	0.120756E+01	-0.135618E-01	18	0.151490E+01	-0.107688E-01
19	0.136693E+01	-0.531235E-02						

FLAGP = 4 -- TAPE CONTAINS THE EPSILON-RAR (FR) VALUES

1	-0.368013E-02	-0.574841E-03	2	-0.152729E-01	-0.235866E-02	3	-0.336063E-01	-0.508433E-02
4	-0.571160E-01	-0.838712E-02	5	-0.841213E-01	-0.118752E-01	6	-0.102196E+00	-0.135835E-01
7	-0.967499E-01	-0.115889E-01	8	-0.801373E-01	-0.822229E-02	9	-0.102091E+00	-0.916240E-02
10	-0.105001E+00	-0.804217E-02	11	-0.772026E-01	-0.501745E-02	12	-0.145645E-01	-0.841083E-03
13	-0.102517E+00	-0.548857E-02	14	-0.202497E+00	-0.111750E-01	15	-0.211533E+00	-0.151780E-01
16	-0.659443E-01	-0.158000E-01	17	0.207560E+00	-0.135618E-01	18	0.514896E+00	-0.107688E-01
19	0.366935E+00	-0.531235E-02						

N	SYMMETRIC	CF-N	LABEL	RFAL	CF(N)	MODE	I	IMAG.
1			CL	0.492999E+01				-0.431901E-06
2			CM-1/4	-0.157000E+01				0.181608E-07
3			CH-3/4	-0.530001E-01				-0.276486E-09

Subroutine Description

The computer program for generating correction factors (EIGC) consists of twenty subroutines. The MAIN of this program reads and writes the header card and reads the control dimensions for a case; the latter are used for dimensioning most of the complex arrays that are passed into Subroutine WEYT via the argument list. Subroutine WEYT is the actual working main of the program, which calls all the major subroutines, supplying these with the necessary information via their argument lists. The following is a detailed description of all subroutines of program EIGC including their flow charts, where applicable, given in alphabetical order. The computer program is written in the FORTRAN IV programming language.

SUBROUTINE CEMN(NPOT, IGO, MODE, NTAPSA, NP, NMON, LABEL, NUTL,
SAI, DCPTIL, CE)

Functional Description

This subroutine integrates the corrected pressures, ΔC_{pe} , into coefficients, C_e , which are used to monitor the results (See Eq. (3)). The integration procedure is identical to that required for obtaining the imposed constraints.

$$\{C_e\} = [S] \{\Delta C_{pe}\}$$

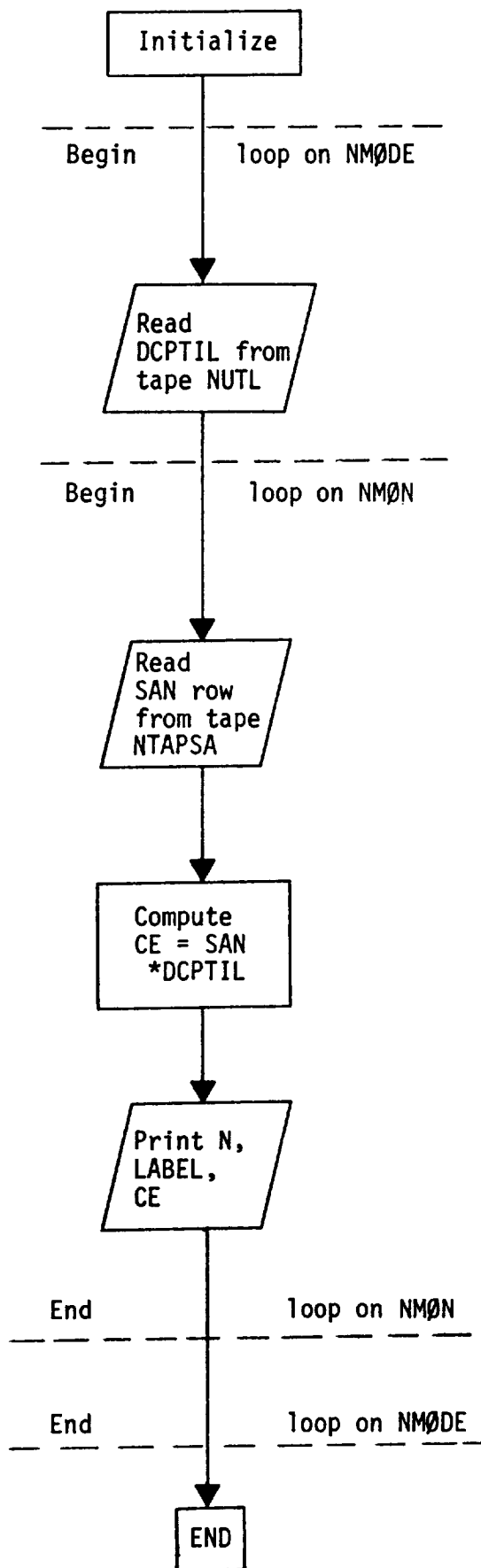
The coefficients C_e are part of the printed output.

Description of Argument List

NPOT	Data set number of the system output data set
IGØ	1 for symmetric modes 2 for antisymmetric modes
MØDE	Mode number
NTAFSA	Data set (tape) number of tape containing the integration matrix [S]
NP	Number of rows in the ΔC_p matrix
NMØN	Number of integration rows used for monitoring
LABEL	Alphanumeric label describing the aerodynamic parameters
NUTL	Data set (tape) number of tape containing columns of the weighted pressures, ΔC_p
SAI	A row of the integration matrix [S]
DCPTIL	A column of the weighted pressures $\{\Delta C_p\}$
CE	A column of the aerodynamic parameters $\{C_e\}$

Calling Subroutine WEYT

Flow Chart



SUBROUTINE DCPB(NTDCP, NTAPW, NTAPDI, IG0, IFP, IFW, NR0W, NC0L,
NMAX, DCP, C0L, W0RK)

Functional Description

This subroutine computes the theoretical pressure distribution if it is not input. Specifically

$$\{\Delta C_{p_t}\} = [D]^{-1} \{W\}$$

where W is the normalwash and $[D]^{-1}$ is the inverse of the aerodynamic influence coefficient matrix. This corresponds to Equation (1) where $[D]^{-1} = [A]$. ΔC_{p_t} is called DELCPB in this subroutine.

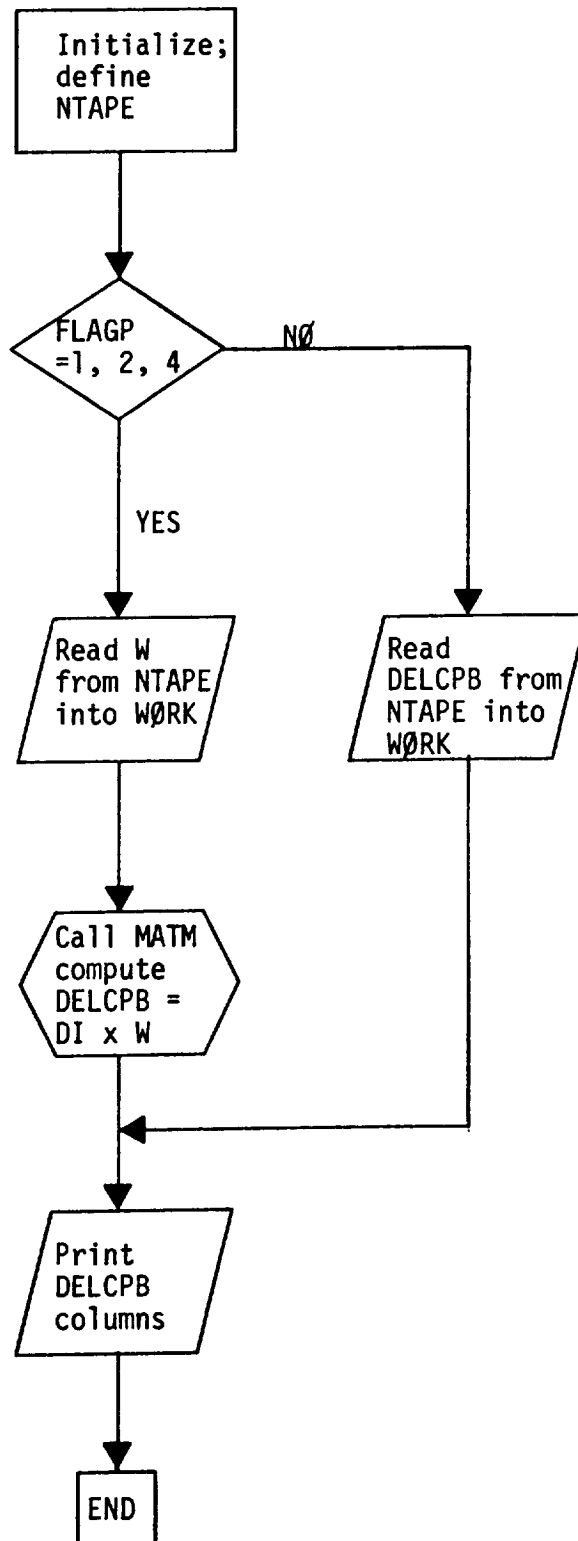
Description of Argument List

NTDCP	Tape number containing the matrix of pressure coefficients, $[\Delta C_{p_t}]$, in column order
NTAPW	Tape number containing the normalwash matrix, $[W]$, in column order
NTAPDI	Tape number containing the inverse-D matrix, $([A])$ $[DI]$, in row order
IGØ	1 for symmetric modes, 2 for antisymmetric modes
IFP	Control flag (see input flag FLAGP). IFP = 0, 2, 3 means premultiplying correction factors, IFP = 1, 4 means post-multiplying correction factors
IFW	Normalwash flag. IFW = 0 means normalwash is tape input (if any), IFW = 1 means normalwash is card input
NRØW	Number of rows in the ΔC_{p_t} matrix
NCØL	Number of columns in the ΔC_{p_t} matrix
NMAX	Maximum number of columns in the ΔC_{p_t} matrix
DCP	One column of the ΔC_{p_t} matrix (complex)
CØL	Temporary work array (complex)
WØRK	The NROW x NMAX complex array containing the ΔC_{p_t} matrix

Calling Subroutine

WEYT

Flow Chart



SUBROUTINE DCPT(NPOT, FLAGB, IG0, M0DE, NP, NSCRCH, NUTL, NTAPDI,
NTAPW, NTAPCF, X, Y, Z, GMA, DELA, NMAX, NEM, W,
DI, EPS, DCPBAR, DCPTIL, W0RK, EB)

Functional Description

This subroutine modifies the theory with the calculated correction factors. If a premultiplier is used the theoretical pressure, ΔC_{p_t} , is modified to produce the modified pressures ΔC_{p_e} (see eqs.(2) and (5)).

$$\{ \Delta C_{p_e} \} = [1+\epsilon] \{ \Delta C_{p_t} \}$$

If a postmultiplier is used then the downwash, W, is modified to produce the corrected pressures ΔC_p (see eqs. (5) and (28)).

$$\{ \Delta C_{p_e} \} = [D]^{-1} [1+\epsilon] \{ W \}$$

If the new postmultiplier is used then

$$\{ \Delta C_{p_e} \} = [D]^{-1} \{ W + [\bar{\phi}] \{ \bar{\epsilon} \} \}$$

$$[\bar{\phi}] = [\phi] [\lambda]$$

$$\{ \lambda \} = [\phi]^T \{ \Delta C_{p_t} \}$$

(See eq. 65)

Also the correction factors, CF, are written on tape where

$$CF = 1 + \epsilon$$

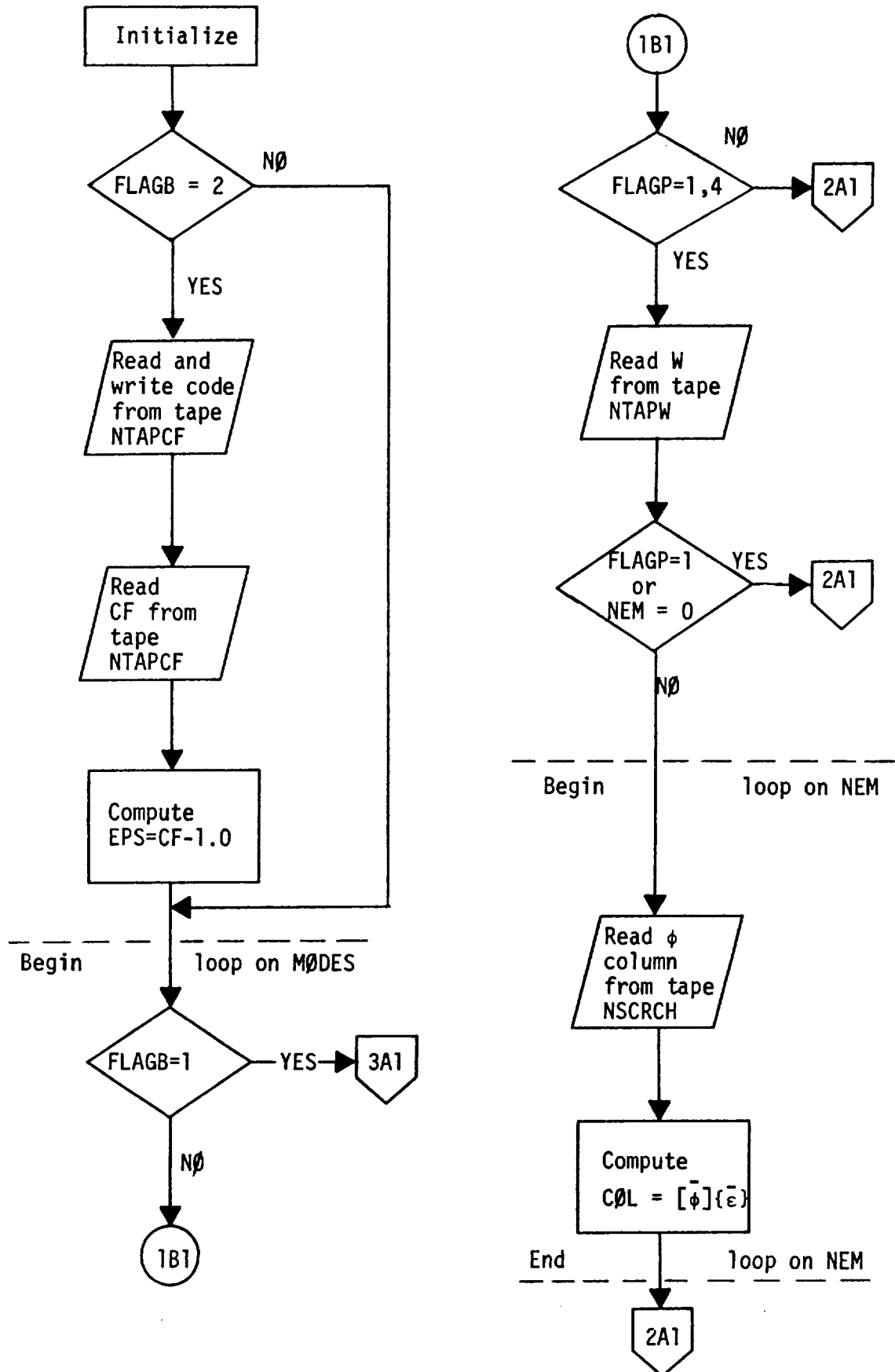
Description of Arguments

NPØT	Data set number of the system output data set
FLAGB	Option flag for correction matrix calculation and/or monitoring of data
IGØ	1 for symmetric modes 2 for antisymmetric modes
MØDE	Mode number
NP	Number of row elements in the ΔC_p matrix
NSCRCH	Data set (tape) number containing the $\bar{\phi}$ matrix in row order (for FLAGP=4 cases only)
NUTL	Data set (tape) number on which the ΔC_{p_e} columns are saved
NTAPDI	Data set (tape) number containing the D^{-1} matrix rows (if needed) ($D^{-1} = A$)
NTAPW	Data set (tape) number containing the W matrix columns (if needed)
NTAPCF	Data set (tape) number on which the matrix of correction factors, CF, is saved in column order
X	x coordiantes } y coordinates } of the pressure points or the ΔC_{p_t} z coordinates }
Y	
Z	
GMA	Dihedral angle array of the boxes over which the pressures act
DELA	Array of box areas
NMAX	Column dimension of the two-dimensional complex array WØRK
NEM	Number of correction factor modes

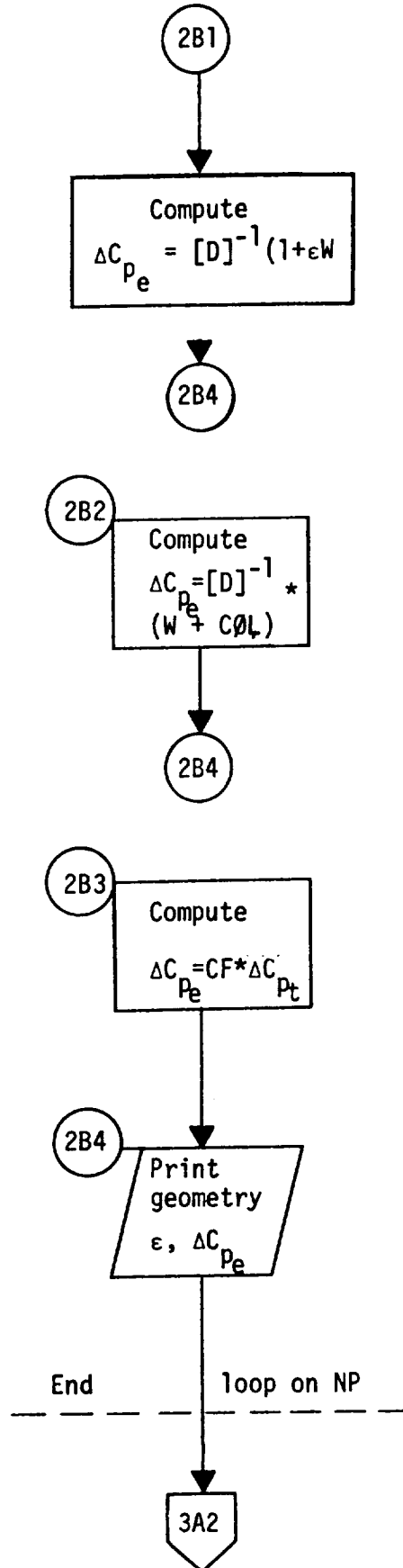
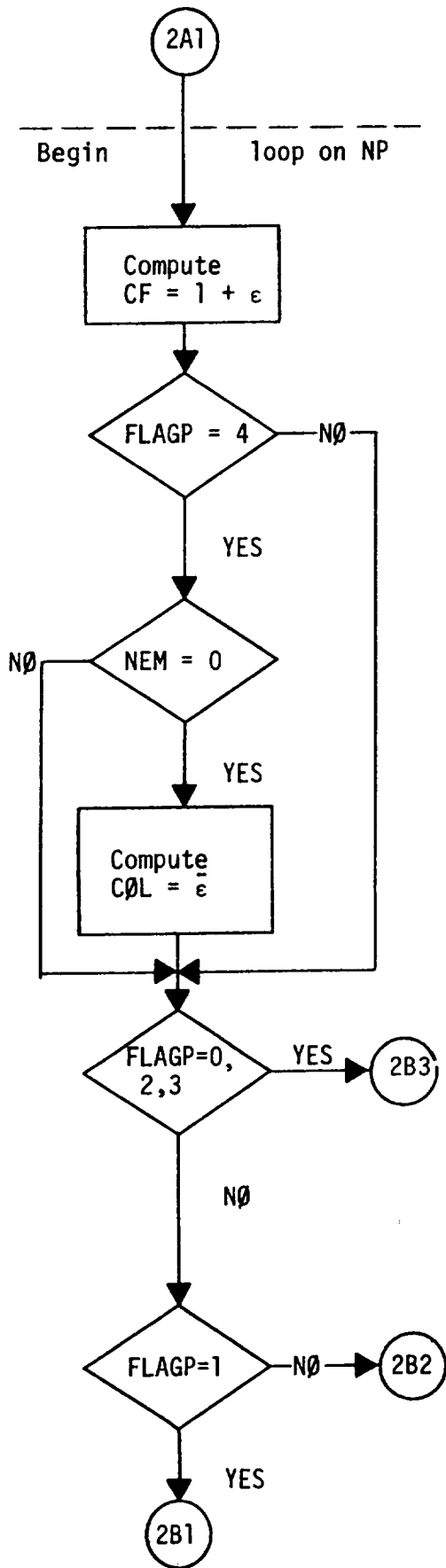
W	A column of the W matrix (complex)
DI	A row of the D^{-1} matrix (complex), ([A] matrix)
EPS	ϵ array
DCPBAR	A column of the ΔC_{p_t} matrix (complex)
DCPTIL	A column of the ΔC_{p_e} matrix (complex)
WORK	Two dimensional complex array containing the ΔC_{p_t} matrix
EB	$\bar{\epsilon}$ array ($\epsilon = \phi \bar{\epsilon}$)

Calling Subroutine WEYT

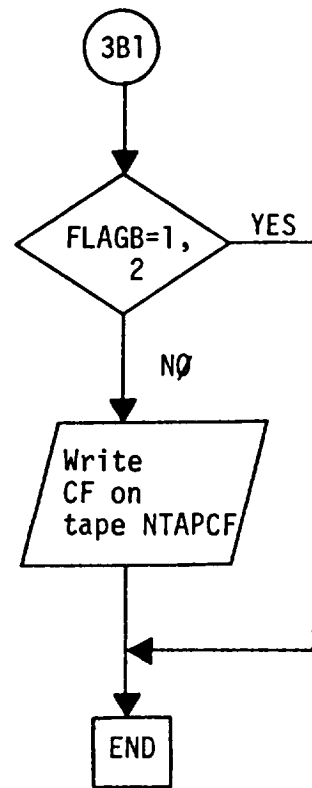
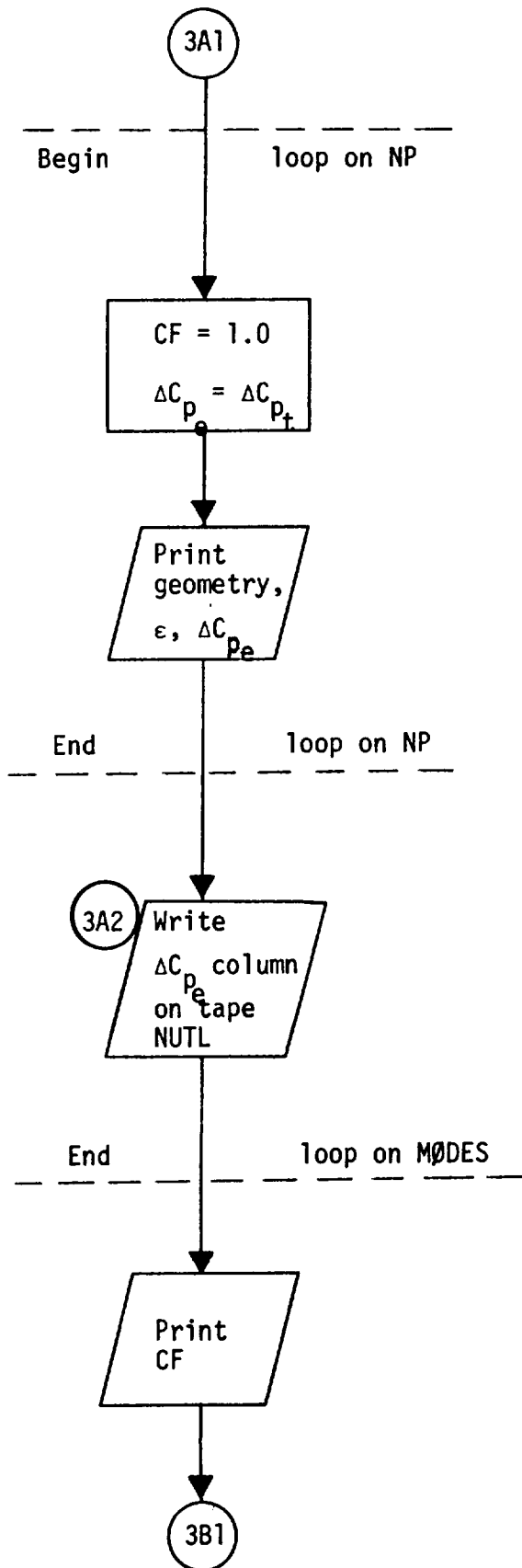
Flow Chart



Flow Chart



Flow Chart



SUBROUTINE DELC(NTAPE, NPOT, NC, NP, NMØDE, NMAX, CIE, DCI, SAI, WØRK)

Functional Description

This subroutine forms the difference between the theoretical, C_t , and the experimental (constrained) C_e coefficients (see Equations (9) and (10)).

$$\{\Delta C_e\} = \{C_e\} - [S] \{\Delta C_{p_t}\}$$

It also prints out C_t (= $[S] \{\Delta C_{p_t}\}$) and ΔC .

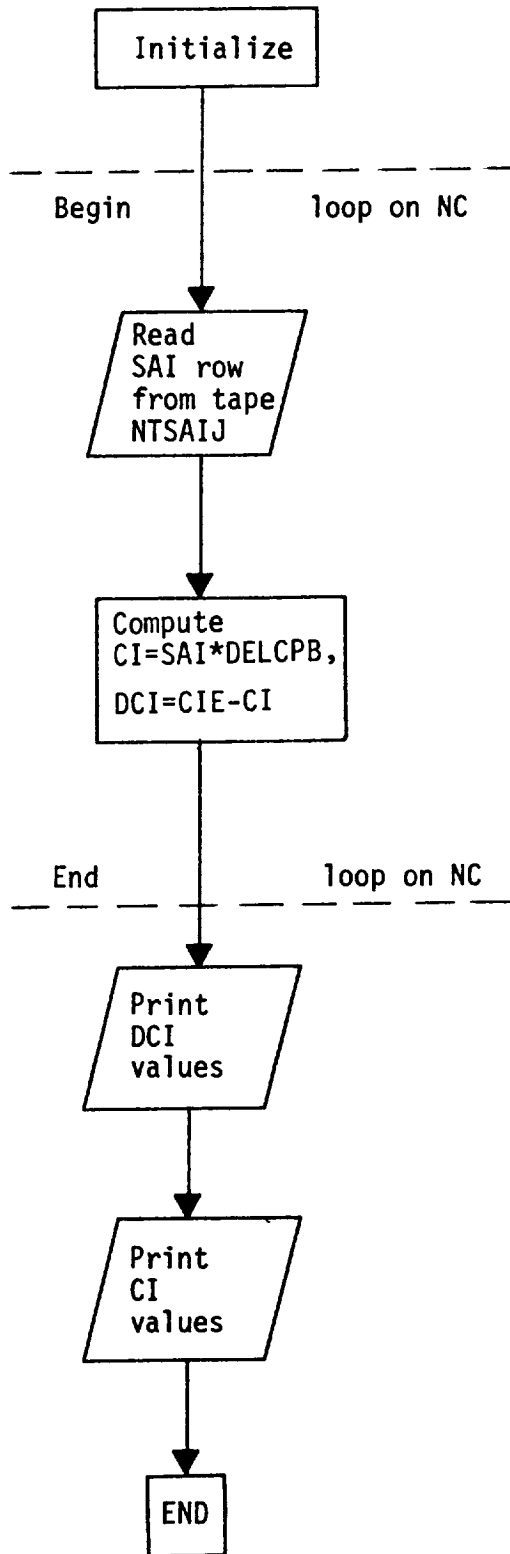
Description of Argument List

NTAPE	Tape containing rows of the integration matrix, [S]
NPØT	Data set number of the system output data set
NC	Number of constraints applied to ΔC_p values
NP	Number of row elements in the ΔC_p matrix
NMØDE	Number of modes
NMAX	Maximum number of columns in the two-dimensional WORK array
CIE	Array containing the input values C_e (experimental constraints)
DCI	The $[\Delta C_e]$ matrix
SAI	A row of the integration matrix [S.]
WORK	The NP by NMAX complex array containing the ΔC_{p_t} matrix

Calling Subroutine

WEYT

Flow Chart



SUBROUTINE EDBL(NPOT, NELIMS, NP, NS, LIMK, JARR, NSMOD, EBMIN,
EBMAX, EB, ELIM)

Functional Description

This subroutine compares the correction factors, $\bar{\epsilon}$, with the input limits $\bar{\epsilon}_{\min}$, $\bar{\epsilon}_{\max}$. If any $\bar{\epsilon}$ falls outside of the limits it replaces $\bar{\epsilon}$ with the closest limit. (The values of $\bar{\epsilon}$ are correction factors if correction factor modes do not exist). This subroutine forms the final correction factor array $\bar{\epsilon}$ (see paragraph below Eq. (60)).

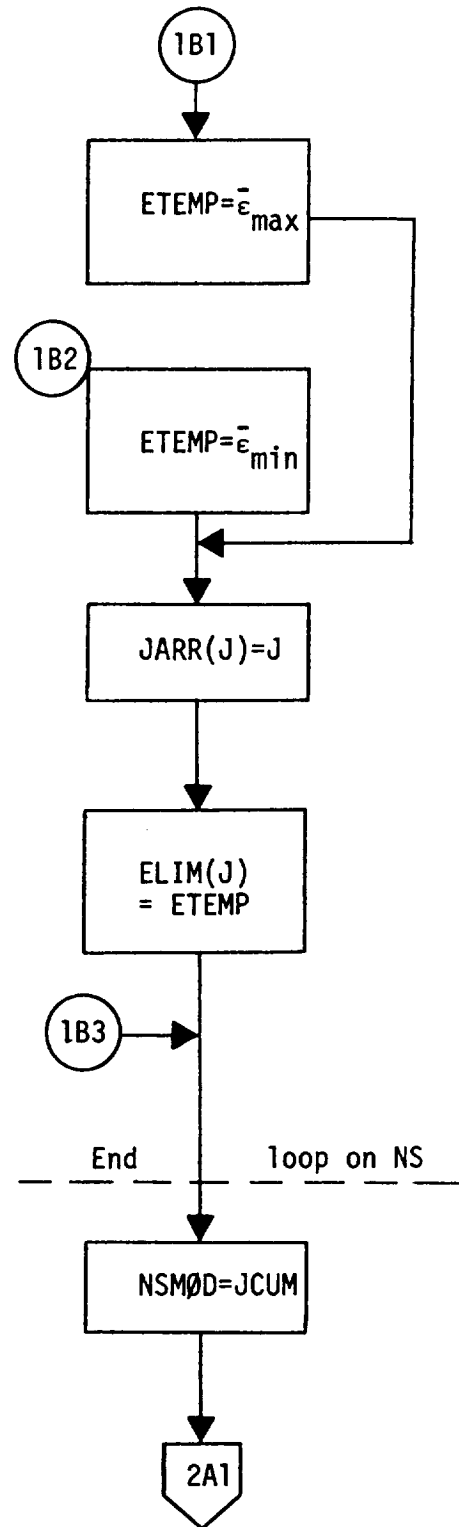
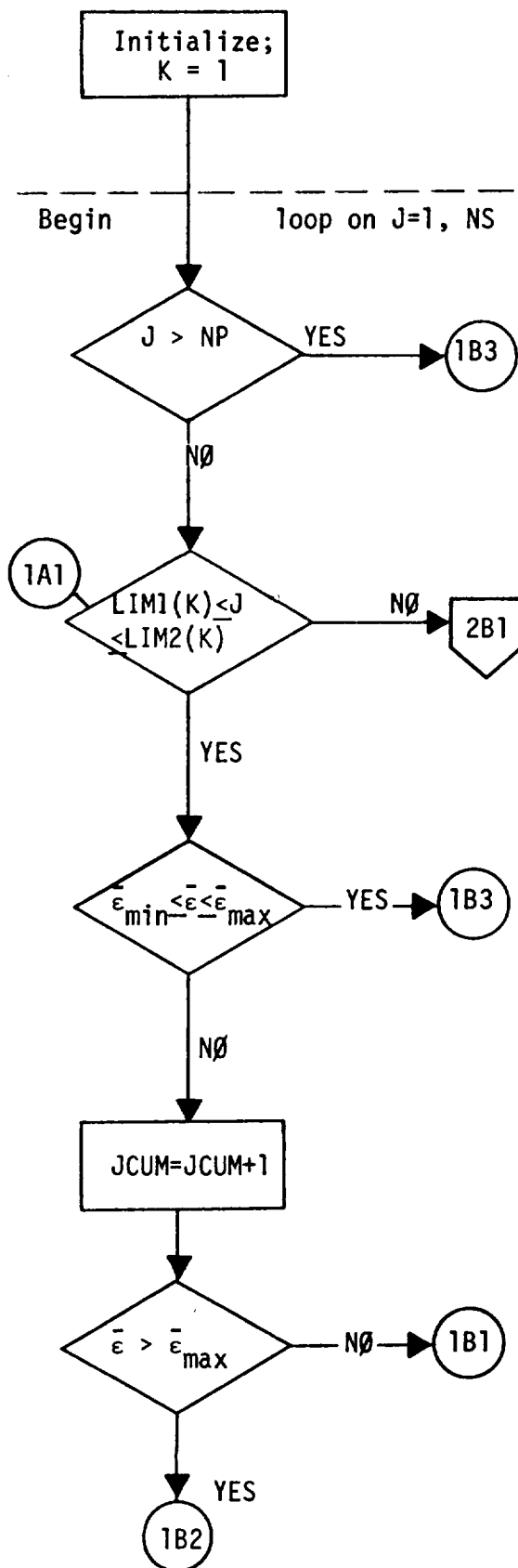
Description of Argument List

NPØT	Data set number of the system output data set
NELIMS	Number of input cards for EBMIN and EBMAX - see below
NP	Number of row elements in the ΔC_p matrix
NS	NS = NP + NC when NEM \leq NP NS = NEM + NC when NEM > NP
LIMK	A two-dimensional array containing the first- and last box numbers that define a range of boxes (or ΔC_p) over which a limit is to be placed on ϵ
JARR	Array of the box numbers for which the ϵ values are modified
NSMØD	The number of ϵ values which are modified due to the limits placed on these
EBMIN	The minimum- and maximum value allowed for the values
EBMAX	of ϵ for boxes (or ΔC_p) in the range defined by LIMK
EB	Array of the calculated $\bar{\epsilon}$ values
ELIM	Array of the ϵ values that were modified due to the $\bar{\epsilon}_{\min}$, $\bar{\epsilon}_{\max}$ restrictions

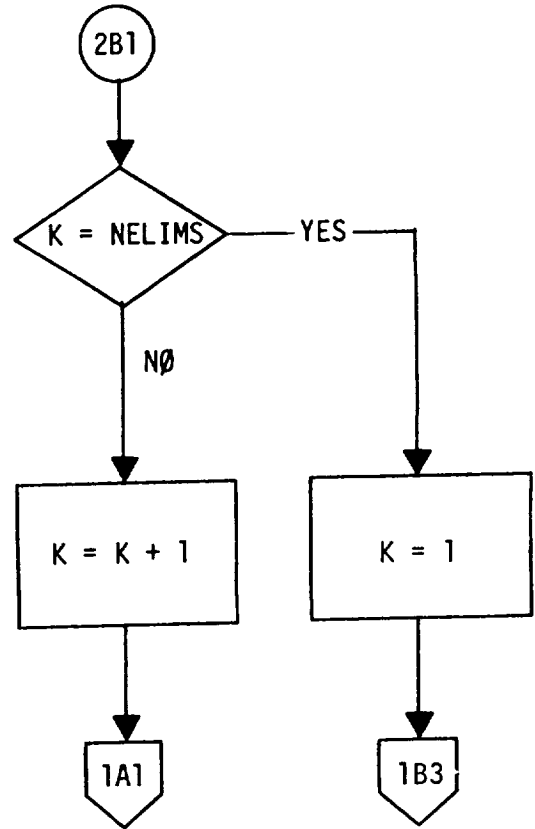
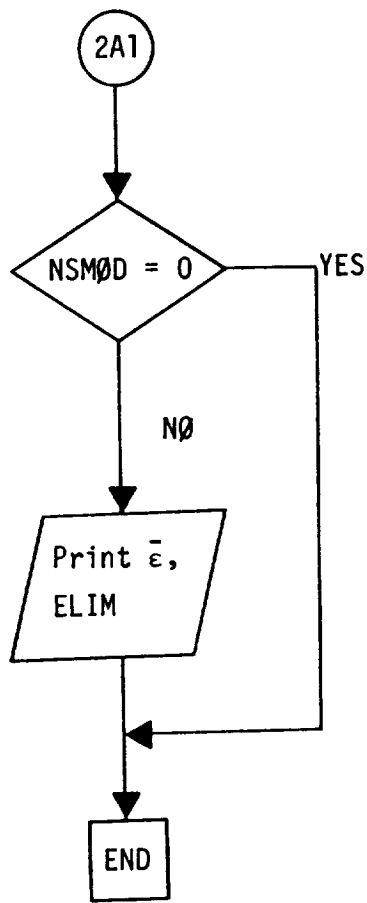
Calling Subroutine

WEYT

Flow Chart



Flow Chart



SUBROUTINE EPSJ(NTPHIJ, NP, NEM, NS, EB, EPS, PHI)

Functional Description

This subroutine relates ϵ to $\bar{\epsilon}$, as in Equation (53).

$$\{\epsilon\} = [\phi] \{\bar{\epsilon}\}$$

where $[\phi]$ are correction factor modes and where

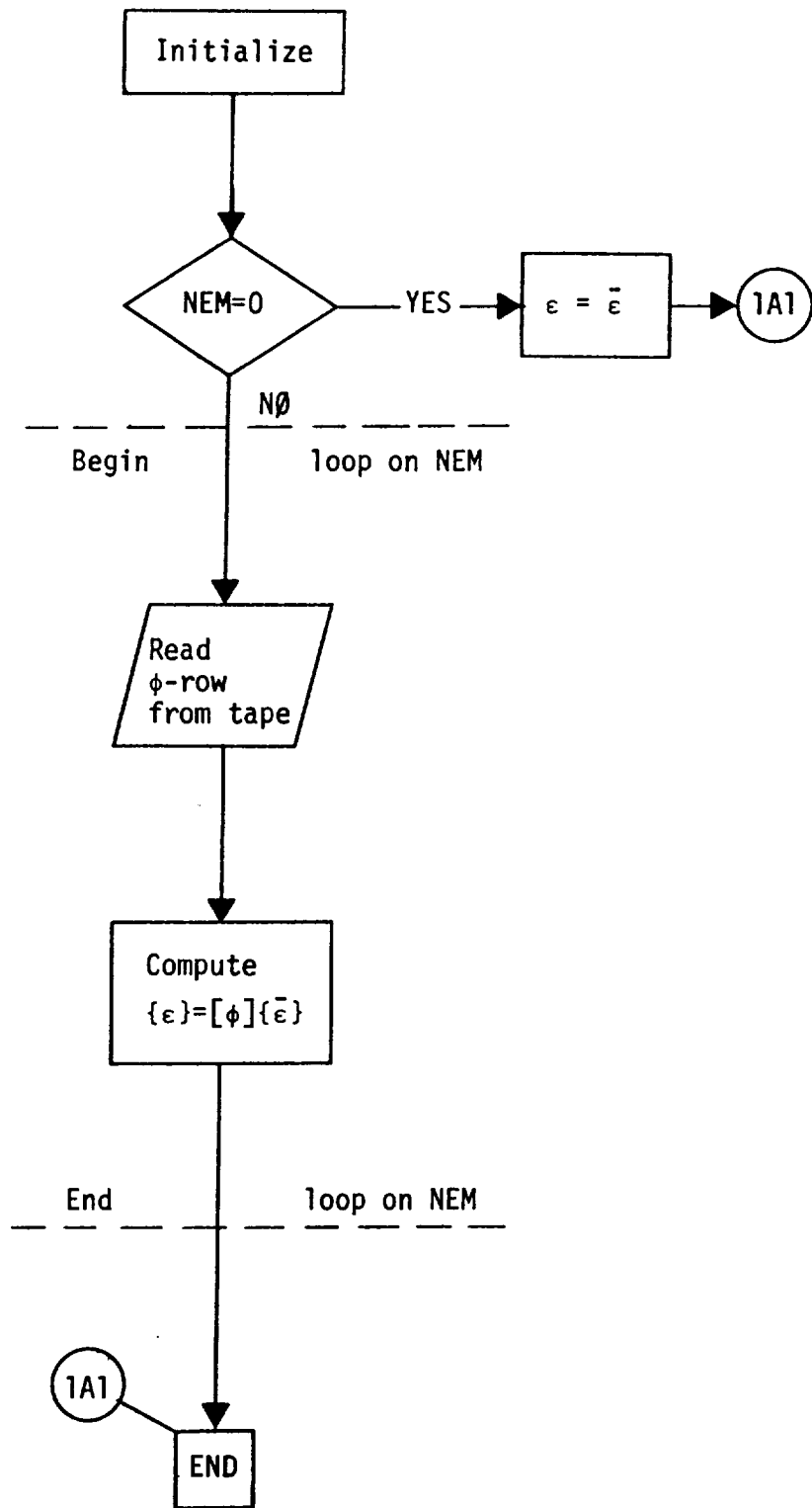
$$\epsilon = \begin{cases} \epsilon_p & \text{for premultiplying correction factors} \\ \epsilon_w & \text{for postmultiplying correction factors} \end{cases}$$

Description of Argument List

NTPHIJ	Tape number containing the ϕ matrix
NP	Number of row elements in the ϕ matrix
NEM	Number of correction factor modes
NS	NS = the greater of (NP+NC) and (NEM+NC)
EB	Array of the $\bar{\epsilon}$ values
EPS	The final ϵ array
PHI	A column of the matrix of weight factor mode shapes, ϕ

Calling Subroutine WEYT

Flow Chart



SUBROUTINE GINV(NPOT, NTAPSB, NC, NS, NX, DC, EB, B, S, SBB)

Functional Description

This subroutine provides a general inverse of the following set of equations:

$$NC \downarrow \{\Delta C_e\} = [\tilde{S}] \{\tilde{\epsilon}\} \downarrow NS$$

When $NC = NS$ (Direct Solution)

$$\{\tilde{\epsilon}\} = [\tilde{S}]^{-1} \{\Delta C_e\}$$

When $NC < NS$ (Minimization Solution, $\sum \tilde{\epsilon}^2 = \min$ (see Eq. (20))

$$\{\tilde{\epsilon}\} = [\tilde{S}]^H \{\lambda\}$$

$$\{\lambda\} = [[\tilde{S}] [\tilde{S}]^H]^{-1} \{\Delta C_e\}$$

When $NC > NS$ (Least Squares Solution $\sum \Delta C_e^2 = \min.$)

$$\{\tilde{\epsilon}\} + [[\tilde{S}]^H [\tilde{S}]]^{-1} \{\Delta C_e\}$$

$$\{\lambda\} = [\tilde{S}]^H \{\Delta C_e\}$$

In the above;

$$[\tilde{S}] = [\bar{S}] [\sqrt{T_p}]^{-1}$$

where $[\bar{S}]$ given in Eq. (51). The term $\tilde{\epsilon}$ is given in Eq. (22). The superscript H indicates the Hermitian transpose.

Description of Argument List

NPØT	Data set number of the system output data set
NTAPSB	Tape number containing the \tilde{S} matrix
NC	Number of constraints; number of rows in the \tilde{S} matrix (SBB)
NS	NS = the greater of (NP+NC) and (NEM+NC); number of columns in the \tilde{S} matrix
NX	NX=NS if NEM=0, NX=NEM + NC otherwise
DC	The complex ΔC_e array
EB	The complex array $\{\tilde{\epsilon}\}$, output of subroutine GINV
B	An array of intermediate solutions (complex)
S	A complex two-dimensional work array of dimension NC by NC
SBB	The complex NC by NS matrix, \tilde{S}

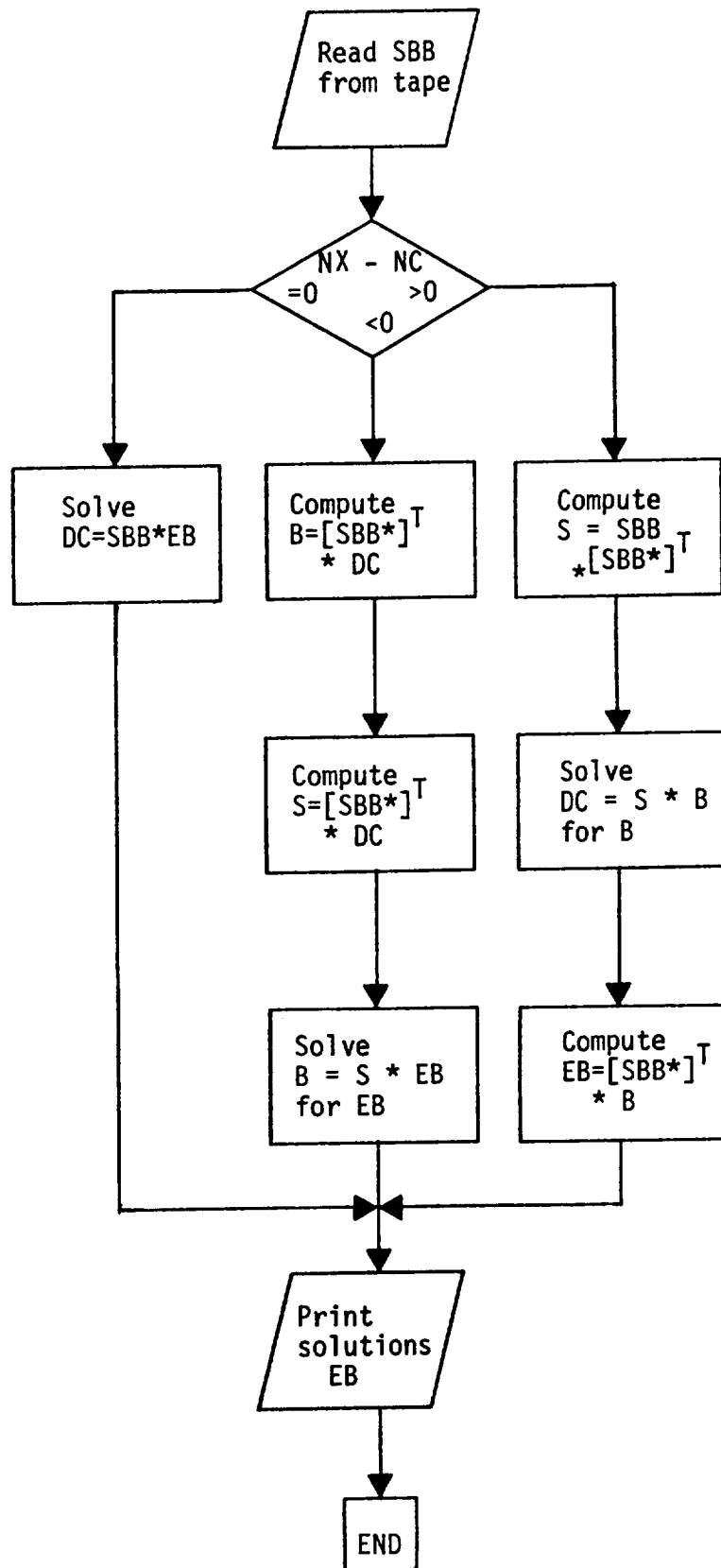
Calling Subroutine

WEYT

Called Subroutine

MIS2, the standard IBM system subroutine
for solving complex matrix equations

Flow Chart



SUBROUTINE MATM(NT, IGØ, NR, NC, NMAX, A, C, B)

Functional Description

Subroutine MATM is essentially a matrix multiplication routine. It obtains the DI matrix ([A]) rows from tape NT and the W matrix from the two-dimensional array B. The results of the matrix multiplication, ΔC_{p_t} , are saved in array B which is returned to the calling routine, DCPB, via the argument list.

Description of Argument List

NT	Tape number containing the inverse-D matrix
IGØ	1 for symmetric modes 2 for antisymmetric modes
NR	Number of rows in the ΔC_{p_t} matrix
NC	Number of columns in the ΔC_{p_t} matrix
NMAX	Maximum number of columns in the ΔC_{p_t} matrix
A	A row of the inverse-D matrix, [A]
C	Complex work array
B	Two-dimensional complex array in which the ΔC_{p_t} matrix is stored

Calling Subroutine

DCPB

SUBROUTINE MODF(NC, NS, MASTSB, NEWTSB, JARR, SQRTT, ELIM,
SBB, DCI, DCMOD)

Functional Description

When some of the values of $\bar{\epsilon}$ have exceeded their limits and have been replaced by the limit values, these new values of $\bar{\epsilon}$ (called ϵ_d in Equation (56)) are then considered fixed and known. However the constraints are now not satisfied and a change in the constraint ΔC_e , i.e., ΔC_{mod} , is calculated (see Equation (59)).

$$\Delta C_{mod} = \Delta C_e - [\bar{S}_d] \{\epsilon_d\}$$

Since the new values of $\bar{\epsilon}$, i.e., ϵ_d , can not influence solution further the \bar{S} matrix must be changed to delete the influence of ϵ_d . Thus the elements of \bar{S} that give the influence of ϵ_d , i.e., \bar{S}_d , must be eliminated resulting in \bar{S}_u . This subroutine forms \bar{S}_u , or in the notation of the computer program $[\bar{S}_{mod}]$.

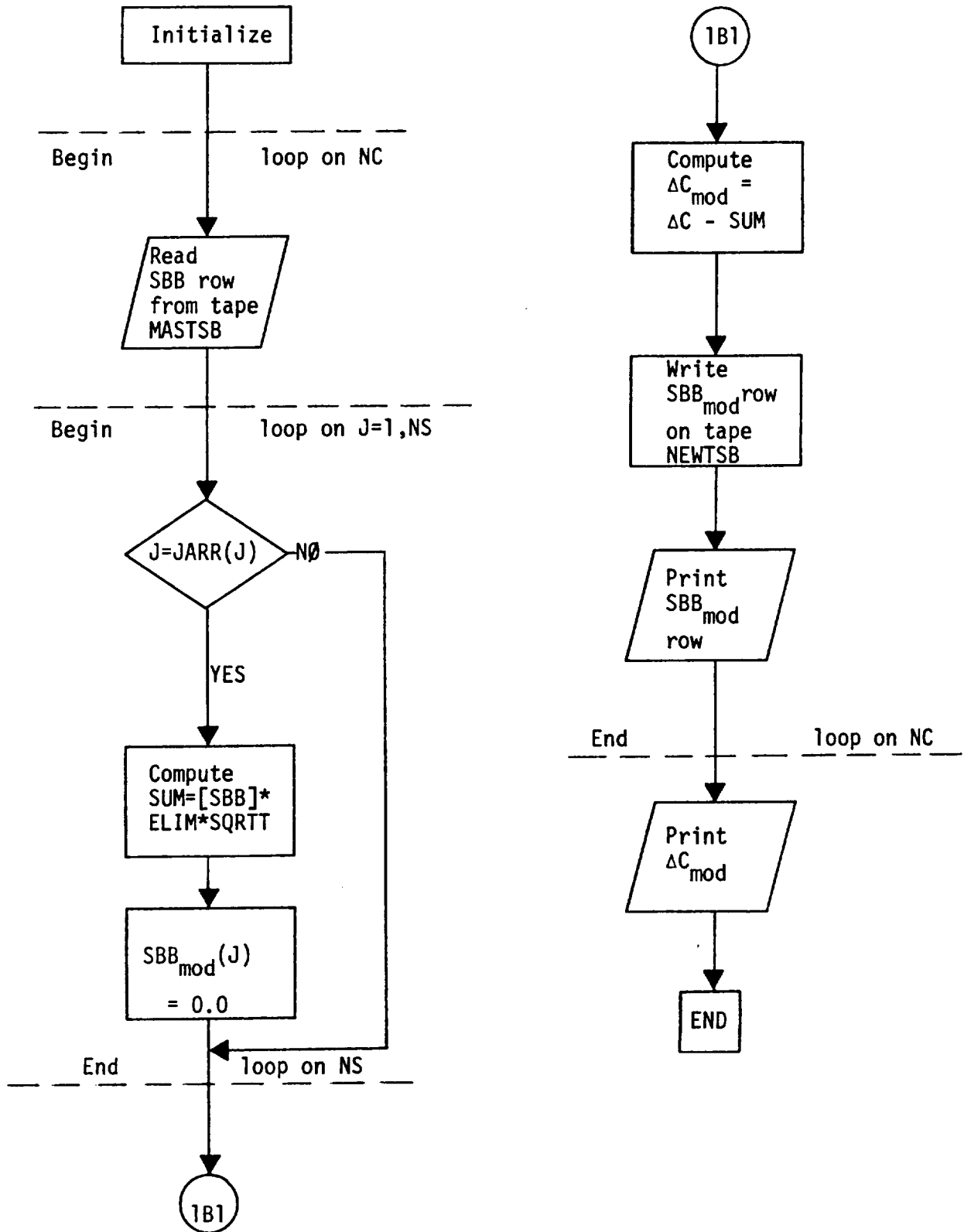
Description of Argument List

NC	Number of constraints - dimension of the complex arrays DCI and DCMØD
NS	Dimension of the complex array SBB
MASTSB	Tape number containing SBB arrays (i.e., rows of the \bar{S} matrix)
NEWTSB	Tape number containing the modified SBB arrays (i.e. rows of the \bar{S}_{mod} matrix) $\bar{S}_{\text{mod}} = \bar{S}_u$
JARR	Array of the element numbers for which the \bar{S} -values are replaced by zeroes
SQRTT	$\sqrt{T_j}$ - see Equations (23) and (34)
ELIM	ϵ_{limj} , array of the modified ϵ values
SBB	Complex array containing rows of the \bar{S} matrix
DCI	Complex array containing ΔC_e
DCMØD	Complex array containing ΔC_{mod}

Calling Subroutine

WEYT

Flow Chart



SUBROUTINE PHIJ(NPIT, NPOT, NTPHIJ, NEM, NP, KODE, MØDES, X, Y, Z, PHI)

Functional Description

This subroutine forms the correction factor modes. If ϕ is input element by element (TYPE = 0) then this subroutine simply arranges the data into arrays. If TYPE = 1 then modes are calculated as follows:

$(x_j - a_\ell)^{n_\ell}$	TYPE = 1
$(y_j - a_\ell)^{n_\ell}$	2
$(z_j - a_\ell)^{n_\ell}$	3
$\exp[b_\ell(x_j - a_\ell)^{n_\ell}]$	4
$\exp[b_\ell(y_j - a_\ell)^{n_\ell}]$	5
$\exp[b_\ell(z_j - a_\ell)^{n_\ell}]$	6

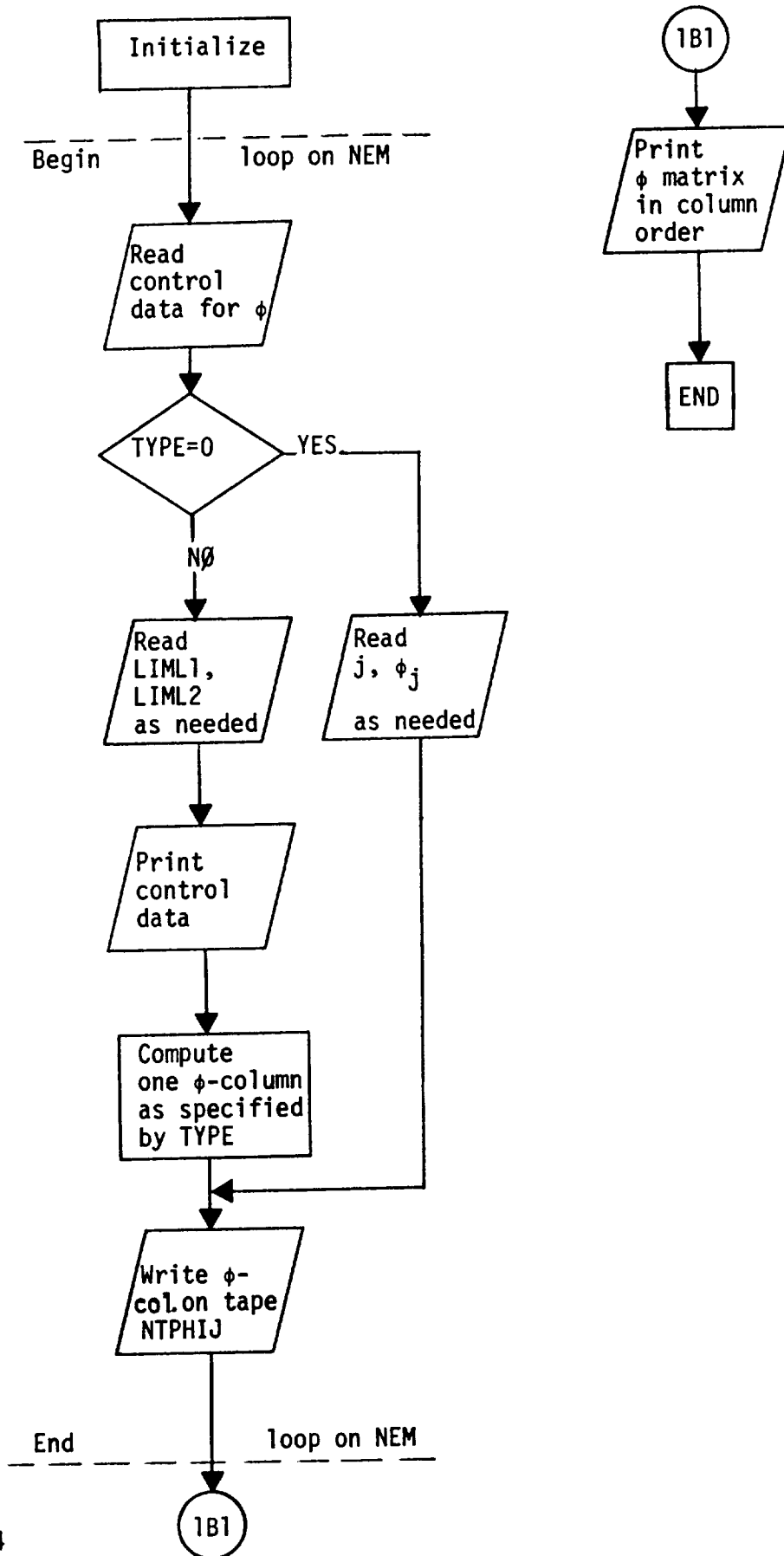
where a b n are input per mode and where $\phi_{j\ell} = 0$ over boxes are not considered.

Description of Argument List

NPIT	Data set number of the system input data set
NPOT	Data set number of the system output data set
NTPHIJ	Tape number containing columns of the NP by NEM ϕ matrix
NEM	Row dimension of the ϕ matrix
NP	Column dimension of the ϕ matrix
KODE	-1 (end indicator of card input sets)
MDES	not used
X	x } y } coordinates of the pressure points or z } of the ΔC_p 's
Y	
Z	
PHI	Complex array containing one column of the ϕ matrix

Calling Subroutine WEYT

Flow Chart



SUBROUTINE POSN(NT, IGØ)

Functional Description

This subroutine positions tapes of a certain uniform format for reading; see Tape Description for NTDCP, NTAPW and NTAPDI.

Description of Argument List

NT	Tape number to be positioned for reading
IGØ	1 for symmetric modes, 2 for antisymmetric modes

Calling Subroutines DCPB, DCPT, MATM, SBAR

SUBROUTINE RECD(NTAPE, A, N)

Functional Description

This subroutine reads arrays of real numbers A of length N from tape NTAPE one record at a time. It is used for the reading of the geometry arrays when these are input from tape NTGEØM.

Description of Argument List

NTAPE	Tape number
A	Array to be read from tape
N	Length of array A

Calling Subroutine WEYT

SUBROUTINE SAIJ(NPIT, NPOT, NTSAIJ, NTSANJ, NC, NP, NMØN, NAXIS,
AIT, CIE, X, Y, Z, CG, SG, DELA, FLAGA, FLAGF,
KØDE, IPRINT, LABEL, SAI)

Functional Description

This subroutine sets up proper argument lists for SROW so that integration matrices, [S], can be calculated for both constraining and monitoring purposes.

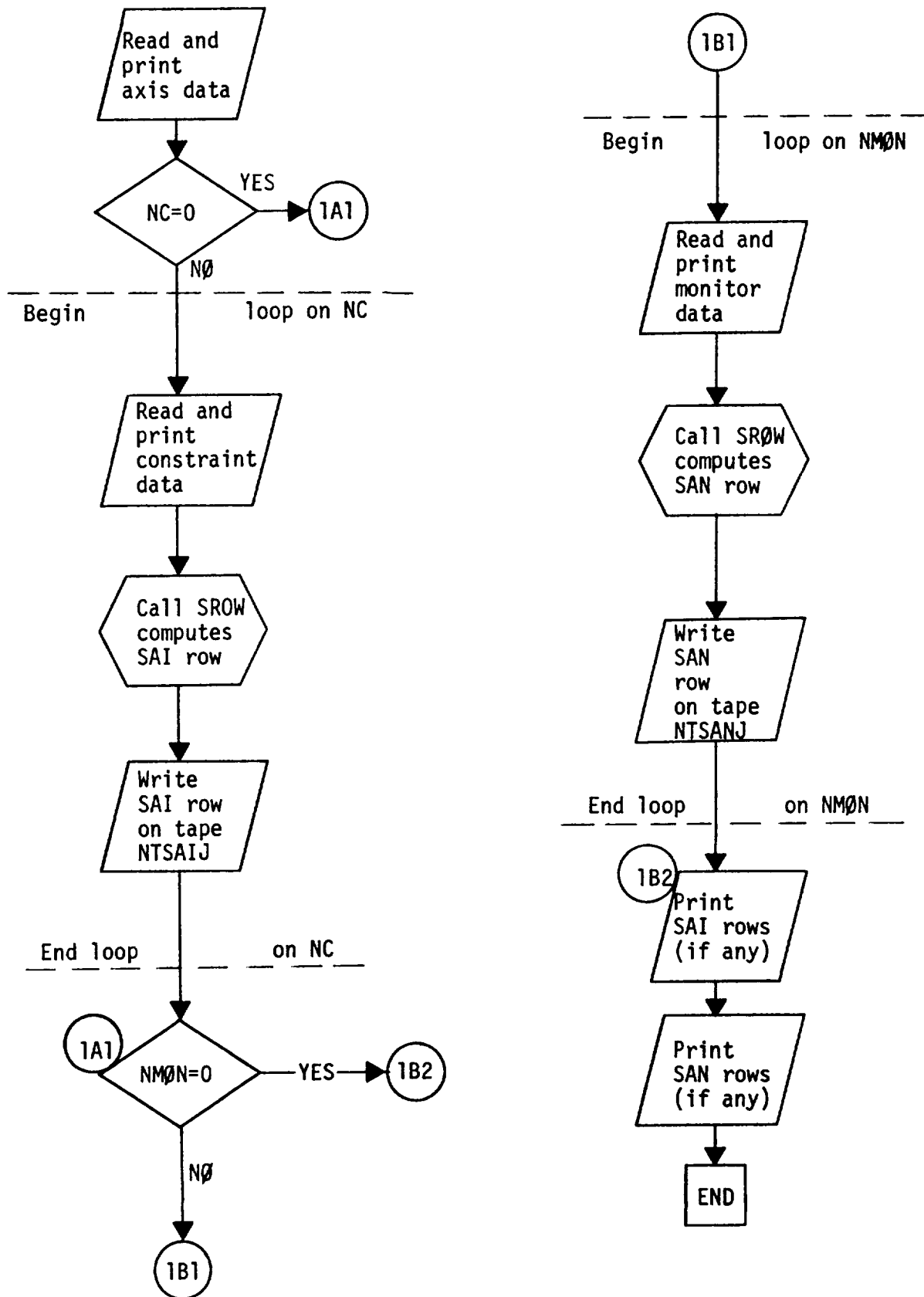
Description of Argument List

NPIT	Data set number of the system input data set
NPOT	Data set number of the system output data set
NTSAIJ	Tape number containing the integration matrix rows, SA_{ij} , for constraints
NTSANJ	Tape number containing the integration matrix rows, SA_{nj} , for monitoring
NC	Number of constraints
NP	Number of ΔC_p elements
NMON	Number of sets of the monitoring data
NAXIS	Number of axes
AIT	Constraining effectiveness of the experimental data, \tilde{a}_i
CIE	Experimental (or any other) constraint on the data, C_e
X, Y, Z	Coordinates of the pressure points (boxes)
CG, SG	Cosine-, sine of box dihedral angles
DELA	Box areas
FLAGA	Axis flag = 0, axis endpoints are input = 1, direction cosines are input
FLAGF	Force/moment flag = 0, C_e is a force in the direction of axis = 1, C_e is a moment about axis

KØDE = -1
IPRINT Detail print flag
IPRINT = 1, print SA_{ij}
and SA_{nj} rows
IPRINT = 0, bypass print
LABEL Alphameric identifier of the integrated parameters
SAI Complex array containing a row of either one of the
integration matrices SA_{ij} or SA_{nj}

Calling Subroutine WEYT
Called Subroutine SRØW

Flow Chart



SUBROUTINE SBAR(NTSBIJ, NTAPDI, NC, NP, NS, FLAGP, FLAGT, FLAGW,
I, IG0, SQRTT, AIW, SAI, DI, W, DELCPB, SBI)

Functional Description

This subroutine solves for the matrix SBI where

$$SBI = [\bar{S}] [\sqrt{T^*}]^{-1}$$

The matrix $[\bar{S}]$ contains all the capability of the program except modes and limits. This capability is outlined in Eqs. (45), (26) and (9) for pre-multipliers and (45), (39) and (30) for postmultipliers. The weights T^* are defined below Equation (47).

$$SBI = \begin{cases} \bar{S}A_{ij} & \text{when } j = 1, 2 \dots NP, i = 1, 2 \dots NC \\ WT_i & \text{when } j = NP + i \\ 0 & \text{otherwise} \end{cases}$$

where NP = number of pressure values and NC = number of constraints.

$$\bar{S}A_{ij} = \begin{cases} SA_{ij} \Delta C_{p_j} / \sqrt{T_j} & \text{when } \Delta C_p \text{ available} \\ \sum SA_{i_k} DI_{k_j} W_j / \sqrt{T_j} & \text{when } \Delta C_{p_j} \text{ not available} \end{cases}$$

$$WT_i = \begin{cases} (1 - \tilde{a}_i) / \tilde{a}_i & \tilde{a}_i > 0.0001 \\ 10^4 & \tilde{a}_i \leq .0001 \end{cases}$$

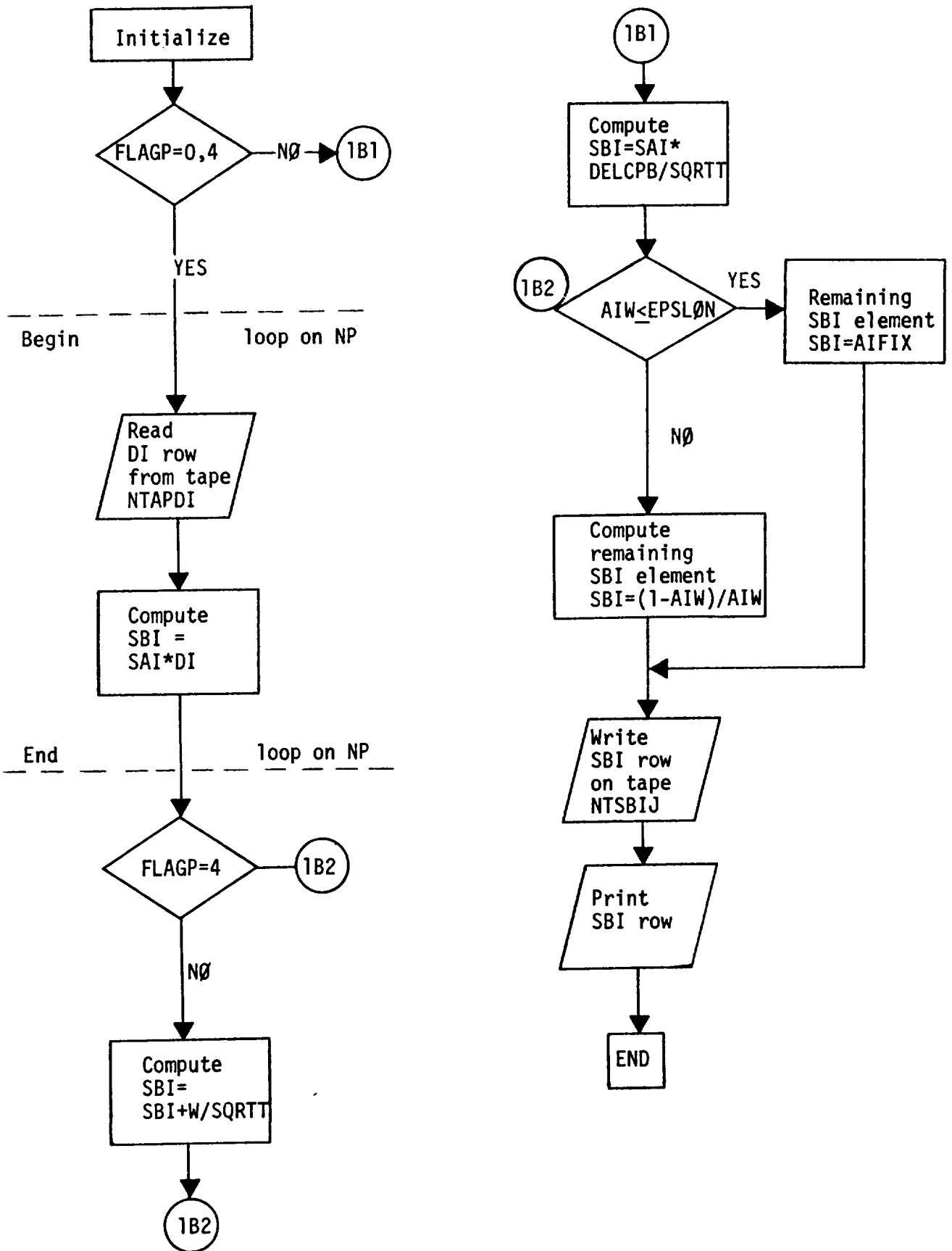
$$T_j = \begin{cases} |\Delta C_{p_t}| \Delta A & \text{FLAGP} \neq 1 \\ \text{or} & \\ |W| & \text{FLAGP} = 1 \\ 1, 0 & \text{FLAGT} = 1 \end{cases} \quad \text{FLAGT} = 0$$

Description of Argument List

NTSBIJ	Tape number containing rows of the integration matrix without weight factor modes, \bar{S}
NTAPDI	Tape number containing rows of the inverse-D matrix
NC	Number of constraints
NP	Number of ΔC_p elements
NS	Length of the SBI matrix rows
FLAGP	Option flag for ΔC_p and/or pre- or post-multiplying correction factors
FLAGT	Option flag for weights
FLAGW	Option flag for normalwash input
I	An intermediate index
IGØ	1 for symmetric modes 2 for antisymmetric modes
SQRTT	$= \sqrt{T}$; see equations
AIW	Constraining effectiveness \tilde{a}_i
SAI	A row of the integration matrix S'_{ij}
DI	A row of the inverse-D matrix
W	A column of the normalwash matrix
DELCPB	A column of the ΔC_{pe} matrix (lifting pressure coefficients, either input, ΔC_p , or computed as $[D]^{-1} \{W\}$)
SBI	A row of the integration matrix without weight factor modes, $[\bar{S}] [\sqrt{T^*}]^{-1}$, $T^* = \begin{cases} T & \text{for constraints} \\ \frac{1-\tilde{a}}{\tilde{a}} & \text{for estimates} \end{cases}$

Calling Subroutine SDBL

Flow Chart



SUBROUTINE SDBL(NSCRCH, NUTL, MASTSB, NTPHIJ, NTAPW, NTSAIJ,
NTAPDI, IGØ, FLAGW, FLAGP, FLAGT, NC, NP, NS,
NEM, SQRTT, AIT, DELA, SBB, SBI, SAI, DI, W, PHI, DELCP)

Functional Description

This subroutine calculates $\bar{[S]}$ described in Equation (54). The quantity calculated in this routine includes estimates and thus

$$\bar{[S]} = [SBB] = [\tilde{S}] \begin{bmatrix} \phi & 10 \\ - & - & - \\ 0 & I \end{bmatrix}$$

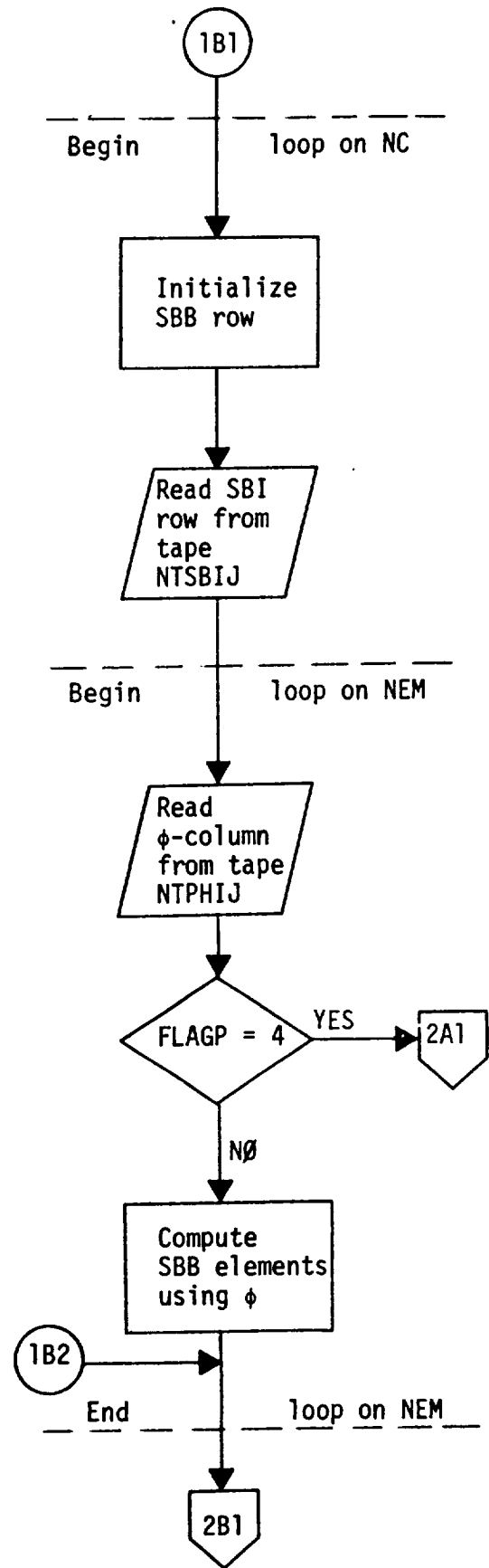
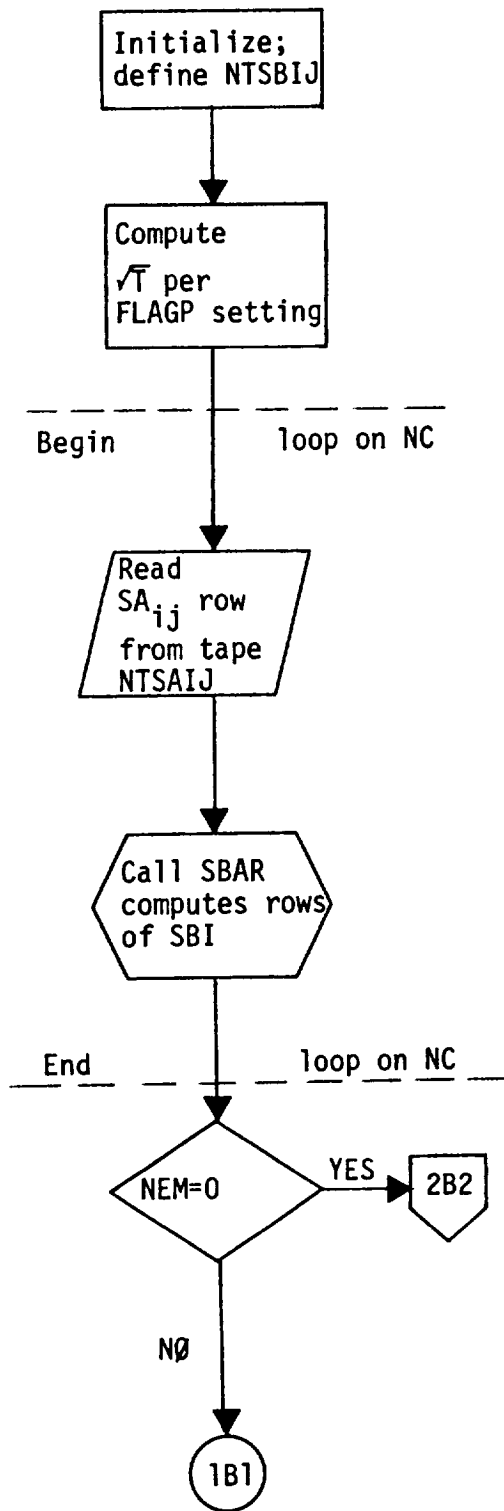
Description of Argument List

NSCRCH	Tape number containing columns of the $\bar{\phi}$ matrix (if any)
NUTL	Utility (scratch) tape number
MASTSB	Tape number containing the \bar{S} matrix rows
NTPHIJ	Tape number containing the ϕ matrix columns
NTAPW	Tape number containing columns of the normalwash matrix
NTSAIJ	Tape number containing rows of the integration matrix, SA_{ij}
NTAPDI	Tape number containing rows of the inverse-D matrix
IGØ	1 for symmetric modes 2 for antisymmetric modes
FLAGW	Option flag for normalwash input
FLAGP	Option flag for ΔC_p input and/or pre- or post-multiplying corrections
FLAGT	Option flag for weights
NC	Number of constraints
NP	Number of ΔC_p elements
NS	= max (NP+NC, NEM+NC)
NEM	Number of correction factor modes
SQRTT	$\sqrt{T_j}$, see equations
AIT	Constraining effectiveness \tilde{a}_i
DELA	Box areas
SBB	A row of the \bar{S} matrix (integration matrix with weight factor modes)
SBI	A row of the $[\bar{S}] [\sqrt{T^*J}]^{-1}$ matrix
SAI	A row of the S_{ij} elements

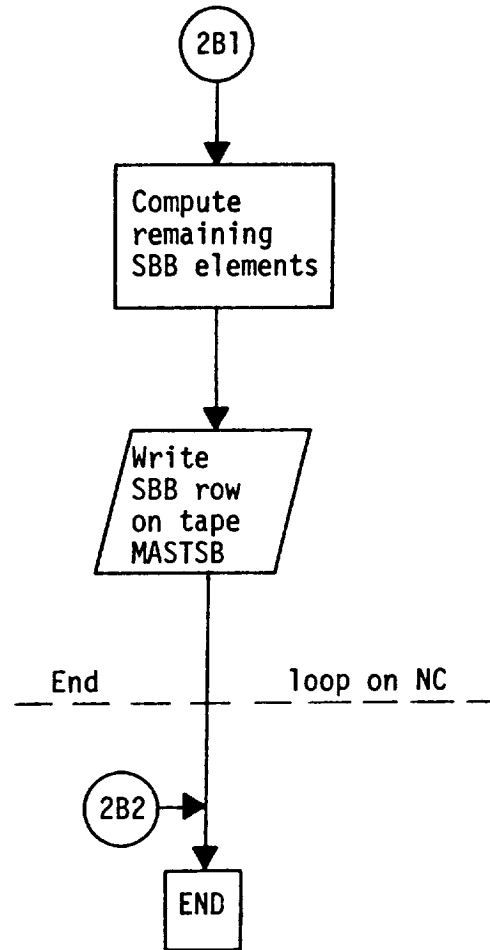
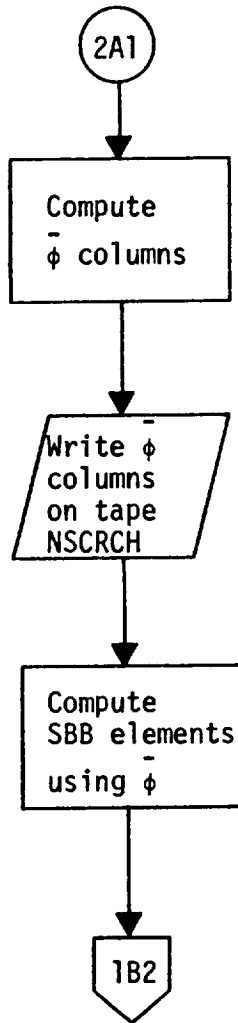
DI	A row of the inverse-D matrix
W	A column of the normalwash matrix
PHI	A column of the ϕ matrix (weight factor mode shapes)
DELCPB	A column of the ΔC_{p_t} matrix

<u>Calling Subroutine</u>	WEYT
<u>Called Subroutine</u>	SBAR

Flow Chart



Flow Chart



SUBROUTINE SRØW(FLAGA, FLAGF, XI1, ETA1, ZETA1, CG, SG, CTIL,
X, Y, Z, DELA, LIM1, IIMAX, I, NP, IR, XI2,
ETA2, ZETA2, SAI)

Functional Description

This subroutine constructs the integration matrix [S] described in Equation (3) a row at a time.

$$S_{ij} = SAIJ = \begin{cases} A_{ij} \Delta A_j & \text{for force calc.} \\ B_{ij} \Delta A_j & \text{for moment calc.} \end{cases}$$

$$A_{ij} = [-\cos\beta_i \sin\bar{\gamma}_j + \cos\gamma_i \cos\bar{\gamma}_j] / \tilde{c}_i$$

$$B_{ij} = \{ \cos\alpha_i [(y_i - \eta_i^{(1)}) (\cos\bar{\gamma}_j) + (z_j - \zeta_i^{(1)}) \sin\bar{\gamma}_j] \\ - \cos\beta_i (x_j - \xi_i^{(1)}) \cos\bar{\gamma}_j \\ - \cos\gamma_i (x_j - \xi_i^{(1)}) \sin\bar{\gamma}_j \} / \tilde{c}_i$$

where $\cos\alpha_i$, $\cos\beta_i$, $\cos\gamma_i$ are the direction cosines of the input axis and where x_j , y_j , z_j , $\bar{\gamma}_j$ are the coordinates and dihedral of the aerodynamic box and $\xi_i^{(1)}$, $\eta_i^{(1)}$, $\zeta_i^{(1)}$ are the coordinates of the one edge of the input axis. SAIJ is of course zero on boxes that are not to be integrated.

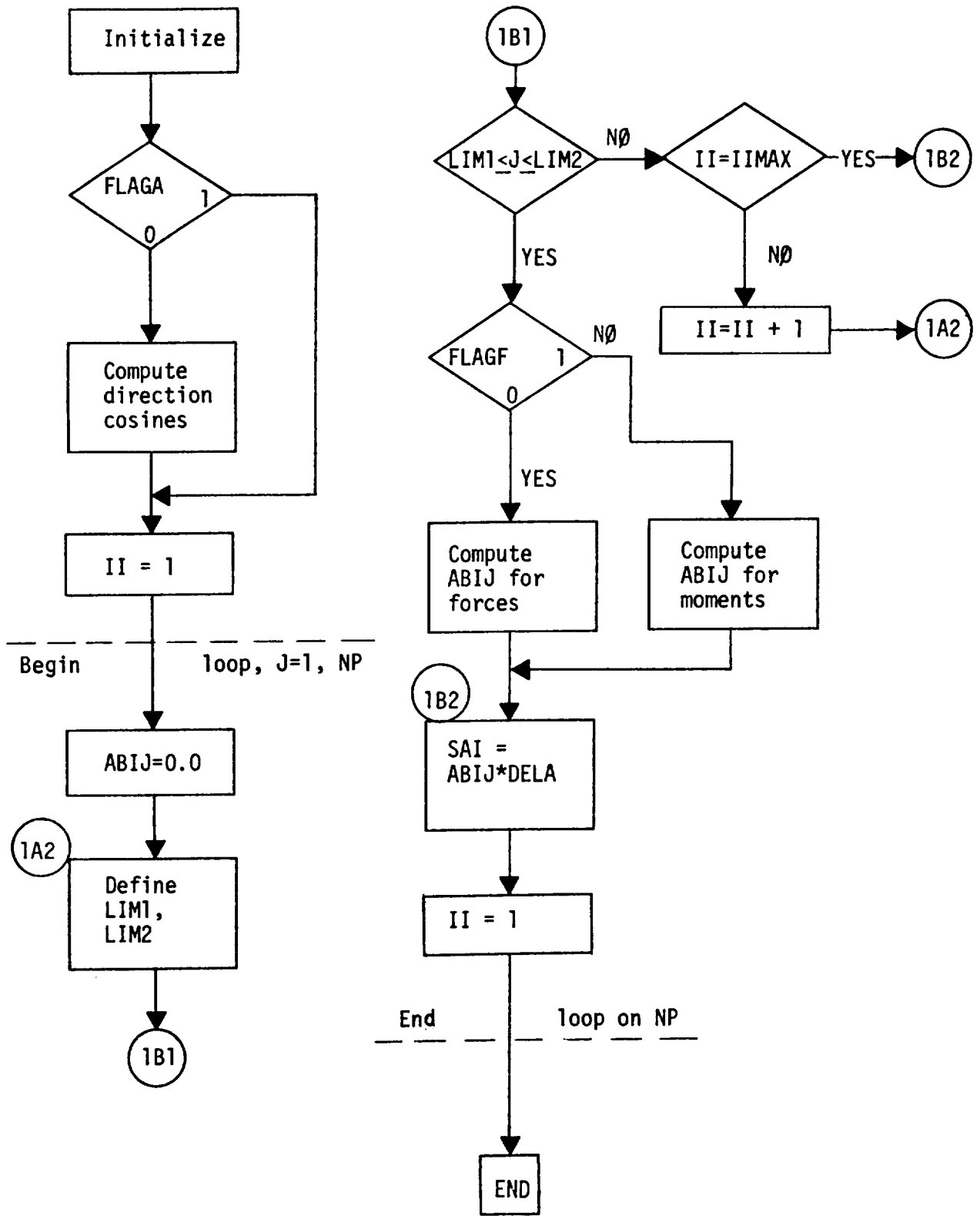
Description of Argument List

FLAGA	Axis input option flag = 0, axis endpoints are input = 1, direction cosines are input
FLAGF	Force/moment flag = 0, $C_i^{(e)}$ is a force in direction of axis = 1, $C_i^{(e)}$ is a moment about axis
XI1	} Axis endpoint coordinates, $\xi^{(1)}$, $\eta^{(1)}$, $\zeta^{(1)}$
ETA1	
ZETA1	
CG, SG	Cosine-, sine of box dihedral angles
CTIL	Constant used to nondimensionalize integrated data (\tilde{c})
X, Y, Z	Coordinates of the pressure points (boxes)
DELA	Box areas
LIMI	First-, last box numbers for the integration of the ΔC_p values
IIMAX	Number of LIM I sets input for one constraint
I	Intermediate index
NP	Number of ΔC_p values
IR	Row index of the S_{ij} matrix
XI2	} Second axis endpoint coordinates when FLAGF = 0, direction cosines when FLAGF = 1
ETA2	
ZETA2	
SAI	A row of the integration matrix S

Calling Subroutine

SAIJ

Flow Chart



SUBROUTINE WEYT(NP, NC, NEM, NELIMS, NMØN, NAXIS, NMIN, NMAX, NS,
NPIT, NPØT, W, DI, DCP, EPS, PHI, SAI, DCPTIL,
DELCPB, CØL, CIE, DCMØD, EBMIN, EBMAX, EB, ELIM,
SBB, SBI, S, SBMAT, DCI, WØRK)

Functional Description

This subroutine is the core of the correction factor method. All logic for the method is established here. This subroutine uses input to decide what is to be done and sets up the argument lists for and executes the calls to all required subroutines. The following flow charts document the logic flow of this subroutine. This subroutine sets up the logic for various forms of input data and various types of calculations. The input data ranges over geometry, pressures, downwashes, aerodynamic influence matrices, previously generated correction factors, integration matrix data, etc. This data can enter the program by cards, tapes or both.

There are three basic computational branches; (1) correction factor calculation, (2) monitoring of data (integration of pressures into aerodynamic parameters) and (3) application of previously generated correction factors to pressure distributions. Within branch (1) there exists a choice of what type of correction factors to generate, premultiplier, postmultiplier and new postmultiplier. Also a choice as to the type of weighting to be used (i.e. the T) is available. The program also tests to see if limits are placed on the correction factors and if modes are used. The constraining power \tilde{a} is always input since a constraint is simply $\tilde{a} = 1.0$.

Description of Argument List

NP	Number of ΔC_p elements
NC	Number of constraints
NEM	Number of correction factor modes
NELIMS	Number of input cards for the EBMIN, EBMAX pairs
NMØN	Number of sets of monitoring data
NAXIS	Number of axes for use in the inegration of the ΔC_{p_t} values
NMIN	= max (1, NELIMS)
NMAX	= max (NC, NMIN, 10)
NS	= max (NP+NC, NEM+NC)
NPIT	Data set number of the system input data set
NPØT	Data set number of the system output data set
W	A column of the normalwash matrix
DI	A row of the inverse-D matrix , (A matrix)
DCP	A column of the theoretical ΔC_{p_t} matrix
EPS	Incremental weight factors array, ϵ
PHI	A column of the weight factor mode shape matrix, ϕ
SAI	Integration matrix row array , [S]. SAN = [S] for monitoring
DCPTIL	A column of pressures modified by weight matrix, $\tilde{\Delta C}_{p_e}$
DELCPB	A column of the unmodified lifting pressure coefficients, ΔC_{p_t} (either input, ΔC_{p_t} , or computed as $[D]^{-1} \{W\}$)

CØL	Complex array for intermediate use
CIE	Array of the experimental constraints, C_{e_i}
DCMØD	Array of the modified ΔC_e values
EBMIN, EBMAX	Minimum-, maximum values allowed for the ϵ array to take
EB	$\bar{\epsilon}$ array (incremental weight factors) ($\epsilon = \phi \bar{\epsilon}$)
ELIM	Array of the modified ϵ values
SBB	A row of the \bar{S} matrix
SBI	A row of the $[\bar{S}] [\sqrt{T^*}]^{-1}$ matrix
S	A two-dimensional complex work array of dimension NC by NC
SBMAT	\bar{S} matrix of maximum dimension NC by NS
DCI	Array of the ΔC_e values
WØRK	A two-dimensional complex array of dimension NP by NMAX in which the ΔC_{p_t} matrix is stored

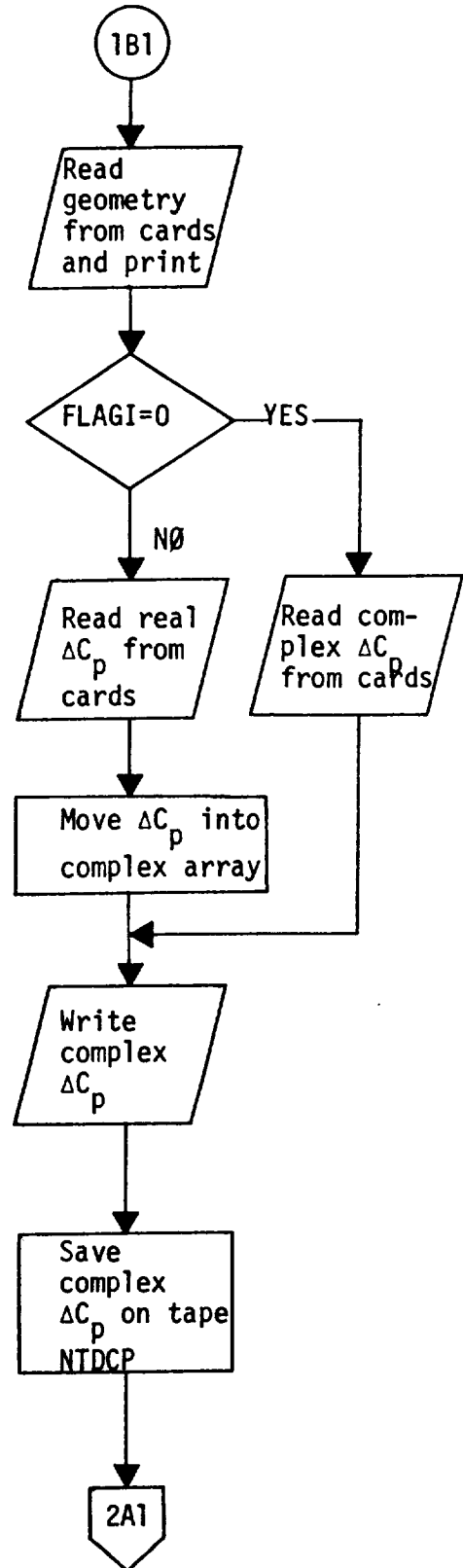
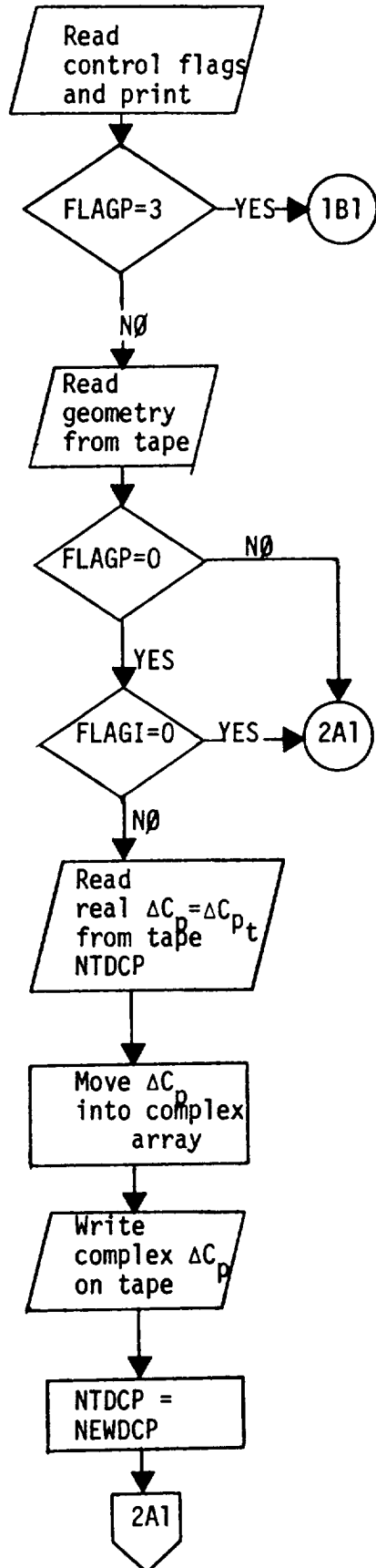
Calling Subroutine

MAIN

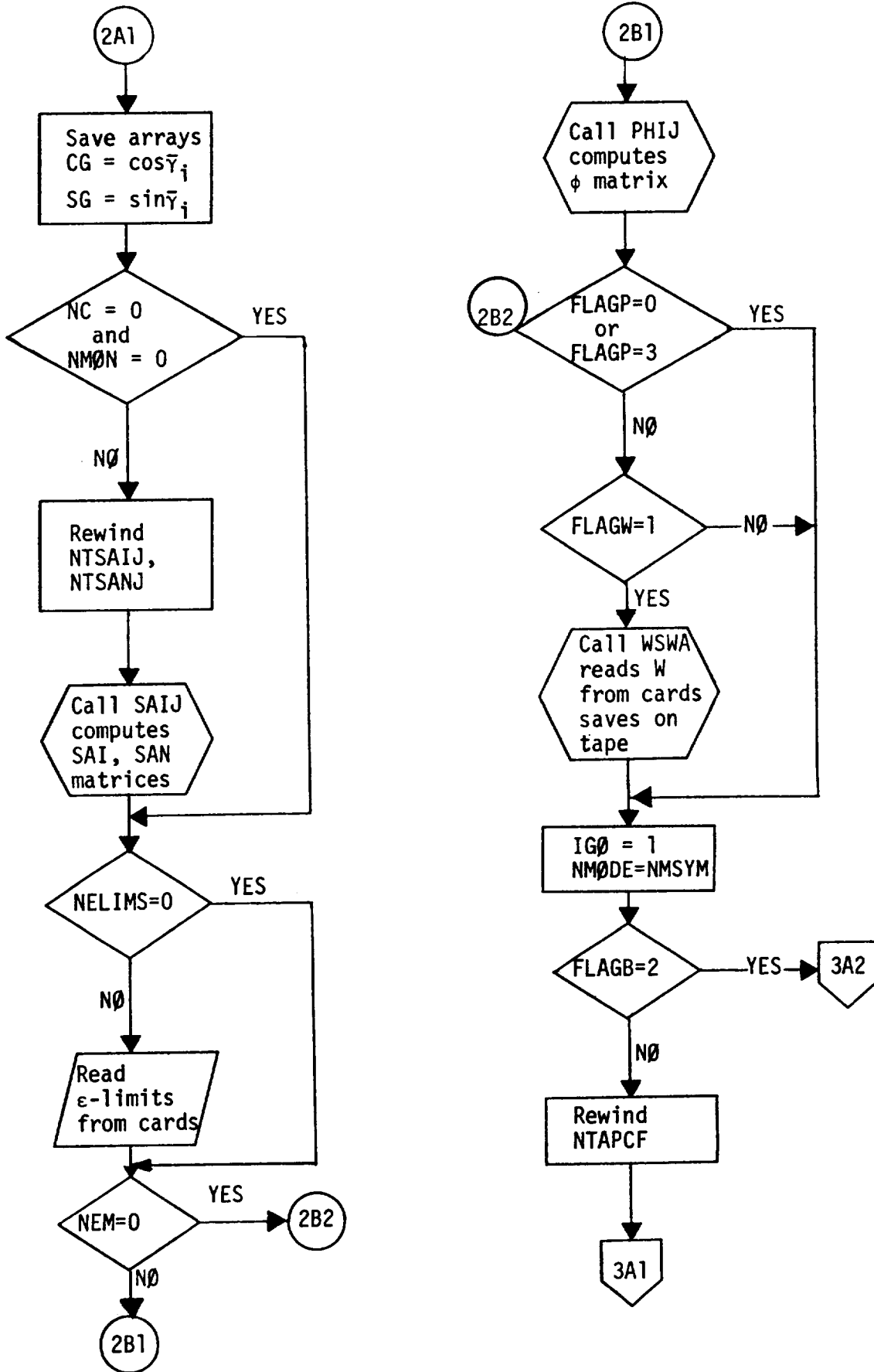
Called Subroutines

CEMN, DCPB, DCPT, DELC, EDBL, EPSJ,
GINV, MØDF, PHIJ, RECD, SAIJ, SDBL,
WSWA

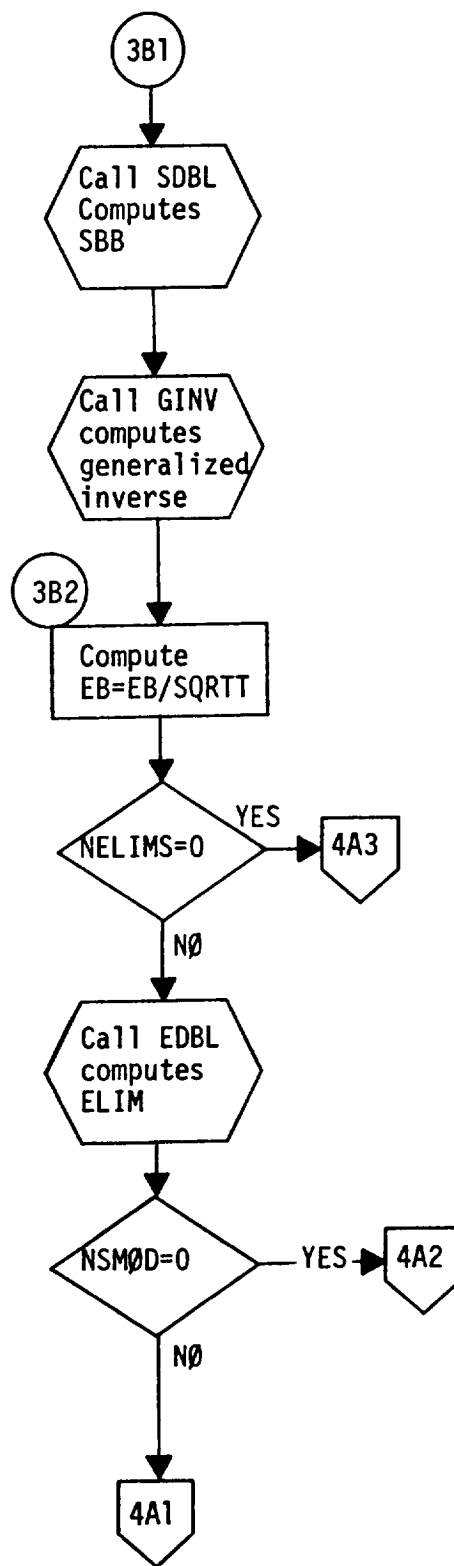
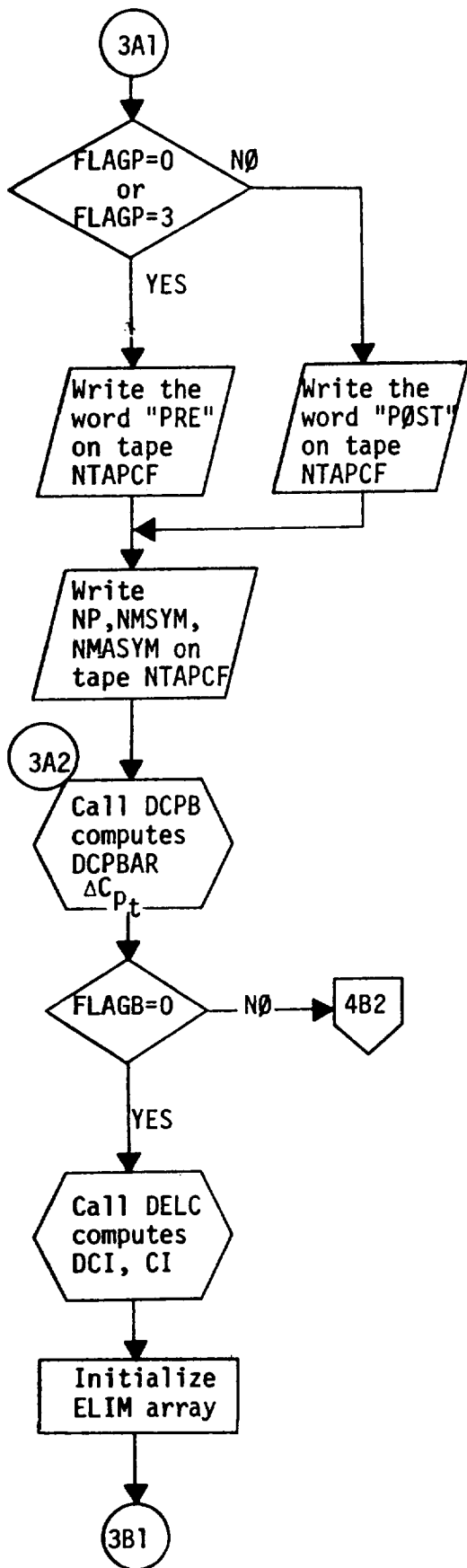
Flow Charts (Read in geometry and pressures)



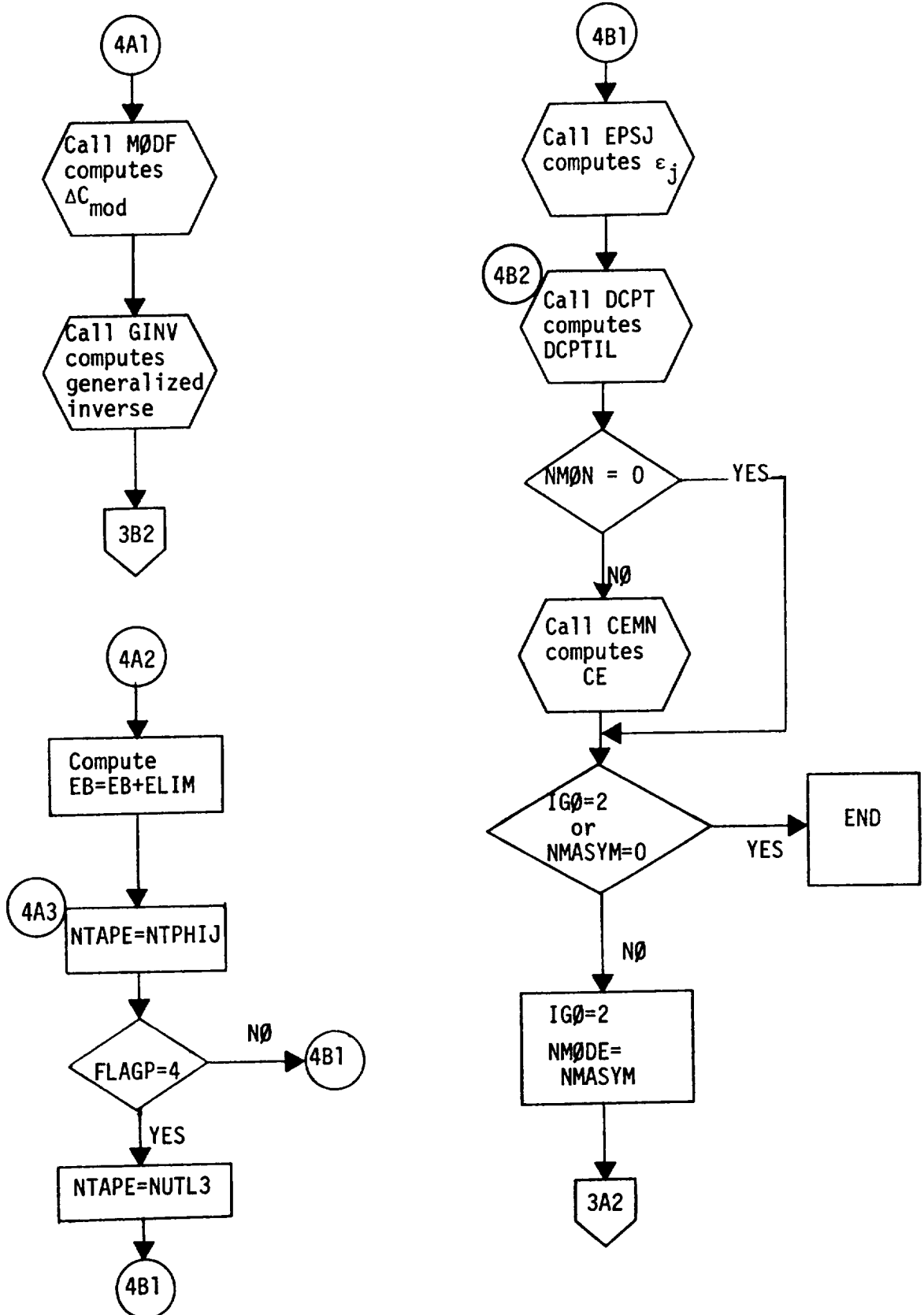
Flow Charts (Calculation of S , ϕ , W)



Flow Charts (Basic method)



Flow Charts (Accounting for limits)



SUBROUTINE WSWA(NPIT, NPOT, NUTL1, NTAPW, KODE, NP, NCOL,
NMAX, NMSYM, NMASYM, W)

Functional Description

Subroutine WSWA is called from WEYT only if the input flag FLAGW = 1. It reads and prints the mode number and symmetry flag identifying the mode, the range of boxes over which the input W value applies, and the normalwash, W for this range of boxes. This card input is repeated for all ranges as needed, but only the non-zero W values are required as input. The complete W matrix is assembled from the input and is saved on tape NTAPW in column order.

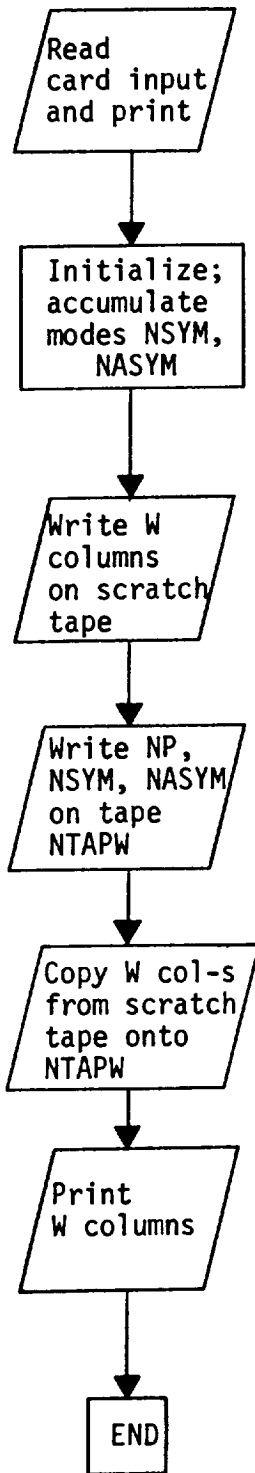
Description of Argument List

NPIT	Data set number of the system input data set
NPOT	Data set number of the system output data set
NUTL1	Utility (scratch) tape number
NTAPW	Tape number containing columns of the W matrix
KODE	= -1
NP	Number of row elements in the W matrix
NCOL	Number of columns in the W matrix
NMAX	Maximum number of columns in the W matrix
NMSYM	Number of symmetric modes
NMASYM	Number of antisymmetric modes
W	Two-dimensional complex array containing the W matrix

Calling Subroutine

WEYT

Flow Chart



SUBROUTINE ZEROUT(WORK, LENGTH, LOOP, ITAPE)

Functional Description

This subroutine initializes a complex array WORK of length LENGTH to zeroes. In addition to this, when the argument ITAPE \neq 0, the complex zeroes stored in WORK are written on tape ITAPE as many times as specified by the argument LOOP.

Description of Argument List

WORK	Complex array to be initialized to zeroes
LENGTH	Length of the complex array WORK
LOOP	Number of times the array WORK is to be written on tape ITAPE (only if ITAPE \neq 0)
ITAPE	Tape number on which the array WORK is saved LOOP-times (if any)

Calling Subroutines EPSJ, MAIN, MATM, SDBL

LISTING

CORRECTION FACTORS (EIGC) 02/03/76

```

1 SUBROUTINE CEMN(NPOT, IGO, NMODE, NTAPSA, NP, NMON, LABEL, NUTL,
  SAI, DCPTIL, CE)
  DATA SET NUMBER OF THE SYSTEM OUTPUT DATA SET
  I FOR SYMMETRIC MODES, 2 FOR ANTISYMMETRIC MODES
  NUMBER OF MODES
  TAPE NUMBER CONTAINING THE INTEGRATION MATRIX SA
  NP
  NMON
  NUTL
  SAI
  DCPTIL
  CE
  DIMENSION LABEL(10, 35)
  COMPLEX ( 1HI// 40H ) DCPTIL( NP ), CE( 35 )
  10 FORMAT ( 1HI// 40H ) SYMMETRIC CE-N
  20 FORMAT ( 1HI// 40H ) ANTISYMMETRIC CE-N
  30 FORMAT ( / 40H N LABEL CE(N)
  40 FORMAT ( 14, 8X, 10A1, 2E16.6 ) REAL IMAG./ )

  REWIND NUTL
  DO 120 MODE = 1, NMODE
  READ (NUTL) IGO, N, MD, DCPTIL
  GO TO (50, 60), IGO
  50 WRITE (NPOT, 10) MODE
  GO TO 70
  60 WRITE (NPOT, 20) MODE
  REWIND (NPOT, 30)
  DO 110 N = 1, NMON
  READ (NTAPSA) NDN, MN, SAI
  CE(N) = (0.0, 0.0)
  DO 100 I = 1, NP
  CE(N) = CE(N) + SAI(I) * DCPTIL(I)
  100 CONTINUE

  WRITE (NPOT, 40) N, ( LABEL(M, N), M = 1, 10), CE(N)
  110 CONTINUE
  120 CONTINUE

  RETURN
  END
SUBROUTINE DCPB(NTDCP, NTAPW, NTAPDI, IGO, IFP, NROW,
  NCOL, NMAX, DCP, COL, IFW, WORK )
  NTDCP
  NTAPW
  NTAPDI
  IGO
  IFP
  DCPB(NTDCP, NTAPW, NTAPDI, IGO, IFP, NROW,
  NCOL, NMAX, DCP, COL, IFW, WORK )
  TAPE NUMBER CONTAINING THE PRESSURE COEFFICIENTS
  TAPE NUMBER CONTAINING THE NORMALWASH MATRIX
  I FOR SYMMETRIC MODES, 2 FOR ANTISYMMETRIC MODES
  DELTA-CP-OPTION FLAG (0, 1, 2, 3 OR 4)

```



```

IFW          NPOT
NROW         NUTL, NTAPDI, IGO, FLAGB, FLAGP, MODES, NP, NSCRCH,
NCOL        NEM, W, DI, EPS, DCPBAR, X, Y, Z, GMA, DELA, EB
DCP         DCPT0070
CJL         DCPT0080
NMAX        DCPT0090
WORK        DCPT0100
              DCPT0110
              DCPT0120
              DCPT0130
              DCPT0140
              DCPT0150
              DCPT0160
              DCPT0170
              DCPT0180
              DCPT0190
COMPLEX     DCP(NROW), COL(NROW), WORK(NROW, NMAX)

NTAPE = NTDCP
IF (IFP.EQ.1.OR.IFP.EQ.2.OR.IFP.EQ.4) NTAPE = NTAPW
CALL POSN( NTAPE, IGO )

DO 10 J = 1, NCOL
READ (NTAPE) (WORK(I, J), I = 1, NROW)
CONTINUE
IF (IFP.EQ.0.OR.IFP.EQ.3) GO TO 30
CONTINUE
CALL MATM(NTAPDI, IGO, NROW, NCOL, NMAX, DCP, COL, WORK )
CONTINUE

      WORK NOW CONTAINS THE ENTIRE DELTA-CP-BAR MATRIX

WRITE (6,50) NCOL
DO 40 J = 1, NCOL
WRITE (6,60) J, (I, WORK(I, J), I = 1, NROW)
IF (J.NE.NCOL) WRITE (6,70)
CONTINUE
50 FORMAT ( 1H1 /// 6H THE , I4, 55H COLUMNS OF THE DELTA-CP-BAR
1  MATRIX (
60 // 9H COLUMN , I4 // ( 3 ( I6, 2E14.6 ) ) )
70 FORMAT ( 1H1 // )
END
SUBROUTINE DCPT(NPOT, LINES, IGO, FLAGB, FLAGP, MODES, NP, NSCRCH,
NUTL, NTAPDI, NTAPW, NTAPCF, X, Y, Z, GMA, DELA, EB,
NEM, W, DI, EPS, DCPBAR, DCPBAR, WORK, EB )
1  2
DATA SET NUMBER OF THE SYSTEM OUTPUT DATA SET
OPTION FLAG FOR DATA MONITORING
1 FOR SYMMETRIC MODES, 2 FOR ANTISYMMETRIC MODES
NUMBER OF MODES
LENGTH OF THE DCPBAR ARRAY
TAPE NUMBER ON CONTAINING THE PHI-BAR MATRIX (IF ANY)
TAPE NUMBER ON WHICH THE DELTA-CP-TILDA MATRIX
COLUMNS ARE SAVED
TAPE NUMBER CONTAINING THE INVERSE-D MATRIX ROWS
(IF NEEDED)
TAPE NUMBER CONTAINING THE W MATRIX COLUMNS
(IF NEEDED)

```

DCPB0120
DCPB0130
DCPB0140
DCPB0150
DCPB0160
DCPB0170
DCPB0180
DCPB0190
DCPB0200
DCPB0210
DCPB0220
DCPB0230
DCPB0240
DCPB0250
DCPB0260
DCPB0270
DCPB0280
DCPB0290
DCPB0300
DCPB0310
DCPB0320
DCPB0330
DCPB0340
DCPB0350
DCPB0360
DCPB0370
DCPB0380
DCPB0390
DCPB0400
DCPB0402
DCPB0410
DCPB0420
DCPB0430
DCPB0440
DCPB0442
DCPB0450
DCPB0460
DCPT0040
DCPT0050
DCPT0060
DCPT0070
DCPT0080
DCPT0090
DCPT0100
DCPT0110
DCPT0120
DCPT0130
DCPT0140
DCPT0150
DCPT0160
DCPT0170
DCPT0180
DCPT0190

CORRECTION FACTORS (EIGC) 02/03/76

```

NTAPCF
X, Y, Z
GMA
DELA
NMAX
NEM
W
DI
EPS
DCPBAR
DCPTIL
WORK
EB

INTEGER FLAGB, FLAG
DIMENSION X(NP), Y(NP), Z(NP), GMA(NP), DELA(NP)
COMPLEX ONE, EPS(NP), DCPBAR(NP), DCPTIL(NP), CF(350),
1 W(NP), DI(NP), WORK(NP, NMAX), EB(1)
COMPLEX COL(350), PHIBAR(350)
DATA COL / 350*0.0 /
DATA WORD / 4H /

10 FORMAT ( 1H1/// 38H SYMMETRIC DELTA-CP-TILDA, MODE, 13 /)
20 FORMAT ( 1H1/// 38H ANTISYMMETRIC DELTA-CP-TILDA, MODE, 13 /)
30 FORMAT ( 97H J X(J) Y(J) GAMMA(J) / DELTA-A(J)
1 EPS(J) IMAG. F12.6 / 4F12.6 )
2 42HREAL I4, 4F9.4, F12.6 )
40 FORMAT ( 1H1/// 34H FLAGB = 1, MONITOR-STEP ONLY / )
50 FORMAT ( 1H1/// 50H CORRECTION FACTORS ** PREMULTIPLIER
1 CASE / )
60 1CASE / )
70 1CASE / )
80 1CASE / )
82 1CASE / )
90 1CASE / )

IF (FLAGB.EQ.1) WRITE (NPOT,50)
IF (FLAGB.EQ.4) REWIND NSCRCH
IFP FLAGB = FLAGP + 1
ONE REWIND NUTL
IF (FLAGB.NE.2) GO TO 110
IF (FLAGB.NE.4) REWIND NSCRCH
READ (NTAPCF) WORD
WRITE (NPOT,80) WORD
READ (NTAPCF)
READ (NTAPCF) (CF(I), I = 1, NP)
IF (FLAGB.EQ.4) WRITE (NPOT, 82)

```

DCPT0200
DCPT0210
DCPT0220
DCPT0230
DCPT0240
DCPT0250
DCPT0260
DCPT0270
DCPT0280
DCPT0290
DCPT0300
DCPT0310
DCPT0320
DCPT0330
DCPT0340
DCPT0350
DCPT0360
DCPT0370
DCPT0380
DCPT0390
DCPT0400
DCPT0410
DCPT0420
DCPT0430
DCPT0440
DCPT0450
DCPT0460
DCPT0470
DCPT0480
DCPT0490
DCPT0500
DCPT0510
DCPT0520
DCPT0530
DCPT0540
DCPT0550
DCPT0560
DCPT0570
DCPT0572
DCPT0574
DCPT0580
DCPT0590
DCPT0600
DCPT0610
DCPT0620
DCPT0630
DCPT0640
DCPT0650
DCPT0660
DCPT0670
DCPT0680
DCPT0692

CCCCCCCCCCCCCCCC

C

CORRECTION FACTORS (E1GC) 02/03/76

```

WRITE (NPOT, 90) (I, CF(I), I = 1, NP)
IF (FLAG.EQ. 4) GO TO 102
DO 100 I = 1, NP
EPS(I) = CF(I) - ONE
CONTINUE
100 GO TO 110
CONTINUE
102 CONTINUE
DO 104 I = 1, NP
EB(I) = CF(I)
CONTINUE
DO 310 MODE = 1, MODES
IF (IGD.EQ. 2) GO TO 120
WRITE (NPOT, 10) MODE
GO TO 130
120 WRITE (NPOT, 20) MODE
130 CONTINUE (NPOT, 30)
WRITE (NPOT, 30)
CONTINUE
IF (FLAGB.EQ. 1) GO TO 280
GO TO (180, 140, 180, 140), IFP
CONTINUE
CALL POSN( NTAPW, IGD )
DO 150 M = 1, MODE
READ (NPOT, 10) W
IF (FLAGP.EQ. 1 .OR. NEM.EQ. 0) GO TO 180
IF (MODE.GT. 1) GO TO 180
REWIND NSCRCH
DO 170 K = 1, NEM
READ (NSCRCH) KK, (PHIBAR(M), M = 1, NP)
DO 160 M = 1, NP
COL(M) = COL(M) + PHIBAR(M) * EB(K)
CONTINUE
160 CONTINUE
170 CONTINUE
CONTINUE
DO 270 I = 1, NP
DCPTIL(I) = (0.0, 0.0)
IF (FLAGB.NE. 2) CF(I) = ONE + EPS(I) IFP
GO TO (250, 220, 250, 250, 190), I
IF (NEM.NE. 0) GO TO 210
DO 200 N = 1, NP
COL(N) = EB(N)
CONTINUE
200 CONTINUE
IF (FLAGB.NE. 2 .OR. MODE.GT. 1) GO TO 220
DO 212 M = 1, NP
EPS(M) = COL(M)
CONTINUE
212 CONTINUE
DO 240 (NTAPDI) DI
IF (FLAGP.EQ. 1) GO TO 230

```

DCPT0694
DCPT0696
DCPT0700
DCPT0710
DCPT0720
DCPT0722
DCPT0724
DCPT0726
DCPT0728
DCPT0730
DCPT0740
DCPT0750
DCPT0760
DCPT0770
DCPT0780
DCPT0790
DCPT0800
DCPT0810
DCPT0820
DCPT0830
DCPT0840
DCPT0850
DCPT0860
DCPT0870
DCPT0880
DCPT0890
DCPT0900
DCPT0902
DCPT0910
DCPT0920
DCPT0930
DCPT0940
DCPT0950
DCPT0960
DCPT0970
DCPT0980
DCPT0990
DCPT1000
DCPT1010
DCPT1020
DCPT1030
DCPT1040
DCPT1050
DCPT1060
DCPT1070
DCPT1072
DCPT1074
DCPT1080
DCPT1090
DCPT1100
DCPT1110
DCPT1120

```

DCPTIL(I)= DCPTIL(I) + DI(J)*(W(J)+COL(J))
GO TO 240
CONTINUE
C 230
DCPTIL(I)= DCPTIL(I) + DI(J)*(ONE+EPS(J))*W(J)
CONTINUE
GO TO 260
C 240
DCPTIL(I)= CF(I) * WORK(I, MODE)
CONTINUE
GO TO 270
C 250
DCPTIL(I)= DCPTIL(I) + DI(J)*GMA(I), DELA(I)
CONTINUE
GO TO 270
C 260
WRITE (NPOT,40) I, X(I), Y(I), Z(I), GMA(I), DELA(I)
1 IF ((I/L) .LT. LINES) GO TO 270
L=L+1
IF (IGD .EQ. 1) WRITE (NPOT,10) MODE
IF (IGJ .EQ. 2) WRITE (NPOT,20) MODE
WRITE (NPOT,30)
C 270
CONTINUE
C
GO TO 300
C 280
CONTINUE I = 1, NP
DO 290 I = 1, NP
DCPTIL(I)= WORK(I, MODE)
CF(I) = ONE + EPS(I)
WRITE (NPOT,40) I, X(I), Y(I), Z(I), GMA(I), DELA(I)
1
C 290
CONTINUE
C 300
CONTINUE (NUTL) IGO, MODE, DCPTIL
C
C 310
CONTINUE .EQ. 2 .AND. FLAGP .EQ. 4) RETURN
IF (FLAGB .EQ. 2 .AND. FLAGP .EQ. 4) RETURN
GO TO (330,320,330,320),
C 320
CONTINUE (NPOT,70)
WRITE (NPOT,40)
GO TO 340
C 330
CONTINUE (NPOT,60)
WRITE (NPOT,60)
C 340
CONTINUE
C
WRITE (NPOT,90) ( I, CF(I), I = 1, NP)
IF (FLAGP .EQ. 4) GO TO 350
IF (FLAGB .EQ. 0)
1WRITE (NTAPCF) (CF(I), I = 1, NP)
REWIND NUTL
C
RETURN (NTAPCF) (EB(I), I = 1, NP)
C 350
WRITE (NPOT,82)
WRITE (NPOT,90) ( I, EB(I), I = 1, NP)
REWIND NUTL
C

```

DCPTI1130
DCPTI1140
DCPTI1150
DCPTI1160
DCPTI1170
DCPTI1180
DCPTI1190
DCPTI1200
DCPTI1210
DCPTI1220
DCPTI1230
DCPTI1240
DCPTI1250
DCPTI1260
DCPTI1270
DCPTI1280
DCPTI1290
DCPTI1300
DCPTI1310
DCPTI1320
DCPTI1330
DCPTI1340
DCPTI1350
DCPTI1360
DCPTI1370
DCPTI1380
DCPTI1390
DCPTI1400
DCPTI1410
DCPTI1420
DCPTI1430
DCPTI1440
DCPTI1442
DCPTI1450
DCPTI1460
DCPTI1470
DCPTI1480
DCPTI1490
DCPTI1500
DCPTI1510
DCPTI1520
DCPTI1530
DCPTI1532
DCPTI1540
DCPTI1550
DCPTI1560
DCPTI1570
DCPTI1580
DCPTI1582
DCPTI1584
DCPTI1586
DCPTI1590

CORRECTION FACTORS (EIGC) 02/03/76

```

RETURN
END
SUBROUTINE DELC(NTAPE, NPOT, NC, NP, NMODE, NMAX,
1 CIE, DCI, SAI, WORK
)
NTAPE TAPE NUMBER CONTAINING THE INTEGRATION MATRIX SA
NPOT DATA SET NUMBER OF THE SYSTEM OUTPUT DATA SET
NC NUMBER OF CONSTRAINTS
NP LENGTH OF THE DELTA-CP COLUMNS
NMODE NUMBER OF MODES
NMAX MAXIMUM NUMBER OF COLUMNS IN THE DELTA-CP MATRIX
CIE ARRAY OF THE INPUT VALUES C-I(E)
DCI THE DELTA-C ARRAY
SAI A ROW OF THE INTEGRATION MATRIX SA
WORK THE NP-BY-NMAX COMPLEX ARRAY CONTAINING THE
DELTA-CP-BAR MATRIX
)
COMPLEX CIE(NC), DCI(NC ), WORK(NP, NMAX), SAI(NP), CI(35)
WRITE (NPOT,40)
REWIND NTAPE
DO 20 I = 1, NC
DCI(I) = (0.0, 0.0)
READ 10 (NTAPE) NDI, MI, SAI
DO 10 J = 1, NP
DCI(I,J) = DCI(I) + SAI(J) * WORK(J, MI)
10 CONTINUE
CI(I) = DCI(I)
DCI(I) = CIE(I) - DCI(I)
20 CONTINUE
WRITE (NPOT,50) (DCI(I), I = 1, NC)
WRITE (NPOT,60) (CI(I), I = 1, NC)
30 CONTINUE
40 FORMAT ( 1H1 /// 12H DELTA-C / )
50 FORMAT ( 8F13.6 )
60 FORMAT ( /// 25H THEORETICAL C-VALUES / )
RETURN
END
SUBROUTINE EDBL(NPOT, NELIMS, NP, NS, LIMK, JARR, NSMOD
1 EBMIN, EBMAX, EB, ELIM
)
NPOT DATA SET NUMBER OF THE SYSTEM OUTPUT DATA SET
NELIMS NUMBER OF INPUT CARDS FOR THE EBMIN, EBMAX PAIRS
NP LENGTH OF THE DELTA-CP COLUMNS
NS = MAX (NP+NC, NEM+NC)
LIMK FIRST AND LAST BOX NUMBERS FOR THE EBMIN, EBMAX
JARR ARRAY OF BOX NUMBERS FOR WHICH THE EPSILON VALUES
WERE MODIFIED
NSMOD NUMBER OF MODIFIED EPSILON VALUES
EBMIN MINIMUM VALUE ALLOWED FOR EPSILON
EBMAX MAXIMUM VALUE ALLOWED FOR EPSILON
)

```

DCPT1600
DELC0040
DELC0050
DELC0060
DELC0070
DELC0080
DELC0090
DELC0100
DELC0110
DELC0120
DELC0130
DELC0132
DELC0134
DELC0136
DELC0140
DELC0150
DELC0160
DELC0170
DELC0180
DELC0190
DELC0200
DELC0210
DELC0220
DELC0230
DELC0240
DELC0250
DELC0260
DELC0270
DELC0280
DELC0290
DELC0300
DELC0310
DELC0320
DELC0330
DELC0340
DELC0350
DELC0360
DELC0370
DELC0380
DELC0390
EDBL0040
EDBL0050
EDBL0060
EDBL0070
EDBL0080
EDBL0090
EDBL0100
EDBL0110
EDBL0120
EDBL0122
EDBL0130

CORRECTION FACTORS (E1GC) 02/03/76

```

C      EBMX
C      EB
C      ELIM
C      DIMENSION LIMK(2, 100), JARR( 350 )
C      COMPLEX EBMIN( NELIMS), EBMAX( NELIMS), EB( NS) ,
C      ELIM( NS) , ETEMP
10 I FORMAT ( 1H1///8H , 7X, 11HEPSILON-BAR , 17X, / )
20 I FORMAT ( 18, 6F14.6 )
C      J = 0
C      JMOD = 0
C      J = 1
C      J = 1
40 CONTINUE = LIMK(1, K)
C      LIM1 = LIMK(2, K)
C      IF (J .GT. NP) GO TO 80
C      IF (J .LT. LIM1 .OR. J .GT. LIM2) GO TO 70
C      THE INDEX J IS BETWEEN THE TWO PRESCRIBED LIMITS
C      EB1 = REAL(EBMIN(K))
C      EB2 = REAL(EBMAX(K))
C      ABSEB = REAL(EB(J))
C      IF (ABSEB .GE. EB1 .AND. ABSEB .LE. EB2) GO TO 80
C      JCUM = JCUM + 1
C      IF (ABSEB .GT. EB2) GO TO 50
C      ETEMP = EBMIN(K)
C      GO TO 60
50 CONTINUE = EBMAX(K)
C      ETEMP = ETEMP
60 CONTINUE = J
C      ELIM(J) = ETEMP
C      GO TO 90
70 CONTINUE
C      IF (K .EQ. NELIMS) GO TO 80
C      K = K + 1
C      GO TO 40
80 CONTINUE
C      CONTINUE
90 CONTINUE
C      IF (J .EQ. NS) GO TO 100
C      J = J + 1
C      GO TO 30
100 CONTINUE

```

EDBL0140
EDBL0150
EDBL0160
EDBL0170
EDBL0180
EDBL0190
EDBL0200
EDBL0210
EDBL0220
EDBL0230
EDBL0240
EDBL0250
EDBL0260
EDBL0270
EDBL0280
EDBL0290
EDBL0300
EDBL0310
EDBL0320
EDBL0330
EDBL0340
EDBL0350
EDBL0360
EDBL0370
EDBL0380
EDBL0390
EDBL0400
EDBL0410
EDBL0420
EDBL0430
EDBL0440
EDBL0450
EDBL0460
EDBL0470
EDBL0480
EDBL0490
EDBL0500
EDBL0510
EDBL0520
EDBL0530
EDBL0540
EDBL0550
EDBL0560
EDBL0570
EDBL0580
EDBL0590
EDBL0600
EDBL0610
EDBL0620
EDBL0630
EDBL0640
EDBL0650
EDBL0660

CORRECTION FACTORS (EIGC) 02/03/76

```

NSMOD = JCUM
IF (NSMOD.EQ. 0) RETURN
WRITE (NPOT,10)

DO 110 J = 1, NS
ETEMP = EB(J)
IF (J.EQ. JARR(J)) ETEMP = ELIM(J)
WRITE (NPOT,20) J, EB(J), ELIM(J), ETEMP
CONTINUE
110

RETURN
END
SUBROUTINE EPSJ(NTPHIJ, NP, NEM, NMIN, EB, EPS, PHI)
NTPHIJ TAPE NUMBER CONTAINING THE PHI MATRIX COLUMNS
NP NUMBER OF ROW ELEMENTS IN THE PHI MATRIX
NEM NUMBER OF COLUMNS IN THE PHI MATRIX
NS = MAX (NP+NC, NEM+NC)
EB ARRAY OF THE EPSILON-BAR VALUES
EPS THE FINAL EPSILON ARRAY
PHI A COLUMN OF THE PHI MATRIX (WEIGHT FACTOR MODE
SHAPES)

COMPLEX EPS(NP), EB( 1), PHI(NP)
CALL ZEROUT( EPS, NP, 0, 0 )
IF (NEM.EQ. 0) GO TO 30
REWIND NTPHIJ
DO 20 J = 1, NEM
READ ( NTPHIJ) MODENO, PHI

DO 10 I = 1, NP
EPS(I) = EPS(I) + PHI(I) * EB(J)
CONTINUE
10

CONTINUE
RETURN
20

CONTINUE
DO 40 I = 1, NP
EPS(I) = EB(I)
CONTINUE
40

RETURN
END
SUBROUTINE GINV(NPOT, NTAPS8, NC, NS, NX, DC, EB,
1
)
NPOT DATA SET NUMBER OF THE SYSTEM OUTPUT DATA SET
NTAPS8 TAPE NUMBER CONTAINING THE S-DOUBLE-BAR MATRIX ROWS
NC NUMBER OF CONSTRAINTS
NS = MAX (NP+NC, NEM+NC)
NX = NS IF NEM=0, NX=NEM+NC OTHERWISE
DC THE COMPLEX DELTA-C ARRAY

```

DBL0670
EDBL0680
EDBL0690
EDBL0700
EDBL0710
EDBL0720
EDBL0730
EDBL0740
EDBL0750
EDBL0760
EDBL0770
EDBL0780
EPSJ0040
EPSJ0050
EPSJ0060
EPSJ0070
EPSJ0080
EPSJ0090
EPSJ0100
EPSJ0110
EPSJ0120
EPSJ0122
EPSJ0130
EPSJ0140
EPSJ0150
EPSJ0160
EPSJ0170
EPSJ0190
EPSJ0210
EPSJ0230
EPSJ0240
EPSJ0250
EPSJ0260
EPSJ0270
EPSJ0280
EPSJ0290
EPSJ0300
EPSJ0310
EPSJ0320
EPSJ0330
EPSJ0340
EPSJ0350
EPSJ0360
GINV0040
GINV0050
GINV0060
GINV0070
GINV0080
GINV0090
GINV0100
GINV0110
GINV0120

CORRECTION FACTORS (EIGC) 02/03/76

```

C C C C C C
C      EB
C      B
C      S
C      SBB

C      DC(NC), EB(NS), B(NC), S(NC, NC), SBB(NC, NS), SCALER
C      SBBCT
C      NERR, M, SCALER / 0, 1, (1.0,0.0) /
C
C      NOTE THAT -EB- STANDS FOR EPSILON-TILDA
C
C      NSMNC = NX - NC
C      DO 10 I = 1, NC (SBB(I, J), J = 1, NS)
C      READ (NTAPSB) (SBB(I, J), J = 1, NS)
C      IF (NSMNC .LT. 0) GO TO 10
C      EB(I) = DC(I)
C      CONTINUE
C 10
C
C      IF (NSMNC) 90, 20, 30
C      CONTINUE
C
C      NS = NC
C      FOR EB BRANCH ---- SOLVE THE EQUATION DC = SBB * EB
C      USING MIS2
C
C      CALL MIS2( SBB, NS, NC, EB, M, NERR, SCALER )
C
C      GO TO 140
C
C 30 CONTINUE
C
C      NS-GREATER-THAN-NC BRANCH ----
C      COMPUTE S = SBB * (SBB-CONJUGATE-TRANSPOSE) AND
C      SOLVE THE EQUATION DC = S * B FOR B USING MIS2
C
C      DO 60 I = 1, NC
C      B(I) = DC(I)
C      DO 50 K = 1, NC
C      S(I, K) = (0.0, 0.0)
C      DO 40 J = 1, NX
C      SBBCT = S(I, K) + SBB(K, J) * SBBCT
C      CONTINUE
C      CONTINUE
C      CONTINUE
C      CONTINUE
C      WRITE (NPOT, 180) S
C      WRITE (NPOT, 200)
C      WRITE (NPOT, 170)
C      WRITE (NPOT, 200) DC
C
C      CALL MIS2( S, NC, NC, B, M, NERR, SCALER )
C
C      WRITE (6, 190)

```

GINV0130
GINV0140
GINV0150
GINV0160
GINV0170
GINV0180
GINV0190
GINV0192
GINV0200
GINV0210
GINV0220
GINV0230
GINV0240
GINV0250
GINV0260
GINV0270
GINV0280
GINV0290
GINV0300
GINV0310
GINV0320
GINV0330
GINV0340
GINV0350
GINV0360
GINV0370
GINV0380
GINV0390
GINV0400
GINV0410
GINV0420
GINV0430
GINV0440
GINV0450
GINV0460
GINV0470
GINV0480
GINV0490
GINV0500
GINV0510
GINV0512
GINV0520
GINV0530
GINV0540
GINV0550
GINV0560
GINV0570
GINV0580
GINV0590
GINV0600
GINV0610
GINV0620
GINV0630

-----CORRECTION FACTORS (EIGC) 02/03/76-----

```

C      WRITE (6,200) B
      COMPUTE EB = (SBB-CONJUGATE-TRANSPPOSE) * B
C
C      DO 80 J = 1, NX
      EB(J) = (0.0, 0.0)
C      DO 70 I = 1, NC
      SBBCT = CONJG( SBB(I, J) ) * B(I)
      EB(J) = EB(J) + SBBCT
      CONTINUE
C      GO TO 140
C
C      90 CONTINUE
C
C      NS-LESS-THAN-NC BRANCH ----- THE LEAST SQUARES CASE ----
      COMPUTE B = (SBB-CONJUGATE-TRANSPPOSE) * (DELTA-C)
      COMPUTE S = (SBB-CONJUGATE-TRANSPPOSE) * SBB AND
      SOLVE THE EQUATION B = S * EB FOR EB USING MIS2
C
C      DO 130 J = 1, NX
      EB(J) = (0.0, 0.0)
C      DO 100 L = 1, NC
      SBBCT = CONJG( SBB(L, J) ) * DC(L)
      EB(J) = EB(J) + SBBCT
      CONTINUE
C
C      DO 120 K = 1, NX
      I = 1, NC
      SBBCT = CONJG( SBB(I, J) ) * SBB(I, K)
      S(J, K) = S(J, K) + SBBCT
      CONTINUE
      CONTINUE
      CONTINUE
C      CALL MIS2( S, NC, NS, EB, M, NERR, SCALER )
C
C      140 CONTINUE
C
C      WRITE (NPOT,150) (EB(I), I = 1, NX)
      WFORMAT ( ( //, 40H ) ) OUTPUT OF GEN. INVERSE (EPS-TILDA) /
      150 FORMAT ( ( 8F13.6 ) )
      160 FORMAT ( ( 1H1 //, 16H -DC- COLUMN / ) )
      170 FORMAT ( ( 1H1 //, 16H -S- MATRIX / ) )
      180 FORMAT ( ( 1H1 //, 28H SOLUTION OF MATRIX EQ. / ) )
      190 FORMAT ( ( 6E16.6 ) )
      200
C      RETURN
      END
      PROGRAM EIGC(INPUT, OUTPUT, TAPE5=INPUT, TAPE6=OUTPUT, TAPE1=512,

```

GINV0640
GINV0650
GINV0660
GINV0670
GINV0680
GINV0690
GINV0692
GINV0700
GINV0710
GINV0720
GINV0730
GINV0740
GINV0750
GINV0760
GINV0770
GINV0780
GINV0790
GINV0800
GINV0810
GINV0820
GINV0830
GINV0840
GINV0850
GINV0852
GINV0860
GINV0870
GINV0880
GINV0890
GINV0892
GINV0894
GINV0900
GINV0910
GINV0920
GINV0930
GINV0940
GINV0950
GINV0960
GINV0970
GINV0980
GINV0990
GINV1000
GINV1010
GINV1020
GINV1030
GINV1040
GINV1050
GINV1060
GINV1070
GINV1080
GINV1100
GINV1110
GINV1120
MAIN0002

CORRECTION FACTORS (E1GC) 02/03/76

```

C 60 CONTINUE
C CALL ZEROUT( WORK(LOC), NWORK, 1, 0 )
C
L1 LOC
L2 + NP
L3 + NP
L4 + NP
L5 + NP
L6 + NP
L7 + NP
L8 + NP
L9 + NP
L10 + NP
L11 + NC
L12 + NC
L13 + NMIN
L14 + NS
L15 + NS
L16 + NS
L17 + NS
L18 + NMATR1
L19 + NMATR2
L20 + NMATR3
L21 +
C CALL WEYTNP, NC, NEM, NELIMS, NMON, NAXIS, NMIN, NMAX, NPOT,
1 WORK( L2), WORK( L3), WORK( L4), WORK( L5), WORK( L6),
2 WORK( L7), WORK( L8), WORK( L9), WORK( L10), WORK( L11),
3 WORK( L12), WORK( L13), WORK( L14), WORK( L15), WORK( L16),
4 WORK( L17), WORK( L18), WORK( L19), WORK( L20), WORK( L21)
5
C GO TO 50
END
SUBROUTINE MATM( NT, IGO, NR, NC, NMAX, A, C, B )
NT TAPE NUMBER CONTAINING THE INVERSE-D MATRIX ROWS
IGO 1 FOR SYMMETRIC MODES, 2 FOR ANTISYMMETRIC MODES
NR NUMBER OF ROW ELEMENTS IN THE DELTA-CP-BAR MATRIX
NC NUMBER OF COLUMNS IN THE DELTA-CP-BAR MATRIX
NMAX MAXIMUM NUMBER OF COLUMNS IN ARRAY B
A ROW OF THE INVERSE-D MATRIX
C COMPLEX WORK ARRAY IN WHICH THE DELTA-CP-BAR MATRIX
B IS STORED
C
COMPLEX K A(NR), C(NR), B(NR, NMAX)
DO 40 K = 1, NC
CALL POSN( NT, IGO )
CALL ZEROUT( C, NR, 1, 0 )
DO 20 I = 1, NR

```

MAIN0540
 MAIN0550
 MAIN0560
 MAIN0570
 MAIN0580
 MAIN0590
 MAIN0600
 MAIN0610
 MAIN0620
 MAIN0630
 MAIN0640
 MAIN0650
 MAIN0660
 MAIN0670
 MAIN0680
 MAIN0690
 MAIN0700
 MAIN0710
 MAIN0720
 MAIN0730
 MAIN0740
 MAIN0750
 MAIN0760
 MAIN0770
 MAIN0780
 MAIN0790
 MAIN0800
 MAIN0810
 MAIN0820
 MAIN0830
 MAIN0840
 MAIN0850
 MAIN0860
 MAIN0870
 MAIN0880
 MAIN0890
 MATM0040
 MATM0050
 MATM0060
 MATM0070
 MATM0080
 MATM0090
 MATM0100
 MATM0110
 MATM0120
 MATM0130
 MATM0132
 MATM0140
 MATM0150
 MATM0160
 MATM0170
 MATM0180
 MATM0190

CORRECTION FACTORS (E1GC) 02/03/76

```

30 FORMAT ( 1H1 /// 6H THE, 14, 4H BY, 14, 22H S-DOUBLE-BAR MATR
MODF0410
MODF0412
MODF0420
MODF0420
MODF0430
MODF0440
MODF0450
MODF0460
MODF0470
MODF0480
PHIJ0040
PHIJ0050
PHIJ0060
PHIJ0070
PHIJ0080
PHIJ0090
PHIJ0100
PHIJ0110
PHIJ0120
PHIJ0130
PHIJ0140
PHIJ0150
PHIJ0160
PHIJ0170
PHIJ0180
PHIJ0190
PHIJ0200
PHIJ0202
PHIJ0210
PHIJ0220
PHIJ0230
PHIJ0240
PHIJ0250
PHIJ0260
PHIJ0270
PHIJ0280
PHIJ0290
PHIJ0300
PHIJ0310
PHIJ0320
PHIJ0330
PHIJ0340
PHIJ0350
PHIJ0360
PHIJ0370
PHIJ0380
PHIJ0390
PHIJ0400
PHIJ0410
PHIJ0412
PHIJ0420
PHIJ0430
PHIJ0440
)
1X
32 FORMAT ( //8H ROW, 14 // (3 ( 16, 2E14.6 ) ) )
40 FORMAT ( //8H DELTA-C-MOD / )
50 WRITE (6,50) (DCMOD(I), I = 1, NC)
RETURN
END
SUBROUTINE PHIJ(NPIT, NPOT, NTPHIJ, NEM, NP, KODE, MODES,
1 X, Y, Z, )
NPIT DATA SET NUMBER OF THE SYSTEM INPUT DATA SET
NPOT DATA SET NUMBER OF THE SYSTEM OUTPUT DATA SET
NTPHIJ TAPE NUMBER CONTAINING COLUMNS OF THE PHI MATRIX
NEM NUMBER OF COLUMNS IN THE PHI MATRIX
NP NUMBER OF ROW ELEMENTS IN THE PHI MATRIX
KODE = -1
MODLS NOT USED
X, Y, Z COORDINATES OF THE PRESSURE POINTS
PHI COMPLEX ARRAY CONTAINING ONE COLUMN OF THE
NP-BY-NEM PHI MATRIX
DIMENSION LIML(2, 25), X(NP), Y(NP), Z(NP)
COMPLEX PHI(NP), PHIL, PHIZ
REAL NL
10 FORMAT ( 8I10, 5F10.0 )
20 FORMAT ( 2I10, 2F10.0 )
30 FORMAT ( 2I10, F12.4, 2F13.5, 2I10 / (6(58X, 2I8)) )
40 FORMAT ( /// 79H MODENO(L), TYPE(L) A(L)
50 B(L) LIM1 LIM2 / )
C REWIND NTPHIJ
L = 1
C 60 READ (NPIT,20) MODENO, ITYPE, NL, AL, BL
C
C IF (ITYPE .NE. 0) GO TO 80
CALL ZEROUT( PHI, NP, 1, 0 )
70 READ (NPIT,30) J, PHIL, JPI, PHI2
IF (J .LE. KODE) GO TO 230
PHI(J) = PHIL
IF (JPI .NE. 0) PHI(JPI) = PHI2
GO TO 70
C
C 80 CONTINUE
IF (L .EQ. 1) WRITE (NPOT,50)
LL = 1
90 READ (NPIT,10) (LIML(J, LL), J = 1, 2)
IF (LIML(1, LL) .LE. KODE) GO TO 100

```


CORRECTION FACTORS (EIGC) 02/03/76

```

1 WRITE (NPOT,70) JAX(I), IFF(I), NDI , MI , AIT(I),
  CIT(I), CIE(I)
  I I
  140 READ (NPIT,10) (LIMI(J, I), J = 1, 2)
  IF (LIMI(1, I) .LE. KODE) GO TO 150
  WRITE (NPOT,12) (LIMI(J, I), J = 1, 2)
  I I
  GO TO 140
C 150 CONTINUE = I I - 1
  IIMAX = I I - 1
C COMPUTE ELEMENTS OF THE SA-I-J MATRIX (DIM. NC-BY-NP)
C AND SAVE MATRIX ON TAPE NTSAIJ IN ROW ORDER
C FLAG = IFF(I) + 1
  IR = JAX(I)
  FLGA = IFA(IR)+ 1
C IDO = 1
  CALL SROW(FLGA, FLAG, XI1 , ETAL , ZETA1, CG, SG, CIT
  , X , Y ; Z ; DELA ; LIMI ; IIMAX , I
  , NP ; IR ; XI2 ; ETA2 ; ZETA2,
  )
C WRITE (NTSAIJ) NDI , MI , SAI
  IF (I .EQ. NC) GO TO 160
  I I + 1
  GO TO 130
C 160 CONTINUE
  IF (NMON .EQ. 0) GO TO 200
  WRITE (NPOT,22)
C SAI MATRIX COMPLETE (DIMENSION NC-BY-NP)
C SAVED ON TAPE NTSAIJ IN ROW ORDER
C IF (IDO .EQ. 2) GO TO 200
  IDO = 2
  REWIND NTSANJ
  N WRITE (NPOT,100) NMON
C 170 READ (NPIT,10) NAX(N), IFN(N)
  READ (NPIT,40) NDN , MN , ANT(N), CNT(N),
  (LABEL(M, N), M = 1, 10)
  1 WRITE (NPOT,80) NAX(N), IFN(N), NDN , MN , ANT(N),
  CNT(N), (LABEL(M, N), M = 1, 10)
C NN = 1
  180 READ (NPIT,10) (LIMN(J, NN), J = 1, 2)
  IF (LIMN(1, NN) .LE. KODE) GO TO 190
  WRITE (NPOT,12) (LIMN(J, NN), J = 1, 2)

```

SAIJ0740
 SAIJ0750
 SAIJ0760
 SAIJ0770
 SAIJ0780
 SAIJ0782
 SAIJ0790
 SAIJ0800
 SAIJ0810
 SAIJ0820
 SAIJ0830
 SAIJ0840
 SAIJ0850
 SAIJ0860
 SAIJ0870
 SAIJ0880
 SAIJ0890
 SAIJ0900
 SAIJ0910
 SAIJ0920
 SAIJ0930
 SAIJ0940
 SAIJ0950
 SAIJ0960
 SAIJ0970
 SAIJ0980
 SAIJ0990
 SAIJ1000
 SAIJ1010
 SAIJ1020
 SAIJ1030
 SAIJ1040
 SAIJ1042
 SAIJ1050
 SAIJ1060
 SAIJ1070
 SAIJ1080
 SAIJ1090
 SAIJ1100
 SAIJ1110
 SAIJ1120
 SAIJ1130
 SAIJ1140
 SAIJ1150
 SAIJ1160
 SAIJ1170
 SAIJ1180
 SAIJ1190
 SAIJ1200
 SAIJ1210
 SAIJ1220
 SAIJ1230
 SAIJ1232

CORRECTION FACTORS (EIGC) 02/03/76

```

1      I, IGO, SORTT, AIW, SAI, DI, W, DELCPB, SBI
NTSBIJ      TAPE NUMBER CONTAINING ROWS OF THE S-BAR MATRIX
NTAPDI      TAPE NUMBER CONTAINING ROWS OF THE INVERSE-D MATRIX
NC          NUMBER OF CONSTRAINTS
NP          NUMBER OF DELTA-CP ELEMENTS
NS          LENGTH OF THE S-BAR MATRIX ROWS
FLAGP      OPTION FLAG FOR DELTA-CP AND/OR PRE- OR POST-
FLAGT      MULTIPLYING CORRECTIONS
           OPTION FLAG FOR WEIGHTS
FLAGW      OPTION FLAG FOR NORMALWASH INPUT
I          INTERMEDIATE INDEX
IGO        1 FOR SYMMETRIC MODES, 2 FOR ANTISYMMETRIC MODES
SORTT      SORT(T) INING EFFECTIVENESS
AIW        A ROW OF THE SAI MATRIX (INTEGRATES DELTA-CP
SAI        INTO COEFFICIENTS)
DI         A ROW OF THE INVERSE-D MATRIX
W          A COLUMN OF THE NORMALWASH MATRIX
DELCPB     A COLUMN OF THE LIFTING PRESSURE COEFFICIENTS,
           DELTA-CP-BAR
SBI        A ROW OF THE INTEGRATION MATRIX S-BAR
DIMENSION  SORTT(350)
COMPLEX    SAI(NP), W(NP), DELCPB(NP), SBI(NS), SAXDI
INTEGER    FLAGP, FLAGT, FLAGW
DATA       EPSLON, AIFIX / .0001, 10000. /
***
IF (FLAGP .EQ. 1 .OR. FLAGP .EQ. 4) GO TO 20
-----
FLAGP = 0, 2, 3 OPTIONS (PRE -MULTIPLY BRANCH)
DO 10 J = 1, NP
SAXDI = SAI(J) * DELCPB(J)
SBI(J) = SAXDI / SORTT(J)
10 CONTINUE
GO TO 60
-----
FLAGP = 1, 4 OPTIONS (POST-MULTIPLY BRANCH)
20 CONTINUE
CALL POSN( NTAPDI, IGO )
DO 40 J = 1, NP
READ (NTAPDI) DI
DO 30 K = 1, NP
SBI(K) = SBI(K) + SAI(J) * DI(K)
30 CONTINUE

```

SBAR0050
SBAR0060
SBAR0070
SBAR0080
SBAR0090
SBAR0100
SBAR0110
SBAR0120
SBAR0130
SBAR0140
SBAR0150
SBAR0160
SBAR0170
SBAR0180
SBAR0190
SBAR0200
SBAR0210
SBAR0212
SBAR0220
SBAR0222
SBAR0230
SBAR0232
SBAR0240
SBAR0250
SBAR0260
SBAR0270
SBAR0280
SBAR0290
SBAR0300
SBAR0310
SBAR0320
SBAR0330
SBAR0340
SBAR0350
SBAR0360
SBAR0370
SBAR0380
SBAR0390
SBAR0400
SBAR0410
SBAR0420
SBAR0430
SBAR0440
SBAR0450
SBAR0460
SBAR0470
SBAR0480
SBAR0490
SBAR0500
SBAR0510
SBAR0520
SBAR0530
SBAR0540

```

40 CONTINUE
IF (FLAGP.EQ.4) GO TO 60
DO 50 J = 1, NP
SBI(J) = SBI(J) * W(J) / SORTT(J)
CONTINUE

60 CONTINUE
JJ = NP + I
IF (AIW .LE. EPSLON) GO TO 70
SBI(JJ) = (1.0 - AIW) / AIW
GO TO 80
SBI(JJ) = AIFIX
CONTINUE

      ONE ROW OF THE S-BAR-I-J MATRIX IS COMPLETE ----
      WRITE IT ON TAPE NTSBIJ
      WRITE (NTSBIJ) SBI
      WRITE (6 ,90)
      WRITE (6 ,100) (SBI(J), J = 1, NS)

90 FORMAT ( 1H0 /// 18H ONE S-BAR ROW / )
100 RETURN
END
SUBROUTINE SDBL(NSCRCH,NUTL,MASTSB,NTPHIJ, NTAPW, NTSAIJ, NTAPDI,
1 IGO, FLAGW, FLAGP, FLAGT, NC, NP, NS, NEM, SORTT, AIT,
2 DELA, SBB, SBI, SAI, DI, W, PHI, DELCPB, WORK )

UTILITY (SCRATCH) TAPE NUMBER
TAPE NUMBER CONTAINING THE SBB MATRIX ROWS
TAPE NUMBER CONTAINING THE PHI MATRIX COLUMNS
TAPE NUMBER CONTAINING THE W MATRIX COLUMNS
TAPE NUMBER CONTAINING THE SAI MATRIX ROWS
1 IGO FOR SYMMETRIC MODES, 2 FOR INVERSE-D MATRIX MODES
OPTION FLAG FOR NORMALWASH INPUT
OPTION FLAG FOR DCP-INPUT AND/OR PRE- OR POST-
NUMBER OF CONSTRAINT ELEMENTS
= MAX (NP+NC, NEM+NC)
= NUMBER OF CORRECTION FACTOR MODES
SORTT(T) SEE EQUATIONS FOR DEFINITION
AIT CONSTRAINTING EFFECTIVENESS
DELA BOX AREAS
SBI A ROW OF THE S-DOUBLE-BAR MATRIX
SAI A ROW OF THE S-BAR MATRIX
DI A ROW OF THE SAI MATRIX
W A ROW OF THE INVERSE-D MATRIX
PHI A COLUMN OF THE W MATRIX
      PHI MATRIX (NORMALWASH)

```

SBAR0550
SBAR0560
SBAR0570
SBAR0580
SBAR0590
SBAR0600
SBAR0610
SBAR0620
SBAR0630
SBAR0640
SBAR0650
SBAR0660
SBAR0670
SBAR0680
SBAR0690
SBAR0700
SBAR0710
SBAR0720
SBAR0730
SBAR0740
SBAR0750
SBAR0760
SBAR0770
SBAR0780
SBAR0790
SDBL0040
SDBL0050
SDBL0060
SDBL0070
SDBL0080
SDBL0090
SDBL0100
SDBL0110
SDBL0120
SDBL0130
SDBL0140
SDBL0150
SDBL0160
SDBL0170
SDBL0180
SDBL0190
SDBL0200
SDBL0210
SDBL0220
SDBL0230
SDBL0240
SDBL0250
SDBL0260
SDBL0270
SDBL0280
SDBL0290
SDBL0292
SDBL0300

CORRECTION FACTORS (EIGC) 02/03/76

```

C      NSCRCH      TAPE NUMBER CONTAINING THE PHI-BAR MATRIX (IF ANY)
C      DELCPB      A COLUMN OF THE DELTA-CP-BAR MATRIX
C      INTEGER     FLAGP, FLAGT, FLAGM
C      DIMENSIONN  SORTT(350), AIT(NC), DELA(350)
C      COMPLEX     SBB(NS,J), SBI(NS), SAI(NP), DI(NP), W(NP), DELCPB(NP)
C      1           EL, PHI(NP), WORK(NP, I)
C      NTSBIJ      = MASTSB, PHIBAR(350), COL(350)
C      IFP        (FLAGP + I) REWIND NSCRCH
C      IF (NEM.EQ.0) NTSBIJ = NUTL
C      REWIND NTSBIJ
C      REWIND NTSBIJ
C      MI
C      CONTINUE   J = 1, NP
C      DO 20      J = 1, NP
C      20 DELCPB(J) = WORK(J, MI)
C      GO TO     (50,30,50,50,30), IFP
C      30 CONTINUE
C      CALL      POSN( NTAPW, IGO )
C      40 READ   (NTAPW) W
C      50 CONTINUE
C      DO 110   J = 1, NP
C      SORTT(J) = 1.0
C      IF (FLAG.EQ.1) GO TO 110
C      GO TO   (100,60,100,100,60), IFP
C      60 CONTINUE
C      POSTMULTIPLIER TYPE
C      IF (J.GT.1) GO TO 80
C      CALL 70 POSN( NTAPDI, IGO )
C      DO 70 K = 1, NP
C      70 COL(K) = (0.0, 0.0)
C      80 READ (NTAPDI) DI
C      DO 90 N = 1, NP
C      90 COL(N) = COL(N) + DI(N) * DELA(J)
C      GO TO 110
C      100 CONTINUE
C      PREMULTIPLIER TYPE
C      110 SORTT(J) = SQRT( CABS ( DELCPB(J)*DELA(J) ) )
C      CONTINUE
C      IF (FLAGT.EQ.1) GO TO 140
C      GO TO (140,120,140,140,120), IFP
C      CONTINUE
C      DO 130 N = 1, NP
C      130 SORTT(N) = SQRT( CABS( COL(N) ) )
C      140 CONTINUE

```

SDBL0080
SDBL0310
SDBL0320
SDBL0330
SDBL0340
SDBL0350
SDBL0360
SDBL0370
SDBL0380
SDBL0390
SDBL0400
SDBL0410
SDBL0420
SDBL0430
SDBL0440
SDBL0450
SDBL0460
SDBL0470
SDBL0480
SDBL0490
SDBL0500
SDBL0510
SDBL0520
SDBL0530
SDBL0540
SDBL0550
SDBL0560
SDBL0570
SDBL0580
SDBL0590
SDBL0600
SDBL0610
SDBL0620
SDBL0630
SDBL0640
SDBL0650
SDBL0660
SDBL0670
SDBL0680
SDBL0690
SDBL0700
SDBL0710
SDBL0720
SDBL0730
SDBL0740
SDBL0750
SDBL0760
SDBL0770
SDBL0780
SDBL0790
SDBL0800
SDBL0810
SDBL0820

CORRECTION FACTORS (E1GC) 02/03/76

```

C 200 I = 1, NC
    AIM = AIF(I)
    CALL ZEROUT( SBI, NS, 1, 0 )
    READ (NTSAIJ) NDI, MI, SAI

C 150 CONTINUE
    DO 160 J = 1, NP
    DELCPB(J) = WORK(J, MI)
    GO TO (190, 170, 170, 190, 170), IFP
C 170 CONTINUE
    CALL POSN( NTAPW, IGO )
    DO 180 M = 1, MI
    READ (NTAPW) W
C 190 CONTINUE

C 1 CALL SBAR(NTSBIJ, NTAPDI, NC, NP, NS, FLAGP, FLAGT, FLAGM, )
    I IGO, SORTT, AIW, SAI, DI, W, DELCPB, SBI

C 200 CONTINUE
    IF (NEM .EQ. 0) GO TO 290

C
    REWIND NUTL
    REWIND MASTSB
    DO 205 J = 1, NP
    DELCPB(J) = WORK(J, 1)
    NEM1 = NEM + 1
    NEMNC = NEM + NC
    WRITE (6, 300) NC, NEMNC
    DO 280 I = 1, NC
    REWIND NTPHIJ
    READ (NUTL) SBI
    CALL ZEROUT( SBB, NS, 1, 0 )
    DO 260 K = 1, NEM
    READ (NTPHIJ) MODEND, PHI
    IF (FLAGP .EQ. 4) GO TO 220
    DO 210 J = 1, NP
    SBB(K) = SBB(K) + SBI(J) * PHI(J)
C 210 CONTINUE
    GO TO 260

C 220 CONTINUE = (0.0, 0.0)
    EL 230 L = 1, NP
    EL = EL + PHI(L) * DELCPB(L)
C 230 CONTINUE

C
    CALL ZEROUT( PHIBAR, 350, 1, 0 )
    DO 240 M = 1, NP
    PHIBAR(M) = PHI(M) * EL
C 240 CONTINUE
    WRITE (NSCRCH) K, (PHIBAR(M), M = 1, NP)

```

DBL0830
SDBL0840
SDBL0850
SDBL0860
SDBL0870
SDBL0880
SDBL0890
SDBL0900
SDBL0910
SDBL0920
SDBL0930
SDBL0940
SDBL0950
SDBL0960
SDBL0970
SDBL0980
SDBL0990
SDBL1000
SDBL1010
SDBL1020
SDBL1030
SDBL1040
SDBL1050
SDBL1060
SDBL1070
SDBL1072
SDBL1074
SDBL1080
SDBL1090
SDBL1100
SDBL1110
SDBL1120
SDBL1130
SDBL1140
SDBL1150
SDBL1160
SDBL1170
SDBL1180
SDBL1190
SDBL1200
SDBL1210
SDBL1220
SDBL1230
SDBL1240
SDBL1250
SDBL1260
SDBL1270
SDBL1280
SDBL1290
SDBL1300
SDBL1310
SDBL1320
SDBL1330

CORRECTION FACTORS (EIGC) 02/03/76

```

C      DO 250 J = 1, NP
      SBB(K) = SBB(K) + SBI(J) * PHIBAR(J)
      CONTINUE
C      DO 260 K = NEM1, NEMNC
      NP = NP + K - NEM
      SBI(NPK) = SBI(NPK)
      CONTINUE
      WRITE (6,310) I, (K, SBB(K), K = 1, NEMNC)
      CONTINUE
      REWIND MASTSB
C      DO 290 CONTINUE
      REWIND NTSBIJ
      FORMAT ( 1H1 // 6H THE, I4, 4H BY, I4, 22H S-DOUBLE-BAR MATR
      1X / )
      ROW, I4 // (3 ( I6, 2E14.6 ) )
      IF (FLAGP.EQ. 4) REWIND NSCRCH
      RETURN
      END
      SUBROUTINE SROW(FLAGA, FLAGF, XI1, ETAL, ZETA1, CG, SG, CTIL
      1, X, NP, IR, X12, ETA2, ZETA2, SAI)
      FLAGA = 0, AXIS ENDPOINTS ARE INPUT
      FLAGF = 1, DIRECTION COSINES ARE INPUT
      0, CIE IS A FORCE IN DIRECTION OF AXIS
      1, CIE IS A MOMENT ABOUT AXIS
      XI1, ETAL, ZETA1, AXIS ENDPOINT COORDINATES
      CG, SG, COSINE-, SINE OF BOX DIHEDRAL ANGLES
      CTIL, CONSTANT, USED TO NONDIMENSIONALIZE INTEGRATED DATA
      X, Y, Z, COORDINATES OF THE PRESSURE POINTS (BOXES)
      DELA, BOX AREAS
      LIM1, FIRST- AND LAST BOX NUMBERS FOR THE INTEGRATION OF
      IIMAX, THE DELTA-CP VALUES
      I, NUMBER OF LIMIT SETS INPUT FOR ONE CONSTRAINT
      NP, INTERMEDIATE INDEX
      IR, NUMBER OF DELTA-CP VALUES
      ROW, INDEX OF SAI MATRIX
      XI2, ETA2, ZETA2, SECOND AXIS ENDPOINT COORDINATES WHEN
      SAI, FLAGF=0, DIRECTION COSINES WHEN FLAGF=1
      A ROW OF THE INTEGRATION MATRIX (SA-IJ, OR SA-NJ)
      INTEGER FLAGA, FLAGF
      DIMENSION XI1( 25), ETAL( 25), ZETA1( 25), CG( NP), SG( NP)
      1 DIMENSION X( NP), Y( NP), Z( NP), DELA( NP), LIM1(2, 35)
      COMPLEX SAI( NP)

```

DBL1340
 SDBL1350
 SDBL1360
 SDBL1370
 SDBL1380
 SDBL1390
 SDBL1400
 SDBL1410
 SDBL1420
 SDBL1430
 SDBL1440
 SDBL1450
 SDBL1460
 SDBL1470
 SDBL1480
 SDBL1490
 SDBL1500
 SDBL1510
 SDBL1520
 SDBL1530
 SDBL1540
 SDBL1550
 SDBL1560
 SROW0040
 SROW0050
 SROW0060
 SROW0070
 SROW0080
 SROW0090
 SROW0100
 SROW0110
 SROW0120
 SROW0130
 SROW0140
 SROW0150
 SROW0160
 SROW0170
 SROW0180
 SROW0190
 SROW0200
 SROW0210
 SROW0220
 SROW0230
 SROW0240
 SROW0250
 SROW0260
 SROW0270
 SROW0280
 SROW0290
 SROW0300
 SROW0310
 SROW0320
 SROW0330

```

C
10 GO TO (10,20), FLAGA - XII (IR)
   XID (IR) - ETAL (IR)
   ETAD (IR) - ZETAL (IR)
   ZETAD (IR) - ZETAL (IR)
   P SORT(XID**2 + ETAD**2 + ZETAD**2)
   COSAI XID / P
   COSBI ETAD / P
   COSGI ZETAD / P
   GO TO 30

C
20 CONTINUE = XII (IR)
   COSAI (IR)
   COSBI (IR)
   COSGI (IR)
   ZETA2 (IR)

30 CONTINUE = I, NP
   DO 90 J = I, NP
   ABIJ = 0.0

40 CONTINUE = LIM1(1, II)
   LIM2 = LIM1(2, II)
   IF (J.GE. LIM1.AND. J.LE. LIM2) GO TO 50
   IF (II.EQ. II + 1) GO TO 80
   II = II + 1
   GO TO 40

C
50 CONTINUE (60,70), FLAGF
60 CONTINUE = (-COSBI * SG(J) + COSGI * CG(J)) / CTIL(I)
   GO TO 80
70 CONTINUE = X(J) - XII (IR)
   YDIF = Y(J) - ETAL (IR)
   ZDIF = Z(J) - ZETAL (IR)
   ABIJ = (COSAI * (YDIF * CG(J) + ZDIF * SG(J))
           - COSBI * (XDIF * SG(J))
           ) / CTIL(I)

80 CONTINUE = I
   I I SAI(J) = CMPLX(ABIJ*DELA(J), 0.0)
   CONTINUE

C
END
SUBROUTINE WEYT( NP, NC, NEM, NELIMS, NMDN, NAXIS, NMIN,
1 NMAX, NS, NPIT, NPOT, PHI, SAI,
2 DI, DCP, DELCPCB, CIE, DCMOD,
3 DCPTIL, DELCPB, COL, ELIM,
4 EBMIN, EBMAX, EB, SBMAT, DCI,
5 SBI, S )

```

SRJW0340
SRJW0350
SRJW0360
SRJW0370
SRJW0380
SRJW0390
SRJW0400
SRJW0410
SRJW0420
SRJW0430
SRJW0440
SRJW0450
SRJW0460
SRJW0470
SRJW0480
SRJW0490
SRJW0500
SRJW0510
SRJW0520
SRJW0530
SRJW0540
SRJW0550
SRJW0560
SRJW0570
SRJW0580
SRJW0590
SRJW0600
SRJW0610
SRJW0620
SRJW0630
SRJW0640
SRJW0650
SRJW0660
SRJW0670
SRJW0680
SRJW0690
SRJW0700
SRJW0710
SRJW0720
SRJW0730
SRJW0740
SRJW0750
SRJW0760
SRJW0770
SRJW0780
SRJW0790
WEYT0020
WEYT0030
WEYT0040
WEYT0050
WEYT0060
WEYT0070
WEYT0080

CORRECTION FACTORS (E1GC) 02/03/76

```

30 FORMAT ( // 27H CONTROL FLAGS -- // )
40 FORMAT ( 45H CORRECTION FACTORS CALCULATED )
50 FORMAT ( 75H DATA MONITORED ONLY -- NO CORRECTION )
52 1FACTORS ( 75H DATA MONITORED - CORRECTION FACTORS )
60 1TAKEN FROM TAPE ( 75H PREMULTIPLIER - PRESSURE AND GEOMETR )
70 1Y TAKEN FROM TAPE ( 75H POSTMULTIPLIER - DT INVERSE AND GEOM )
80 1E TRY TAKEN FROM TAPE ( 75H PREMULTIPLIER - DT INVERSE AND GEOM )
90 1TRY TAKEN FROM TAPE ( 75H PREMULTIPLIER - PRESSURE AND GEOMETR )
92 1Y TAKEN FROM CARDS ( 78H NEW POSTMULTIPLIER - DT INVERSE AND )
100 1GEOMETRY ( TAKEN FROM TAPE ( 50H WEIGHTS ARE A FUNCTION OF THE LOADS ) )
110 1FORMAT ( 50H FLAGT = 0 )
120 1FORMAT ( 60H FLAGT = 1 )
130 1FORMAT ( 60H FLAGW = 0 )
134 1DED )
140 1FORMAT ( 10H IPRINT = 12, 23H (DETAIL PRINT FLAG) )
140 1FORMAT ( // 27H CONTROL -- // )
140 1FORMAT ( 10H NP = 14 / 10H NC = 14 / )
140 1FORMAT ( 10H NEM = 14 / 10H NELIMS = 14 / )
140 1FORMAT ( 10H NMON = 14 / 10H NAXIS = 14 / )
150 1FORMAT ( // 34H LIST OF INPUT/OUTPUT TAPES -- // )
19H GEOMETRY TAPE = 13/19H DELTA-CP TAPE = 13 /
19H W TAPE = 13/19H D-INVERSE TAPE = 13 /
19H CORR. FACTORS = 13 /
160 1FORMAT ( 14, 19, 4F16.6 )
170 1FORMAT ( 1H1 // 23H EPSILON LIMITS -- // EPSILON-BAR-MIN )
170 1FORMAT ( 48H LIM-1(K) LIM-2(K) LIM-32X, 20H REAL IMAG. )
170 1FORMAT ( 17X, 15HEPSILON-BAR-MAX / 32X, 20H REAL )
180 1FORMAT ( 1H1 // 32H CARD-READ OPTION IS SPECIFIED // 6H )
180 1FORMAT ( 1HX, 12X, 1HY, 12X, 1HZ, 11X, 5HGAMMA, 8X, 7HDELTA-A / )
190 1FORMAT ( 6F10.0 )
190 1FORMAT ( 8F13.6 )
200 1FORMAT ( 16, 8F13.6 )
210 1FORMAT ( 1H1 // 34H SYMMETRIC DELTA-CP MATRIX / )
220 1FORMAT ( 1H0 // 34H ANTI SYMMETRIC DELTA-CP MATRIX / )
230 1FORMAT ( 1H0 // 34H )
240 1FORMAT ( / 9H COLUMN, 13 / )

```

WEYTO580
WEYTO590
WEYTO600
WEYTO610
WEYTO612
WEYTO614
WEYTO620
WEYTO630
WEYTO640
WEYTO650
WEYTO660
WEYTO670
WEYTO680
WEYTO690
WEYTO692
WEYTO694
WEYTO700
WEYTO710
WEYTO720
WEYTO730
WEYTO740
WEYTO750
WEYTO756
WEYTO760
WEYTO770
WEYTO780
WEYTO790
WEYTO800
WEYTO810
WEYTO820
WEYTO822
WEYTO830
WEYTO840
WEYTO850
WEYTO860
WEYTO870
WEYTO880
WEYTO890
WEYTO900
WEYTO910
WEYTO920
WEYTO930
WEYTO940
WEYTO950
WEYTO1000
WEYTO1010
WEYTO1020
WEYTO1030
WEYTO1040
WEYTO1050
WEYTO1060
WEYTO1062
WEYTO1070

CC

CORRECTION FACTORS (EIGC) 02/03/76

```

IF (FLAGP .EQ. 1) WRITE (NPOT,70)
IF (FLAGP .EQ. 2) WRITE (NPOT,80)
IF (FLAGP .EQ. 3) WRITE (NPOT,90)
IF (FLAGP .EQ. 4) WRITE (NPOT,92)
IF (FLAGT .EQ. 0) WRITE (NPOT,100)
IF (FLAGT .EQ. 1) WRITE (NPOT,110)
IF (FLAGW .EQ. 0) WRITE (NPOT,120)
IF (FLAGW .EQ. 1) WRITE (NPOT,130)
WRITE (NPOT,134) IPRINT

CC WRITE CONTROL DIMENSIONS
CC WRITE (NPOT,140) NP , NC , NEM , NELIMS, NMON , NAXIS
CC READ NUMBER OF MODES AND WRITE LIST OF INPUT/OUTPUT TAPES
C READ (NPIT, 10) NMSYM, NMASYM
C WRITE (NPOT,150) NTGEOM, NTDCP, NTAPW, NTAPOI, NTAPCF
C IFP (FLAGP .EQ. 1) GO TO 310
C IF (FLAGP .EQ. 3) GO TO 310
CC READ GEOMETRY TAPE
CC REWIND (NTGEOM) LENGTH
C CALL RECD( NTGEOM, X , LENGTH )
CALL RECD( NTGEOM, Y , LENGTH )
CALL RECD( NTGEOM, Z , LENGTH )
CALL RECD( NTGEOM, GMA , LENGTH )
CALL RECD( NTGEOM, DELA , LENGTH )
IF (FLAGI .EQ. 0) GO TO 500
IF (FLAGI .EQ. 1) GO TO 500
REWIND NTDCP
READ (NTDCP) LENGTH, NMSYM, NMASYM
WRITE (NEWDCP) LENGTH, NMSYM, NMASYM
MODCP 300 = NMSYM + NMASYM
DO 290 J = 1, MODCP
DO 290 I = 1, NP
DCP(I) = CMPLX(ROW(I), 0.0)
300 CONTINUE
REWIND NEWDCP
NTDCP = NEWDCP
GO TO 500
310 CONTINUE
REWIND NUTL1
WRITE (NPOT, 180)
C

```

WEYTI1080
WEYTI1090
WEYTI1100
WEYTI1102
WEYTI1110
WEYTI1120
WEYTI1130
WEYTI1140
WEYTI1144
WEYTI1150
WEYTI1160
WEYTI1170
WEYTI1180
WEYTI1190
WEYTI1200
WEYTI1210
WEYTI1220
WEYTI1230
WEYTI1240
WEYTI1250
WEYTI1260
WEYTI1270
WEYTI1280
WEYTI1290
WEYTI1300
WEYTI1310
WEYTI1320
WEYTI1330
WEYTI1340
WEYTI1350
WEYTI1360
WEYTI1370
WEYTI1380
WEYTI1390
WEYTI1400
WEYTI1410
WEYTI1420
WEYTI1430
WEYTI1440
WEYTI1450
WEYTI1460
WEYTI1470
WEYTI1480
WEYTI1490
WEYTI1500
WEYTI1510
WEYTI1520
WEYTI1530
WEYTI1540
WEYTI1550
WEYTI1570
WEYTI1580
WEYTI1590

```

C      READ GEOMETRY ARRAYS AND DELTA-CP MATRIX FROM CARDS
C      DO 330 I = 1, NP
      READ (NPIT,190) X(I), Y(I), Z(I), GMA(I), DELA(I)
      WRITE (NPOT,210) I, X(I), Y(I), Z(I), GMA(I), DELA(I)
C
C      CONTINUE
      WRITE (NTDCP) NP, NMSYM, NMASYM
      IGO = 1
      IF (NMSYM .EQ. 0) GO TO 390
      MODES = NMSYM
      WRITE (NPOT,220)
C      CONTINUE
      DO 380 J = 1, MODES
      WRITE (NPOT,240) J
      IF (FLAGI .NE. 0) GO TO 350
      READ (NPIT,190) (DCP(I), I = 1, NP)
      GO TO 370
C      350 READ TO (NPIT,190) (ROW(I), I = 1, NP)
      DO 360 I = 1, NP
      DCP(I) = CMLPX(ROW(I), 0.0)
C      360 DCP(I)
      CONTINUE
      WRITE (NPOT,200) (DCP(I), I = 1, NP)
      WRITE (NTDCP) (DCP(I), I = 1, NP)
C      380 CONTINUE
C
C      390 CONTINUE
      IF (IGU .EQ. 2 .OR. NMASYM .EQ. 0) GO TO 400
      IGO = 2
      MODES = NMASYM
      WRITE (NPOT,230)
      GO TO 340
C      400 CONTINUE = NP
      LENGTH = NP
C      500 CONTINUE
C
C      DO 510 I = 1, LENGTH
      CG(I) = COS(GMA(I))
      SG(I) = SIN(GMA(I))
C      510 CONTINUE
C
C      IF (NC .EQ. 0 .AND. NMON .EQ. 0) GO TO 520
      REWIND NTSAIJ
      REWIND NTSANJ
C
C      CALL SAIJ(NPIT, NPOT, NTSAIJ, NTSANJ, NC, NP, NMON, NAXIS,
1 AIT, CIE, X, Y, Z, CG, SG, DELA, FLAGA, FLAGF, CODE, IPRINT,
2 LABEL, SAI)
C      520 CONTINUE
      IF (NELIMS .EQ. 0) GO TO 540
      K

```

```

WEYTT1600
WEYTT1610
WEYTT1620
WEYTT1630
WEYTT1640
WEYTT1650
WEYTT1710
WEYTT1720
WEYTT1750
WEYTT1760
WEYTT1770
WEYTT1780
WEYTT1790
WEYTT1800
WEYTT1810
WEYTT1820
WEYTT1830
WEYTT1840
WEYTT1850
WEYTT1860
WEYTT1870
WEYTT1880
WEYTT1890
WEYTT1900
WEYTT1910
WEYTT1920
WEYTT1930
WEYTT1940
WEYTT1950
WEYTT1960
WEYTT1970
WEYTT1980
WEYTT1990
WEYTT2000
WEYTT2010
WEYTT2350
WEYTT2360
WEYTT2370
WEYTT2380
WEYTT2390
WEYTT2400
WEYTT2410
WEYTT2430
WEYTT2440
WEYTT2450
WEYTT2460
WEYTT2470
WEYTT2480
WEYTT2490
WEYTT2500
WEYTT2510
WEYTT2520
WEYTT2530

```

CORRECTION FACTORS (EIGC) 02/03/76

```

530 WRITE (NPOT,170)
    READ (NPIT,20)
    WRITE (NPOT,160) K, LIMK(1, K), LIMK(2, K), EBMIN(K), EBMAX(K)
    IF (K.EQ. NELIMS) K, LIMK(1, K), LIMK(2, K), EBMIN(K), EBMAX(K)
    K = K + 1
    GO TO 530
C
540 CONTINUE
C
540 IF (NEM.EQ. 0) GO TO 550
C
    CALL PHIJ(NPIT, NPOT, NTPHIJ, NEM, NP, KODE, PHI, MODES, )
    X, Y, Z,
C
550 CONTINUE = NP
    NROW (FLAGP.EQ. 0 .OR. FLAGP.EQ. 3) GO TO 560
    IF (FLAGW.NE. 1) GO TO 560
C
    REWIND NTAPDI
    READ (NTAPDI)
    NCOL = MAXO(NMSYM, NMASYM)
    REWIND NTAPW
C
    CALL HSWA(NPIT, NPOT, NUTL1, NTAPW, KODE, NP, NCOL, NMAX, )
    NMSYM, NMASYM,
    1
C
    THE TAPE NTAPW CONTAINS THE TWO W-MATRICES, WS AND WA,
    PRECEDED BY THE NUMBERS NP, NMSYM, NMASYM
C
560 CONTINUE = NS
    NX (NEM.NE. 0) NX = NEM + NC
    IGO = 1
    NMODE = NMSYM
    IF (NMSYM.NE. 0) GO TO 562
    IGO = 2
    NMODE = NMASYM
    CONTINUE
    IF (FLAGB.NE. 0) GO TO 600
C
    REWIND NTAPCF
    GO TO (580,570,580,580,570), IFP
    570 WRITE (NTAPCF) POST
    GO TO 590
    580 WRITE (NTAPCF) PRE
    590 CONTINUE
    WRITE (NTAPCF) NP, NMSYM, NMASYM
    600 CONTINUE
C
    CALL DCPB(NTDCP, NTAPW, NTAPDI, IGO, FLAGP, FLAGW, NROW, )
    NMODE, NMAX, DCP, COL,
    1 IF (FLAGB.NE. 0) GO TO 612

```

YTT2540
 WEYTT2550
 WEYTT2560
 WEYTT2570
 WEYTT2580
 WEYTT2590
 WEYTT2600
 WEYTT2610
 WEYTT2620
 WEYTT2630
 WEYTT2640
 WEYTT2650
 WEYTT2660
 WEYTT2670
 WEYTT2680
 WEYTT2690
 WEYTT2700
 WEYTT2710
 WEYTT2720
 WEYTT2730
 WEYTT2740
 WEYTT2750
 WEYTT2760
 WEYTT2770
 WEYTT2780
 WEYTT2790
 WEYTT2800
 WEYTT2810
 WEYTT2820
 WEYTT2830
 WEYTT2840
 WEYTT2842
 WEYTT2844
 WEYTT2850
 WEYTT2860
 WEYTT2862
 WEYTT2864
 WEYTT2866
 WEYTT2868
 WEYTT2870
 WEYTT2872
 WEYTT2880
 WEYTT2890
 WEYTT2900
 WEYTT2910
 WEYTT2920
 WEYTT2930
 WEYTT2940
 WEYTT2950
 WEYTT2960
 WEYTT2970
 WEYTT2980
 WEYTT2982

CORRECTION FACTORS (EIGC) 02/03/76

```

C      CALL      DELC(NTSAIJ, NPOT , NC , NP , NMODE, NMAX ,
C      CIE , DCI , SAI , WORK )
      DO 610 I = 1, NS
      ELIM(I) = (0.0, 0.0)
      CONTINUE
610  IF (FLAGB.EQ. 0) GO TO 616
612  GO TO (672, 614), FLAGB
614  IF (FLAGP.NE. 4 .OR. NEM .EQ. 0) GO TO 672
616  CALL      SDBL(NUTLI, NUTL2, MASTSB, NPHIJ, NTAPW, NTSAIJ, NTAPDI,
      IGO, FLAGH, FLAGP, FLAGT, NC, NP, NS, NEM, SQRTT, AIT,
      DELA, SBB, SBI, SAI, DI, W, PHI, SQRTT, WORK )
      IF (FLAGB.NE. 0) GO TO 672
C      CALL      GINV(NPOT, MASTSB, NC , NS , NX , DCI
      EB , CIE , S , SBMAT )
C
C      CONTINUE I = 1, NP
620  DO 630 EB(I) = EB(I) / SQRTT(I)
630  CONTINUE
C
C      IF (NELIMS.EQ. 0) GO TO 670
      CALL      EDBL(NPOT, NELIMS, NP ; NS, LIMK, JARR, NSMOD
      EBMIN , EBMAX ; EB ; ELIM )
C
C      IF (NSMOD .EQ. 0) GO TO 650
      CALL      MODF( NC, NS, MASTSB, NEWTSB, JARR , SQRTT ,
      ELIM, SBB, DCI , DCMOD )
C
C      CALL      GINV(NPOT, NEWTSB, NC, NS , NX ,
      EB , B , S , SBMAT , DCMOD )
C
C      GO TO 620
C
C      CONTINUE
650  DO 660 IB = 1, NS
660  EB(IB) = EB(IB) + ELIM(IB)
670  CONTINUE
C
      NTAPE = NTPHIJ
      IF (FLAGP .EQ. 4) NTAPE = NUTLI
      CALL      EPSJ(NTAPE , NP , NEM , NMAX,
      EB , EPS , PHI )
C
C      CONTINUE
672  CONTINUE

```

Y2990
 Y3000
 Y3010
 Y3020
 Y3030
 Y3040
 Y3050
 Y3052
 Y3054
 Y3056
 Y3057
 Y3058
 Y3060
 Y3070
 Y3080
 Y3090
 Y3100
 Y3110
 Y3120
 Y3130
 Y3140
 Y3150
 Y3160
 Y3170
 Y3180
 Y3190
 Y3210
 Y3220
 Y3230
 Y3240
 Y3250
 Y3260
 Y3270
 Y3280
 Y3290
 Y3300
 Y3310
 Y3320
 Y3330
 Y3340
 Y3350
 Y3360
 Y3370
 Y3380
 Y3390
 Y3400
 Y3402
 Y3404
 Y3410
 Y3420
 Y3430
 Y3432
 Y3440

CORRECTION FACTORS (EIGC) 02/03/76

```

1 CALL NUTL2, DCPT(NPOT, LINES, IGO, FLAGB, FLAGP, NMODE, NP, NUTL1,
2 NEM, NTAPDI, NTAPW, NTAPCF, X, Y, Z, GMA, DELA, EB
   , W, DI, EPS, DELCPB, DCPTIL, WORK, EB
C IF (NMON.EQ.0) GO TO 690
C CALL CEMN(NPOT, IGO, NMODE, NTSANJ, NP, NMON, LABEL, NUTL2,
1 SAI, DCPTIL, CE
C 690 CONTINUE
IF (IGO.EQ.2.OR.NMASYM.EQ.0) GO TO 700
IGO = 2
NMODE = NMASYM
GO TO 600
700 CONTINUE
RETURN
END
SUBROUTINE WSWA(NPIT, NPOT, NUTL1, NTAPW, KODE, NP, NCOL, NMAX,
1 NMSYM, NMASYM,
C DATA SET NUMBER OF THE SYSTEM INPUT DATA SET
C DATA SET NUMBER OF THE SYSTEM OUTPUT DATA SET
C UTILITY (SCRATH) TAPE NUMBER
C TAPE NUMBER CONTAINING COLUMNS OF THE W MATRIX
= -1
C NUMBER OF ROW ELEMENTS IN THE W MATRIX
C NUMBER OF COLUMNS IN THE W MATRIX
C MAXIMUM OF COLUMNS IN THE W MATRIX
C NUMBER OF SYMMETRIC MODES
C NUMBER OF ANTISYMMETRIC MODES
C 2-D COMPLEX ARRAY CONTAINING THE W MATRIX
COMPLEX WIN(100), W(NP, NMAX)
DIMENSION MODE(100), IDELW(100), LIMW(2, 100)
10 FORMAT (4I10, 4F10.0)
20 1 FORMAT (1H1//, 23H --- IS CARD INPUT // 26H MODE DELTA
LIMITS, 15X, 5H - W - / 35X, 18HREAL IMAG. )
30 FORMAT (16, 2I8, 16, 4F14.6)
40 1 FORMAT (1H1//6H, THE, I4, 41H COLUMNS OF THE SYMMETRIC
MATRIX ( / 8H COLUMN, I4 / ( 3 ( I6, 2E14.6 ) ) )
50 FORMAT (1H1//6H, THE, I4, 41H COLUMNS OF THE ANTISYMMETRIC
60 1 FORMAT (1H1//,
62 1 FORMAT (1H1//,
C
J WRITE (NPOT, 20)
70 CONTINUE (NPIT, 10) MODE(J), IDELW(J), LIMW(1,J), LIMW(2,J), WIN(J)
IF (MODE(J).LE. KODE) GO TO 80
WRITE (NPOT, 30) MODE(J), IDELW(J), LIMW(1,J), LIMW(2,J), WIN(J)
= J + 1

```

WEYT3450
WEYT3460
WEYT3470
WEYT3480
WEYT3500
WEYT3510
WEYT3520
WEYT3530
WEYT3540
WEYT3550
WEYT3560
WEYT3570
WEYT3580
WEYT3590
WEYT3600
WEYT3610
WEYT3620
WEYT3630
WSWA0040
WSWA0050
WSWA0060
WSWA0070
WSWA0080
WSWA0090
WSWA0100
WSWA0110
WSWA0120
WSWA0130
WSWA0140
WSWA0150
WSWA0160
WSWA0170
WSWA0180
WSWA0190
WSWA0200
WSWA0220
WSWA0230
WSWA0240
WSWA0250
WSWA0260
WSWA0270
WSWA0280
WSWA0290
WSWA0300
WSWA0302
WSWA0310
WSWA0320
WSWA0330
WSWA0340
WSWA0350
WSWA0360
WSWA0370
WSWA0380

CORRECTION FACTORS (E1GC) 02/03/76

```

80 GO TO 70
   CONTINUE = NP
   NROW = NUTL1
   DO 100 N = 1, NMAX
   DD 90 M = 1, NROW
   W(M, N) = (0.0, 0.0)
90 CONTINUE
100 CONTINUE = J - 1
   JMAX = J
   IGO = I
   IDEL = I
110 CONTINUE = 0
   MDMAX = J = 1, JMAX
   DD 130 = IDELW(J)
   IF (ND .NE. NDEL) GO TO 130
   MD = MODE(J)
   L1 = LIMW(1, J)
   L2 = LIMW(2, J)
   IF (MDMAX .LT. MD) MDMAX = MD
   DO 120 L = L1, L2
   W(L, MD) = WIN(J)
120 CONTINUE
C 130 CONTINUE
C 140 CONTINUE
   WRITE (NUTL1) W IGO
   GO TO (140, 150), W IGO
C 150 CONTINUE
   NMSYM = MDMAX
   NDEL = -1
   IGO = 2
   GO TO 110
   NMASYM = MDMAX
   REWIND NUTL1
   REWIND NTAPW
   WRITE (NTAPW) NROW, NMSYM, NMASYM
C
   NMD = NMSYM
   IGO = I
   WRITE (NPOT, 40) NMSYM
160 CONTINUE
   READ (NUTL1) W
   DD 170 NM = 1, NMD
C
   WRITE (NTAPW) (W(M, NM), M = 1, NROW)
   WRITE (NPOT, 50) NM, (I, W(I, NM), I = 1, NROW)
   IF (NM .NE. NMD) WRITE (NPOT, 62)
170 CONTINUE
C

```

WSWA0390
WSWA0400
WSWA0410
WSWA0420
WSWA0430
WSWA0440
WSWA0450
WSWA0460
WSWA0470
WSWA0480
WSWA0490
WSWA0500
WSWA0510
WSWA0520
WSWA0530
WSWA0540
WSWA0550
WSWA0560
WSWA0570
WSWA0580
WSWA0590
WSWA0600
WSWA0610
WSWA0620
WSWA0630
WSWA0640
WSWA0650
WSWA0660
WSWA0670
WSWA0680
WSWA0690
WSWA0700
WSWA0710
WSWA0720
WSWA0730
WSWA0740
WSWA0750
WSWA0760
WSWA0770
WSWA0780
WSWA0790
WSWA0800
WSWA0810
WSWA0820
WSWA0830
WSWA0840
WSWA0850
WSWA0860
WSWA0870
WSWA0880
WSWA0890
WSWA0900
WSWA0910

CORRECTION FACTORS (EIGC) 02/03/76

```

180 GO TO (180,190), IGO
CONTINUE
IF (NMASYM .EQ. 0) GO TO 190
WRITE (NPOT,60) NMASYM
NMD = NMASYM
IGO = 2
GO TO 160

C 190 CONTINUE NTAPW
REWIND NTAPW
RETURN
END
SUBROUTINE ZEROOUT( WORK, LENGTH, LOOP, ITAPE )
C
C WORK COMPLEX ARRAY TO BE INITIALIZED TO ZEROES
C LENGTH LENGTH OF ARRAY WORK
C LOOP NUMBER OF TIMES THE ARRAY WORK IS TO BE WRITTEN ON
C ITAPE ITAPE (ONLY IF ITAPE IS NOT ZERO)
C COMPLEX WORK(LENGTH)
DO 10 I = 1, LENGTH
WORK(I) = (0.0, 0.0)
CONTINUE
IF (ITAPE .EQ. 0) RETURN

DO 20 L = 1, LOOP
WRITE (ITAPE) (WORK(I), I = 1, LENGTH)
CONTINUE
RETURN
END

```

WSMA0920
WSMA0930
WSMA0940
WSMA0950
WSMA0960
WSMA0970
WSMA0980
WSMA0990
WSMA1000
WSMA1010
WSMA1020
WSMA1030
ZER00020
ZER00030
ZER00040
ZER00050
ZER00060
ZER00070
ZER00080
ZER00090
ZER00100
ZER00110
ZER00120
ZER00130
ZER00140
ZER00150
ZER00160
ZER00170
ZER00180
ZER00190
ZER00200

REFERENCES

1. Revell, J. D., and Rodden, W. P., "A Rational Method for Utilizing Experimental Aerodynamic Data in Flutter Analyses Through the Use of Aerodynamic Influence Coefficient Matrices", North American Aviation, Inc., Report NA-59-867, 30 January 1959.
2. Rodden, W. P., "An Empirical Weighting Matrix for Use with Aerodynamic Influence Coefficients in Aeroelastic Analyses," Northrop Corp., Report NOR-59-320, 1 April 1959.
3. Rodden, W. P., and Revell, J. D., "The Status of Unsteady Aerodynamic Influence Coefficients," Paper FF-33, presented to IAS 30th Annual Meeting, 20-24 January 1962; preprinted as Rept. TDR-930(2230-09)TN-2, 22 November 1961, Aerospace Corp., El Segundo, Ca.
4. Rodden, W. P., "Comment on 'Convergence Proof of Discrete-Panel Wing Loading Theories'", J. Aircraft, Vol. 9, No. 9, September 1972, pp. 686-688.
5. Bergh, H., "Some Aspects of Unsteady Pressure Measurements," AGARD Report 498 Part II, 1965; also Rept. NLR MP.227, National Aerospace Lab., Amsterdam, The Netherlands, 1964.
6. Bergh, H., and Zwaan, R. J., "A Method for Estimating Unsteady Pressure Distributions for Arbitrary Vibration Modes from Measured Distributions for One Single Mode," Rept. NLR-TR-F.250, National Aerospace Lab., Amsterdam, The Netherlands, February 1966.
7. Ashley, H., "Some Considerations Relative to the Prediction of Unsteady Air Loads on Interfering Surfaces," AGARD-CP-80-71, Paper No. 1, AGARD Symposium on Unsteady Aerodynamics for Aeroelastic Analyses of Interfering Surfaces, Tønsberg, Norway, 3-4 November 1970.
8. Ashley, H., and Rowe, W. S., "On the Unsteady Aerodynamic Loading of Wings with Control Surfaces," Z. Flugwiss., Band 18, Heft 9/10, September/Oktober

1970, pp. 321-330.

9. Rowe, W. S., Winther, B. A., and Redman, M. C., "Unsteady Subsonic Aerodynamic Loadings Caused by Control Surface Motions," J. Aircr., Vol. 11, No. 1, January 1974, pp. 45-54.
10. Tijdeman, H., and Zwaan, R. J., "On the Prediction of Aerodynamic Loads on Oscillating Wings in Transonic Flow," AGARD Report No. 612, Supplement to the Manual on Aeroelasticity, Vol. 11, Ch. 10, January 1974. Also Report NLR MP 73026U June 1965.
11. Tijdeman, H., and Bergh, H., "Analysis of Pressure Distributions Measured on a Wing with Oscillating Control Surface in Two-Dimensional High Subsonic and Transonic Flow," National Aerospace Laboratories Report NLR-TR F.253, March 1967.
12. Traci, R. M., Farr, J. L., Albano, E., "Perturbation Method for Transonic Flows About Oscillating Airfoils," AIAA Paper No. 75-877, June 1975.
13. Tijdeman, H., Schippers, P., "Results of Pressure Measurements on an Airfoil with Oscillating Flap in Two-Dimensional High Subsonic and Transonic Flow (Zero Incidence and Zero Mean Flap Position)," National Aerospace Laboratories Report NLR TR 73078U, July 1973.
14. Hertrich, H., "Druckverteilungsmessungen an Halbflügelmodellen mit Ruder in stationärer Unterschallströmung", Bericht 66J12, Aerodynamische Versuchsanstalt, Göttingen, 23 December 1966.
15. Hertrich, H., "Zur experimentellen Prüfung instationärer dreidimensionaler Tragflächentheorien bei inkompressibler Strömung," Bericht 67J02, Aerodynamische Versuchsanstalt, Göttingen, 25 Mar. 1967.
16. Försching, H., Triebstein, H., and Wagener, J., "Pressure Measurements on an Harmonically Oscillating Swept Wing with Two Control Surfaces in Incompressible Flow," AGARD-CP-80-71, Paper No. 15, AGARD Symposium on

Unsteady Aerodynamics for Aeroelastic Analyses of Interfering Surfaces,
Tønsberg, Norway, 3-4 November 1970.

17. Giesing, J. P., Kalman, T. P., Rodden, W. P., "Subsonic Steady and Oscillatory Aerodynamics for Multiple Interfering Wings and Bodies," *Journal of Aircraft*, Vol. 9, No. 10, Oct. 1972.
18. Schmeer, J. W., "The Effect of Leading-Edge Droop upon the Pressure Distribution and Aerodynamic Loading Characteristics of a 45° Sweptback Wing at Transonic Speeds," *NACA TM RM L55.116*, Nov. 1955.
19. Carlson, H. W., "Pressure Distributions at Mach Number 2.05 on a Series of Highly Swept Arrow Wings Employing Various Degrees of Twist and Camber," *NASA TN D-1264*, May 1962.
20. Giesing, J. P., Kalman, T. P., "Oscillatory Supersonic Lifting Surface Theory Using a Finite Element Doublet Representation," *AIAA Paper No. 75-761* presented Denver, Colo. May 1975.

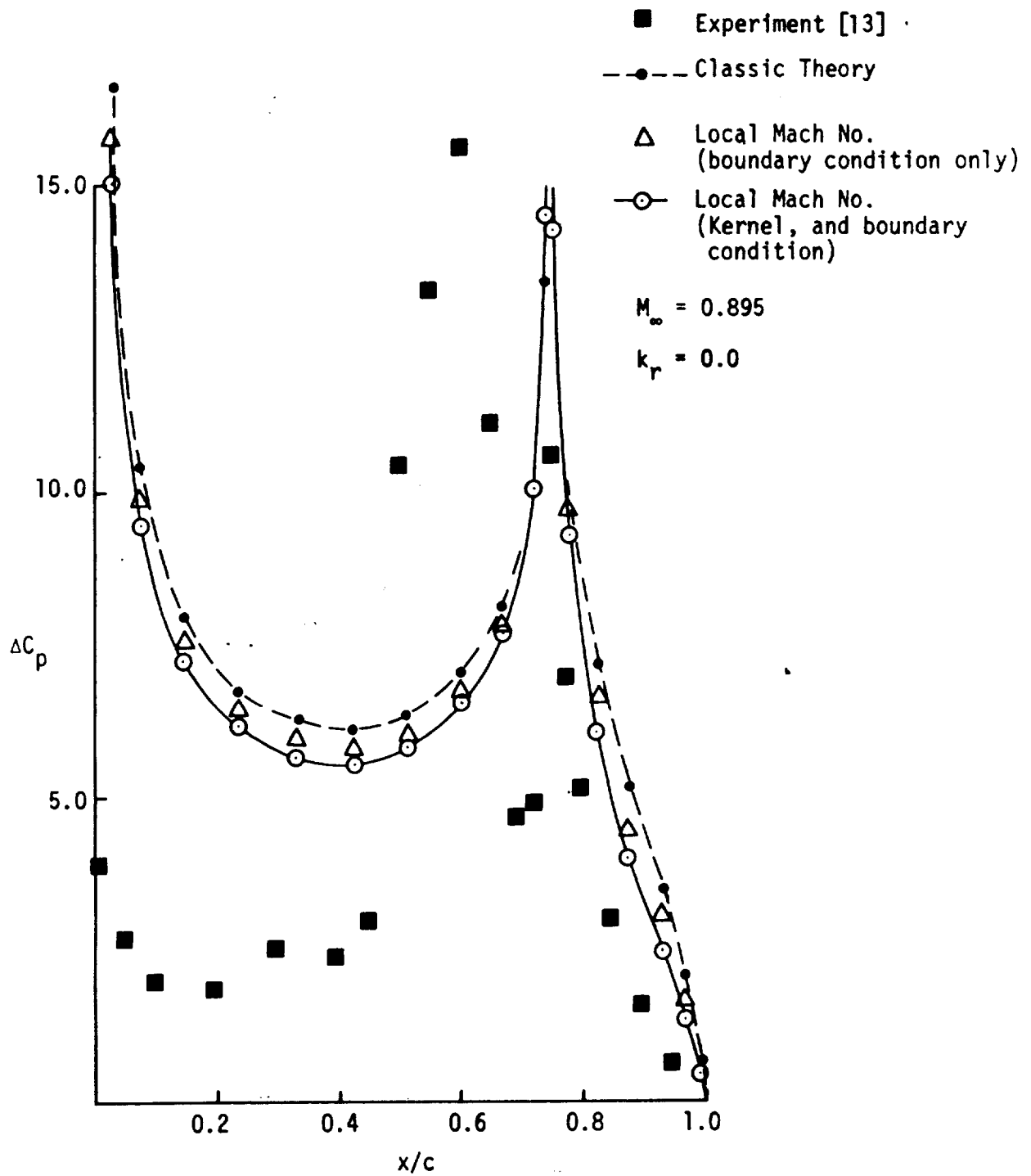


Figure 3. - Effect of applying local Mach Number to the boundary conditions and the kernel of the classic theory.

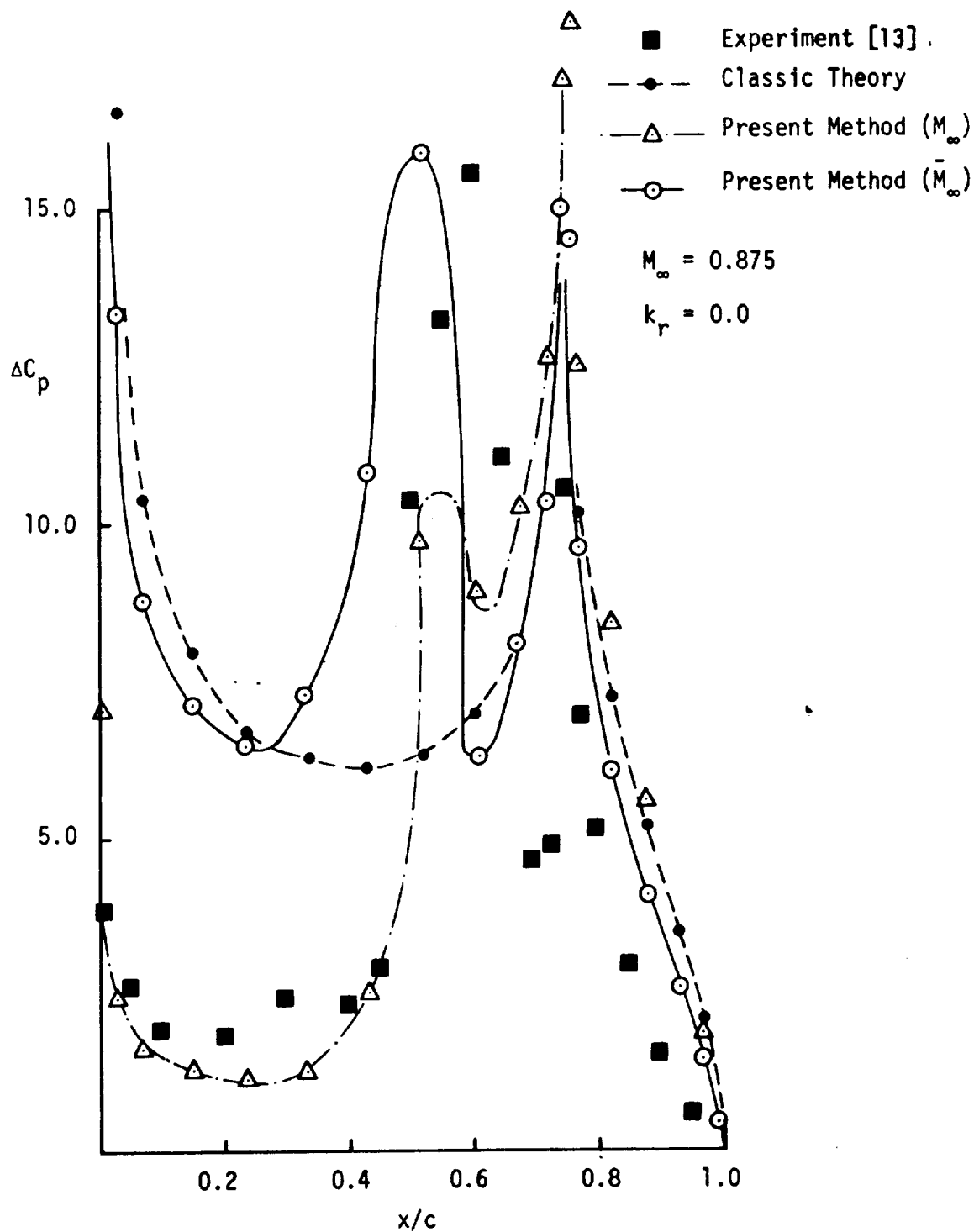


Figure 4. - Comparison of classic theory and two variations of the present method with experimental data for the steady case.

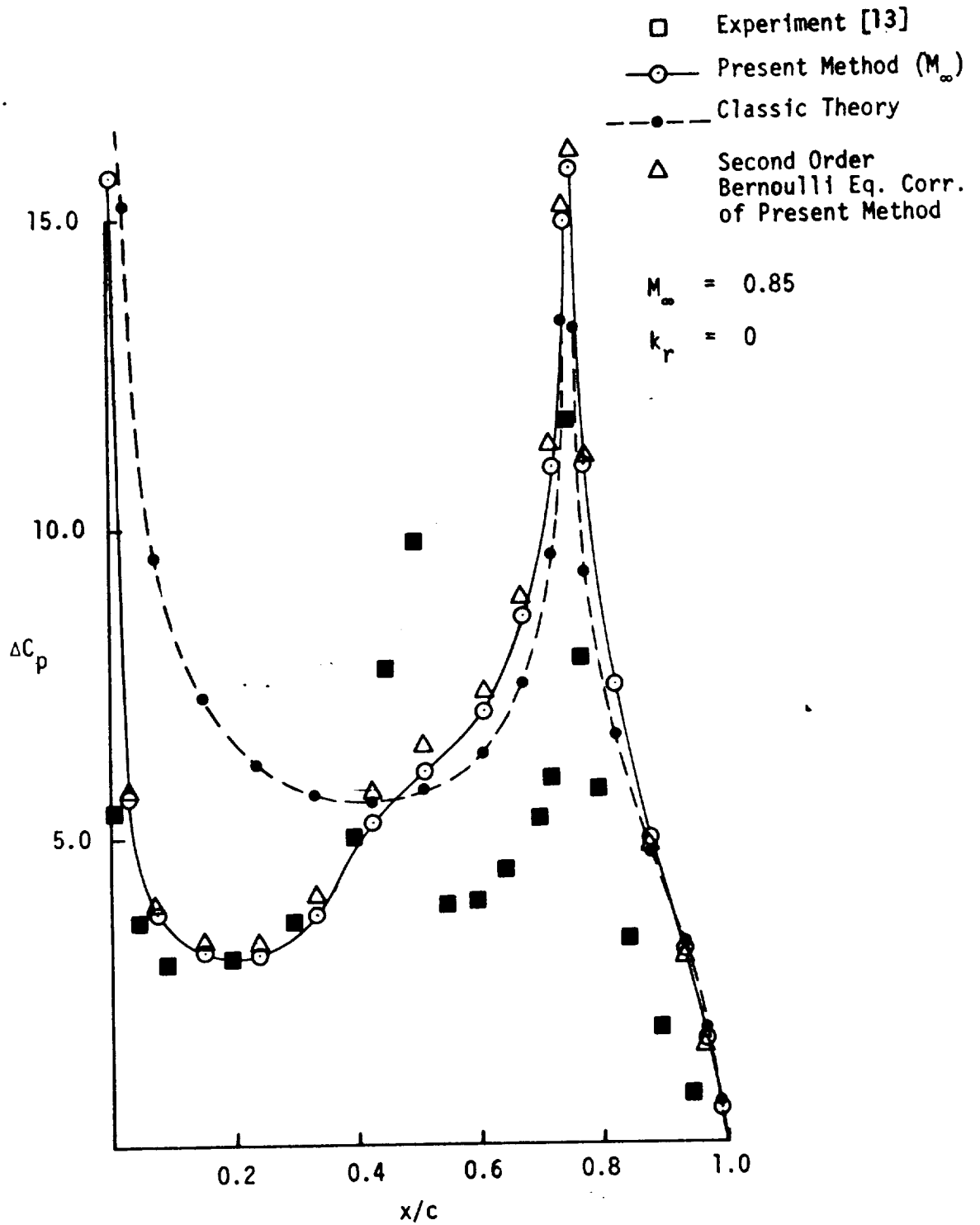


Figure 5. - Comparison of classic theory and the present method (M_∞) (with and without second order Bernoulli correction) with experimental data.

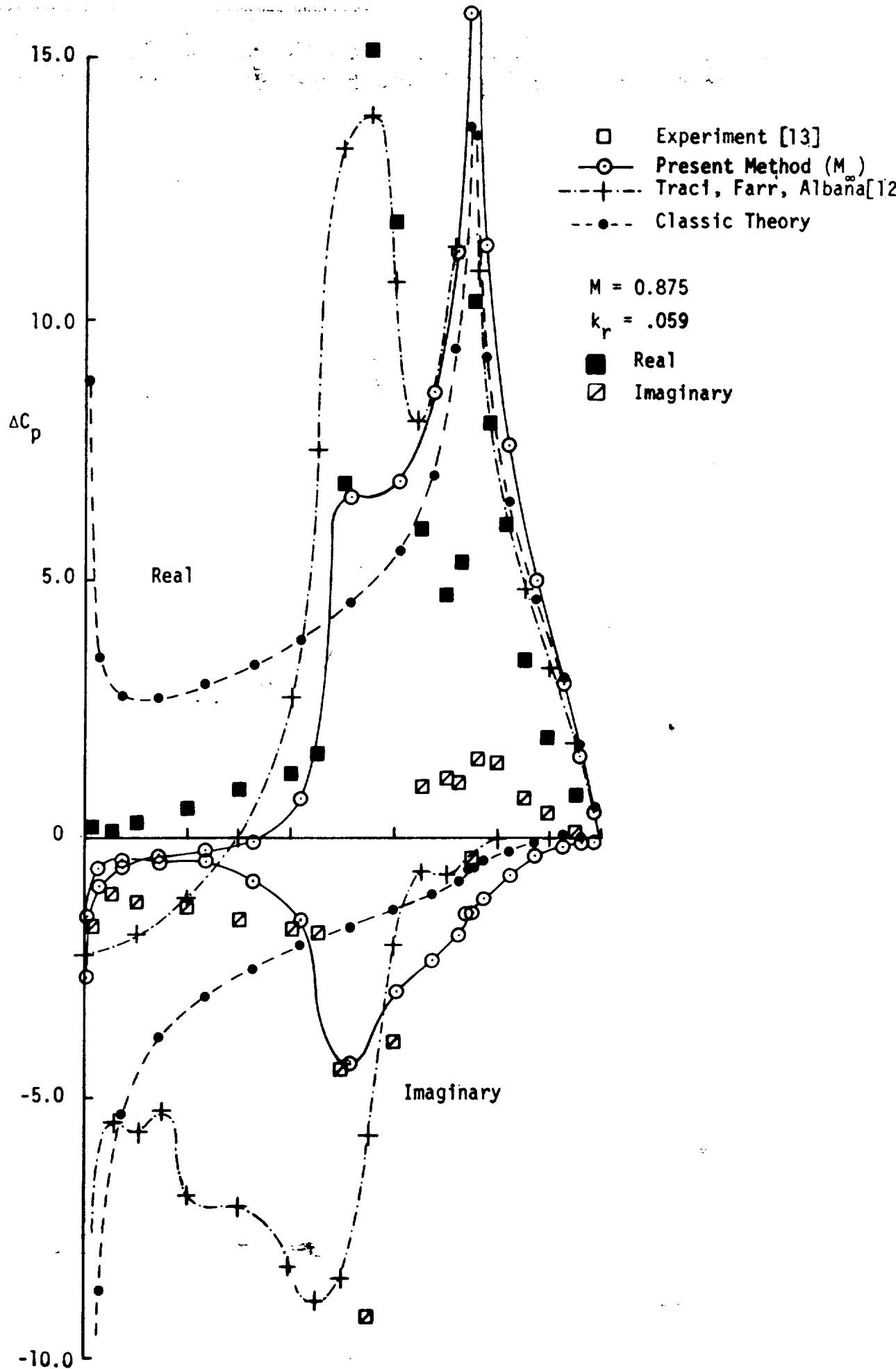


Figure 6. - Comparison of various theories with experimental data for the oscillatory control surface case.

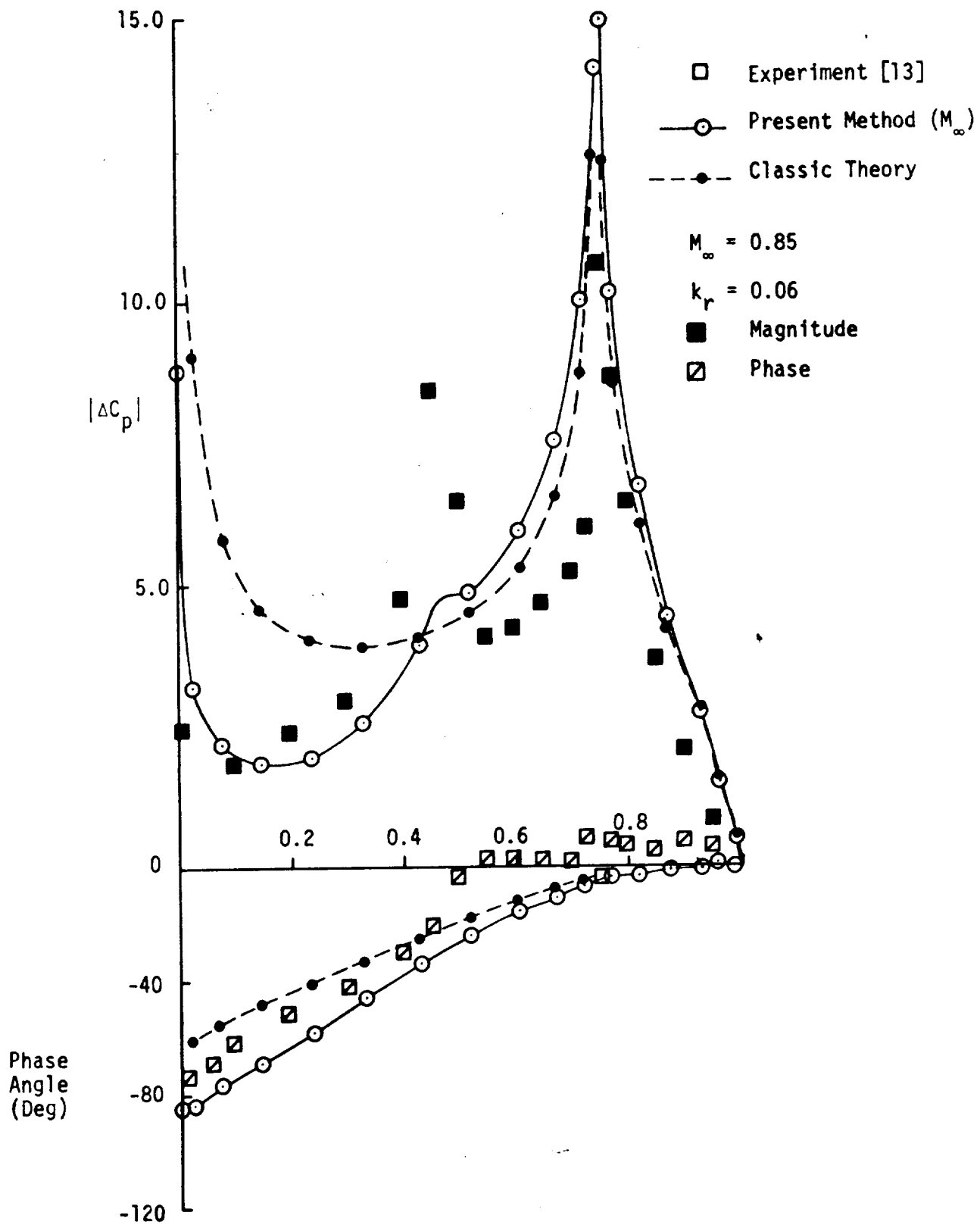


Figure 7. - Comparison of classic theory and the present method (M_∞) with experimental data for the oscillatory case.

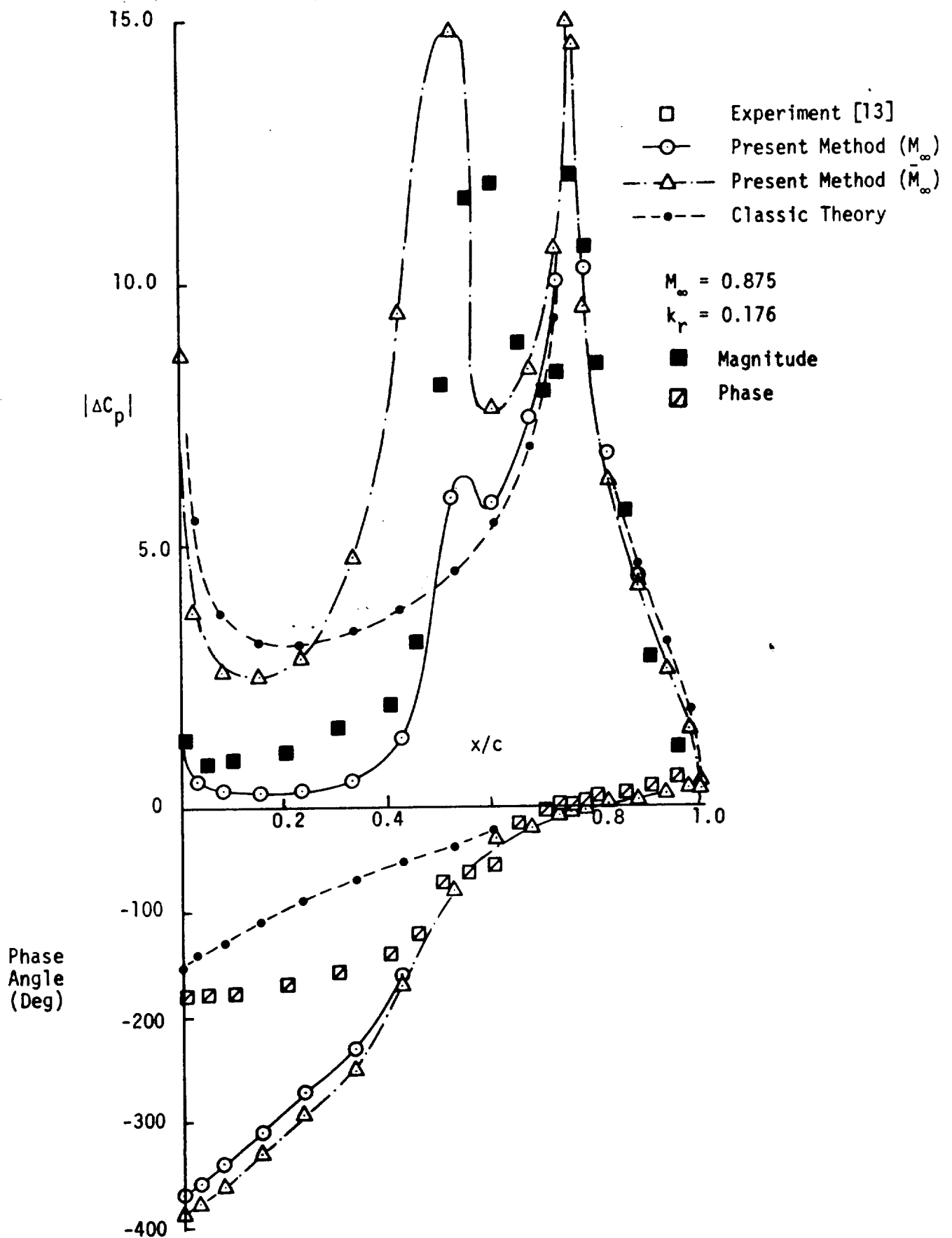


Figure 8. - Comparison of two variations of the Present transonic method with data and classic theory for the oscillatory case.

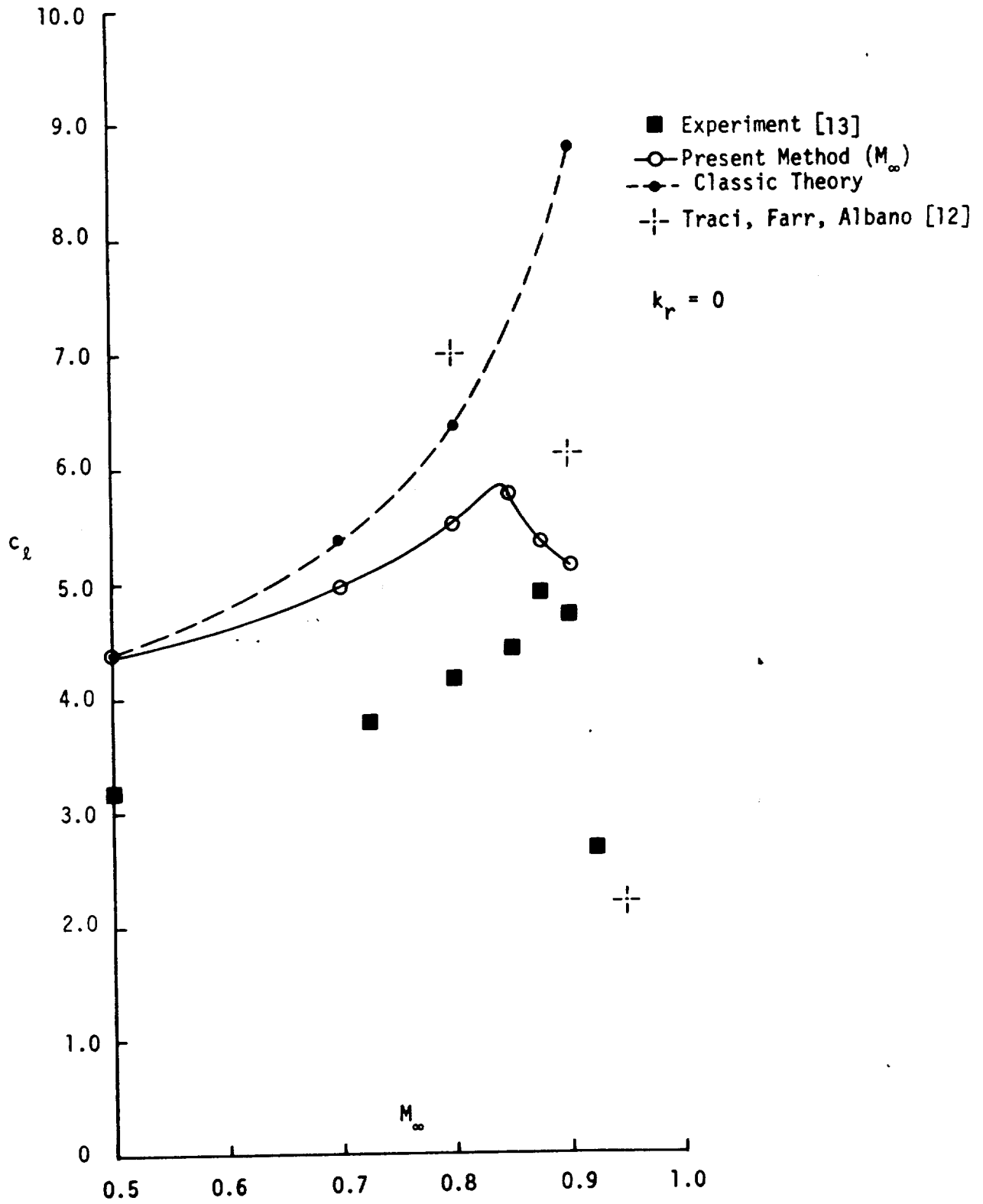


Figure 9. - Comparison of experimental and theoretical lift coefficient for an airfoil with a deflected 25% chord flap.

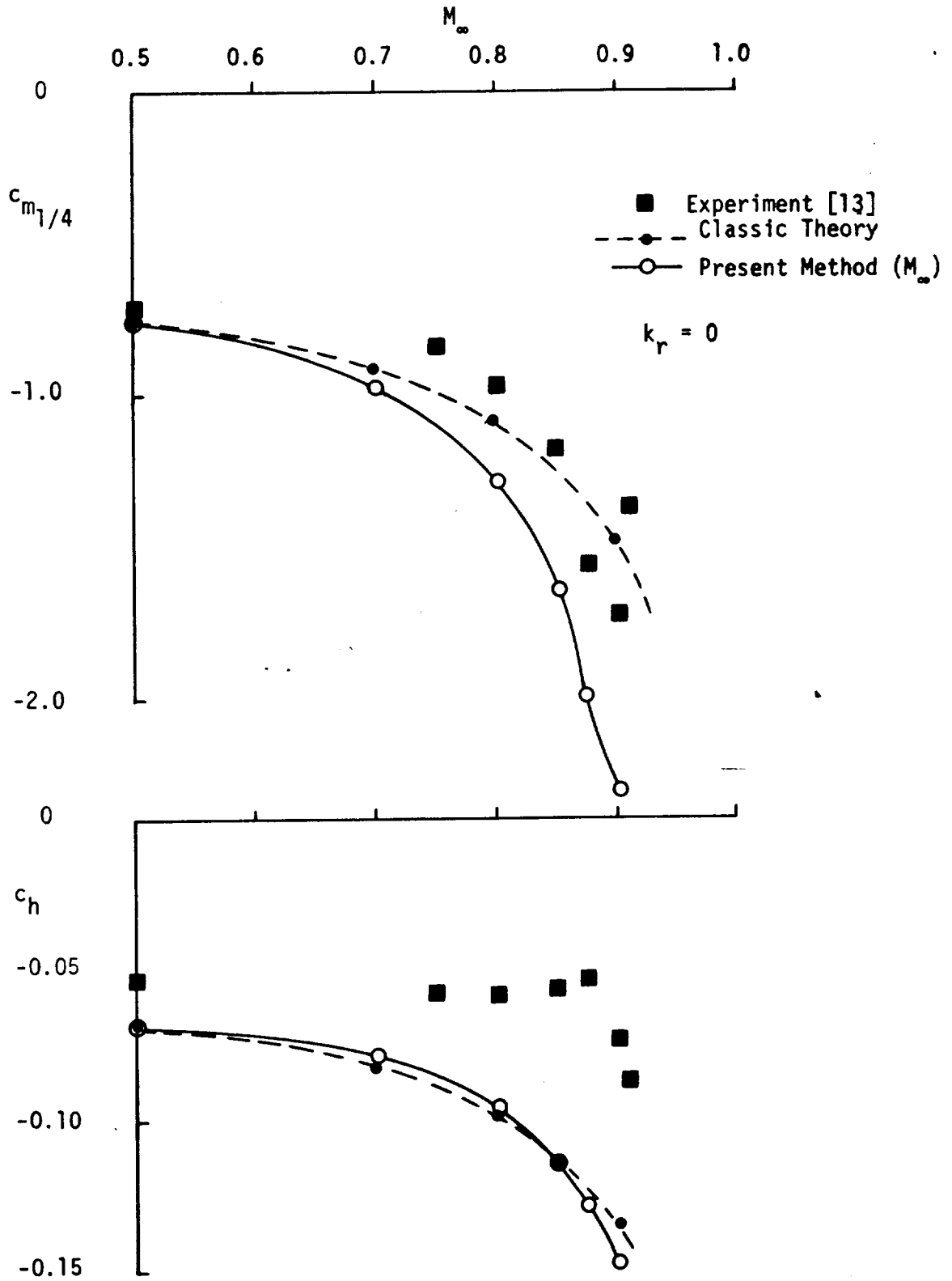


Figure 10 - Comparison of experimental and theoretical pitching (about $c/4$) and hinge moment (about $3c/4$) coefficient for an airfoil with a deflected 25% chord flap.

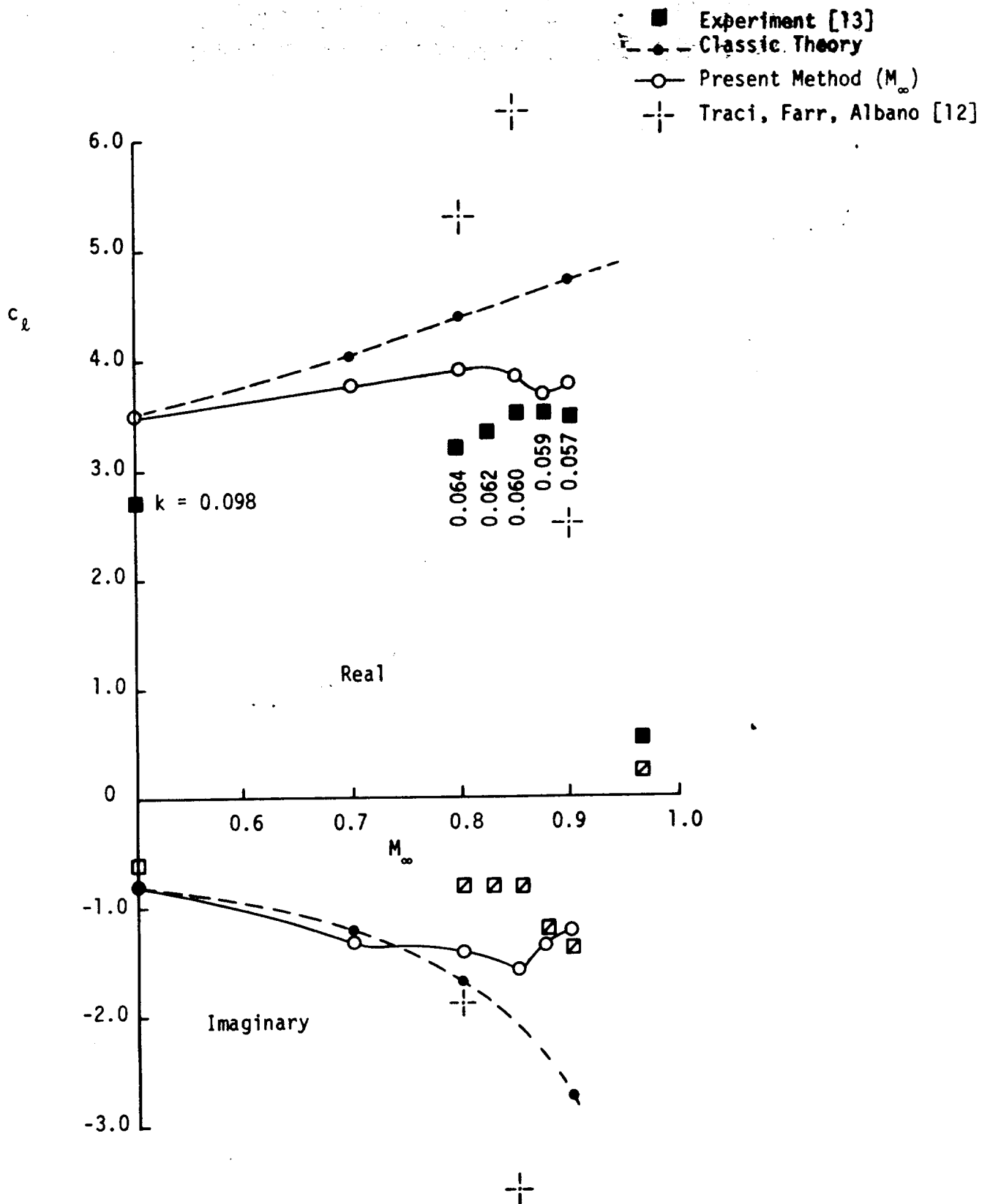


Figure 11. - Comparison of experimental and theoretical lift coefficient for an airfoil with deflected 25% chord flap.

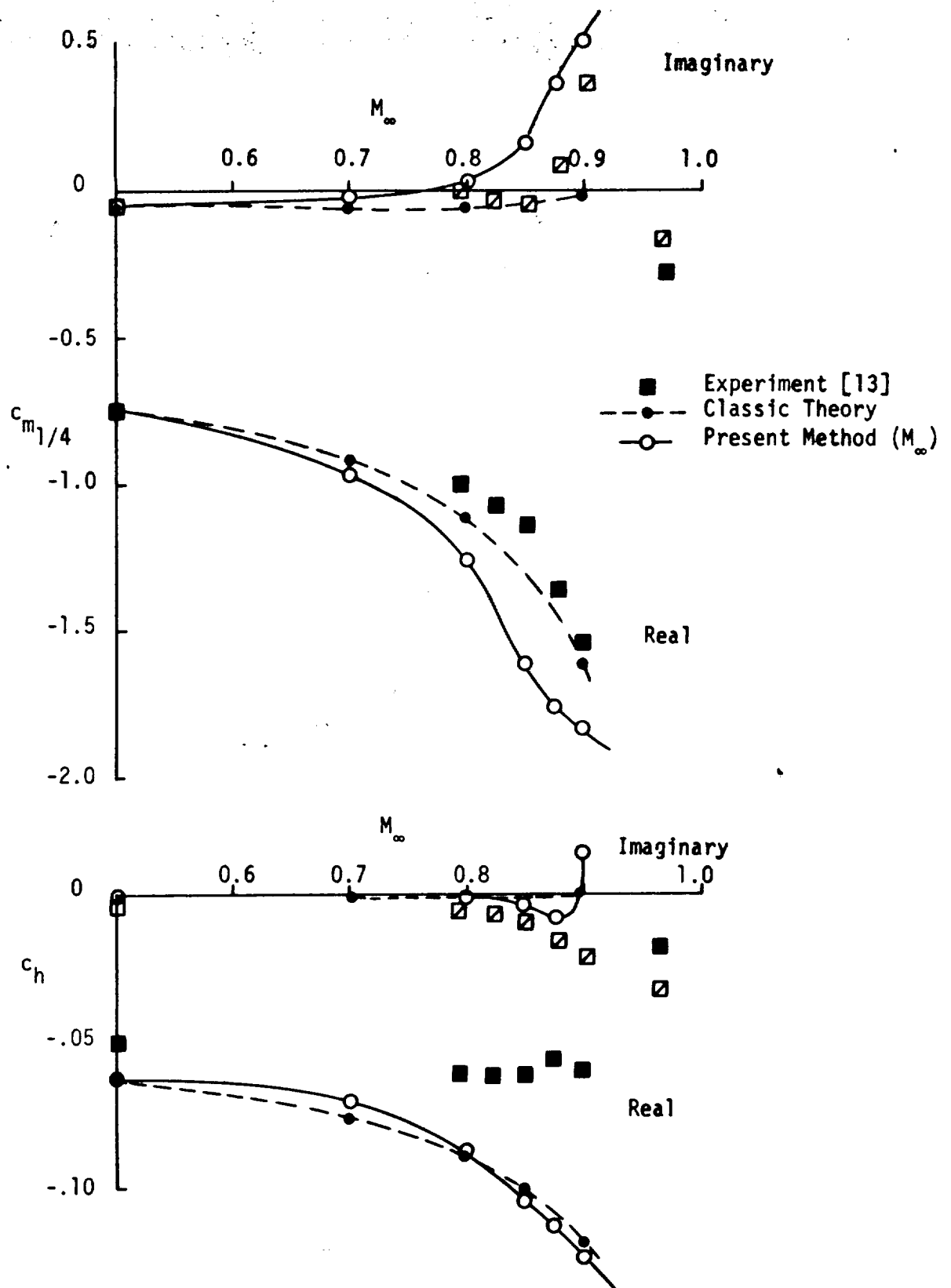


Figure 12. - Comparison of experimental and theoretical pitching moment (about $c/4$) and hinge moment (about $3c/4$) coefficient for an airfoil with an oscillating control surface.

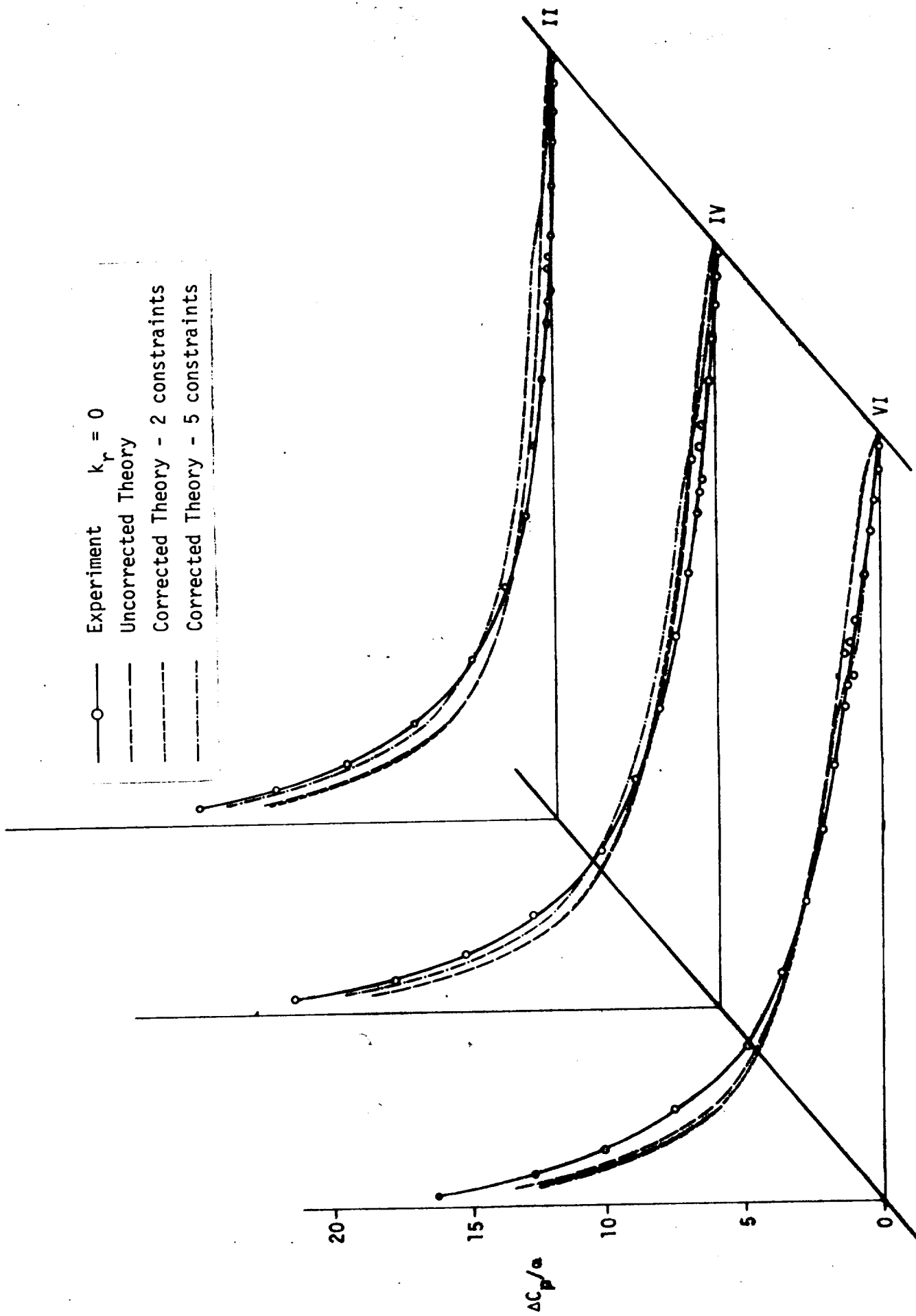
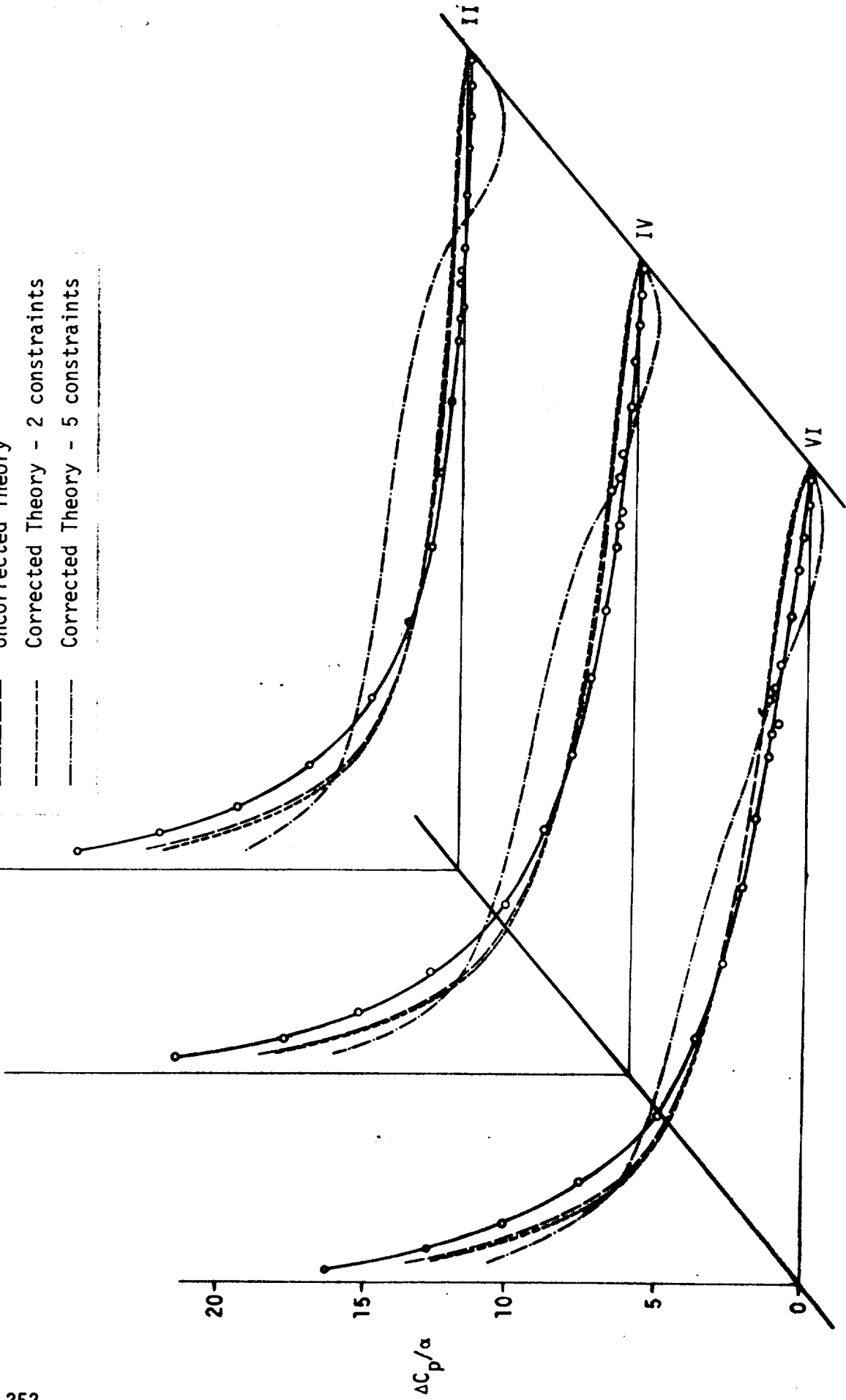


Figure 13. - Experimental, Theoretical and Corrected Pressure Loadings for Angle of Attack Using Pre-multiplying Correction Factors



- Experiment $k_r = 0$
- Uncorrected Theory
- Corrected Theory - 2 constraints
- Corrected Theory - 5 constraints

Figure 14. - Experimental, Theoretical and Corrected Pressure Loadings for Angle of Attack Using Postmultiplying Correction Factors

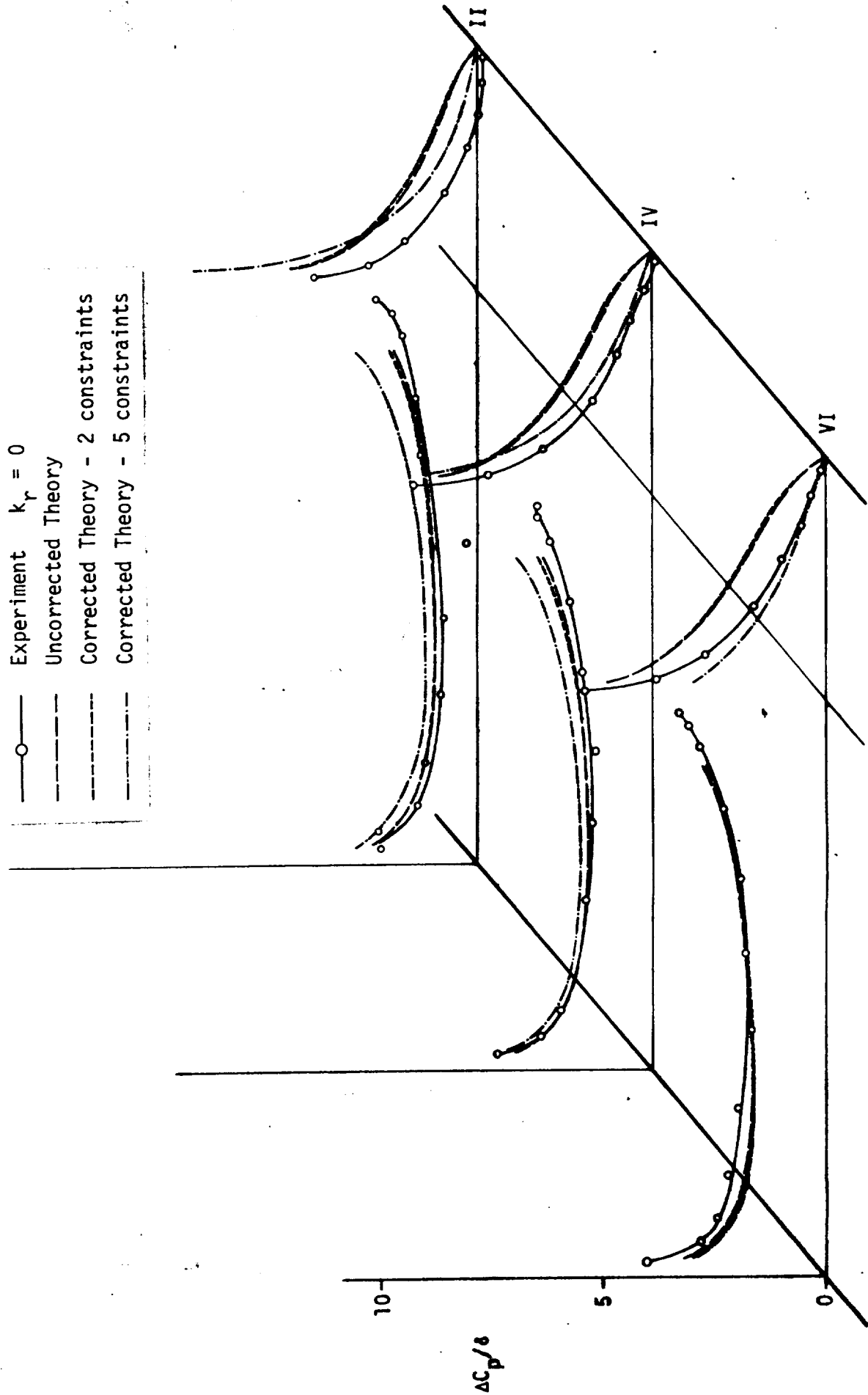


Figure 15. - Experimental, Theoretical and Corrected Pressure Loadings for Flap Rotation Using Premultiplying Correction Factors

○ Experiment $k_r = 0$
 — Uncorrected Theory
 - - - Corrected Theory - 2 constraints
 - - - Corrected Theory - 5 constraints

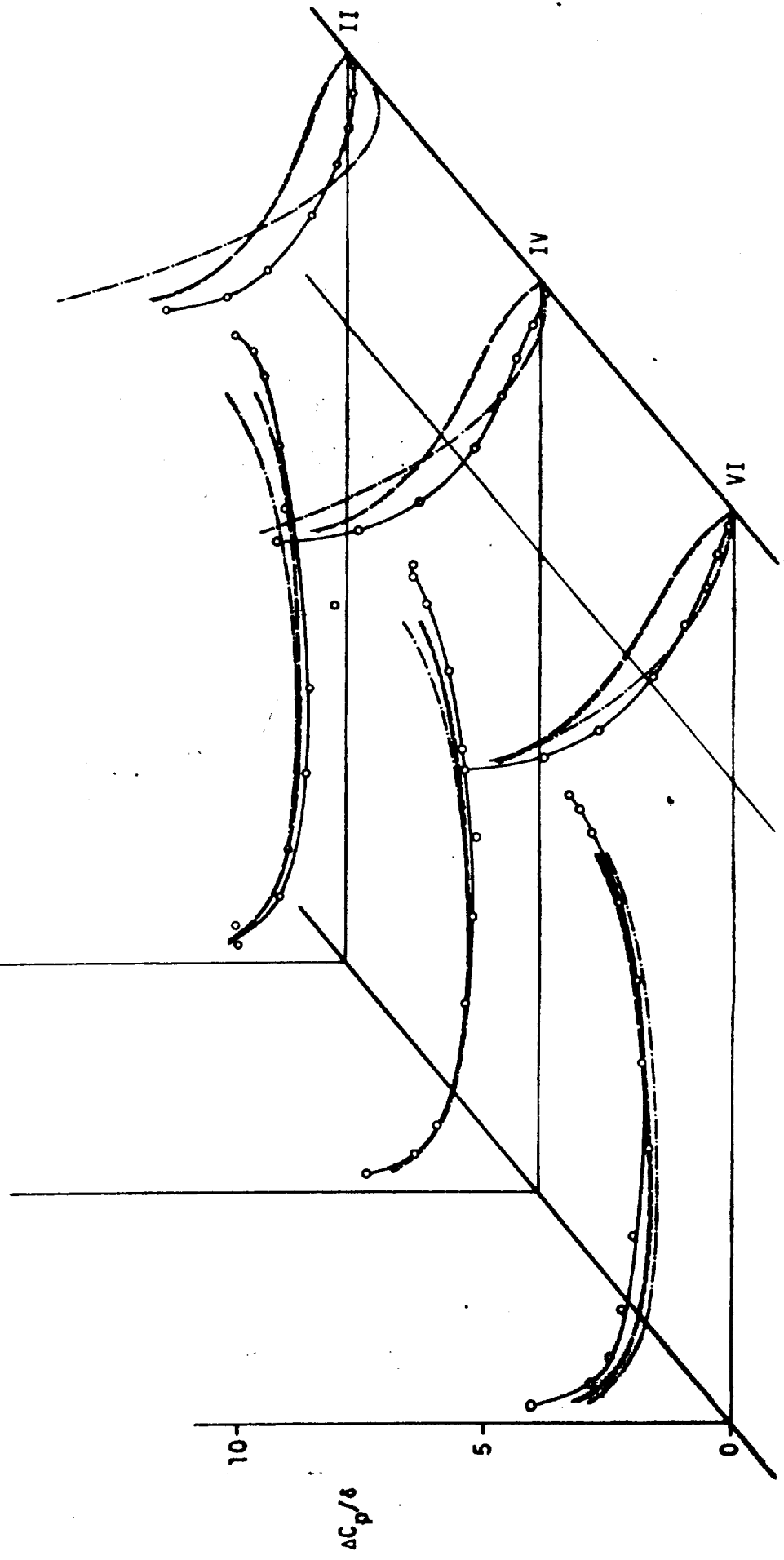


Figure 16. - Experimental, Theoretical and Corrected Pressure Loadings for Flap Rotation Using Postmultiplying Correction Factors

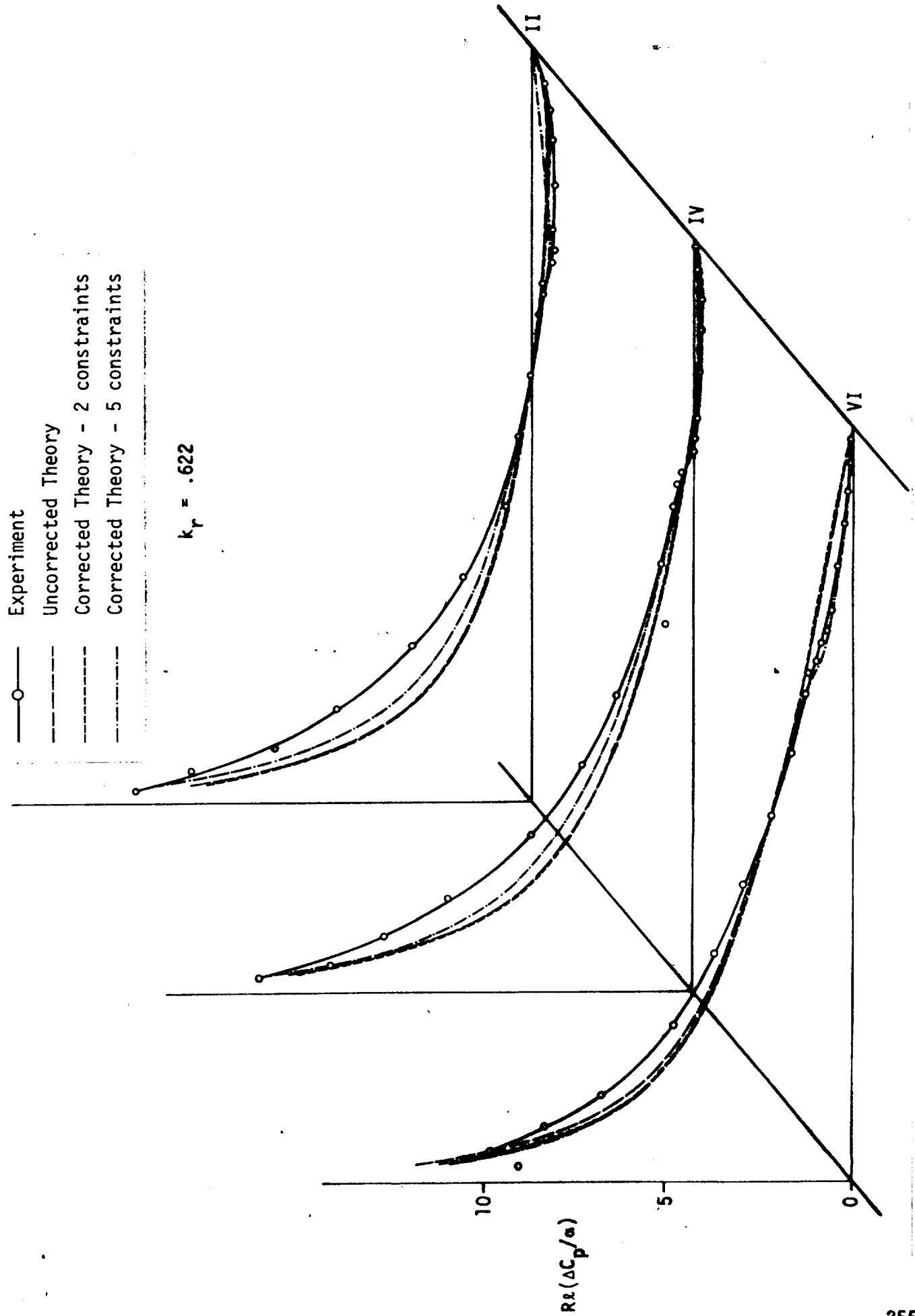


Figure 17. - Real Part of Experimental, Theoretical and Corrected Pressure Loadings for Angle of Attack Using Premultiplying Correction Factors

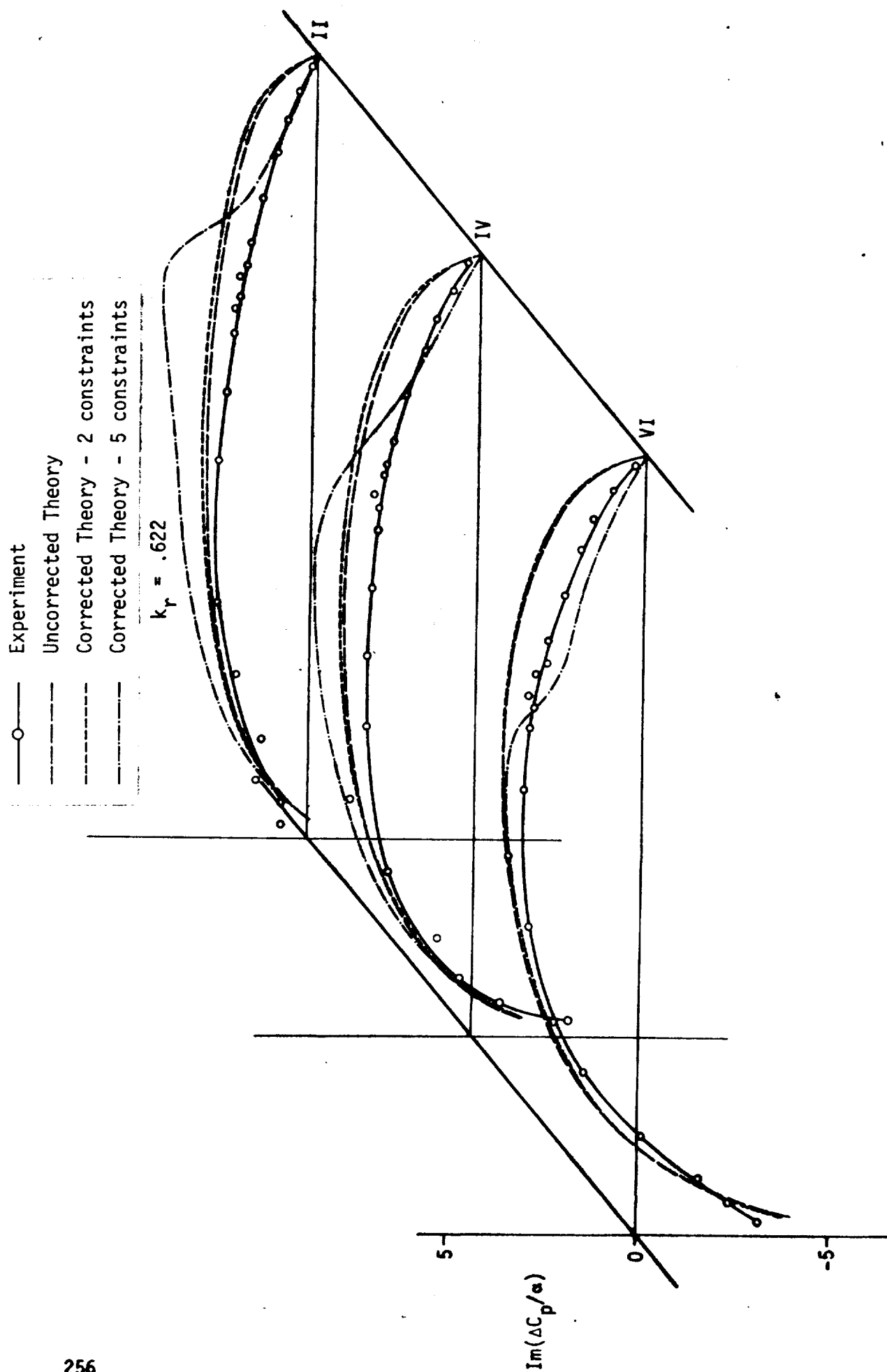


Figure 18. - Imaginary Part of Experimental, Theoretical and Corrected Pressure Loadings for Angle of Attack Using Premultiplying Correction Factors

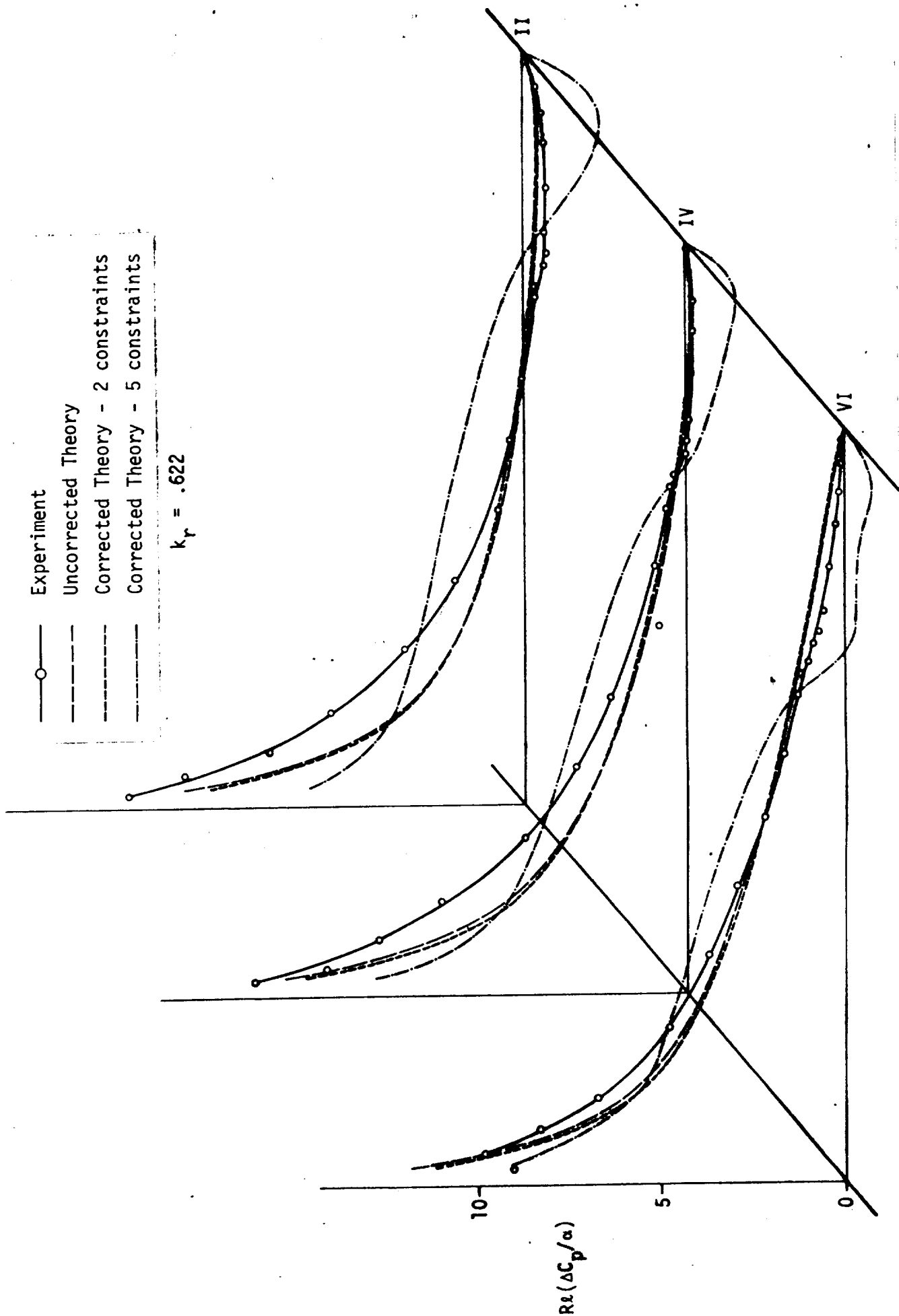


Figure 19. - Real Part of Experimental, Theoretical and Corrected Pressure Loadings for Angle of Attack Using Postmultiplying Correction Factors

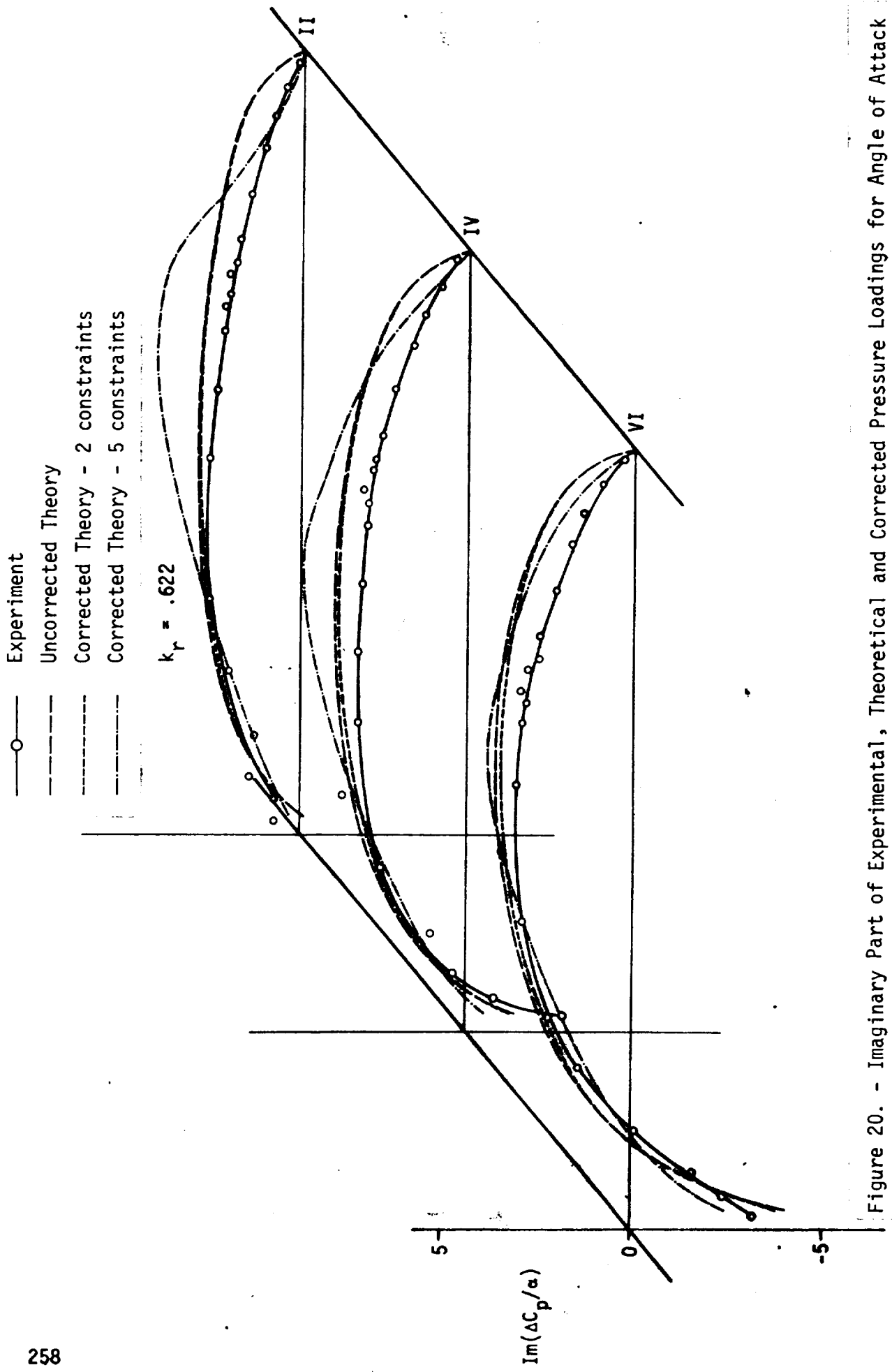


Figure 20. - Imaginary Part of Experimental, Theoretical and Corrected Pressure Loadings for Angle of Attack Using Postmultiplying Correction Factors

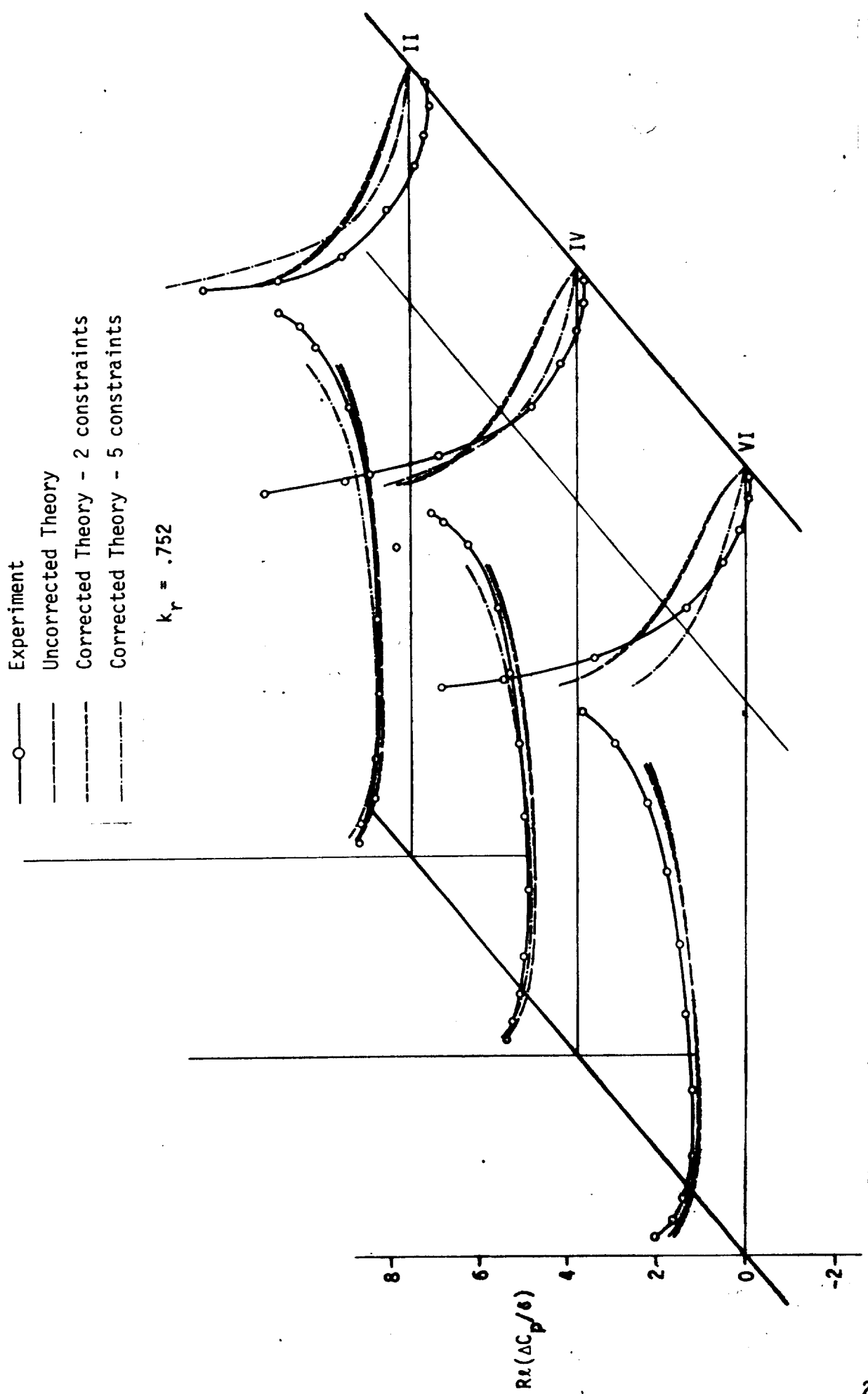


Figure 21. - Real Part of Experimental, Theoretical and Corrected Pressure Loadings for Flap Rotation Using Premultiplying Correction Factors

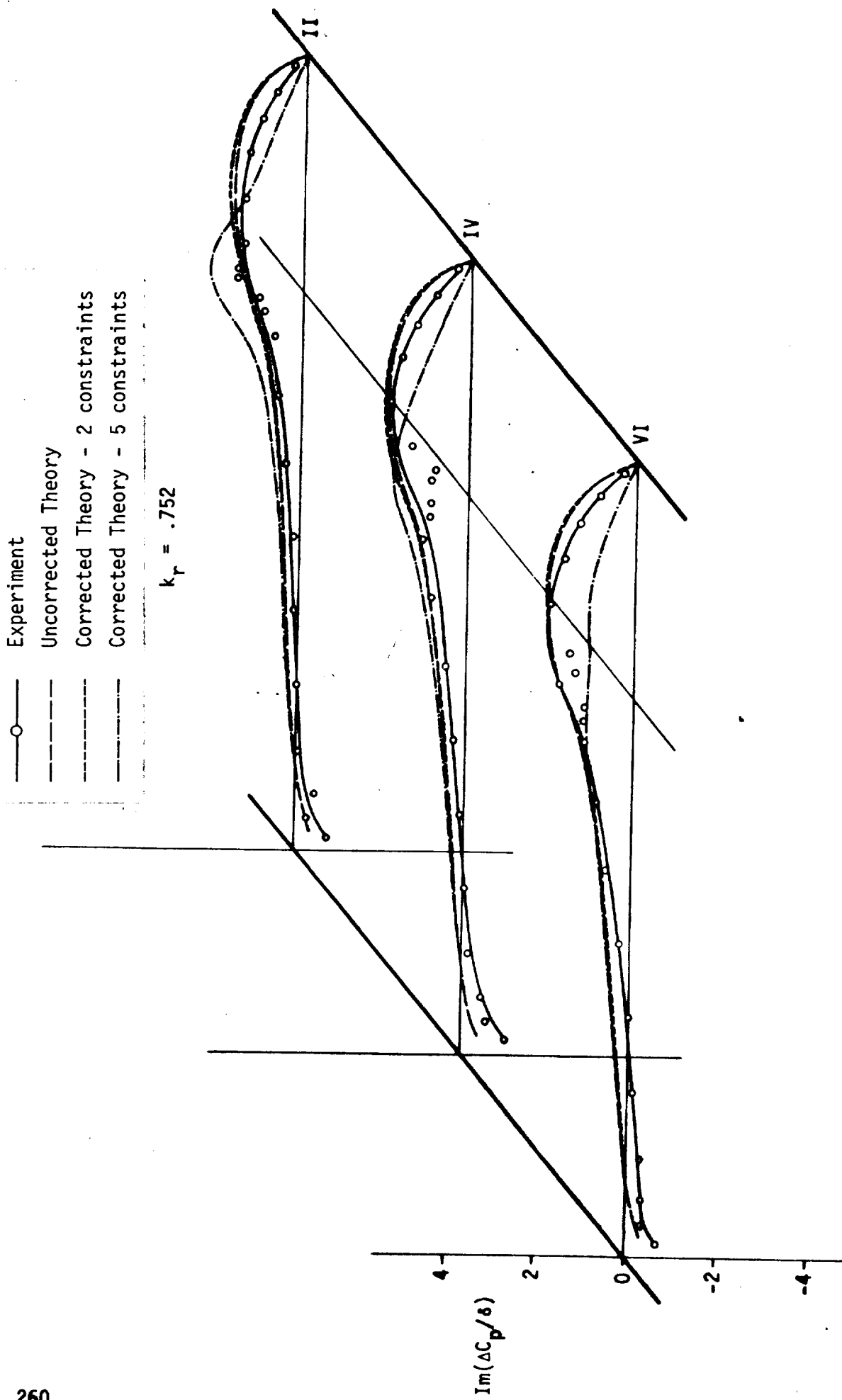


Figure 22. - Imaginary Part of Experimental, Theoretical and Corrected Pressure Loadings for Flap Rotation Using Premultiplying Correction Factors

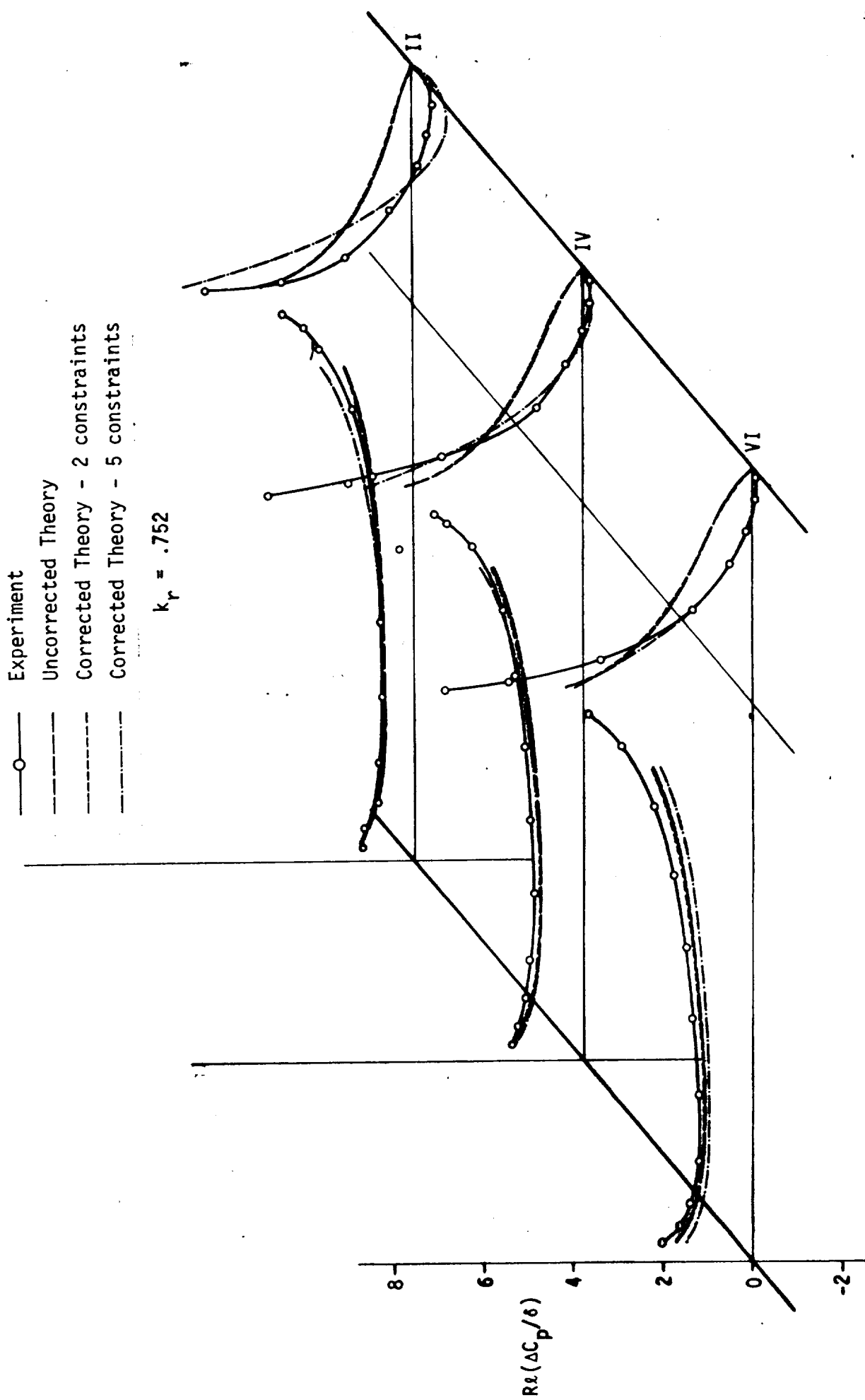


Figure 23. - Real Part of Experimental, Theoretical and Corrected Pressure Loadings for Flap Rotation Using Postmultiplying Correction Factors

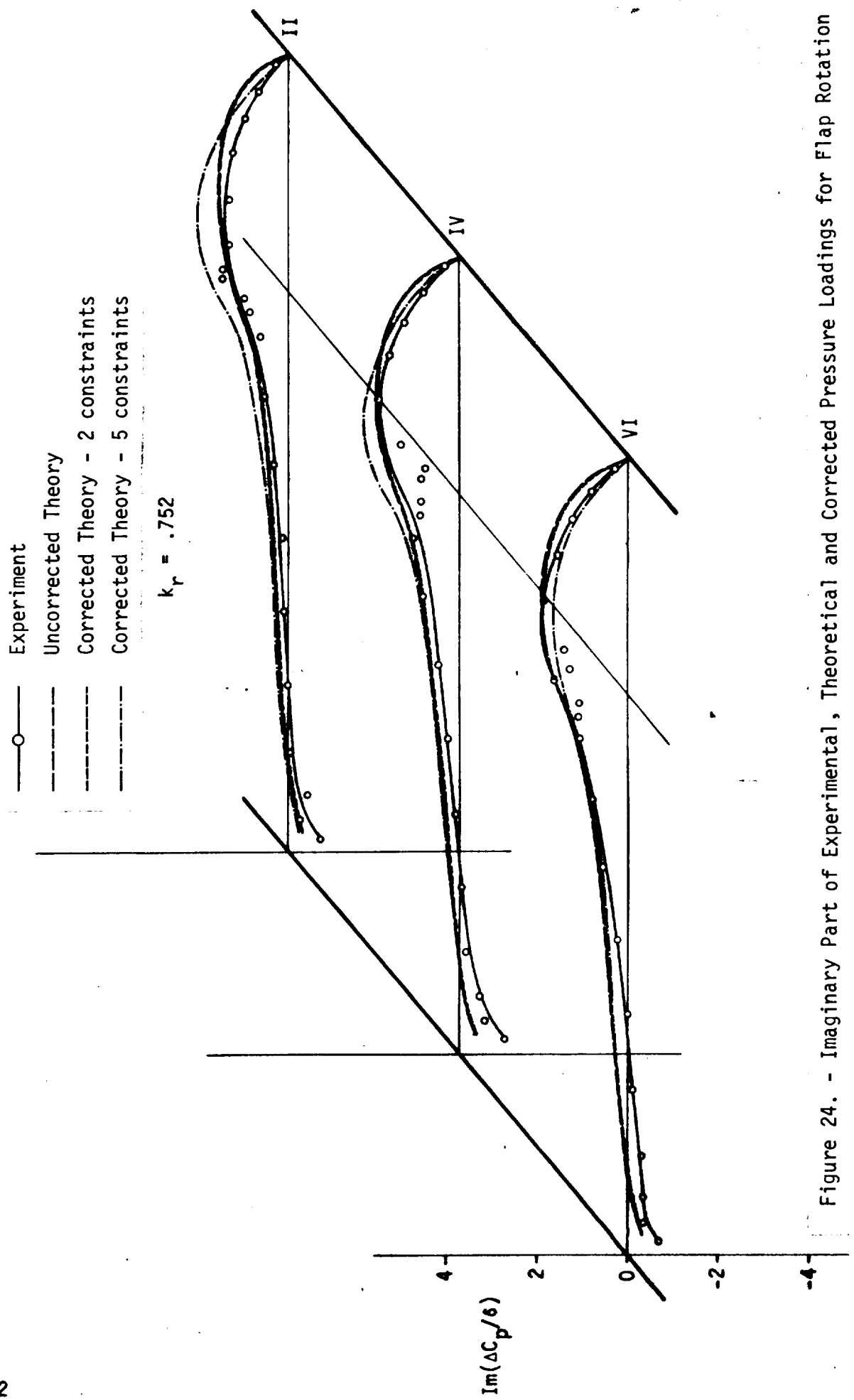


Figure 24. - Imaginary Part of Experimental, Theoretical and Corrected Pressure Loadings for Flap Rotation Using Postmultiplying Correction Factors

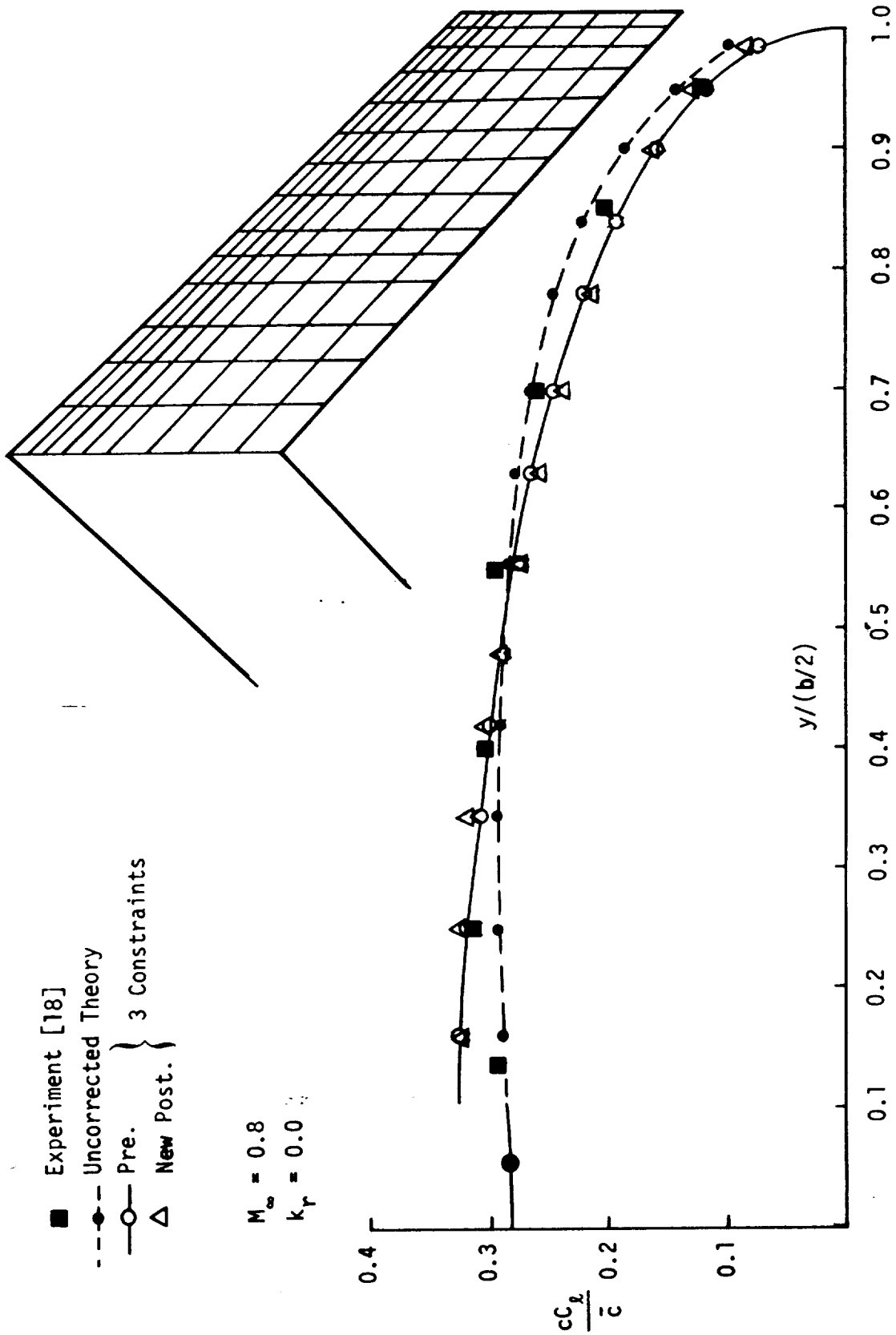


Figure 25. - Comparison of experimental data with corrected and uncorrected theory for a swept wing operating at subsonic speeds and $\alpha = 4^\circ$.

■ Experiment [18]
 -●- Uncorrected Theory
 -○- Corrected Theory (Pre., 3 constraints)

$M_\infty = 0.8$
 $k_r = 0.0$

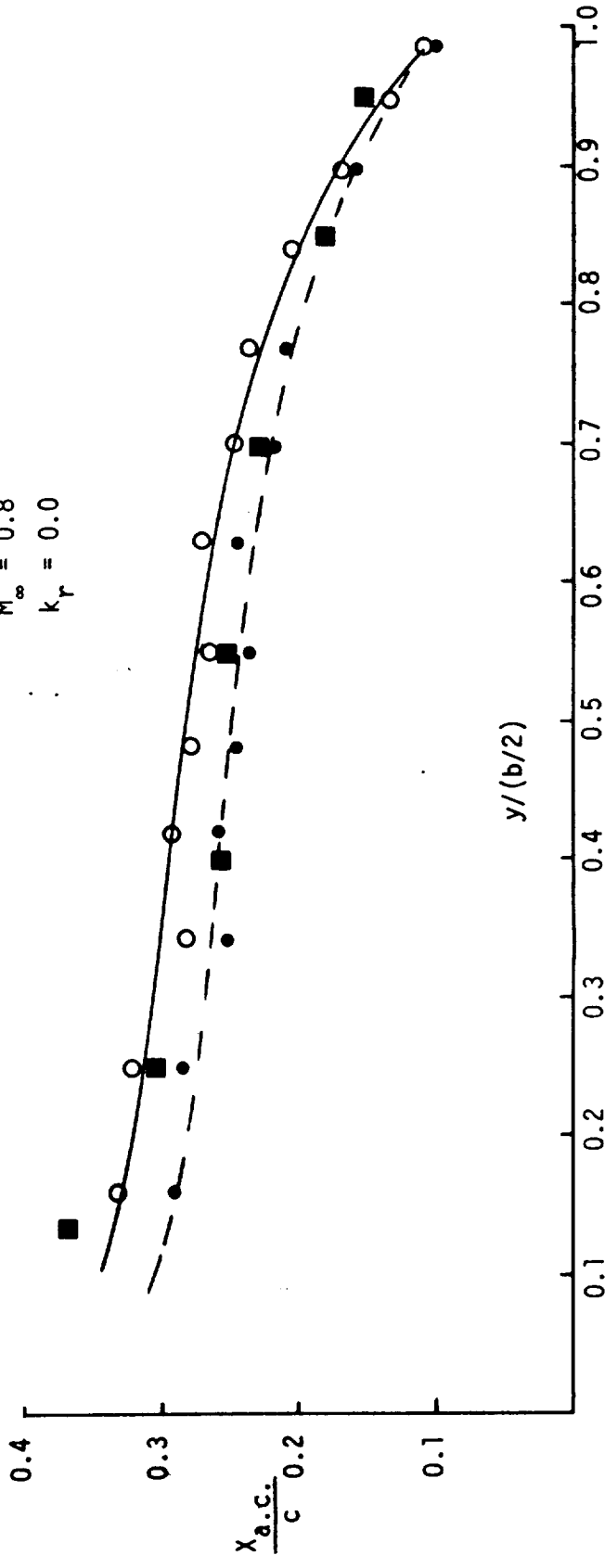


Figure 26. - Comparison of experimental data with corrected and uncorrected theory for a swept wing operating at subsonic speeds at $\alpha = 4^\circ$.

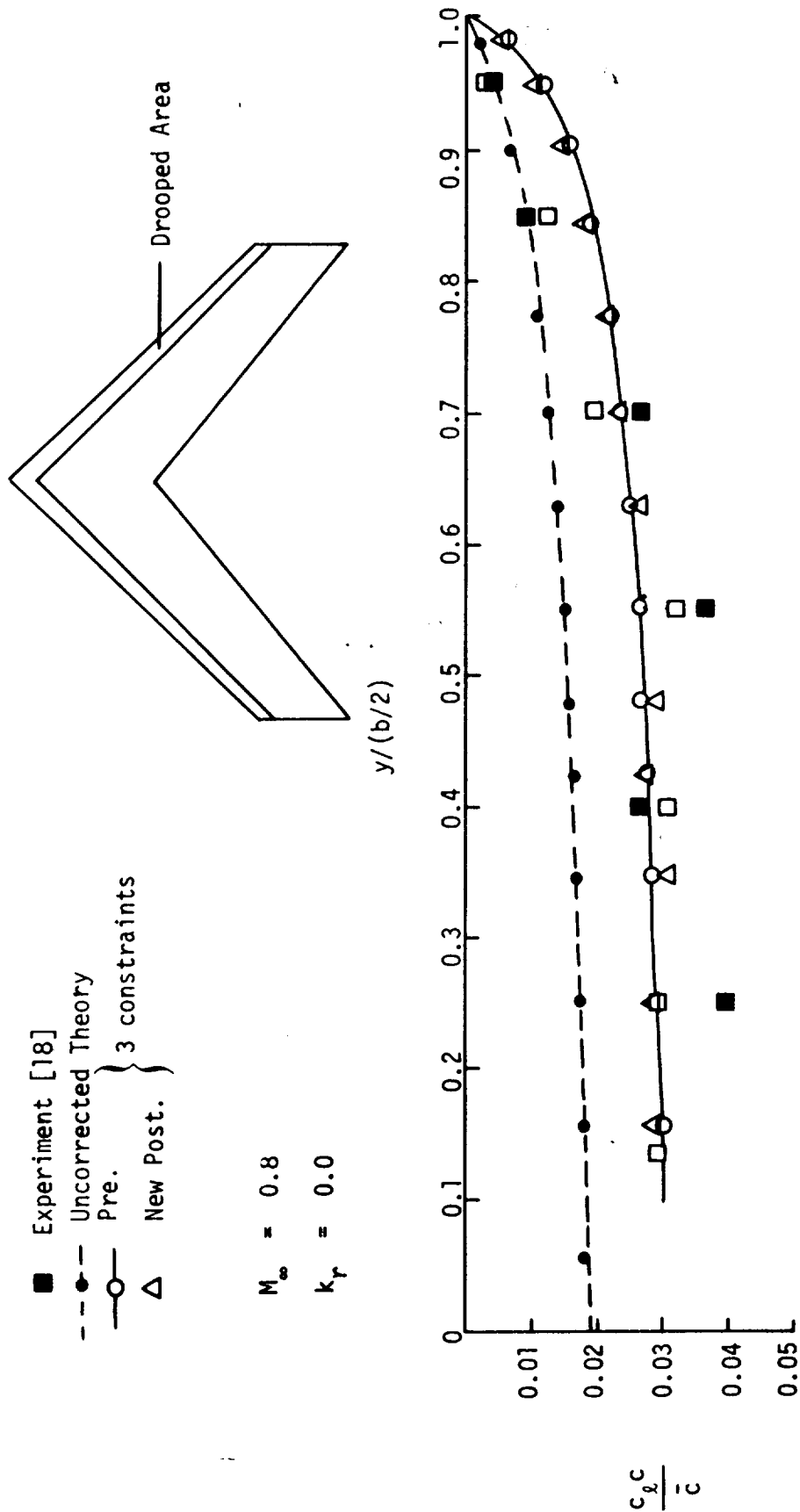


Figure 27. - Comparison of experimental data with corrected and uncorrected theory for a swept wing operating at subsonic speeds with a leading edge droop of 6° .

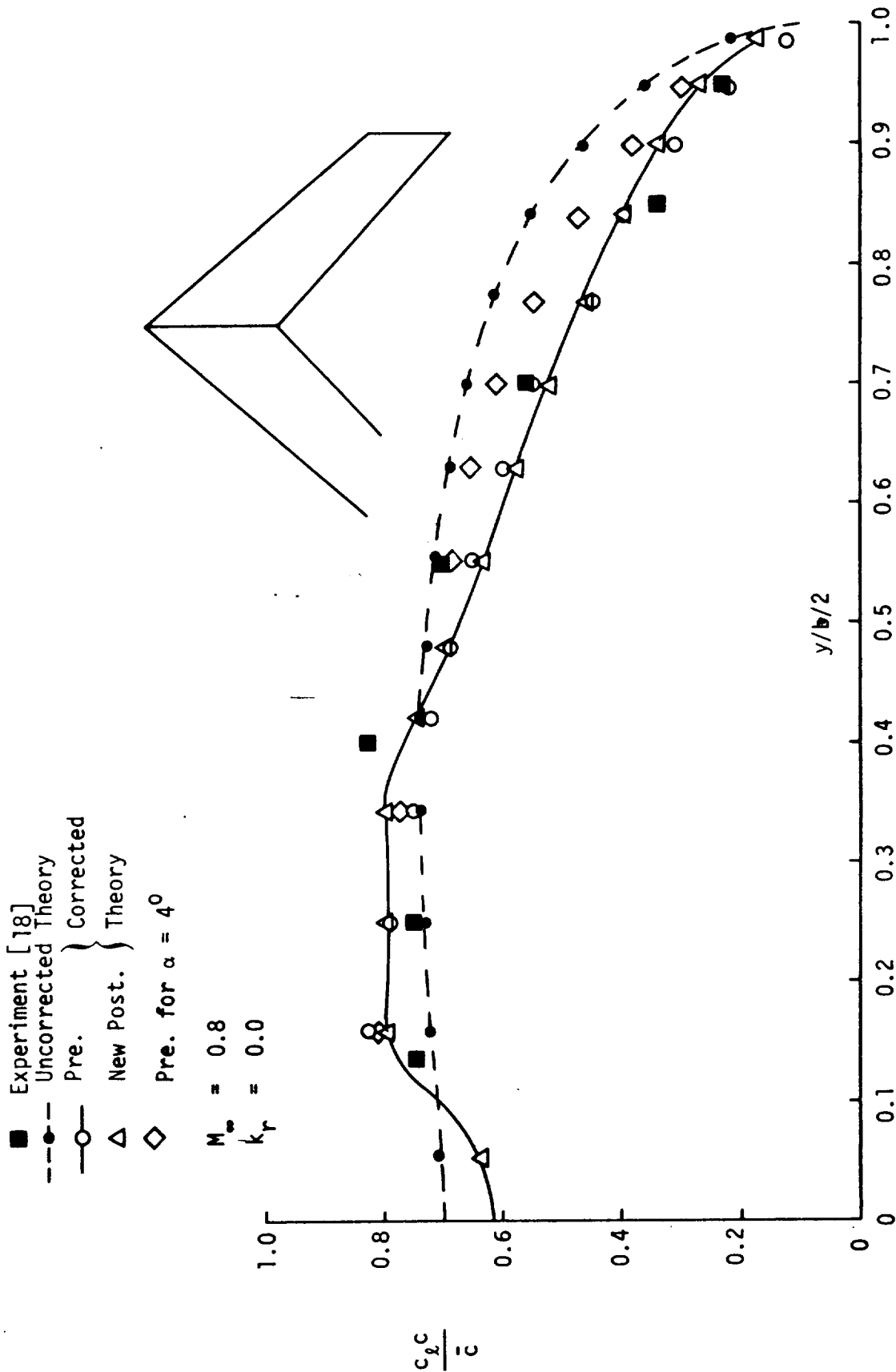


Figure 28. - Comparison of experimental data with corrected and uncorrected theory for a swept wing operating at subsonic speeds at $\alpha = 10^\circ$.

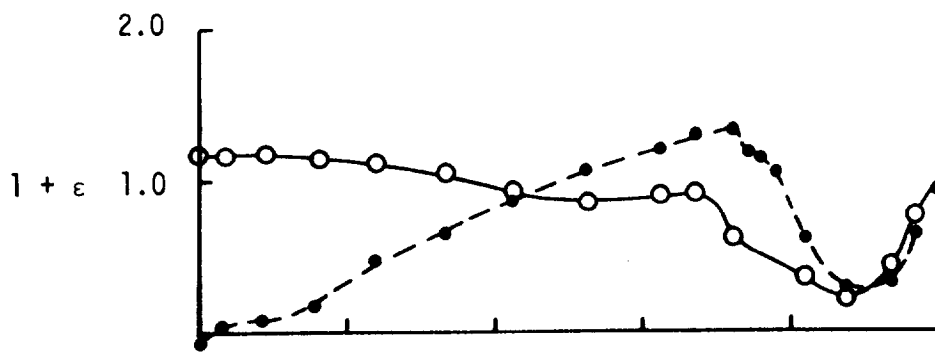
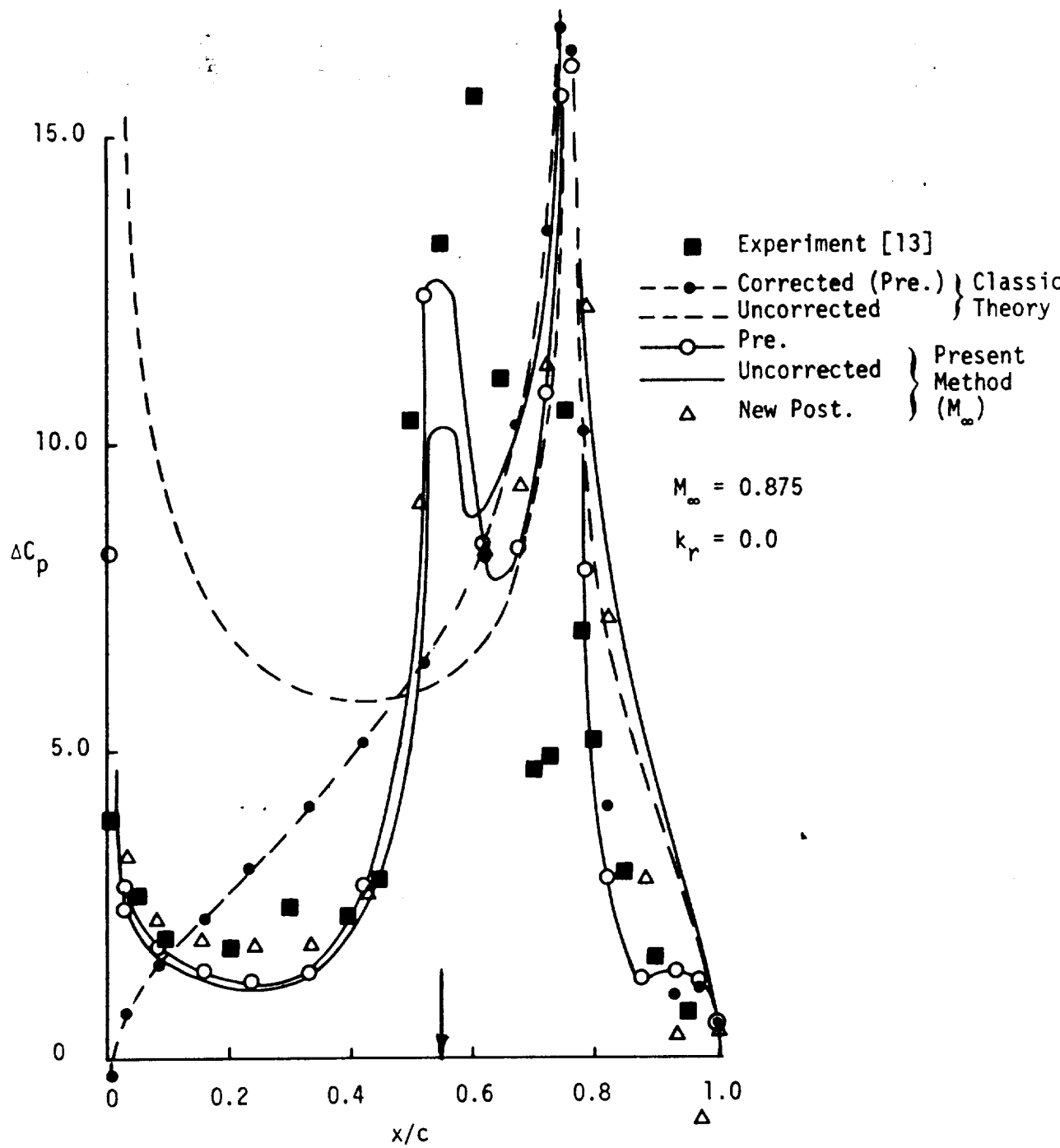


Figure 29. - Comparison of corrected and uncorrected classic theory and Present Method (M_∞) with experimental data.

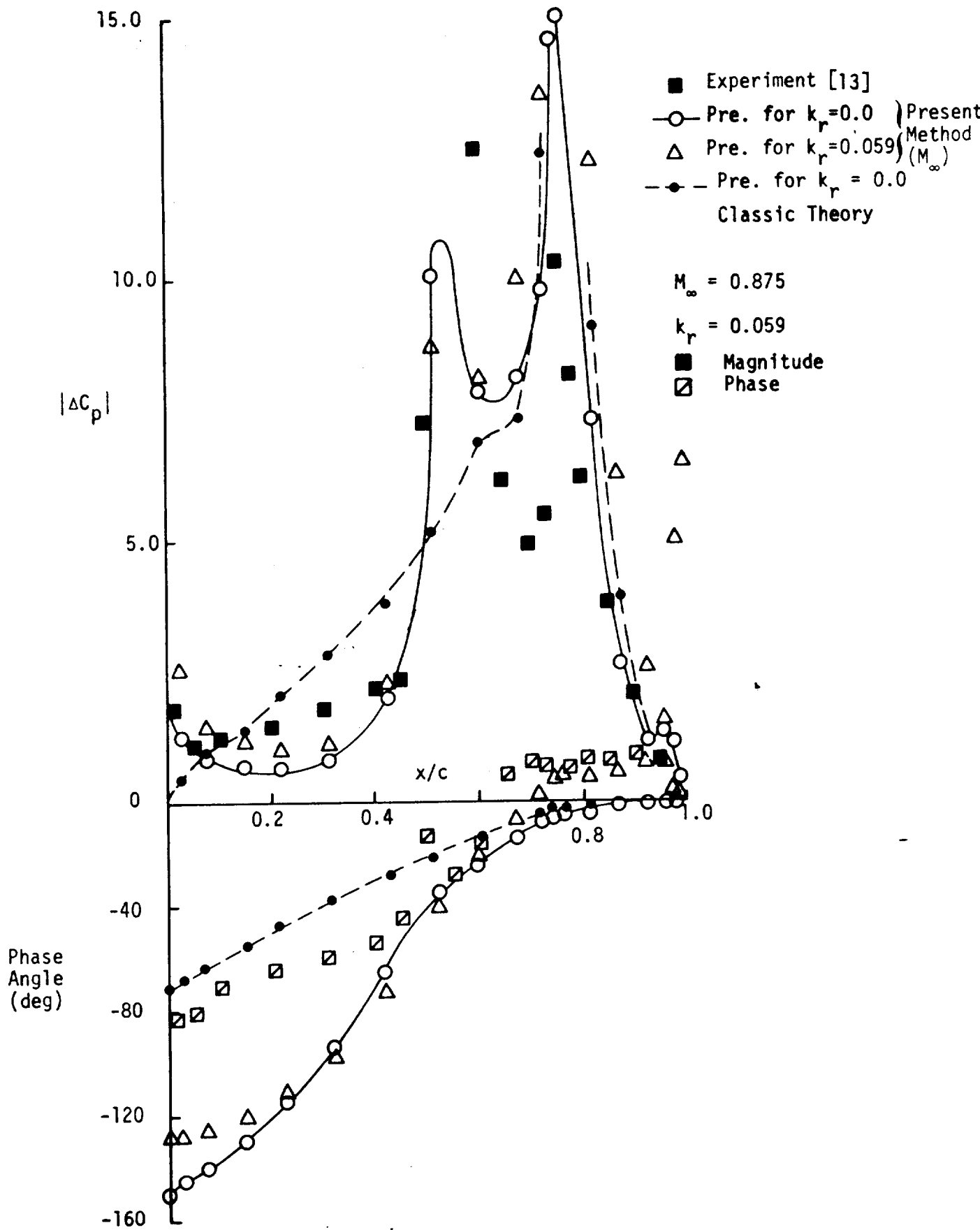


Figure 30. - Comparison of experimental data with corrected theory; the corrections being based on static and oscillatory data.

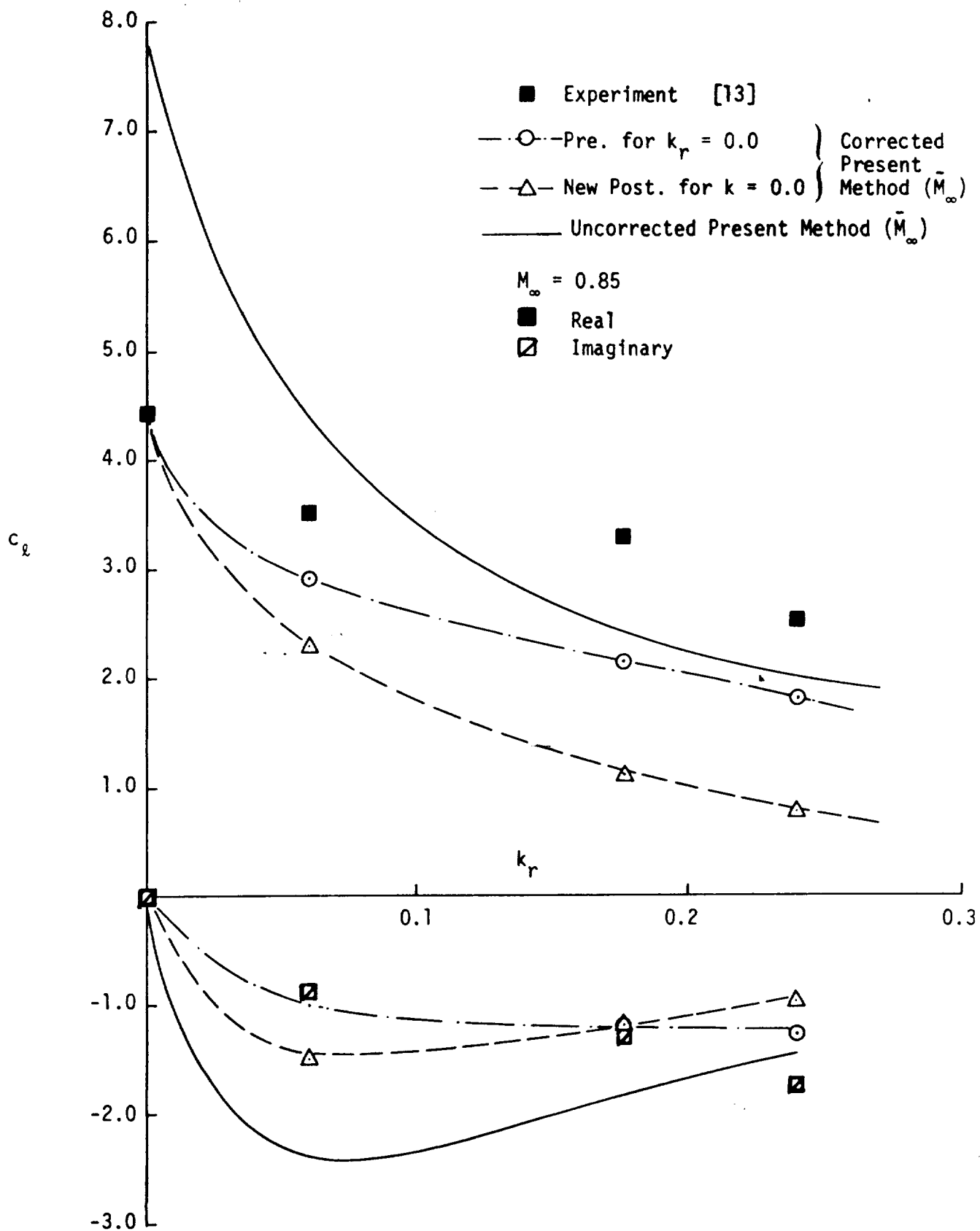


Figure 31. - Effect of applying static correction factors to the Present Method (\bar{M}_∞) for the oscillatory case.

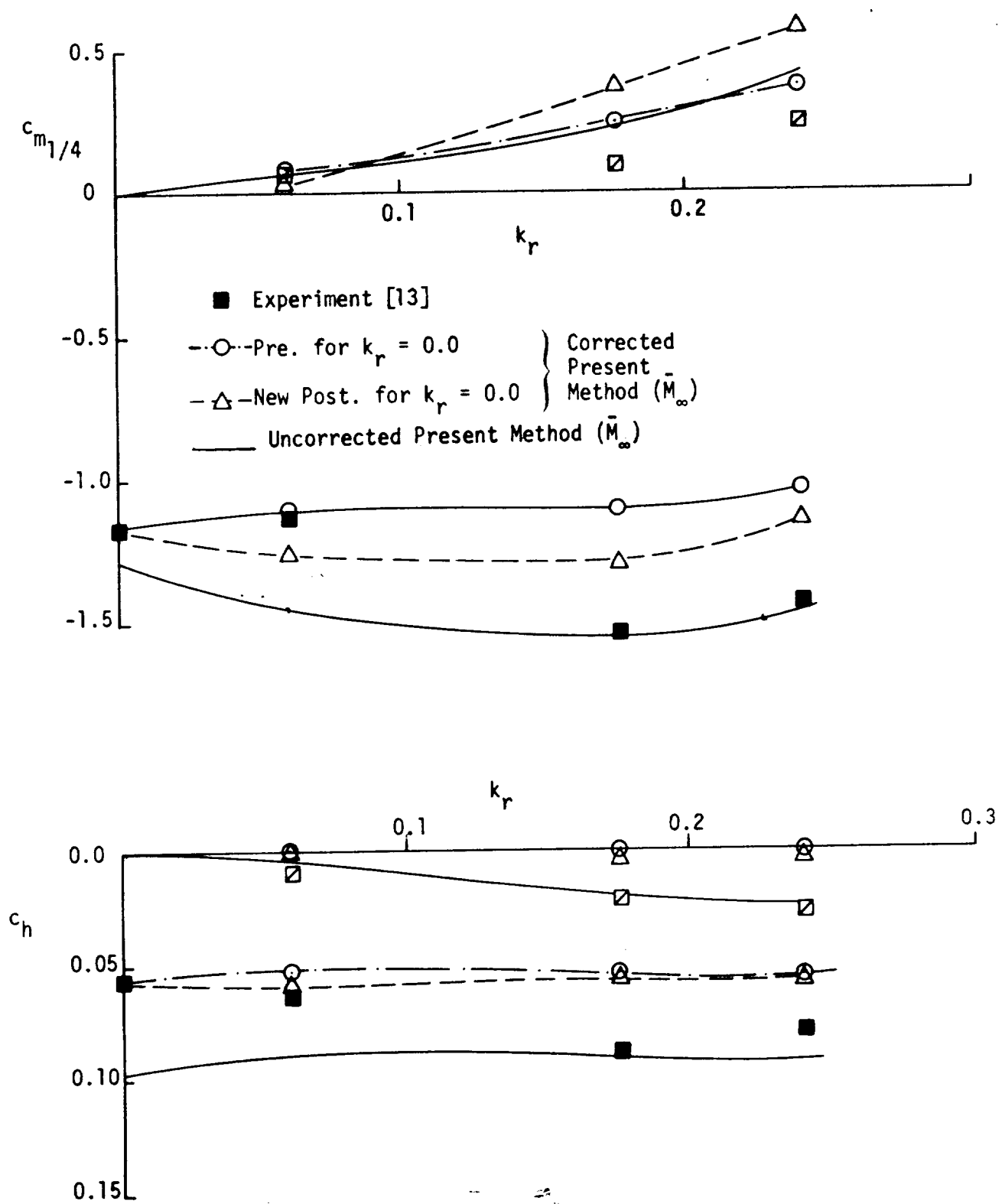


Figure 32. - Effect of applying static correction factors to the Present Method (\bar{M}_∞) for the oscillatory case.

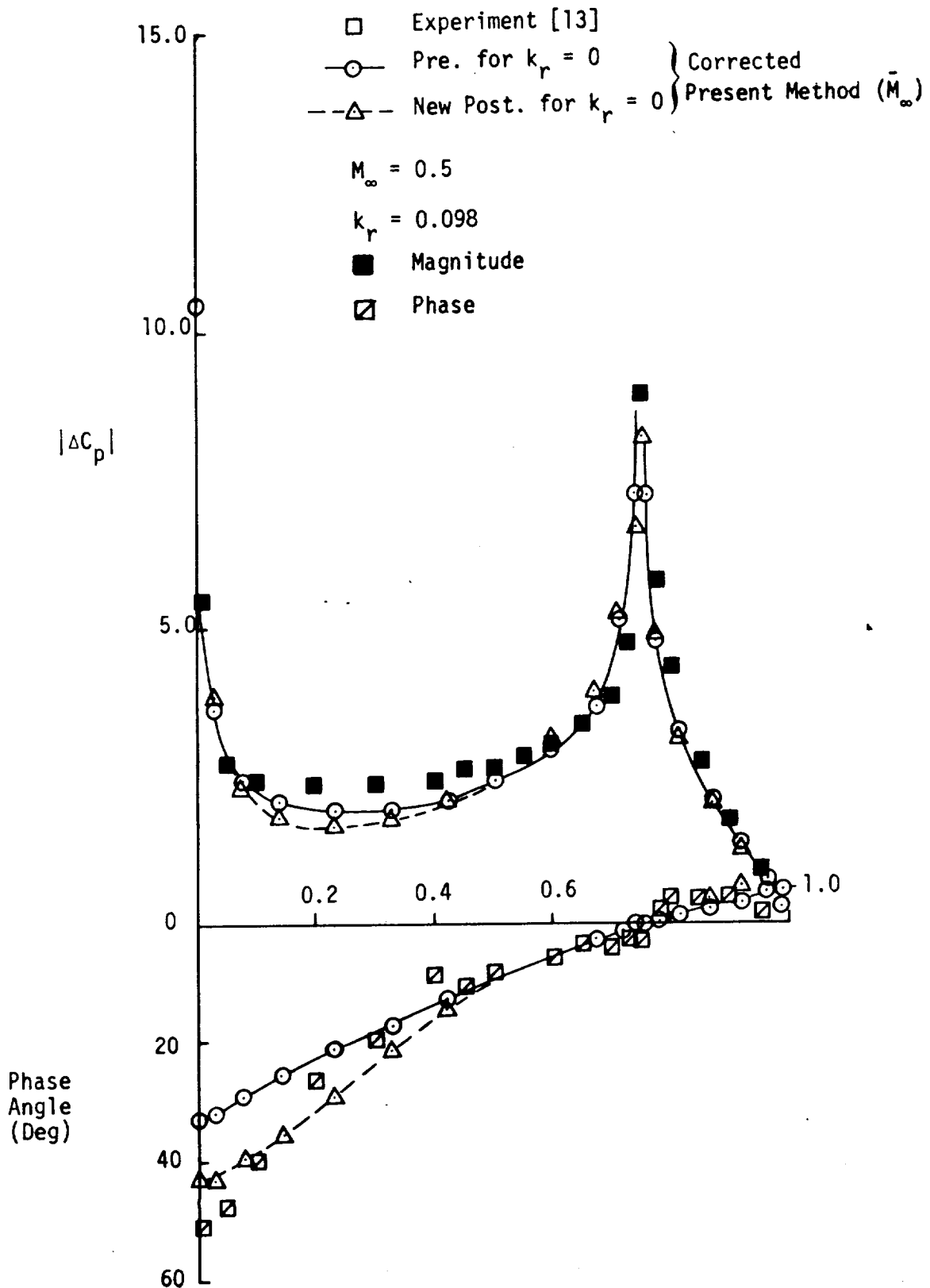


Figure 33. - Application of static correction factors to the oscillatory case.

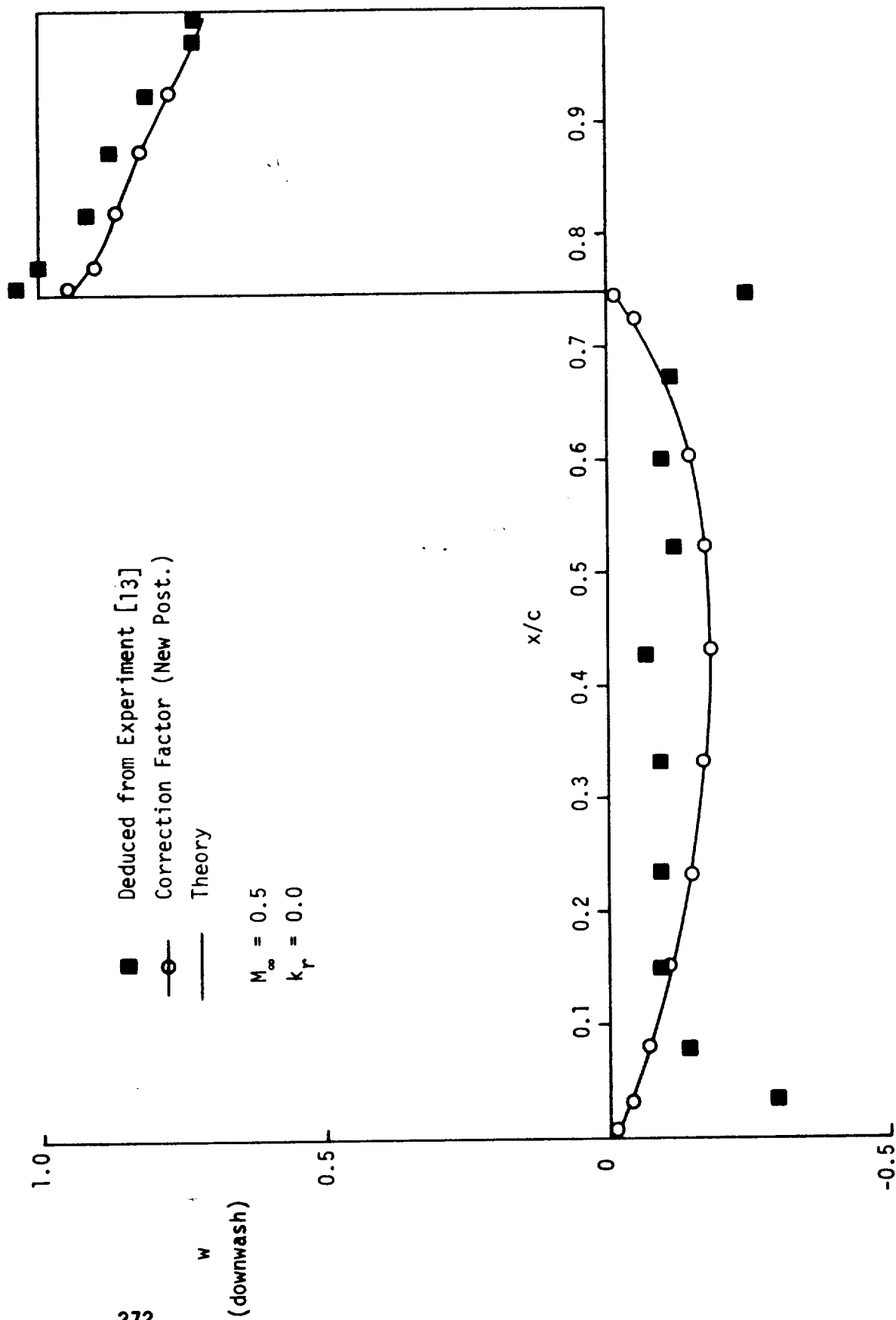


Figure 34. - Comparison of theoretical, corrected, and experimental downwash induced by a control surface deflection on a two-dimensional section.

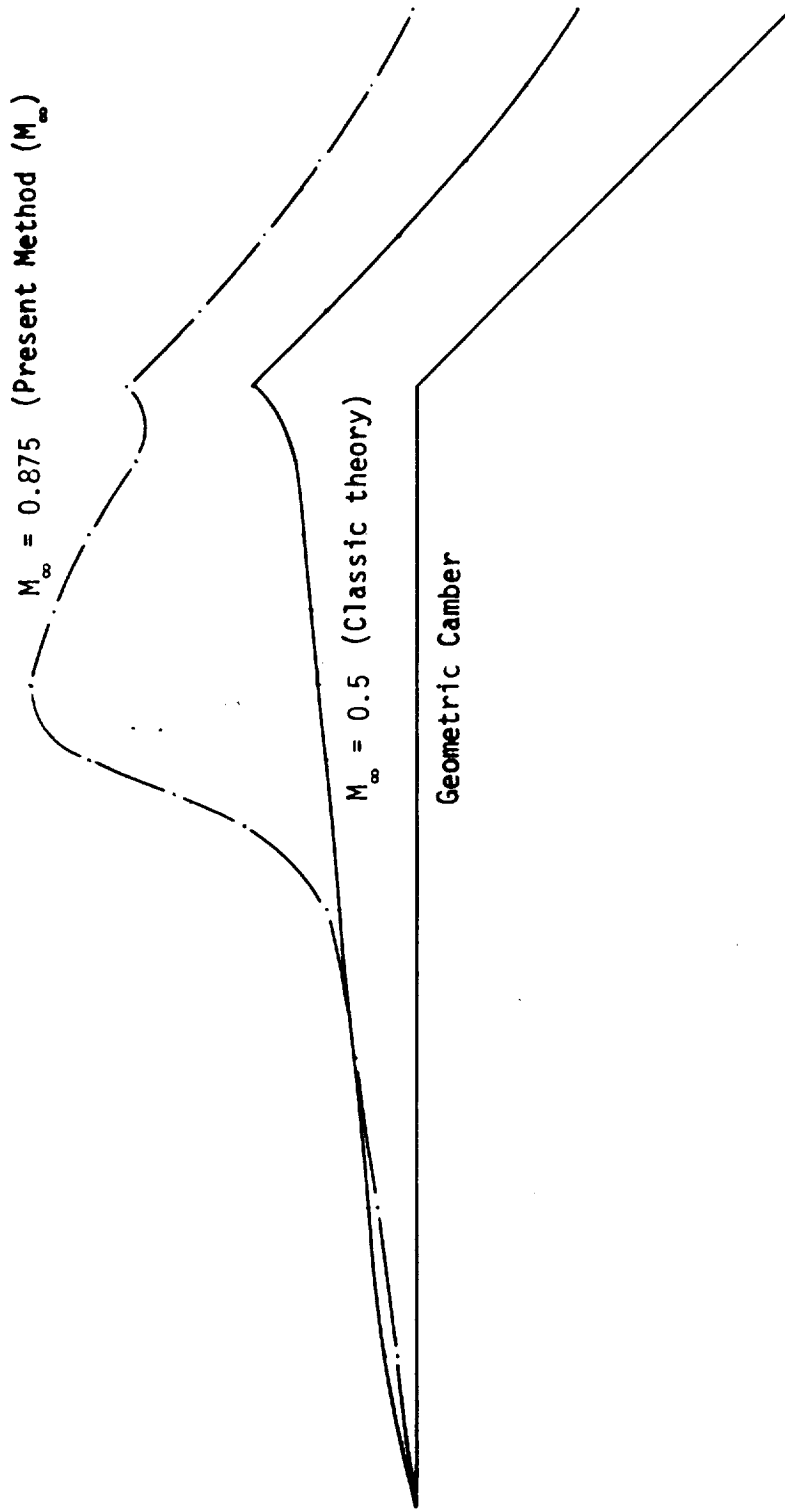


Figure 35. - Comparison of the apparent camber distribution induced at sub- and transonic Mach Numbers with the geometric camber for a control surface deflection on a two-dimensional section.

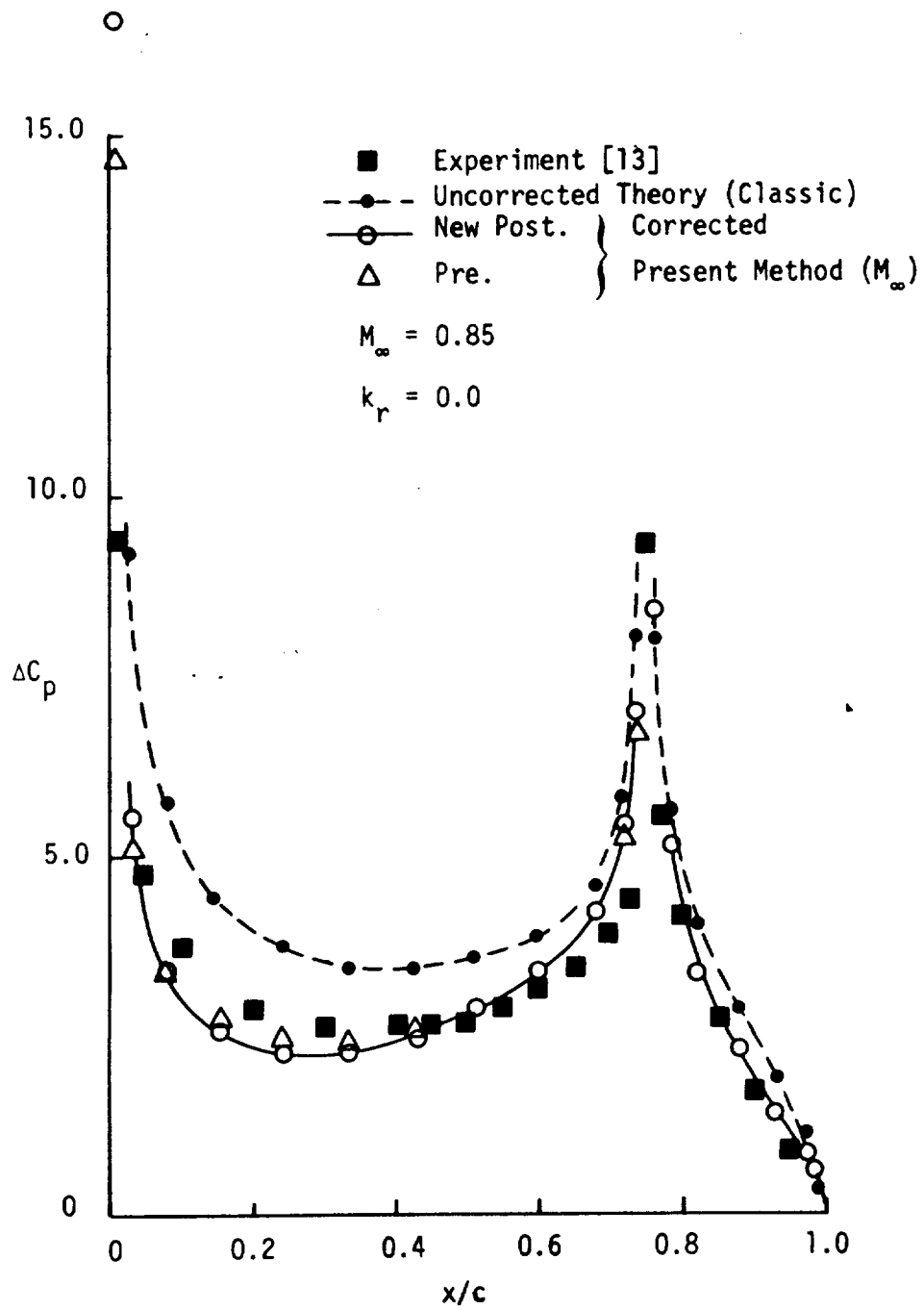


Figure 36. - Comparison of data with premultiplier and postmultiplier (New) corrected theory.

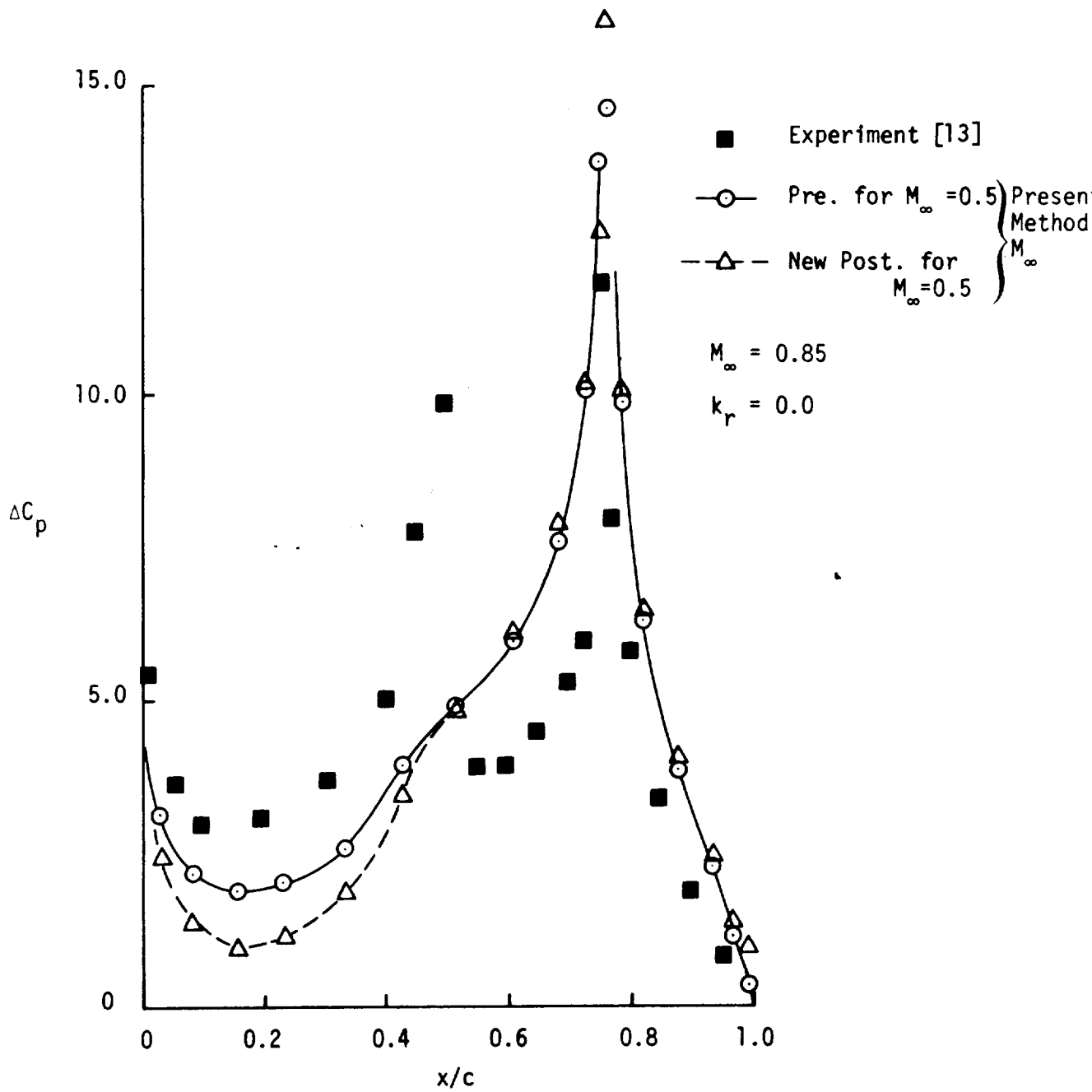


Figure 37. - Application of correction factors obtained at subsonic Mach Number ($M_\infty = 0.5$) to the transonic case ($M_\infty = 0.85$).

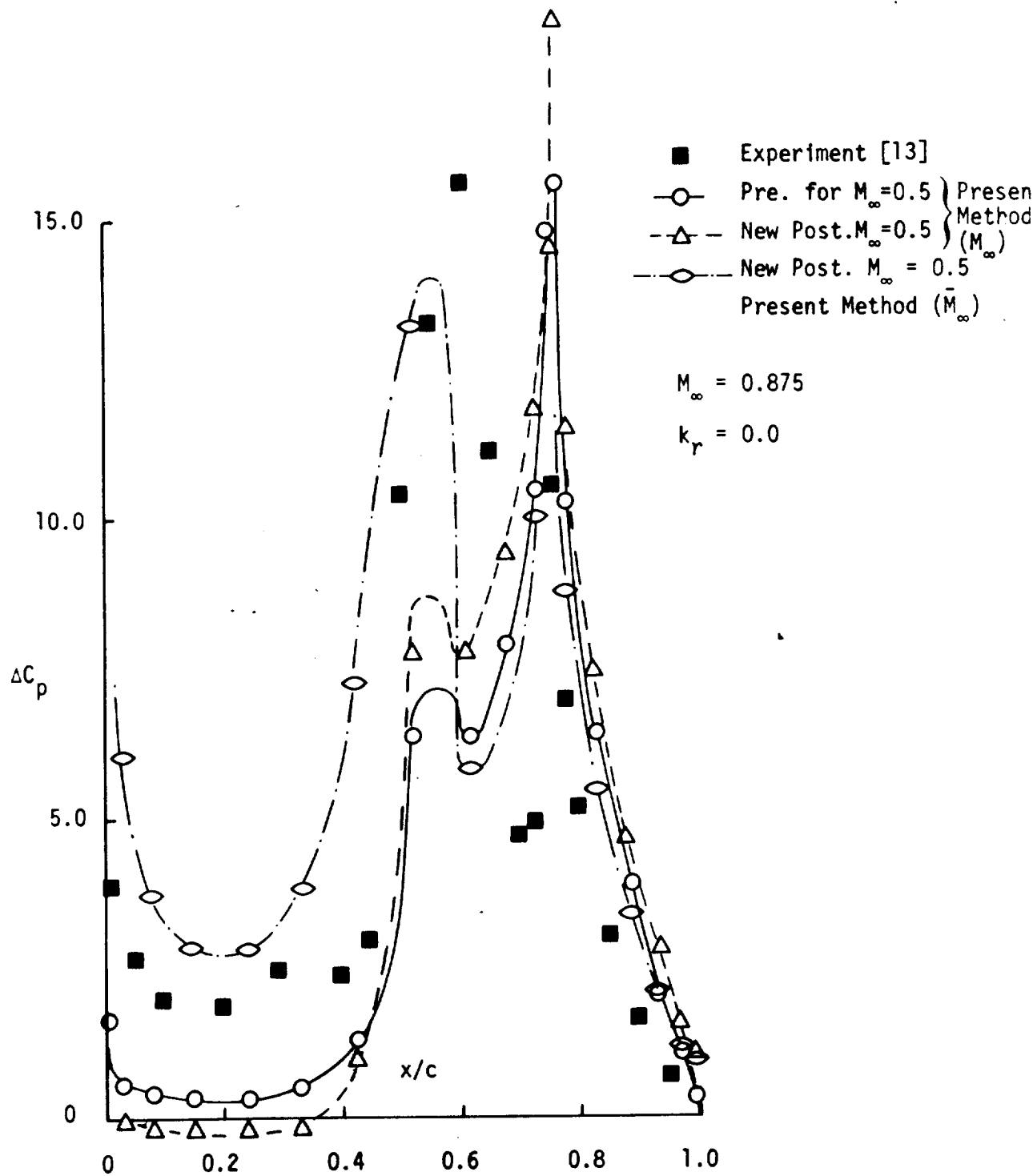


Figure 38. - Application of correction factors obtained at a subsonic Mach Number ($M_\infty = 0.5$) to theory for the transonic case ($M_\infty = 0.875$).

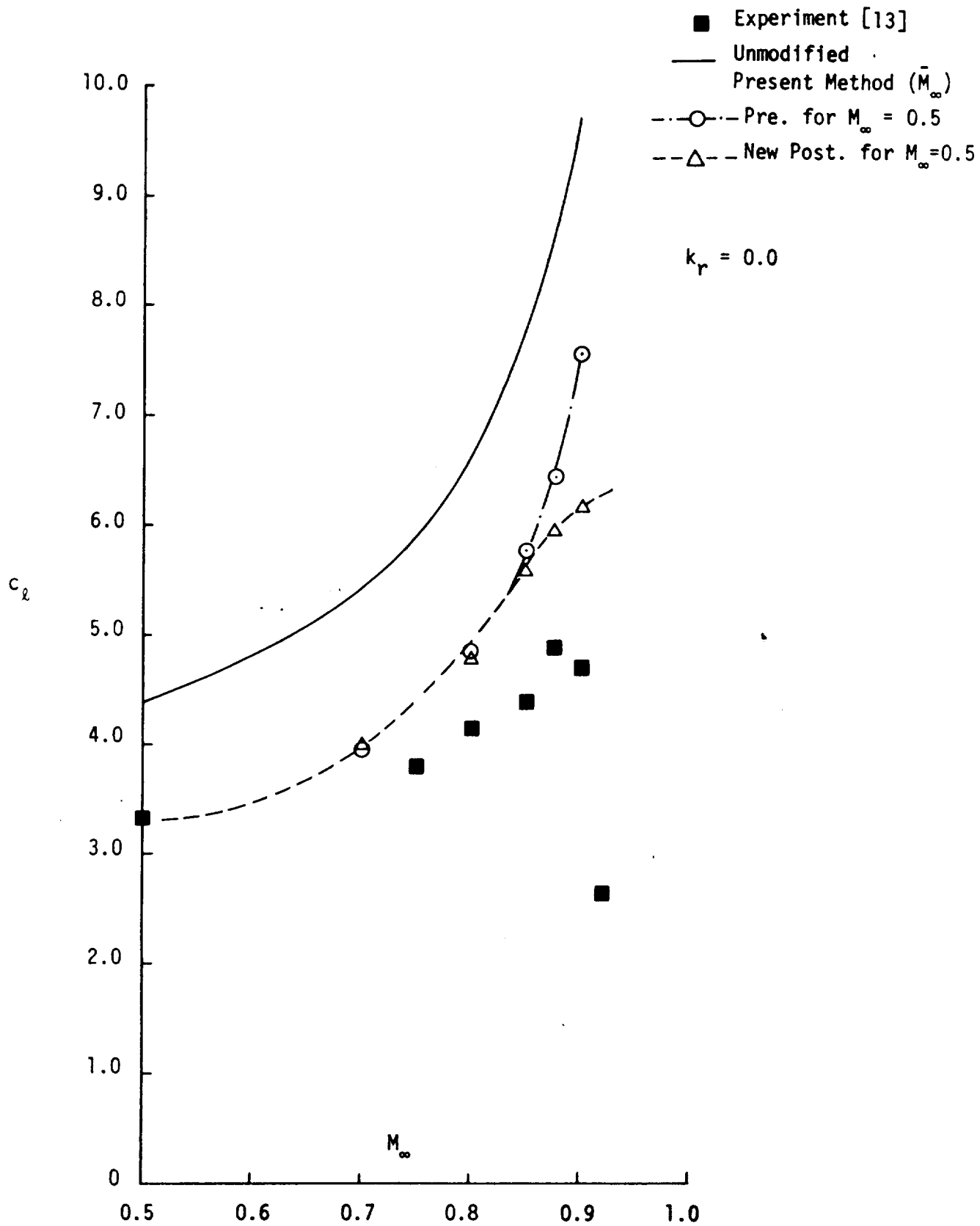


Figure 39. - Effect of applying correction factors obtained at $M_\infty = 0.5$ to other Mach Numbers for the Present Method (\bar{M}_∞).

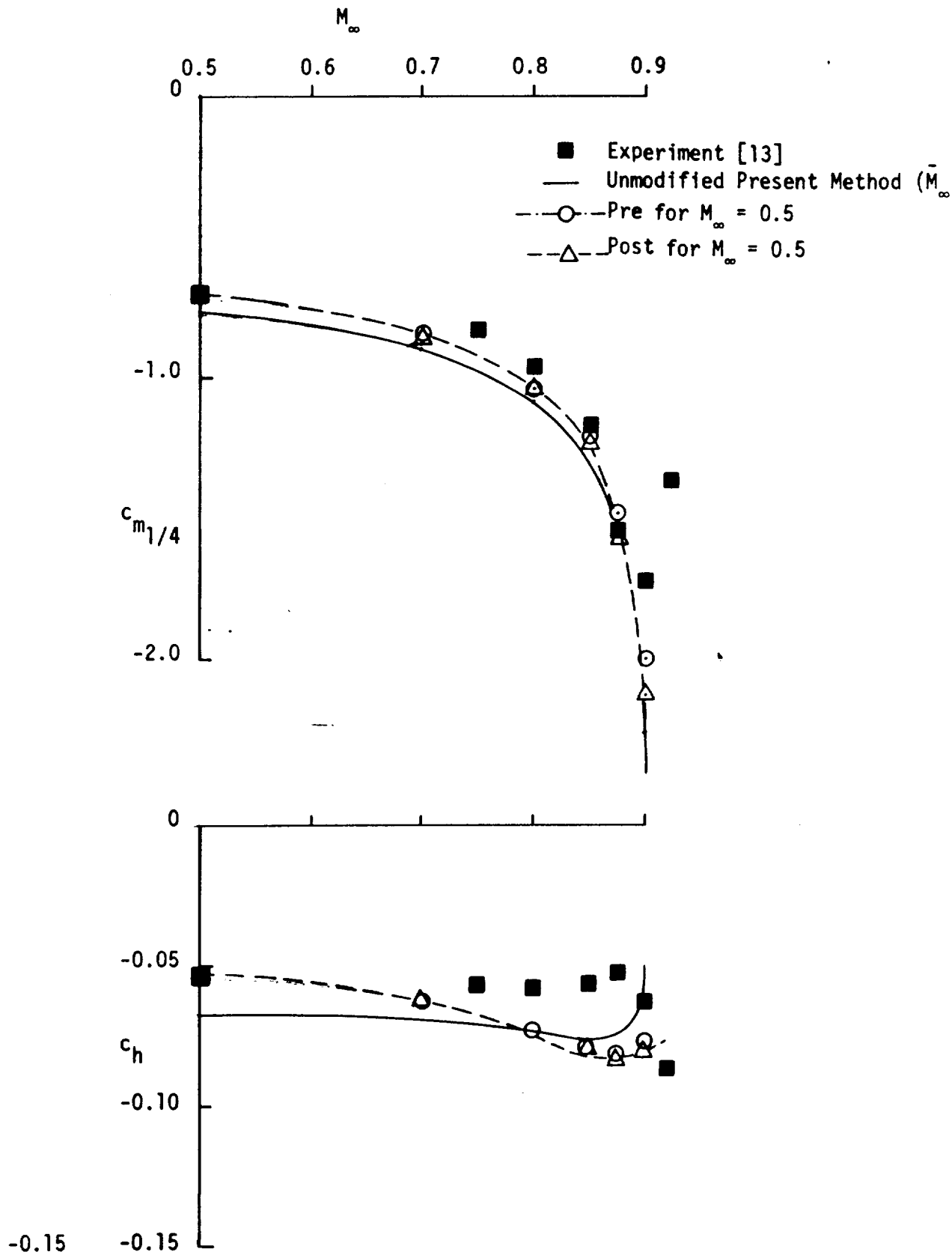


Figure 40. - Effect of applying correction factors obtained at $M_\infty = 0.5$ to other Mach Numbers for the Present Method (\bar{M}_∞)

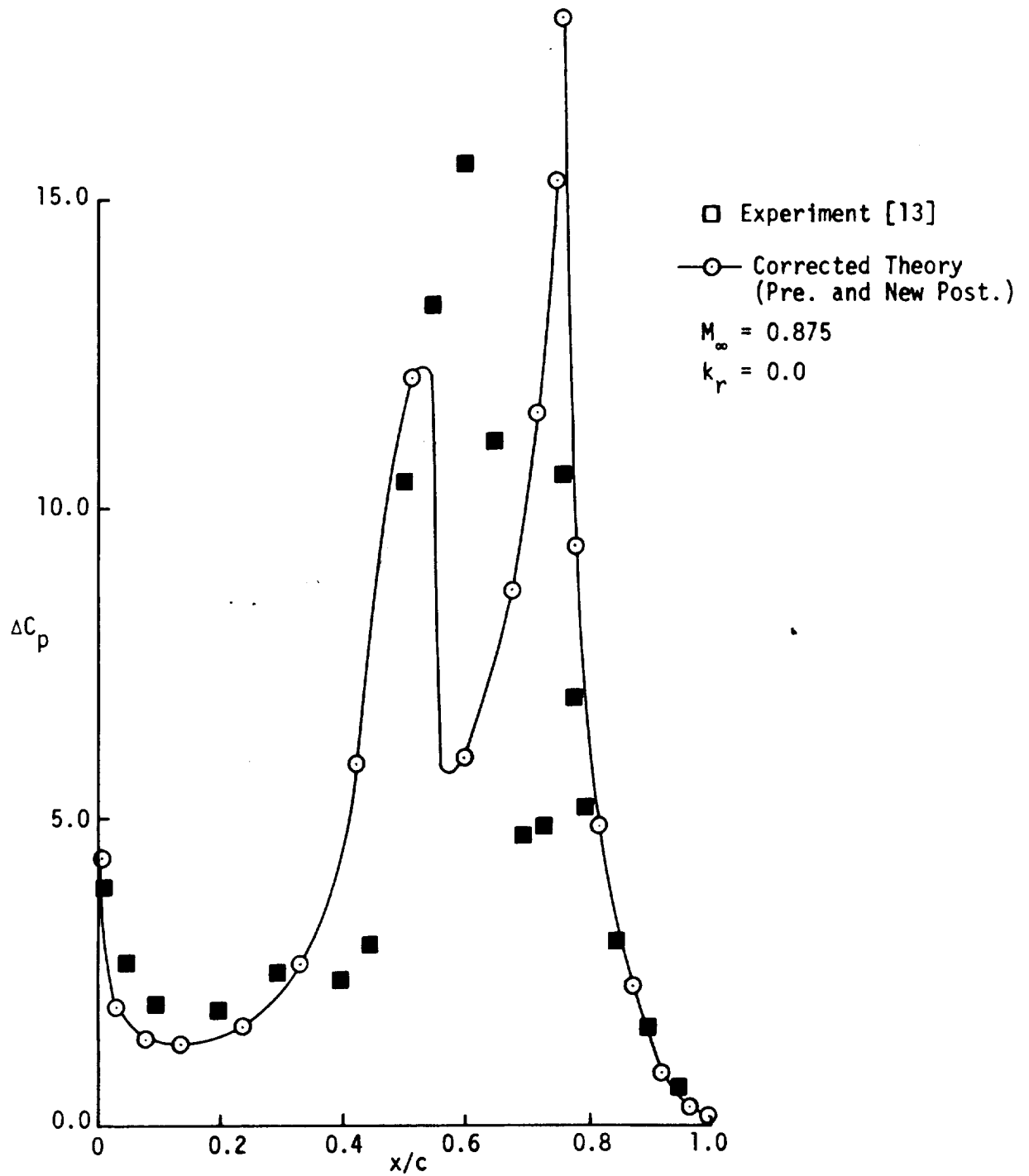


Figure 41. - Results of applying postmultiplying correction factors (New) obtained at $M = 0.5$ and premultiplying factors obtained at $M = 0.875$ to theory.

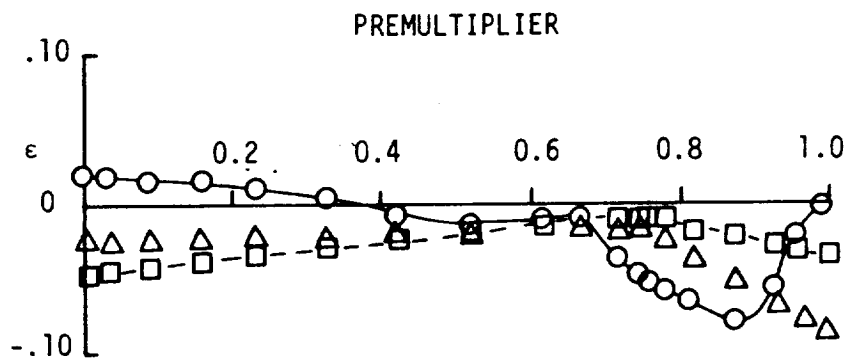
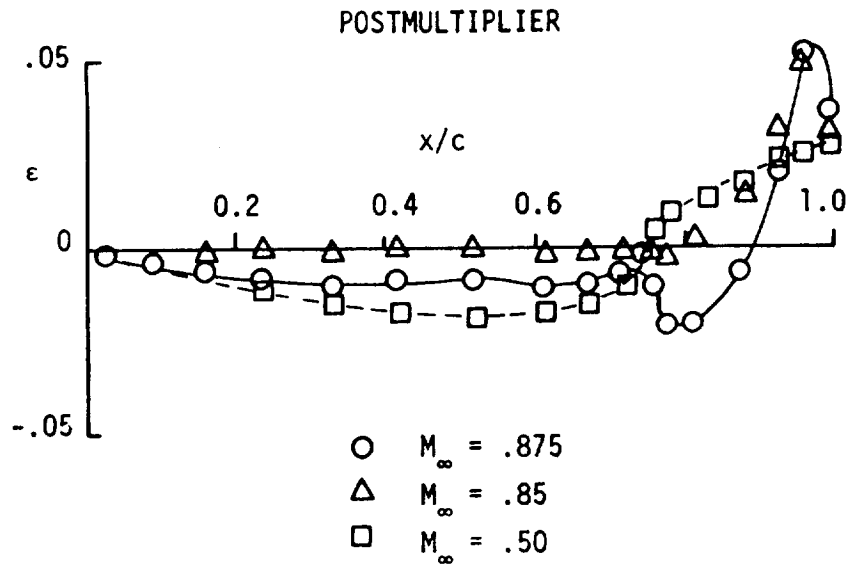


Figure 42. - Comparison of incremental correction factors obtained at various Mach Numbers using the Present Method (M_∞).

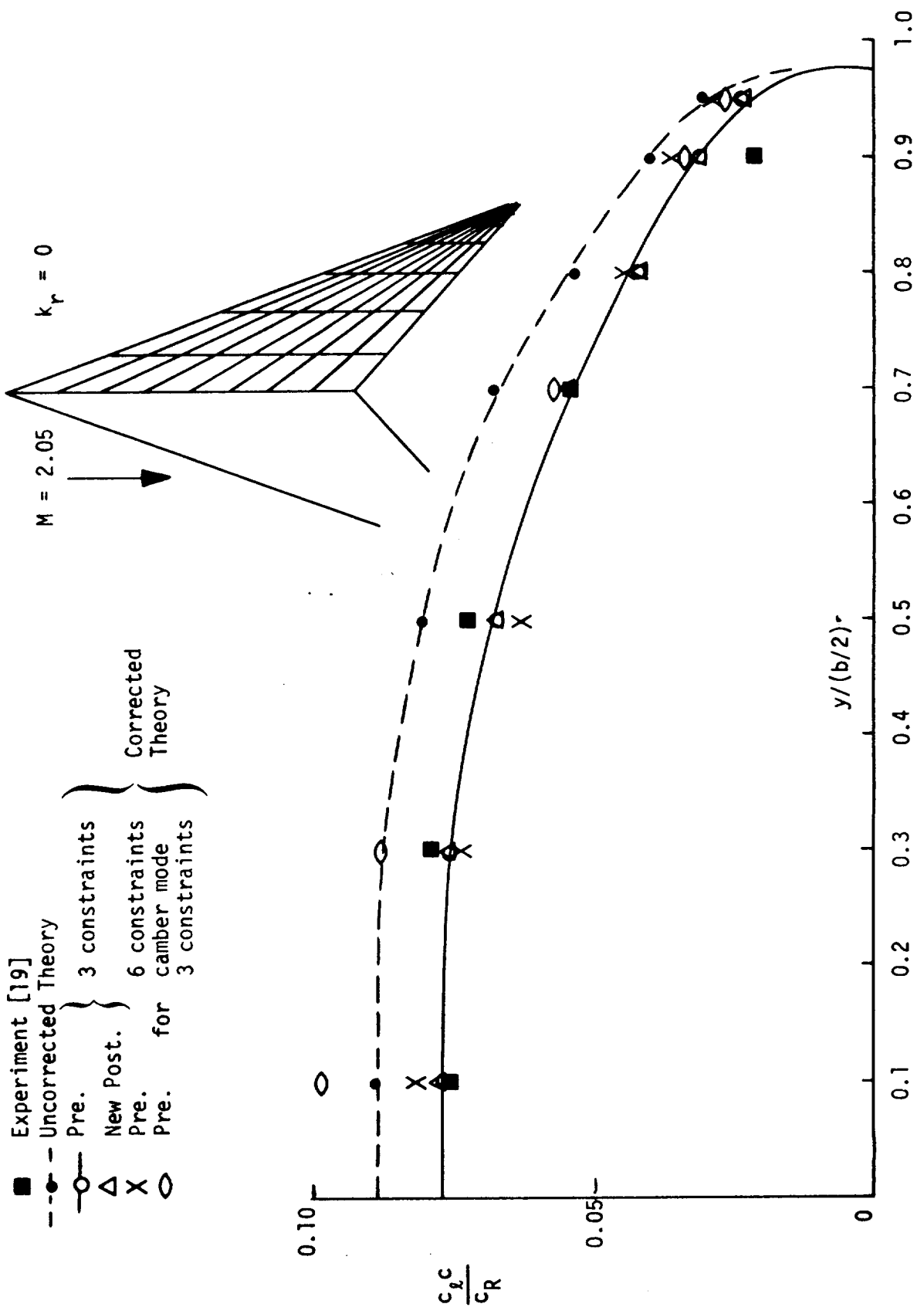


Figure 43. - Comparison of experimental data with corrected and uncorrected theory for an arrow wing in pitch ($\alpha = 4^\circ$) operating at supersonic speeds.

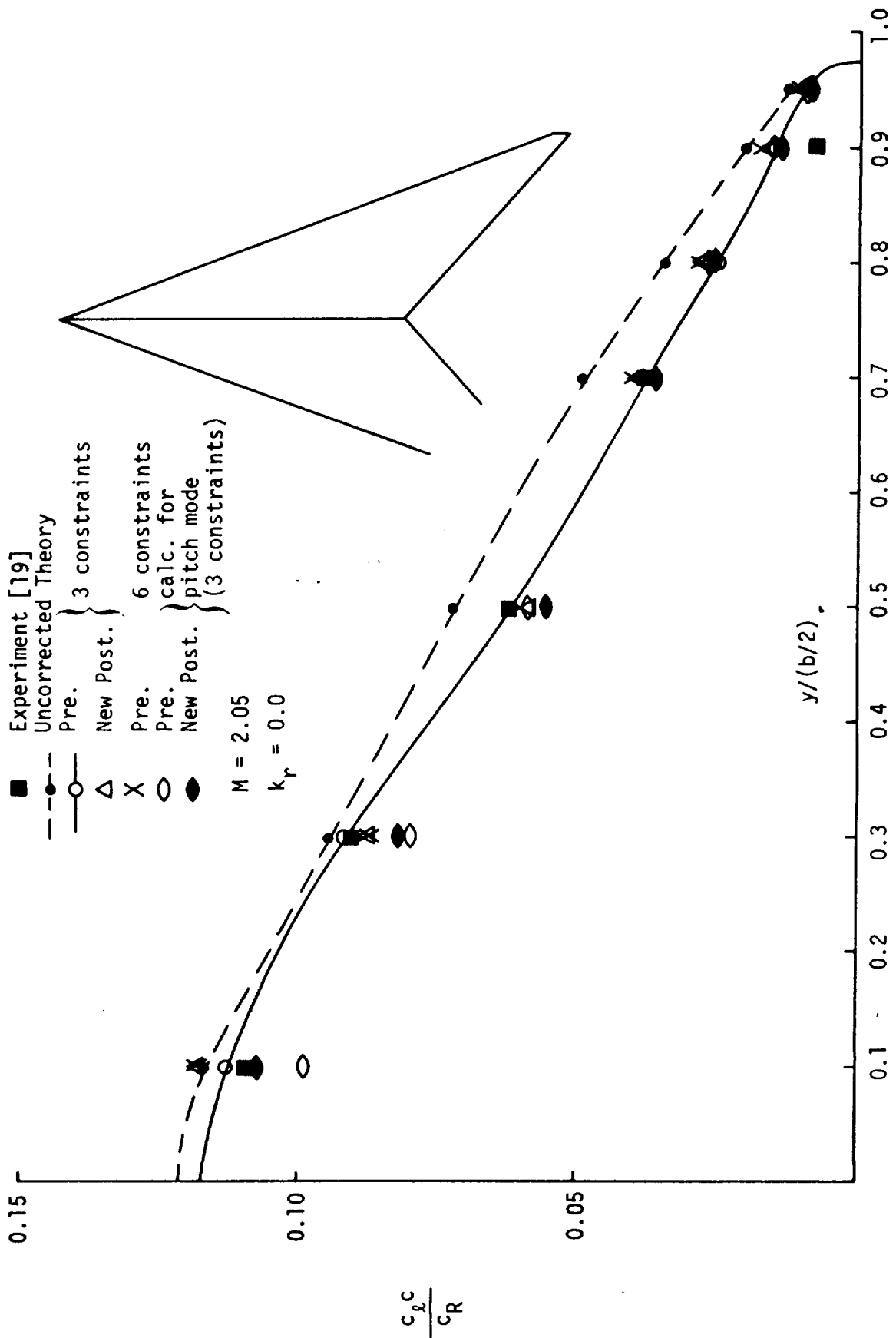


Figure 44. - Comparison of experimental data with corrected and uncorrected theory for an arrow wing with camber operating at supersonic speeds.

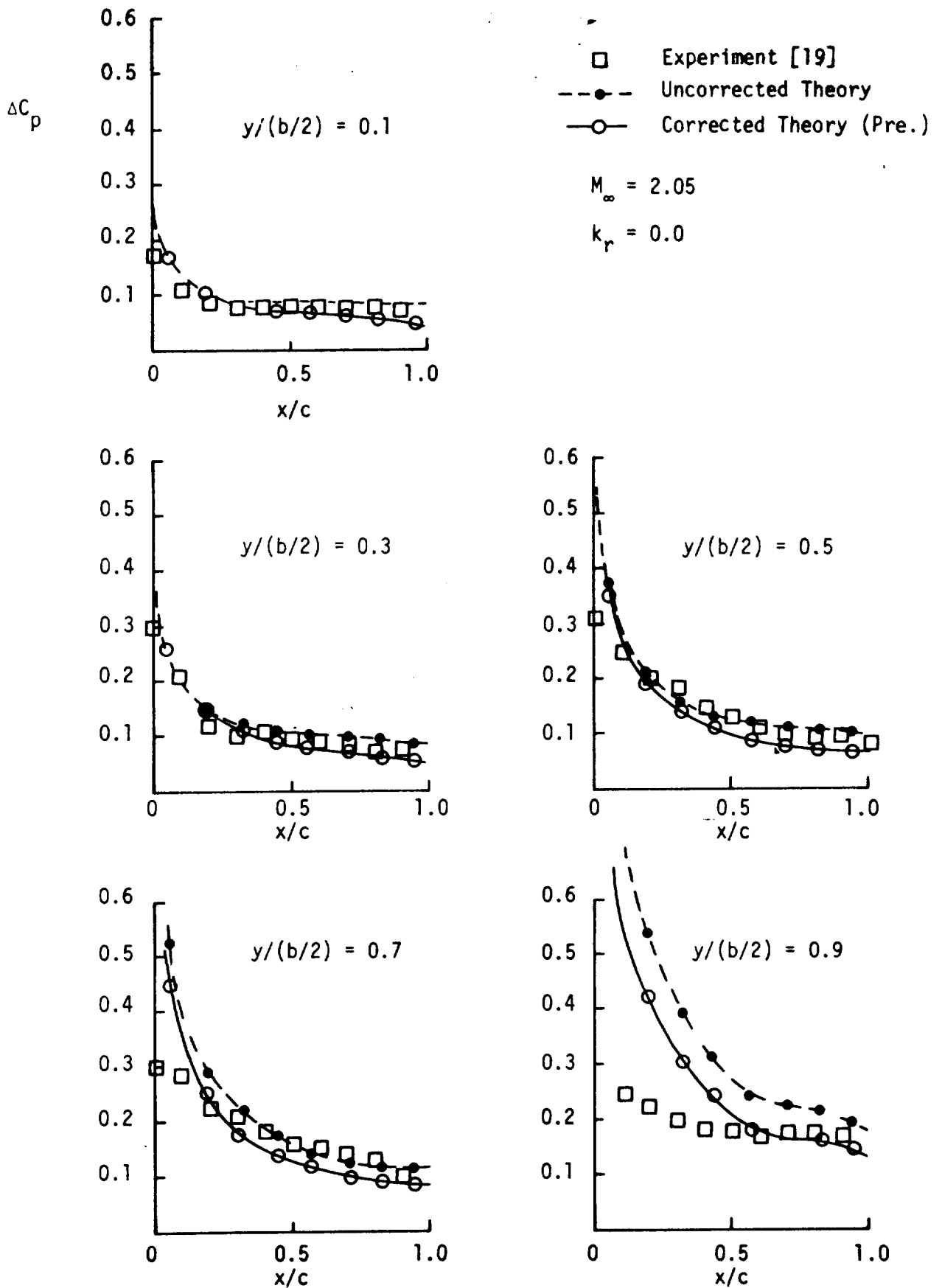


Figure 45. - Comparison of experimental data with corrected and uncorrected theory for an Arrow wing in pitch.

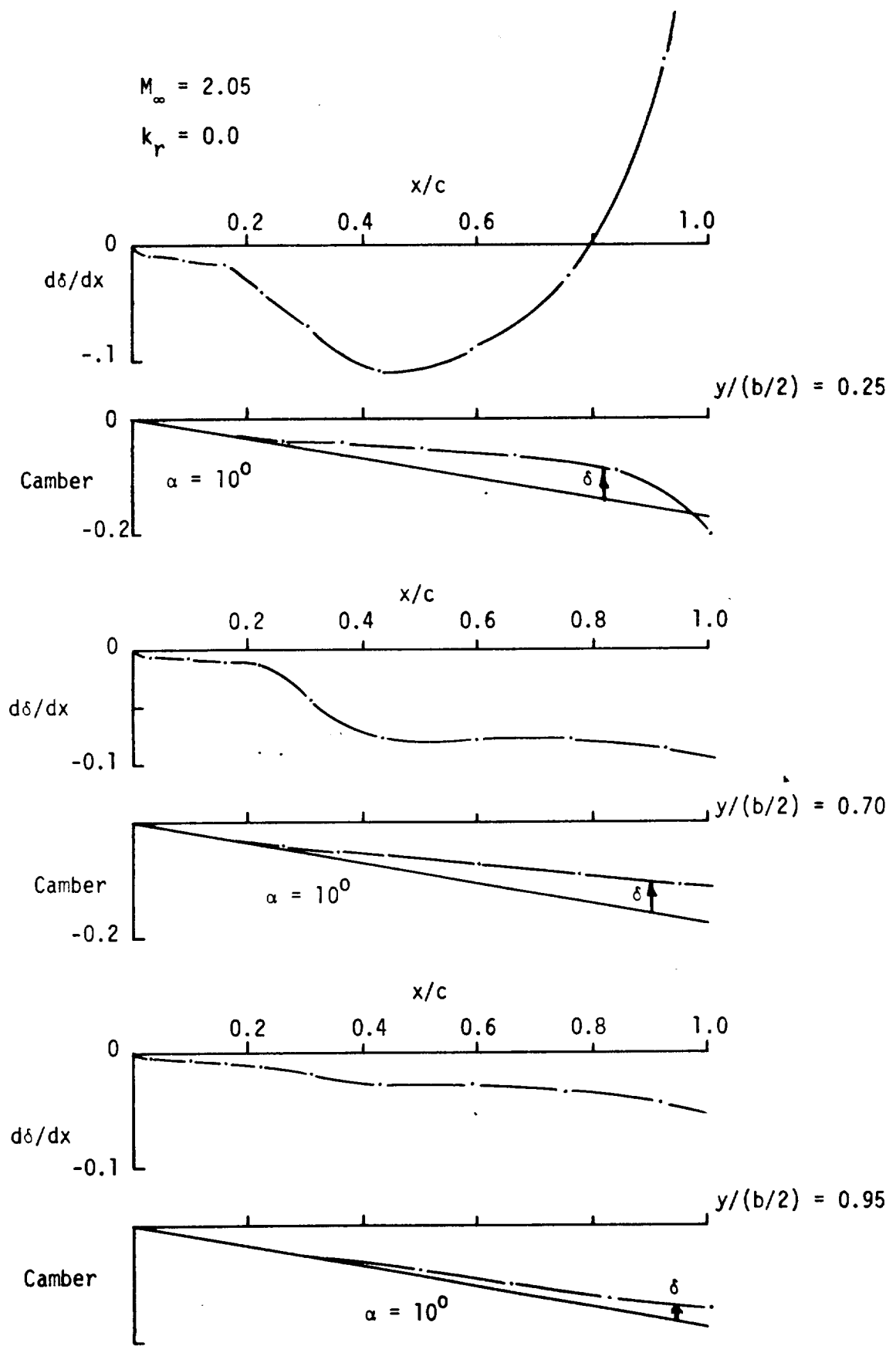
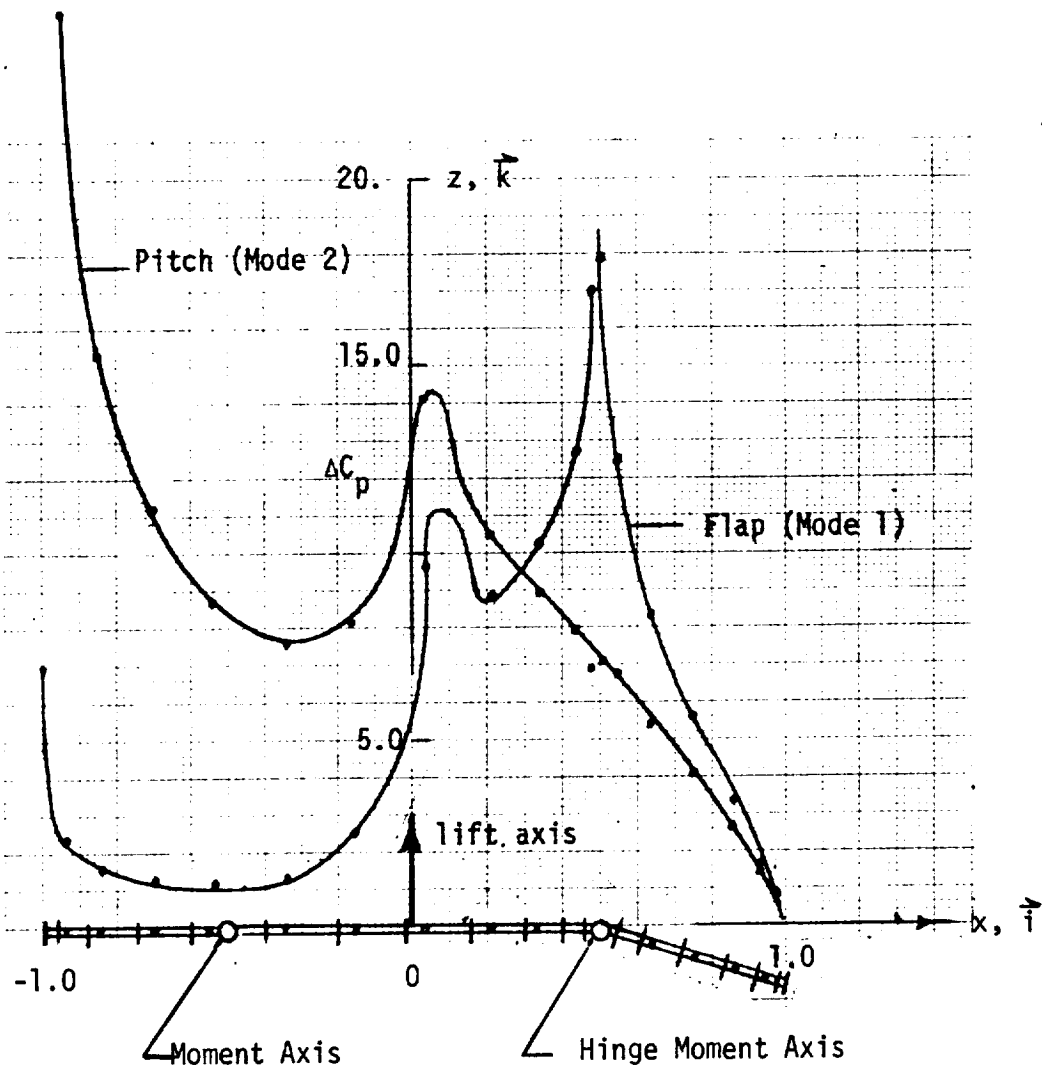


Figure 46. - Camber changes inferred by New Postmultiplying correction factors as applied to an Arrow wing operating at supersonic speeds and $\alpha = 10^\circ$.



Axes Data

Axis No.	Origin			Direction Cosines		
	$\xi(1)$	$\eta(1)$	$\zeta(1)$	$\cos\alpha$	$\cos\beta$	$\cos\gamma$
1	0	0	0	0	0	1
2	-0.5	0	0	0	1	0
3	+0.5	0	0	0	1	0

Lift and Moment Data

	Flap		Pitch	
	Exp.	Theo.	Estimate	Theo.
c_l	4.93	5.56	8.8	10.0
$c_{m1/4}$	-1.57	-2.09		
$c_{h3/4}$	-0.053	-0.141		

Figure 47. - Graphical and Tabulated Data for Program Test Cases

1. Report No. NASA CR-144967	2. Government Accession No.	3. Recipient's Catalog No.	
4. Title and Subtitle CORRECTION FACTOR TECHNIQUES FOR IMPROVING AERODYNAMIC PREDICTION METHODS		5. Report Date May 1976	6. Performing Organization Code
		8. Performing Organization Report No.	
7. Author(s) Joseph P. Giesing, Terez P. Kalman, William P. Rodden		10. Work Unit No.	
		11. Contract or Grant No. NAS1-13835	
9. Performing Organization Name and Address McDonnell Douglas Corporation Douglas Aircraft Company 3855 Lakewood Boulevard Long Beach, California 90846		13. Type of Report and Period Covered Contractor Report	
		14. Sponsoring Agency Code	
12. Sponsoring Agency Name and Address National Aeronautics and Space Administration Washington, D. C.			
15. Supplementary Notes Final Report, for NASA Langley Research Center; Project Manager Irving Able			
16. Abstract <p>A method for correcting discrete element lifting surface theory to reflect given experimental data is presented. Theoretical pressures are modified such that imposed constraints are satisfied (e.g., lift, moment, etc.) while minimizing the changes to the pressures. Several types of correction procedures are presented and correlated; (1) scaling of pressures; (2) scaling of downwash values and (3) addition of an increment to the downwash that is proportioned to pressure. Some special features are included in these methods and they include: (1) consideration of experimental data from multiple deflection modes, (2) limitation of the amplitudes of the correction factors and (3) the use of correction factor mode shapes. These methods are correlated for cases involving all three Mach Number ranges using a FORTRAN IV computer program. Subsonically, a wing with an oscillating partial span control surface and a wing with a leading edge droop are presented. Transonically a two-dimensional airfoil with an oscillating flap is considered. Supersonically an arrow wing with and without camber is analyzed.</p> <p>In addition to correction factor methods an investigation is presented dealing with a new simplified transonic modification of the two-dimensional subsonic lifting surface theory. Correlations are presented for an airfoil with an oscillating flap.</p>			
17. Key Words (Suggested by Author(s)) Correction factors Oscillatory aerodynamics Control surface aerodynamics Semiempirical aerodynamic corrections Transonic flow		18. Distribution Statement Unclassified - unlimited	
19. Security Classif. (of this report) Unclassified	20. Security Classif. (of this page) Unclassified	21. No. of Pages 285	22. Price*

* For sale by the National Technical Information Service, Springfield, Virginia 22151